LONG RANGE FORECAST MODELING ON CHAOTIC ENVIRONMENTAL TIMES SERIES AND STUDY ON RAINFALL PATTERNS IN DIFFERENT REGIONS OF INDIA

A THESIS SUBMITTED IN PARTIAL FULFILLMENT OF THE REQUIREMENTS FOR THE DEGREE OF DOCTOR OF PHILOSOPHY

MARINA LALLAWMZUALI
MZU REGISTRATION NUMBER: 2108961
Ph.D. REGISTRATION NO: MZU/Ph.D./1778 of 17.09.2021

DEPARTMENT OF MATHEMATICS AND COMPUTER SCIENCE

SCHOOL OF PHYSICAL SCIENCES

NOVEMBER, 2025

LONG RANGE FORECAST MODELING ON CHAOTIC ENVIRONMENTAL TIMES SERIES AND STUDY ON RAINFALL PATTERNS IN DIFFERENT REGIONS OF INDIA

BY

MARINA LALLAWMZUALI

Department of Mathematics and Computer Science

Supervisor : Prof. M. Sundararajan

Submitted

In partial fulfillment of the requirement of the Degree of Doctor of Philosophy in Mathematics of Mizoram University, Aizawl

Dedicated to,

My family.

DEPARTMENT OF MATHEMATICS AND COMPUTER SCIENCE
(School of Physical Sciences)
MIZORAM UNIVERSITY
TANHRIL : 796004
Aizawl : Mizoram
(DST-FIST & NBHM – DAE SUPPORTED)

Prof. M. Sundararajan
Professor

Post Box No. 190
Gram:
Mob: 8936088405
E-Mail: dmsrajan@mzu.edu.in
University Website: www.mzu.edu.in

CERTIFICATE

This is to certify that the thesis entitled "Long Range Forecast Modeling on Chaotic Environmental Times Series and Study on Rainfall Patterns in Different Regions of India", submitted by Marina Lallawmzuali (Registration No. : MZU/Ph.D./1778 of 17.09.2021) for the award of the degree of Doctor of Philosophy (Ph. D.) in Mathematics, is a bonafied record of the original research carried out by her under my supervision. She has been duly registered, and the thesis is worthy of being considered for the award of the Ph. D. degree. This work has been done under my supervision and has not been submitted for any degree in any other university/Institute.

Place: Aizawl

Date:

(Prof. M. SUNDARARAJAN)
Supervisor

DECLARATION

MIZORAM UNIVERSITY

NOVEMBER, 2025

I, **Ms. Marina Lallawmzuali**, hereby declare that the subject matter of this thesis is the record of work done by me, that the contents of this thesis did not form basis of the award of any previous degree to me or to do the best of my knowledge to anybody else, and that the thesis has not been submitted by me for any research degree in any other University/Institute.

This is being submitted to the Mizoram University for the degree of Doctor of Philosophy in Mathematics.

(MARINA LALLAWMZUALI)
Candidate

(Prof. S. SARAT SINGH)
Head of Department
Dept. of Maths. and Comp. Sc.,
Mizoram University, Mizoram.

(Prof. M. SUNDARARAJAN)
Supervisor
Dept. of Maths. and Comp. Sc.,
Mizoram University, Mizoram.

ACKNOWLEDGEMENTS

I would like to express my sincere gratitude to Prof. Samba Shiva Rao, former Vice-Chancellor of Mizoram University, for his valuable guidance and encouragement during the early stage of my research. I am also thankful to Prof. Diwakar Chandra Deka, Vice-Chancellor of Mizoram University, for his continuous support and for providing an academic environment that enabled me to complete this work.

My heartfelt thanks go to Prof. Diwakar Tiwari, former Dean of the School of Physical Sciences, for his advice and encouragement, and to Prof. Suman Rai, Dean of the School of Physical Sciences, for his support and constructive feedback. Their guidance has been very important for the progress of my study.

I am deeply grateful to my supervisor, Prof. M. Sundararajan, Department of Mathematics and Computer Science, for his expert guidance, patience, and constant motivation. His support and valuable suggestions have been central to the completion of this thesis.

I am highly obliged to Prof. S. Sarat Singh, Head of Department, Mathematics and Computer Science, Mizoram University, for providing all the necessary facilities and his faithful advice during the course of my research work.

I would also like to thank the faculty members who encouraged me and shared helpful feedback: Prof. Jamal Hussain, Mr. Laltanpuia, Dr. M. Saroja Devi, Mr. Sajal Kanti Das, Dr. Tanay Saha, and Dr. Sandipan Dutta. Their valuable feedback and discussions contributed immensely to the depth of this study. I gratefully acknowledge all the staff of the Department of Mathematics and Computer Science for their assistance and support during my research.

I also thank to Dr. Mohan Khatri, Dr. A. Lalchhuangliana, Dr. Sanjay Debnath, Dr. C. Zosangzuala, Dr. Robert Sumlalsanga, Dr. Lalnunenga Colney, Dr. Bidyabati Thangjam and Dr. Shrabanika Boruah, for their valuable advice, co-operation and full support during my research work.

My heartfelt thanks also go to my fellow research scholars— Ms. Biakkim K.C., Mr. Laltluangkima, Ms. Panchalika Dutta, Ms. K. Lalnunsiami, Ms.

Jenny Lallawmzuali, Ms. Lalruatpuii, Ms. Vanlalchhandami, Mr. Zenith Oinam, Ms. Nancy Lalremsangi, Mr. Pranab Modak, Mr. H. Lalhriatpuia and all the research scholars in the department—whose support, discussions, and companionship made this academic journey both productive and enjoyable.

Furthermore, I would like to acknowledge every single one who helped to the successful completion of this research.

Finally, I would like to thank my parents, K. Lalramnghaka and B. Lalchhuankimi, my sisters K. Lalthianghlimi and Lucy Lalhriatpuii, and my brother Franky Lalsangzuala for their love, encouragement, and constant support.

Above all, I dedicate this thesis to God Almighty, whose blessings and guidance have been my constant strength.

(MARINA LALLAWMZUALI)

Place: Aizawl

Date:

PREFACE

The present thesis entitled "Long Range Forecast Modeling on Choatic Environmental Times Series and Study on Rainfall Patterns in Different Regions of India" is the result of research conducted by the author under the supervision of Prof. Sundararajan Muniyan, Professor in the Department of Mathematics and Computer Science at Mizoram University, Aizawl, Mizoram.

The thesis is organized into six chapters, each divided into smaller sections. Chapter 1 introduces the background and motivation for the study. It defines the research problem, reviews existing literature, and clearly outlines the research objectives, scope, and significance.

Chapter 2 outlines the methodological framework of this study. In this work, we develop a Modified Holt Winters method (MOHW) and an Innovative Rainfall Predictive Method (IRPM), along with two multivariate extensions—MAHW and MMOHW—that incorporate temperature and humidity. The model parameters are optimized using both Brute-force approach and Bayesian optimization techniques. Model performances are evaluated through multiple error metrics to ensure reliability.

Chapter 3 applies the AHW, MHW, and MOHW models to rainfall forecasting in Mizoram and five South Indian states—Andhra Pradesh, Telangana, Tamil Nadu, Kerala, and Karnataka. The findings indicate that the MOHW model consistently outperforms both the AHW and MHW models, as well as the SARIMA method by achieving lower RMSE and MAE, thereby establishing it as the preferred forecasting method for these regions and used it to forecast rainfall.

Chapter 4 applies the IRPM model to districts of Mizoram and subdivision of India. First, rainfall trends were assessed using the Mann–Kendall test, Sen's slope, and ITA on monthly data from 1986–2023 for Mizoram districts; the results indicated mostly decreasing trends. IRPM was then used to forecast rainfall from 2024 to 2064. The second part extends the analysis to 34 meteorological subdivisions of India using data from 1972–2022. Mann–Kendall and Sen's slope tests revealed significant spatial and temporal variability: increasing trends in

March and September in West Rajasthan, Konkan & Goa, and Coastal/North Interior Karnataka; July showed increases in some regions, while declines were observed in Northeast and Eastern India. No significant changes were noted in May and December. IRPM forecasts up to 2075 achieved RMSE values between 21.39 and 102.26 and R^2 values between 0.67 and 0.95. These projections highlighted sharp rainfall declines in Northeast India during February and July, and in Jharkhand, Bihar, and Uttar Pradesh during peak monsoon months, whereas increases occurred in parts of Karnataka, Kerala, and Konkan & Goa. These mixed patterns underscore the complexity of monsoon dynamics and the need for region-specific forecasting models. The results provide essential insights for water resource planning, food security, and agricultural management in a changing climate.

Overall, the IRPM model outperformed the ARIMA and SARIMA models in every region we evaluated.

Chapter 5 develops the multivariate framework (MAHW and MMOHW) to address limitations of univariate models. Using data from Mizoram (1986–2023), these multivariate models showed significantly lower RMSE and MAE values compared to univariate Holt Winters, Multiple Linear Regression (MLR), and Vector Autoregression (VAR). Their integration of temperature and humidity makes them powerful tools for enhancing long range rainfall forecasts.

Chapter 6 provides a summary and conclusion of the research discussed in the preceding chapters and suggests future research directions.

Additionally, a list of references is given at the end.

Contents

LIST OF FIGURES

LIST OF TABLES

LIST OF ACRONYMS

Acronym	Meaning
ADF	Augmented Dickey-Fuller
AHW	Additive Holt Winters
AI	Artificial Intelligence
AIC	Akaike Information Criterion
ARIMA	Autoregressive Integrated Moving Average
BIC	Bayesian Information Criterion
EI	Expected Improvement
IMD	Indian Meteorological Department
IRPM	Innovative Rainfall Predictive Method
ITA	Innovative Trend Analysis
LRF	Long Range Forecast
MAE	Mean Absolute Error
MAHW	Multivariate Additive Holt Winters
MAPE	Mean Absolute Percentage Error
MHW	Multiplicative Holt Winters
MK	Mann-Kendall
MLR	Multi Linear Regression
MMOHW	Multivariate Modified Holt Winters
MOHW	Modified Holt Winters
MSE	Mean Square Error
NSE	Nash–Sutcliffe Efficiency coefficient
RMSE	Root Mean Square Error
SARIMA	Seasonal Autoregressive Integrated Moving Average
SD	Standard Deviation
VAR	Vector Autoregression

Chapter 1

Introduction

1.1 Background and Motivation

Rainfall is a crucial component of the hydrological cycle, and any alterations in its patterns have a direct impact on water resources (Islam *et al.*, 2012). The shifts in rainfall patterns due to climate change have become a significant concern for water resource managers and hydrologists (Gajbhiye *et al.*, 2015). Previous studies, such as those by Srivastava *et al.* (2014) and Islam *et al.* (2012) have highlighted that changes in rainfall volume and frequency can significantly influence streamflow patterns, water demand, runoff distribution, groundwater levels, and soil moisture. These variations lead to far-reaching effects on water resources, ecosystems, biodiversity, agriculture, and food security. Additionally, extreme changes in rainfall trends are linked to an increased occurrence of hazardous events like droughts and floods (Srivastava *et al.*, 2014). Gupta *et al.* (2014) emphasize that the availability of soil moisture, critical for crop production, depends heavily on rainfall. In India, monsoon rainfall is vital for agriculture, with approximately 68% of cultivated land relying on rain-fed farming. This form of agriculture supports nearly 60% of the livestock population and 40% of the human population (Matham *et al.*, 2024). Consequently, studying climate change particularly changes in rainfall patterns and their spatial distribution, is essential for sustainable water resource management. Different parts of the country experience significant variations in rainfall during the monsoon season. While some regions receive substantial rainfall, others face extremely low levels, often leading to severe water shortages. Moreover, the agricultural sector has been heavily impacted by the adverse effects of climate change, particularly changes in rainfall patterns (Attri and Tyagi, 2010). Rainfall often fails to occur during expected periods or takes place unpredictably, resulting in considerable damage. Therefore, it is essential to assess whether there are discernible trends in rainfall and patterns in its variability (Kumar *et al.*, 2010).

In a developing country like India where agriculture has been considering a prime profession, the biggest worry is always water scarcity, no matter the year. The southwest monsoon season (June-September) typically brings the highest precipitation to the country, although regional rainfall patterns vary significantly from year to year, the overall southwest monsoon rainfall across India remains relatively stable. Statistical analysis indicates that the average seasonal rainfall from 1941 to 1990 was 89 cm for half the century, with a variation of approximately 10% (Charaniya and Dudul, 2011). Even minor fluctuates in seasonal rainfall can profoundly impact the agricultural sector. Despite a decline in the agricultural sector's contribution to national income to less than 30% in the assessment year, its performance remains crucial to India's economy. The deficient monsoon rainfall experienced in 2002 and 2004 had adverse effects on the economy (Rajeevan *et al.*, 2007).

The state of Mizoram is particularly vulnerable to climatic variability. More than 70% of its population depends on agriculture, primarily through shifting cultivation (Sati and Rinawma, 2014). Given its mountainous topography and heavy rainfall, the state is prone to abnormal climate variability and long term climate change impacts. Both rural and urban communities rely heavily on agriculture and allied sectors, which are highly sensitive to changing rainfall patterns. This vulnerability manifests in shifts in sowing and harvesting periods, reduced yields, and disruptions to food security. Moreover, Mizoram faces additional climate-induced hazards such as landslides and flash floods, which further threaten its socio-economic development (Lallianthanga *et al.*, 2018). Accurate rainfall prediction is therefore essential to capture the state's rainfall dynamics and mitigate associated risks.

In recent years, there has been a growing focus on scientific research aimed at understanding the transformations occurring within the life support systems of various ecosystems and the impacts of climate change. These investigations have revealed substantial challenges in managing and conserving resources, while also influencing the dynamics of global socio-economics relations. Scholars have been addressing these issues since the early 1970s and have come to regard them as "wicked problems par excellence". due to their complex, multifaceted nature and the conflicting interests surrounding them. Many research studies, therefore, are aimed at contributing towards existing knowledge organization pertaining to climate change in India. One of the major areas in which the climate change has made a great alternation is rainfall patterns in various regions of the world. In India, rainfall during summer is very crucial due to its direct influence on agriculture, and consequently, on the nation's economy. In view of this impact, a reasonable forecast of this rainfall is needed.

At present, most forecasting approaches rely on statistical techniques applied to limited datasets with area wise. These methods typically treat sequential rainfall observations as realizations of stochastic processes, resulting in forecast equations that use one or more predictor variables. However, the accuracy of such methods remains limited. Given the importance of the monsoon to India's economy, the need for robust LRF of rainfall is undeniable. The consequence of the wrong prediction could lead to wrong planning. Thus, researchers and policy makers have long recognized the necessity of developing improved LRF models that are not restricted to a particular region or state but can be applied more broadly. Such models would enable policy makers to prepare sustainable development strategies, manage agricultural production more effectively, and ensure the conservation of natural resources and life-support systems.

1.2 Literature Review

Rainfall is one of the most vital hydro-meteorological variables, capturing the sustained attention of hydrologists and climate researchers worldwide over the past several decades. Investigating rainfall trends under changing climate conditions remains a key focus, yet predicting these trends continues to pose a considerable challenge. Global warming and its impacts on rainfall, runoff, and precipitation, have captured researchers' attention globally. In India, climate change and shifts in rainfall patterns are pressing concerns (Goswami *et al.*, 2006), even though developing countries often receive less global and local attention despite facing urgent environmental, agricultural, and water resource issues (Mahmoud and Smadi, 2006). Climate variability directly impacts water resources, which are integral to socioeconomic stability and ecosystem health. Freshwater availability in many Indian river basins is projected to decline due to climate change (Gosain *et al.*, 2006). Moreover, a lack of awareness about changing climate conditions and poor adaptive planning have worsened environmental problems and disrupted communities (Uba and Bakari, 2005). Responding to these challenges, researchers are exploring a variety of approaches to adapt to environmental change. A clear understanding of rainfall trends, examining both magnitude and variability is essential (Zhang *et al.*, 2008). Additionally, reliable rainfall forecasting is critical for agricultural planning, urban and industrial water supply, and food security (Sharma *et al.*, 2016). Thus, many researchers have conducted trend analyses and developed forecasting models for different region using various statistical and mathematical models. Each method has its own strengths and limitations. Reviewing previous approaches creates a bridge to improving and refining conceptual frameworks, and supports the development of reliable long term rainfall forecasting. Thus, conducting long term time series analysis of past trends can support the development of dependable tools for forecasting rainfall (Feng *et al.*, 2016). The review of previous research focusing on trend analysis using Mann-Kendall (MK) test, Sen's slope estimator test, and mathematical models for rainfall forecasting are presented in this section.

1.2.1 Trend Analysis of Rainfall

Trend analysis is a statistical approach used to investigate the long term direction or behaviour of a variable over time. In the context of hydro climatology, it helps assess whether variables such as rainfall exhibit any significant increasing or decreasing trends. Various methods exist to analyze such trends, broadly classified into parametric and non-parametric techniques (Duhan and Pandey, 2013). The primary goal of trend analysis is to determine whether there is a statistically significant directional change in a variable over a given period (Jain and Kumar, 2012).

The parametric method is based on linear regression and therefore checks only for a linear trend. In addition, the method is less flexible as it requires the recorded data to be normally distributed. On the other hand, there is no such restriction for the non-parametric test. Parametric tests can be applied when the data are normally distributed. But many hydrology or climate time series data in real time are not normally distributed and hence non-parameter tests are considered as more robust than over parameter tests (Karpouzos *et al.*, 2010; Hamid *et al.*, 2014).

One major advantage of non-parametric tests is that the data do not have to fit into any particular probability distribution, allowing broader application across various types of data. Commonly used non-parametric tests for rainfall trend detection are Mann-Kendall (MK) test, Spearman's Rho, Sen's Slope estimator, Seasonal Kendall, and Sen's T-test (Yue *et al.*, 2002; Krishnakumar *et al.*, 2009; Paulo *et al.*, 2012; Shadmani *et al.*, 2012; Subash and Sikka, 2014). Among these, the Mann-Kendall test is widely recognized and frequently applied in climatological and hydrological trend studies. It is a rank-based, non-parametric test designed to evaluate whether a variable shows a monotonic upward or downward trend over time (Subash and Sikka, 2014). The MK test is particularly useful for datasets affected by outliers or skewed distributions, as it is not influenced by extreme values. Its robustness and simplicity make it a preferred choice over linear tests (Onoz and Bayazit, 2003; Kahya and Kalayci, 2004). The significance of identified trends is typically assessed at a 5% significance level ($p < 0.05$).

The MK method has been widely used in rainfall analysis (Partal and Kahya, 2006; Kumar *et al.*, 2010; Tabari *et al.*, 2011; Shadmani *et al.*, 2012; Soltani *et al.*, 2012, 2013), as well as in broader fields of time series analysis (Kalayci and Kahya, 2006; Tian *et al.*, 2010; Sulaiman *et al.*, 2015). The World Meteorological Organization also recommends the MK test for detecting trends in climatic and hydrologic data (Chowdhury *et al.*, 2010).

To complement the MK test, the Sen's slope estimator (Sen, 1968) is often used to quantify the magnitude of the trend. This non-parametric method estimates the rate of change per year in a time series and effectively handles seasonal variability in precipitation data. While the MK test identifies the presence of a trend, Sen's slope provides a numerical estimate of its magnitude when the trend is statistically significant (Paulo *et al.*, 2012).

Numerous studies have been conducted on rainfall trends both globally (Longobardi and Villani, 2010; Caloiero *et al.*, 2011; Marumbwa *et al.*, 2019; He *et al.*, 2022; Treppiedi *et al.*, 2023; Wu *et al.*, 2023) and within India (Guhathakurta and Rajeevan, 2008; Subash and Sikka, 2014; Praveen *et al.*, 2020; Ahmed, 2023). The changes in rainfall patterns across India, as observed in various studies, reveal no definitive trend in annual rainfall increase or decrease (Mooley and Parthasarathy, 1984; Sarker and Thapliyal, 1988; Thapliyal and Kulshreshtha, 1991). However, subsequent research identified significant long term trends in Indian rainfall (Dash *et al.*, 2007; Kumar and Jain, 2009; Gajbhiye *et al.*, 2015; Mondal *et al.*, 2018).

Guhathakurta and Rajeevan (2008) analyzed annual rainfall data from 1901 to 2003 for 36 meteorological subdivisions in India. Their findings revealed that eight subdivisions exhibited a significant increasing trend, while three subdivisions—Kerala, Jharkhand, and Chhattisgarh—showed a significant decreasing trend.

Similarly, Kumar *et al.* (2010) also reported a significant decline in rainfall in Chhattisgarh. Patra *et al.* (2012) conducted a trend analysis of rainfall patterns in Odisha, examining monthly, seasonal, and annual variations and their findings indicated a long term, statistically insignificant decline in both annual and monsoonal rainfall, whereas a positive trend was observed during the post-monsoon season. Jaswal *et al.* (2015) reported a significant decreasing trend in Himachal Pradesh's annual rainfall between 1951 and 2005. Kumar *et al.* (2020) analyzed rainfall in Rajasthan from 1971 to 2019 and found no significant trend. Junaid and Santhannakrishna (2021) examined 30 years (1990–2019) of daily rainfall data for Tamil Nadu, concluding that there was no significant trend, despite the presence of both increasing and decreasing tendencies. A similar lack of significant trends was reported in Uttarakhand by Alam *et al.* (2018). Goswami and Prasad (2023) studied annual rainfall from 1901 to 2002 in Arunachal Pradesh and identified a decreasing trend. Praveen *et al.* (2020) applied innovative trend analysis to annual and seasonal rainfall data from 1901 to 2015 across 34 meteorological subdivisions. Their results indicated that most subdivisions exhibited significant negative trends, with only seven exceptions. Gouda *et al.* (2024) assessed the spatial and temporal distribution of monsoon rainfall in Karnataka, analyzing its climatology, variability, and trends and their time series analysis revealed an overall increasing trend in rainfall, although the rate of increase has slowed in recent decades compared to the long term trend. Pandey *et al.* (2024) examined rainfall trends in Mizoram over a 25-year period (1996–2020), considering both short term and long term persistence of seasonal and annual rainfall trends across districts in the state. Most existing studies focus primarily on seasonal and annual rainfall trends, leaving monthly rainfall patterns underexplored. To address this gap, our study focuses on the monthly rainfall trend analysis of India.

1.2.2 Forecasting of Rainfall using Time Series Models

India's agricultural and industrial sectors are heavily influenced by regional weather patterns. However, the frequent and unpredictable fluctuations in climatic conditions across the country pose significant challenges to both governmental and non-governmental planning bodies. Accurate and dependable forecasting of the Indian monsoon, especially at seasonal and monthly time scales, has therefore become not only a priority for future development planning but also a complex scientific task.

Statistical forecasting methods that utilize historical time series data are often employed to predict weather parameters for a specific region and time-frame. Yet, the dynamic and variable nature of weather conditions makes consistent and precise forecasting difficult. Among all climatic variables, rainfall prediction is particularly critical due to its direct impact on agriculture, water resources, and disaster preparedness.

Reliable rainfall forecasts can play a vital role in mitigating the adverse effects of natural calamities and enhancing the preparedness of communities. Developing an accurate and timely rainfall prediction system remains a major interdisciplinary challenge, attracting the attention of researchers across various fields (Li and Lai, 2004; Yang *et al.*, 2007).

A time series is defined as a sequence of observations recorded at successive points in time, typically at uniform intervals. Time series analysis involves the study of such data to understand underlying patterns and structures, enabling the analysis of historical behaviour and the prediction of future. It finds widespread applications across diverse domains such as energy production and consumption (Deb *et al.*, 2017; Li *et al.*, 2019; Saxena *et al.*, 2019), finance and stock markets (Callot *et al.*, 2017; Singh *et al.*, 2023), health and welfare monitoring (Piccialli *et al.*, 2021; Mishra *et al.*, 2024), urban traffic flow modeling (Tedjopurnomo *et al.*, 2020; Lv *et al.*, 2014), and rainfall prediction (Mudelsee, 2019; Praveen *et al.*, 2020). Time series forecasting has emerged as a vital analytical tool for modeling historical rainfall data and predicting future rainfall patterns (Malik *et* *al.*, 2023). Blanford (1884) was the first person to issue LRF of summer monsoon rainfall over India based on the connection between the Himalayan snow cover and the seasonal monsoon rainfall in India but forecast based on this single parameter were not accurate after a few years because of failure of prediction for the drought of 1899 and 1901. The Indian Meteorological Department (IMD) has been providing LRF for southwest monsoon rainfall since 1886. However, it was the extensive and pioneering work of Walker (1923, 1925) that paved the way for the development of the first objective models. These models were based on statistical correlations between monsoon rainfall and various antecedent atmosphere, land, and ocean parameters. Since then, IMD's operational LRF system has evolved, undergoing changes in its approach. Over time, efforts have been made to improve these models by refining the selection of parameters associated with rainfall. Several models have been proposed by researchers such as Banerjee *et al.* (1978), Hastenrath (1988), Gowariker *et al.* (1989, 1991), Rajeevan (2001), Delsole and Shukla (2002), Thapliyal and Rajeevan (2003), and Sahai *et al.* (2003). However, the 2002 and 2004 droughts were unpredicted by any of these models (Gadgil *et al.*, 2005).

Many studies have been conducted by various researchers to forecast rainfall using statistical models (Chander and Wheater, 2002; Bari *et al.*, 2015; Alivia and Biswas, 2016; Reddy *et al.*, 2017), machine learning models (Ingsrisawang *et al.*, 2008; Singh and Borah, 2013), deep learning models (Poornima and Pushpalatha, 2019; Kanchan and Shardoor, 2021), and hybrid or ensemble models (Shejule and Pekkat, 2024; Jyostna *et al.*, 2025).

Numerous reviews have been conducted on the models i.e., Thapliyal and Kulshreshtha (1991), Hastenrath (1995), Kumar *et al.* (1995), Rajeevan *et al.* (2000), Ramesh and Iyengar (2017), Mohanty *et al.* (2019), and Madolli *et al.* (2022).

Among the available methods, Linear regression is one of the most fundamental and widely used statistical techniques for modeling the relationship between a dependent variable and one or more independent variables. In the context of rainfall analysis, it has been extensively applied to assess trends in precipitation over time (Ahasan *et al.*, 2010; Islam *et al.*, 2017; Sarkar *et al.*, 2023; Agrawal *et al.*, 2024), highlighting its effectiveness in rainfall forecasting.

Fourier series are a highly effective tool for modeling and predicting the seasonal and periodic components of rainfall patterns (Jou and Mirhashemi, 2023). Kronmal and Tarter (1968) introduced the Fourier series as a nonparametric technique for estimating probability density and cumulative distribution functions. Karmakar and Simonovic (2008) identified cosine-based Fourier series as optimal for defining flood characteristic distributions, outperforming kernel density estimation. Haghighatjou *et al.* (2009) confirmed the Fourier series' accuracy in analyzing annual precipitation in Iran, showing a better fit compared to seven parametric methods. Their later study (Haghighatjou *et al.* 2013) further validated its superiority over other nonparametric and parametric approaches. Zhang *et al.* (2020) highlighted the importance of temporal resolution in evaluating rainfall time series for Rainwater Harvesting systems. Additionally, Afshar and Fahmi (2012) demonstrated the Fourier series' effectiveness in forecasting monthly rainfall, showing reliable accuracy in capturing seasonal patterns and has the ability to forecast long term rainfall.

Asmat *et al.* (2021) concluded that the first two or three harmonics are most accurately captured by a unimodal pattern. Norzaida *et al.* (2016) evaluated both the original space-time Neyman–Scott rectangular pulse model and a modified version incorporating a Fourier series, they discovered that including the Fourier series enhanced the model's performance in rainfall forecasting. Jou and Mirhashemi (2023) demonstrated that a nonparametric Fourier series approach outperformed various parametric techniques—such as normal, two- and three-parameter log-normal, two-parameter gamma, Pearson and log-Pearson type III, extreme value type I (Gumbel), generalized extreme value, and generalized logistic distributions—in predicting rainfall. Probability and frequency analysis of rainfall data can help us understand the likelihood of different rainfall events occurring and their expected intensity (Bhakar *et al.*, 2008).

Trend analysis provides valuable insights into past and present climatic variations; however, future forecasting is essential for planners to formulate effective strategies in response to changing climatic conditions. In this context, a reliable model is required for long-range forecasting. To address this need, we developed an Innovative Rainfall Predictive Model (IRPM) designed to project future climatic variables. The IRPM incorporates three key components: linear, cyclic, and random.

1.2.2.1 Forecasting of Rainfall using Holt Winters Method

Over the past four decades, researchers have extensively studied rainfall forecasting and extreme hydrological events. Mathematical models have proven crucial for predicting rainfall and extreme events by analyzing historical data. Time series analysis, a key tool in this effort, examines data patterns over time to forecast future values. Accurate forecasting relies on identifying four primary data patterns: seasonal patterns, cyclic patterns, trends, and irregularities (Hanke and Wichern, 2005). Seasonal patterns, which refer to periodic fluctuations recurring at regular intervals, are particularly significant in rainfall analysis. These patterns exhibit strong correlations over specific time intervals that correspond to one seasonal cycle (Nusyirwan and Ahmad, 2020). However, traditional forecasting methods, such as moving averages and single or multiple exponential smoothing, often fail to accurately capture seasonal characteristics, necessitating more advanced techniques for improved precision (Hyndman and Athanasopoulos, 2018).

Exponential smoothing is one such advanced method widely used in time series analysis due to its simplicity and adaptability. Unlike simple moving averages, which assign equal weight to all past observations, exponential smoothing applies progressively smaller weights to older data points. This approach is more responsive to recent changes while retaining historical trends. Additionally, exponential smoothing can be customized to account for specific assumptions, such as seasonality, making it suitable for a range of applications. It has been effectively used in diverse fields, including bus passenger demand (Cyril *et al.*, 2019), the spread of COVID-19 (Djakaria and Saleh, 2021), natural gas production (Ribeiro *et al.*, 2019), electricity consumption (Karthika and Karthikeyan, 2021), rainfall prediction (Pertiwi, 2020; Sinay *et al.*, 2017), revenue forecasting (Rahman *et al.*, 2016), and wastewater treatment (Ewa and Chmielowski, 2016). Exponential smoothing is classified into three types; each suited to specific data characteristics. Single exponential smoothing is used for datasets without clear trends or seasonal patterns. It employs a single smoothing parameter, α, which ranges from 0 to 1. Smaller α values result in slower learning, requiring more historical data for accurate forecasts, while larger values prioritize recent observations, enabling faster learning. Double exponential smoothing extends the single method to accommodate data with trends. Developed by Holt (2004), it introduces an additional smoothing parameter, β, alongside α, to capture trend variations. Trends may be additive, indicating linear growth or decline, or multiplicative, reflecting exponential changes. Triple exponential smoothing is designed for time series data with seasonal variations. It incorporates seasonality through three smoothing parameters—α, β, and γ—all ranging from 0 to 1, making it ideal for modeling and forecasting complex seasonal patterns. The Holt Winters method is an advanced exponential smoothing technique that integrates the Holt and Winters approaches to time series forecasting (Kalekar, 2004). Building upon the foundation of simple exponential smoothing, this method incorporates three smoothing parameters: level (α), trend (β), and seasonality (γ), allowing for the modeling of more complex patterns (Encik and Sugiarto, 2016). It is further categorized into two models: the Additive Holt Winters (AHW) model and the Multiplicative Holt Winters (MHW) model. The additive model is best suited for data with relatively constant variance in seasonal patterns, while the multiplicative model is more effective for data with fluctuating seasonal variance (Yang *et al.*, 2017). The versatility of Holt Winters methods has been demonstrated across a wide range of applications. Cyril *et al.* (2019) applied these methods to predict public bus passenger demand using ticket sales data from the Kerala State Road Transport Corporation (KSRTC) for the period 2010–2013.

Their study revealed that the multiplicative model, which better captured proportional seasonal variations, outperformed the additive model. While damping improved trend moderation, even without it, the multiplicative model provided more accurate forecasts, making it particularly suitable for contexts with significant seasonal fluctuations.

Djakaria and Saleh (2021) explored the Holt Winters method for forecasting COVID-19 cases in Gorontalo, Indonesia, from April to October 2020. The optimal model employed smoothing parameters of $\alpha = 0.1$ for level and $\beta = \gamma = 0.5$ for trend and seasonality. This configuration yielded a Mean Absolute Percentage Error (MAPE) of 6.14, demonstrating high accuracy in predicting case totals over the study period. Similarly, Ribeiro *et al.* (2019) evaluated the Holt-Winters additive and multiplicative models for forecasting natural gas production in Brazil. Using data from 2010 to 2017, they predicted production values for 2018 and found that the multiplicative model delivered superior accuracy. The forecasts fell within the 95% confidence interval, affirming the reliability of the multiplicative formulation for estimating Brazilian natural gas production. Rahman *et al.* (2016) investigated the seasonal behaviour of time series data for monthly revenue from the Bangabandhu Multipurpose Bridge. They analyzed this data using both AHW and MHW models. The study concluded that the additive model was most effective for forecasting monthly revenue, providing reliable forecasts extending up to January 2021. Ewa and Chmielowski (2016) examined daily sewage inflow volumes into a wastewater treatment plant in Nowy Sącz from 2008 to 2014. Using the Holt-Winters seasonal method, they forecasted daily sewage inflow and evaluated the model's fit to actual data for 2014 using linear regression. Their findings confirmed the effectiveness of the AHW model for predicting sewage volumes, showcasing its utility in environmental management applications. The collective findings from these studies highlight the versatility and accuracy of Holt Winters models in addressing diverse time series forecasting challenges.

The Holt Winters method has been widely applied for rainfall forecasting across various regions, with studies comparing the performance of its additive

(AHW) and multiplicative (MHW) models. Sinay *et al.* (2017) assessed rainfall prediction in West Java using both models. Their findings indicated that the additive model, with a lower RMSE of 140.174 compared to 150.020 for the multiplicative model, was more effective in capturing the seasonal patterns in the data. Similarly, Pertiwi (2020) evaluated erratic rainfall patterns in Mataram City and concluded that the MHW model outperformed the AHW model, with superior MAPE, MAD, and MSE values, making it more suitable for forecasting rainfall over the next 12 periods. Further studies corroborate these findings. Rafian (2022) and Hutapea and Siahaan (2023) both analyzed rainfall forecasting in West Java. The AHW model, with parameters $\alpha = 0.435$, $\beta = 0$, and $\gamma = 1$, consistently achieved better accuracy, reflected in its lower RMSE of 140.17, compared to the MHW model, which had parameters $\alpha = 0.936$, $\beta = 0$, and $\gamma = 0.247$, and an RMSE of 150.020. Meanwhile, Aini *et al.* (2021) investigated rainfall forecasting in Malang City and Pasuruan, demonstrating that the MHW method was better suited for those regions, achieving improved performance metrics such as MAPE. Wiguna *et al.* (2023) utilized the Holt Winters exponential smoothing method for rainfall forecasting in Bali, while Karthika and Karthikeyan (2022) applied various Holt Winters methods to monsoon data in Tamil Nadu, India, for the period 2004–2018. Their study revealed that the MHW model, optimized with specific smoothing parameters, achieved an RMSE of 96.308% and outperformed the AHW model in capturing seasonal variability. Similar results were observed in Ranchi District, Jharkhand, where Pandit *et al.* (2023) reported the MHW method's superiority. Irwan *et al.* (2023) investigated rainfall forecasting in Makassar City for 2022. They concluded that the MHW model, with parameters $\alpha = 0.001$, $\beta = 0.15$, and $\gamma = 0.002$, was the most effective, achieving the lowest MAPE of 1.18 and MAD of 136.23. It outperformed other methods, including Brown's triple exponential smoothing and the AHW model. However, they also noted a key limitation of the MHW method: its inability to handle zero values in the data series, which can lead to forecasting inaccuracies. To overcome this limitation, Manideep and Sekar (2018) proposed an enhanced additive Holt Winters method capable of effectively managing zero values. Their improvement underscored the importance of selecting the appropriate model based on regional data characteristics. The AHW model is generally more accurate for regions with linear seasonal patterns and consistent variations, while the MHW model is better suited for areas where seasonal effects scale proportionally with data levels, capturing complex seasonal variations more effectively (Yang *et al.*, 2017). Consequently, the choice between AHW and MHW depends on a comprehensive understanding of the seasonal behaviour of the target region. Holt Winters method is valuable for forecasting rainfall, as they often outperform ARIMA and SARIMA models when applied to data with strong, consistent seasonal patterns (Brito *et al.*, 2021; Gowri *et al.*, 2022).

Based on our review, the Holt Winters method has shown considerable success in forecasting rainfall across different regions. Accordingly, within this thesis we have employed both the AHW and MHW methods in the study area. However, the performance of these models varied, with one often outperforming the other depending on the region. To address this limitation and identify a model that performs consistently well across regions, we developed a new Modified Holt Winters method (MOHW) and further extended it to a Multivariate Holt Winters method for incorporating additional meteorological variables.

1.3 Objective of the Proposed Research Work

The main aim of the proposed research work is to develop a LRF model on chaotic time series and thereafter to apply the model to study the rainfall pattern of different regions in India. The objectives of the proposed research work are to study:

- To carry out an extensive statistical analysis of the rainfall data that will be collected from different rainfall regions of India.
- To develop an appropriate mathematical model on chaotic time series for Long Range Forecasting taking into consideration the three components of

linear trend, cyclic trend and random events.

- To develop a LRF System of time series inbuilt with the proposed model.
- To study on the rainfall patterns in different regions of India.

1.4 Significance of the Study

Multiple studies have shown that climate change significantly affects hydro climatic variables, including rainfall, temperature, and runoff. Although climate change is a global phenomenon, its impacts on rainfall can vary considerably between regions (Madhusoodhanan *et al.*, 2016). Numerous researchers have applied statistical and mathematical models to forecast rainfall, highlighting its importance in tropical countries like India (Yeditha *et al.*, 2023). It benefits agriculture by aiding farmers in optimal crop management and water resource utilization. Governments and water management authorities use rainfall information for efficient water resource allocation and disaster preparedness. Meteorologists and emergency services depend on rainfall predictions to prepare for extreme weather events, while urban planners use this information to mitigate urban flooding. Additionally, hydroelectric power generation, tourism, ecosystem research, transportation, and insurance industries all find value in accurate rainfall forecasting. Building on these insights, this study adopts an innovative approach to rainfall forecasting. It focuses on several key areas:

- The Long Range Forecast (LRF) model integrates linear, cyclic, and random components from chaotic rainfall time series, reducing forecast error.
- The LRF model can be adapted for any region in India, enabling authorities to make more accurate, data-driven decisions and better respond to weather-related challenges.
- A Modified Holt Winters method (MOHW) for monthly rainfall outperforms the traditional Holt Winters method, offering improved predictions

that benefit agriculture, water management, and disaster preparedness sectors.

- More accurate detection of shifts in rainfall trends and improved rainfall forecasting are crucial for water resource managers and disaster response teams. Precise forecasts allow them to anticipate floods or droughts ahead of time, stay alert to emerging risks, and take proactive measures to mitigate impacts like crop loss, infrastructure damage, and community disruption.
- Including multiple meteorological variables (temperature and humidity) with a Multivariate Holt Winters method strengthens forecast reliability by capturing real-world climatic interactions.
- Analyzing long term trends in rainfall helps detect and understand local shifts in precipitation patterns, which is essential for planning agricultural and water resources management strategies.

Chapter 2

Methodology

2.1 Introduction

In this chapter, we present the methodological framework guiding our study. The proposed approach incorporates a quantitative, time-series forecasting framework for modeling monthly rainfall data using Additive Holt Winters method (AHW) and Multiplicative Holt Winters method (MHW). Additionally, we intoduced a three methods: the Innovative Rainfall Predictive Method (IRPM), the Modified Holt Winters method (MOHW), and the Multivariate Holt Winters method. To assess long term changes in rainfall patterns, we apply non-parametric trend analysis, specifically the Mann–Kendall test, Sen's slope estimator and Innovative Trend Anaylsis (ITA). Furthermore, we described the performance metrices used to evaluate these models and discuss the strategy for model validation.

2.2 Innovative Rainfall Predictive Method (IRPM)

Rainfall is a critical meteorological parameter that influences agriculture, water resource management, and disaster preparedness. Accurate long term rainfall forecasting is therefore essential for planning and mitigation (Salas, 1993; Wilks, 2011). Rainfall exhibits both predictable patterns and stochastic variations, which can be captured using time series models (Box *et al.*, 2015). A time series consists of data which are arranged chronologically. It establishes a relationship between two variables in which one of the variable is independent variable i.e. the time and other variable is the dependent variable whose value changes with regard to time variable. Several time series models have been successfully applied to rainfall prediction across different regions (Chander and Wheater, 2002; Bari *et al.*, 2015; Alivia and Biswas, 2016; Reddy *et al.*, 2017). Due to the success of this, Innovative Rainfall Predictive Method (IRPM) was developed to predict rainfall by integrating the three components of a time series: trend, cyclic, and random components. These components are combined into a single equation, and adjust using a corrector factor. The overall methodology is illustrated in Figure 2.1.

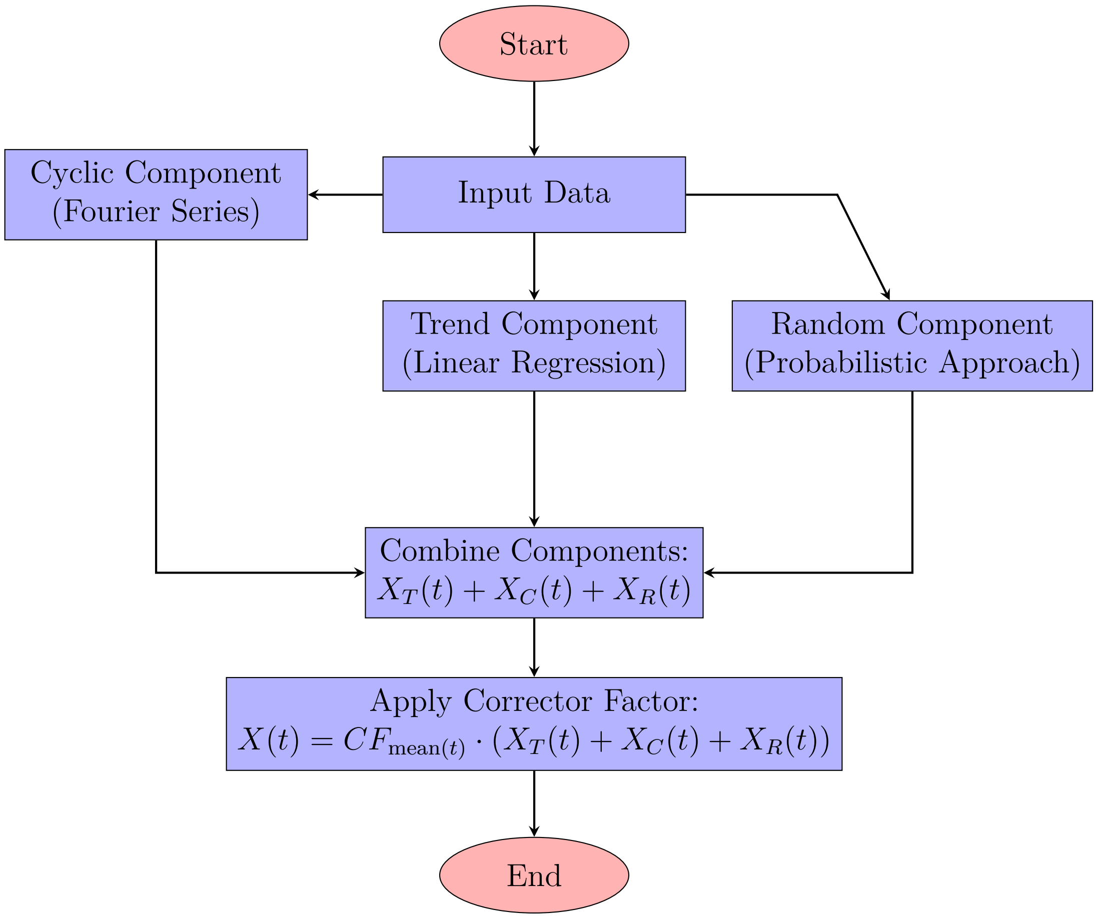

Figure 2.1: Methodology Flowchart of the Innovative Rainfall Predictive Method (IRPM).

2.2.1 Mathematical Formulation of IRPM

The predicted rainfall at time t is expressed as:

$$X(t) = \mathrm{CF}_{\mathrm{mean}}(t) \left(X_T(t) + X_C(t) + X_R(t) \right), \tag{2.1}$$

where:

- $X_T(t)$ is a trend component, which is estimated through simple linear regression, reflecting whether there is an overall increase or decrease in rainfall over the period considered.
- $X_C(t)$ is a cyclic component, which is model using Fourier series to capture the significant frequencies of periodic patterns in the data.
- $X_R(t)$ is a random component, It has been appropriately derived by combining the factors of probability with the rainfall and the expected amount of rainfall in a particular month, for stochastic variations in rainfall.
- $CF_{mean(t)}$ is the mean of the corrector factor.

The corrector factor is calculated as:

$$CF(t) = \frac{X'(t)}{X_T(t) + X_C(t) + X_R(t)}, \tag{2.2}$$

where $X'(t)$ is the observed rainfall at time t, and its mean over N years:

$$CF_{\mathrm{mean}}(t) = \frac{1}{N} \sum_{i=1}^{N} CF(t_i). \tag{2.3}$$

2.2.1.1 Trend Component

Linear regression is a statistical method used to model the relationship between a dependent variable and one or more independent variables. It assumes a linear relationship between them and aims to find the best-fitting line that minimizes the difference between actual and predicted values. The trend component $X_T(t)$ represents the long term increase or decrease in rainfall and is estimated using linear regression:

$$y = a + bx, \tag{2.4}$$

where y is the dependent variable (rainfall), x is the independent variable (time), a is the intercept, and b is the slope. The slope and intercept are computed using the least squares method.

$$b = \frac{n\sum x_i y_i - \left(\sum x_i\right)\left(\sum y_i\right)}{n\sum x_i^2 - \left(\sum x_i\right)^2}, \tag{2.5}$$

$$a = \frac{\sum y_i - b\sum x_i}{n}. \tag{2.6}$$

2.2.1.2 Cyclic Component

Fourier series are widely used in time series modeling and forecasting to capture cyclic patterns by decomposing data into sums of sine and cosine functions (Hippenstiel, 2017). The technique has several advantages, including its ability to capture and model the underlying periodicity of time-series data and its versatility to handle nonlinear and nonstationary time-series data (Danbatta *et al.*, 2025). A Fourier series can be used to can be used to forecast future values (Wang *et al.*, 2022). Asmat *et al.* (2021) found that the first two or three harmonics are most accurately captured by a unimodal pattern. The cyclic component $X_C(t)$ captures recurring periodic patterns in rainfall. It is modeled using a Fourier series (Talbot *et al.*, 2020; Wilson *et al.*, 2018):

$$X_C(t) = A_0 + \sum_{n=1}^{\infty}\left[A_n \cos\left(\frac{\pi n t}{T}\right) + B_n \sin\left(\frac{\pi n t}{T}\right)\right], \quad \text{for } 0 < t < 2T, \tag{2.7}$$

The coefficients A_0, A_n and B_n are estimated as:

$$A_0 = \frac{1}{2T}\int_0^{2T} X'(t)\,dt, \tag{2.8}$$

$$A_n = \frac{1}{T}\int_0^{2T} X'(t)\,\cos\left(\frac{\pi n t}{T}\right)\,dt, \tag{2.9}$$

$$B_n = \frac{1}{T}\int_0^{2T} X'(t)\,\sin\left(\frac{\pi n t}{T}\right)\,dt. \tag{2.10}$$

2.2.1.3 Random Component

The random component $X_R(t)$ captures stochastic variations in rainfall. Let X_{ij} represent rainfall for the i^{th} year and j^{th} month in a data matrix:

$$\langle X_{(i,j)}\rangle_{NM} = \begin{bmatrix} X_{11} & X_{12} & X_{13} & \cdots & X_{1M} \\ X_{21} & X_{22} & X_{23} & \cdots & X_{2M} \\ X_{31} & X_{32} & X_{33} & \cdots & X_{3M} \\ \vdots & \vdots & \vdots & \ddots & \vdots \\ X_{N1} & X_{N2} & X_{N3} & \cdots & X_{NM} \end{bmatrix}. \tag{2.11}$$

Now, let us proceed to use the concepts of probability theory to identify the random experiment or trial, event, random variable, sample space and probability etc. In fact, we do not see here any experiment or trial as the rainfall occurrence in particular month of certain year is a natural phenomenon. There may or may not be rainfall in the month. Further, if rainfall occurs, it may be any measure. Hence, we may assume the event of rainfall in a certain range of measure is an event of random phenomenon. Thus, if the maximum value of the observed rainfall in the entire period of observation considered for forecast falls within the interval $(n-1)I \leq X_n < nI$ where I is the length of interval considered for each event of the random phenomenon and each column of the rainfall observation may be divided into n number of events, $E_1, E_2, E_3, ..., E_n$ as follows:

$$E_1 = 0 \leq X_1 < I,$$
$$E_2 = I \leq X_2 < 2I,$$
$$E_3 = 2I \leq X_3 < 3I,$$
$$\vdots$$
$$E_n = (n-1)I \leq X_n < nI.$$

Further let n_k be the number of observations fall within the interval $E_k = (k-1)I \leq X_k < kI$, and the total number of observation for each month is N.Therefore, the probability for the event E_k to occur, i.e., the rainfall X_k to fall within the interval $(k-1)I \leq X_k < kI$ in the random phenomenon is

$$P(X_k) = \frac{n_k}{N} = P_k. \tag{2.12}$$

This represents the likelihood that the rainfall in a particular month lies within the specified interval, based on the observed data. As we know the total rainfall prediction observed during a certain month for N years is discrete random variables, the expectation of the random variable X is defined to be

$$E(X) = \sum_{k=1}^{n} X_k' \, P(X_k), \tag{2.13}$$

where X_k' is the midpoint of the interval. This provides the predicted stochastic contribution for the $(N+1)^{\text{th}}$ year.

2.3 Exponential Smoothing

Exponential smoothing is a widely used time series forecasting method that applies exponentially decreasing weights to past observations. It is useful for forecasting data with or without trends and seasonality. Exponential Smoothing was introduced by Brown (1956) and has been widely used in forecasting applications due to its simplicity and effectiveness. Unlike simple moving averages, where each past observation is given equal weight, exponential smoothing places progressively less importance on older data points. The core idea is to give more weight to recent observations while gradually reducing the influence of older data.

The simplest form of exponential smoothing, known as simple exponential smoothing, is used when there are no clear trends or seasonal patterns (Yorucu, 2003). Single exponential smoothing utilizes a single parameter, α, which ranges from 0 to 1, which controls how much weight will be given to its most recent data (Fahrudin *et al.*, 2021).The simple exponential smoothing is given by (Brown and Meyer, 1961):

$$L_t = \alpha Y_t + (1 - \alpha) L_{t-1}, \tag{2.14}$$

$$F_{t+h} = L_t, \tag{2.15}$$

where L_t is the level components (or smoothed value), Y_t is the actual value and α is the smoothing parameters for level.

In case of data with no trend, simple exponential smoothing yields a good results, but it fails in case of existence of trend.

For time series data that exhibit a trend, Holt (1957) extended simple exponential smoothing to handle data with trends, also known as double exponential smoothing. This method uses an additional smoothing parameter, β, along with α to account for changes in trend. The equation for double exponential smoothing method are as follows:

$$L_t = \alpha \left(Y_t\right) + (1 - \alpha) \left(L_{t-1} + B_{t-1}\right), \tag{2.16}$$

$$B_t = \beta \left(L_t - L_{t-1}\right) + (1 - \beta) B_{t-1}, \tag{2.17}$$

$$F_{t+h} = \left(L_t + B_t\, h\right), \tag{2.18}$$

where L_t is the level components, B_t is the trend component, Y_t refers to the actual data for time period t, and $F_{(t+h)}$ is the forecast for the period ahead (h). Then, α and β are the smoothing parameters for the level and trend, respectively, which lies in the interval [0,1].

When the data exhibit only a linear trend, double exponential smoothing yields good results but it fails to capture seasonality in case of existence of linear and seasonality. In order to avoid this limitation, and also to involve both trend and seasonality, Winters (1960) extended Holt method by incorporating seasonality, also known as triple exponential smoothing. This approach relies on three smoothing parameters incorporates seasonality and relies on three smoothing parameters: α, β, and γ, each of which ranges between 0 and 1.

2.4 Holt Winters Method

The Holt Winters method is an exponential smoothing method combining the Holt and Winters methods (Kalekar, 2004). The Holt Winters method employs a forecasting equation alongside three smoothing equations: one for the level (L_t), one for the trend (B_t), and one for the seasonal components (S_t). These components are adjusted using smoothing parameters α, β,and γ, which controls how much weight is given to recent observations versus past data. The smoothing parameter α is used for the level, β for the trend, and γ for the seasonal component. The parameter m represents the frequency of the seasonal cycle, indicating the number of seasons within a year. For instance, for quarterly data, m is taken as 4, while for monthly data, m is taken as 12 (Hyndman and Athanasopoulos, 2018).

The Holt Winters method features two variations based on the type of seasonal component: additive and multiplicative. The additive method is appropriate when seasonal variations are consistent over time. In this approach, the seasonal component is given in absolute terms, and the series is adjusted for seasonality by subtracting this component. This adjustment ensures that the seasonal component averages close to zero each year. On the other hand, the multiplicative method is used when seasonal variations are proportional to the level of the series. In this approach, the seasonal component is represented as percentages, and the series is adjusted by dividing it by this seasonal factor, leading to the seasonal component summing to approximately the number of seasons, m (Hyndman and Athanasopoulos, 2018). Holt Winters method has been widely used in various time series applications, including bus passenger demand forecasting (Cyril *et al.*, 2019), COVID-19 spread analysis (Djakaria and Saleh, 2021), natural gas production (Ribeiro *et al.*, 2019), electricity usage (Karthika and Karthikeyan, 2021), rainfall prediction (Irwan *et al.*, 2023); Pertiwi, 2020; Sinay *et al.*, 2017), revenue forecasting (Rahman *et al.*, 2016), and wastewater treatment processes (Ewa and Chmielowski, 2016).

2.4.1 Additive Holt Winters Method (AHW)

The additive model assumes that the seasonal effects are constant and can be represented as fixed values added to the level of the series. The AHW method employs three key components: level, trend, and seasonal effects. The level represents the baseline value of the series, the trend indicates the underlying direction of the data over time, and the seasonal component captures regular fluctuations that repeat at specific intervals. By adjusting these components with smoothing parameters (α for level, β for trend, and γ for seasonality, which lies in the interval [0,1]), the model effectively balances the influence of recent observations with historical data, enabling more accurate forecasts. This method is particularly well-suited for datasets with a clear and stable seasonal pattern, such as monthly sales figures, monthly rainfall, or temperature readings. The additive approach facilitates straightforward interpretation and application, making it a preferred choice for practitioners in various fields, including finance, meteorology, and supply chain management. By effectively modeling seasonality and trends, the Additive Holt Winters method enhances decision-making processes by providing reliable predictions for future values. The equation are as follows (Holt, 1957; Winters, 1960):

$$L_t = \alpha\big(Y_t - S_{t-m}\big) + (1-\alpha)\big(L_{t-1} + B_{t-1}\big), \tag{2.19}$$
$$B_t = \beta\big(L_t - L_{t-1}\big) + (1-\beta)B_{t-1}, \tag{2.20}$$
$$S_t = \gamma\big(Y_t - L_t\big) + (1-\gamma)S_{t-m}, \tag{2.21}$$
$$F_{t+h} = \big(L_t + B_t h\big) + S_{t-m+h}, \tag{2.22}$$

where m is the seasonality length, L_t is the level components, B_t is the trend component, S_t is the seasonal component, Y_t refers to the real data for time period t, and $F_{(t+h)}$ is the forecast for the period ahead (h). Then, α, β, and γ are the smoothing parameters for the level, trend, and seasonality, respectively, which lies in the interval [0,1]. For initializing the level (L_0), trend (B_0), and seasonality ($S_{01}, S_{02}, S_{03}, \ldots\ldots, S_{0m}$), we adopt the following relations:

$$L_0 = \frac{Y_1 + Y_2 + \cdots + Y_m}{m}, \tag{2.23}$$
$$B_0 = \frac{Y_{m+1} - Y_1}{m}, \tag{2.24}$$
$$S_{01} = Y_1 - L_0, \quad S_{02} = Y_2 - L_0, \quad \ldots, \quad S_{0m} = Y_m - L_0. \tag{2.25}$$

2.4.2 Multiplicative Holt Winters Method (MHW)

The Multiplicative Holt Winters method is particularly effective for datasets where seasonal fluctuations change in magnitude as the overall level of the series increases or decreases. In contrast to AHW method, the Multiplicative Holt Winters method models seasonal variations as percentage changes rather than fixed amounts. This characteristic makes it particularly suitable for data exhibiting exponential growth or decline, such as sales figures, economic indicators, or environmental measurements like rainfall and temperature. The method incorporates three primary components: level, trend, and seasonal effects. The level represents the baseline value, the trend captures the direction of the data over time, and the seasonal component reflects the variations that occur at specific intervals. The model adjusts these components using smoothing parameters (α for level, β for trend, and γ for seasonality, in the interval of [0,1]), allowing it to effectively weigh recent observations against historical data. Equation for level (L_t), trend (B_t), seasonal (S_t) and forecast (F_t) components are as follows (Holt, 1957; Winters, 1960):

$$L_t = \alpha \left(\frac{Y_t}{S_{t-m}} \right) + (1-\alpha)\left(L_{t-1} + B_{t-1}\right), \tag{2.26}$$

$$B_t = \beta \left(L_t - L_{t-1}\right) + (1-\beta)B_{t-1}, \tag{2.27}$$

$$S_t = \gamma \left(\frac{Y_t}{L_t} \right) + (1-\gamma)S_{t-m}, \tag{2.28}$$

$$F_{t+h} = \left(L_t + B_t\, h\right)\, S_{t-m+h}. \tag{2.29}$$

For initializing the level (L_0), it is same as Equation (2.23), and for trend (B_0), it is the same as Equation (2.24), and seasonality ($S_{01}, S_{02}, S_{03}, \ldots\ldots, S_{0m}$) obtained from the relation as given by

$$S_{01} = \frac{Y_1}{L_0}, \quad S_{02} = \frac{Y_2}{L_0}, \quad \ldots, \quad S_{0m} = \frac{Y_m}{L_0}. \tag{2.30}$$

2.4.3 Modified Holt Winter Method (MOHW)

In certain cases, the AHW method outperforms the MHW method in forecasting rainfall as reported by Rafian (2022), Hutapea and Siahaan (2023) , while in other situations, MHW provides better results than AHW as observed in the studies of Aini *et al.* (2021), Irwan *et al.* (2023), Pertiwi (2020). A notable limitation of MHW is its inability to handle zero values in the data (Manideep and Sekar, 2018). To address this issue and to develop a method that both accommodates zeros and improves forecasting over traditional approaches, we introduced the Modified Holt Winters method (MOHW). In the MOHM method, the forecasting process involves updating key components—level, trend, and seasonality effects, as shown below:

$$L_t = \alpha\big(Y_t - S_{t-m}\big) + (1-\alpha)\big(L_{t-1} - B_{t-1}\big), \tag{2.31}$$

$$B_t = \beta\left(\frac{L_t - L_{t-1}}{S_{t-m} + B_{t-1}}\right) + (1-\beta)\big(B_{t-1} + S_{t-m} + L_{t-1}\big), \tag{2.32}$$

$$S_t = \gamma\big(Y_t - L_t\big) + (1-\gamma)\big(S_{t-m} + B_t\big), \tag{2.33}$$

$$F_{t+h} = \big(L_t + B_t\, h\big) + S_{t-m+h}. \tag{2.34}$$

The three initial values are the same as that of the AHW method.

In Equation (2.31), the estimate of the level at time t is adjusted to account for the trend from the previous period by subtracting the previous period's trend estimate ($B_{(t-1)}$), to the last smoothed level value, $L_{(t-1)}$. This adjustment corrects for lag and brings L_t closer to the current data value. The smoothing parameter dictates how the estimate of the level is influenced by recent observations and the most recent forecast value, with α weighing the current observation and $(\alpha - 1)$ weighting the forecasted value for smoothing purposes. Since trends are present in the time series, the next value is expected to deviate from the current one. In essence, we modified the trend component (B_t), by taking a weighted average of two terms: the trend estimated from level changes, which is $(L_t - L_{(t-1)})/(S_{(t-m)} + B_{(t-1)})$, representing the trend based on the change in the level component relative to the seasonal component and previous trend estimate; and the previous trend adjusted by seasonal and level components, given by $(B_{(t-1)} + S_{(t-m)} + L_{(t-1)})$. The parameter β controls the weighting between these two terms, balancing the responsiveness to recent changes with stability derived from historical data. We improved the seasonal component (S_t) by adding the trend component (B_t) to the seasonal effect from the previous cycle ($S_{(t-m)}$).

2.5 Multivariate Holt Winters Method

According to Pfeffermann and Allon (1989), just as the Vector Autoregressive (VAR) model is designed to handle multiple variables in time series analysis, multiple exponential smoothing techniques can also be applied to account for multivariate dependencies. Holt Winters method is a univariate method, it relies only in one variable. Building on this, Since rainfall is influenced by many other factors, we extend both the AHW and MOHW to a multivariate framework by incorporating additional climatic variables. Furthermore, the MHW method was excluded from consideration because it cannot handle zero values, which are common in many meteorological datasets.

2.5.1 Multivariate Additive Holt Winters Method (MAHW)

Traditionally, the AHW method is designed for univariate time series data, where a single set of smoothing parameters is used for level, trend, and seasonality. However, to extend this approach for multivariate time series, we introduce the Multivariate Additive Holt Winters method (MAHW) method. In this extension, instead of using scalar smoothing parameters, we use $k \times k$ matrices for each component, where k represents the number of variables in the model. This allows each variable to influence the level, trend, and seasonal components dynamically, capturing the interdependencies between variables. In the MAHW, the update equations for level, trend, and seasonality are modified to accommodate multiple variables, ensuring that each component is updated based on the relationships among all variables. This enhancement improves forecasting accuracy by incorporating additional climatic factors rather than relying solely on rainfall data.

The equation are given by,

$$L_{t,i} = A(Y_{t,i} - S_{t-m,i}) + (I - A)(L_{t-1,i} + B_{t-1,i}), \tag{2.35}$$

$$B_{t,i} = C(L_{t,i} - L_{t-1,i}) + (I - C)B_{t-1,i}, \tag{2.36}$$

$$S_{t,i} = G(Y_{t,i} - L_{t,i}) + (I - G)S_{t-m,i}, \tag{2.37}$$

$$F_{t+h,i} = (L_{t,i} + B_{t,i}h) + S_{t-m+h,i}, \tag{2.38}$$

where I is the identity matrix, $L_{(t,i)}$ is the level component for variable i at time t, $B_{(t,i)}$ is the trend component for variable i at time t, $S_{(t,i)}$ is the seasonal component for variable i at time t, $Y_{(t,i)}$ represents the observed data for variable i at time period t, and $F_{(t+h,i)}$ is the forecast value for variable i at time $t+h$, where, $i = 1, 2, ...k$. The smoothing parameters for level (A), trend (C), seasonality (G) are as follows:

$$A = \begin{bmatrix} \alpha_{11} & \alpha_{12} & \cdots & \alpha_{1k} \\ \alpha_{21} & \alpha_{22} & \cdots & \alpha_{2k} \\ \vdots & \vdots & \ddots & \vdots \\ \alpha_{k1} & \alpha_{k2} & \cdots & \alpha_{kk} \end{bmatrix}, \tag{2.39}$$

$$C = \begin{bmatrix} \beta_{11} & \beta_{12} & \cdots & \beta_{1k} \\ \beta_{21} & \beta_{22} & \cdots & \beta_{2k} \\ \vdots & \vdots & \ddots & \vdots \\ \beta_{k1} & \beta_{k2} & \cdots & \beta_{kk} \end{bmatrix}, \tag{2.40}$$

$$G = \begin{bmatrix} \gamma_{11} & \gamma_{12} & \cdots & \gamma_{1k} \\ \gamma_{21} & \gamma_{22} & \cdots & \gamma_{2k} \\ \vdots & \vdots & \ddots & \vdots \\ \gamma_{k1} & \gamma_{k2} & \cdots & \gamma_{kk} \end{bmatrix}. \tag{2.41}$$

The three initial values for level, trend, and seasonality are the same as those in Equations (2.23), (2.24), and (2.25) respectively.

2.5.2 Multivariate Modified Holt Winters Method (MMOHW)

Since rainfall is influenced by various meteorological factors, we aim to extend the Modified Holt Winters method (MOHW) form a univariate to a multivariate framework. By incorporating multiple variables, such as temperature and humidity, the model can better capture dependencies and interactions, making the forecasting process more reliable and accurate. In this multivariate adaptation, each component—level, trend, and seasonality—is updated for each variable, with smoothing parameters represented as $k \times k$ matrices to account for inter-variable relationships. The modified equations for the Multivariate Modified Holt Winters method (MMOHW) are detailed below:

$$L_{t,i} = A\left(Y_{t,i} - S_{t-m,i}\right) + (I - A)\left(L_{t-1,i} - B_{t-1,i}\right), \tag{2.42}$$

$$B_{t,i} = C\left(\frac{L_{t,i} - L_{t-1,i}}{S_{t-m,i} + B_{t-1,i}}\right) + (I - C)\left(B_{t-1,i} + S_{t-m,i} + L_{t-1,i}\right), \tag{2.43}$$

$$S_{t,i} = G\left(Y_{t,i} - L_{t,i}\right) + (I - G)\left(S_{t-m,i} + B_{t,i}\right), \tag{2.44}$$

$$F_{t+h,i} = \left(L_{t,i} + B_{t,i}h\right) + S_{t-m+h,i}. \tag{2.45}$$

The smoothing matrices used in MMOHW remain the same as those defined in Equations (2.39), (2.40), and (2.41). Similarly, the initial values for level, trend, and seasonality are adopted as given in Equations (2.23), (2.24), and (2.25).

2.6 Trend Analysis

Trend analysis is a statistical method used to predict the future behaviour of a variable by examining historical data. It aims to forecast future patterns by identifying and analyzing past trends. In this study, The Mann-Kendall (MK) test was applied to detect changes in rainfall trends over time at a 95% confidence level, while the Sen's slope test was used to quantify the magnitude of these trends. Additionally, Innovative Trend Analysis (ITA) for graphical approach.

2.6.1 Mann-Kendall (MK) Test

The Mann-Kendall (MK) test, originally introduced by Mann (1945) and later refined by Kendall (1975), is a non-parametric method designed to identify trends in time series data. This test evaluates monotonic (consistently increasing or decreasing) trends in climatic data over time. The MK test has been widely applied to determine the presence of significant or non-significant trends in hydrological and climatic variables, such as precipitation, rainfall, temperature, and streamflow, particularly in the context of climate change. It has been effectively utilized in numerous studies, including those by Jain *et al.* (2013), Abeysingha *et al.* (2017), Mondal *et al.* (2018), Khaniya *et al.* (2019), and Monir *et al.* (2023). The Mann-Kendall test statistic (S) is calculated using the following equation (Kendall, 1975):

$$S = \sum_{i=1}^{n-1} \sum_{j=i+1}^{n} \operatorname{sgn}(x_j - x_i), \tag{2.46}$$

here, x_j and x_i represent the time series values, and n denotes the total number of data points in the series. The sgn function is further defined as:

$$\operatorname{sgn}(x_j - x_i) = \begin{cases} +1, & \text{if } x_j - x_i > 0 \\ 0, & \text{if } x_j - x_i = 0 \\ -1, & \text{if } x_j - x_i < 0 \end{cases} . \tag{2.47}$$

When the sample size n is greater than 8, the test statistic S approximately follows a normal distribution. The mean $E(S)$ and variance $Var(S)$ are calculated as follows:

$$E(S) = 0, \tag{2.48}$$

$$\mathrm{Var}(S) = \frac{n(n-1)(2n+5) - \sum t_p(t_p-1)(2t_p+5)}{18}, \tag{2.49}$$

where, t_p is the number of ties of length p.

The Z value is utilized to determine whether the time series data exhibits a significant trend or not. It is calculated using Equation (2.32).

$$Z = \begin{cases} \frac{S+1}{\sqrt{\mathrm{Var}(S)}}, & \text{if } S < 0 \\ 0, & \text{if } S = 0 \\ \frac{S-1}{\sqrt{\mathrm{Var}(S)}}, & \text{if } S > 0 \end{cases} . \tag{2.50}$$

Positive Z values indicate an upward or increasing trend, while negative Z values signify a downward or decreasing trend (Anand *et al.*, 2020). For this study, the significance level was set at a 95% confidence level.

2.6.2 Sen's Slope Test

The Sen's Method (Sen, 1968) is used to estimate the magnitude of a trend, assuming a linear pattern in the time series. It has been extensively applied to analyze trends in hydro-meteorological data (Jayawardene *et al.*, 2015, Isabella *et al.*, 2020, and Kumar *et al.*, 2023). This method calculates both the slope and intercept using the Sen's Slope Estimator test. Initially, linear slopes are determined for all possible data pairs using the following equation (Sen, 1968).

$$T_i = \frac{x_j - x_k}{j-k}, \quad \text{for } i = 1, 2, \ldots, n \text{ and } j > k, \tag{2.51}$$

here, T_i represents the slope, while x_j and x_k are the data values at times j and k, respectively. The median of the n slope values T_i is referred to as Sen's slope estimator (Q_i) and is calculated as:

$$Q_i = \begin{cases} T_{\frac{n+1}{2}}, & \text{if } n \text{ is odd} \\ \frac{1}{2}\left(T_{\frac{n}{2}} + T_{\frac{n+2}{2}}\right), & \text{if } n \text{ is even} \end{cases}. \tag{2.52}$$

A positive Q_i value indicates an upward or increasing trend, while a negative Q_i value signifies a downward or decreasing trend.

2.6.3 Innovative Trend Analysis

The Innovative Trend Analysis (ITA) method, introduced by Sen (2012), is a graphical approach used to detect trends in time series data without relying on statistical assumptions such as normality or independence. Unlike traditional methods like the Mann-Kendall test and Sen's slope estimator, ITA allows for direct visualization of trends. The method involves dividing the time series into two equal halves, where the first half represents the earlier period and the second half represents the later period, each half is arranged in ascending order before plotting. A scatter plot is then created, with values from the first half plotted on the x-axis and values from the second half on the y-axis, along with a 45-degree reference line representing a no-trend scenario. Data points positioned above the 1:1 reference line indicate an increasing trend, while those below the line signify a decreasing trend. Points that lie on the reference line suggest no significant trend (Caloiero *et al.*, 2018). To determine statistical significance, lower and upper trend limits are calculated at a 95% confidence level. If the slope falls within these limits, the trend is classified as insignificant; if it exceeds the upper limit, it indicates an increasing trend, whereas falling below the lower limit confirms a decreasing trend. The slope of ITA (Sen, 2012) is calculated by:

$$D = \frac{2(\bar{Y}_2 - \bar{Y}_1)}{n}, \tag{2.53}$$

where, Y_1 represents the arithmetic mean of the first subseries, and Y_2 denotes the arithmetic mean of the second sub-series.

2.7 Optimization Method

Optimization plays a crucial role in solving problems across various sectors. In many cases, complex problems require immediate solutions, making efficient search strategies essential. Artificial Intelligence (AI) offers numerous search algorithms, each with distinct advantages and limitations. Therefore, it is important to develop methods that maximize performance while minimizing resource use. A common challenge in problem-solving is the speed required to identify the optimal solution. An effective algorithm is one that efficiently utilizes both time and memory, allowing for a thorough evaluation of its efficiency and computational complexity (Subaeki, 2017). In practical applications, optimization becomes indispensable because identifying the best solution can be time-consuming. Although search processes often yield results close to the maximum value, the inherent randomness in many algorithms may cause previous solutions to degrade, leading to increased processing time. To determine the optimal smoothing parameters for our model, we employ both a brute-force approach and Bayesian optimization, ensuring that the model achieves the best possible performance efficiently.

2.7.1 Brute-Force Approach

The Brute-Force algorithm is a method that searches for solutions by systematically testing all possible options to identify the best outcome. Fundamentally, it compares patterns or text character by character, shifting the search pattern one position at a time and repeating the comparison until a match is found or the end of the text is reached (Mohammad *et al.*, 2006). As illustrated in Figure 2.2, brute force employs a straightforward, direct approach to problem-solving (Ndaumanu, 2020). Typically, the algorithm explores solutions based on the problem definition and the relevant conceptual framework (Nainggolan *et al.*, 2021). Brute-force algorithms are valued for their simplicity, clarity, and directness in finding solutions (Santoso *et al.*, 2006).

In the context of our study, the brute-force approach was applied to identify the most suitable smoothing parameters, ensuring that the model achieves optimal forecasting performance.

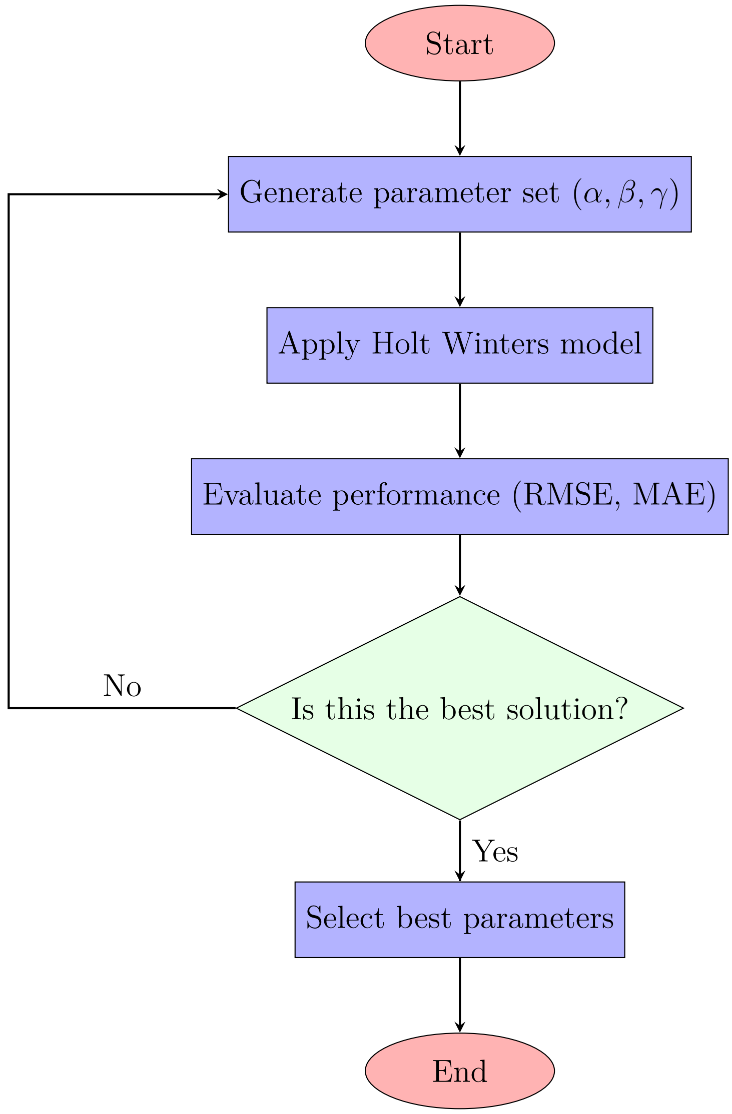

Figure 2.2: Flowchart of Brute-Force approach for optimizing Holt-Winters parameters.

2.7.2 Bayesian Optimization

The selection of optimal smoothing parameters represents a fundamental challenge in statistical modeling and time series forecasting, where the balance between model flexibility and overfitting significantly impacts predictive performance (Bergmeir, and Benítez, 2012). Traditional approaches to parameter optimization often rely on grid search or random search methods, which can be computationally intensive and inefficient, particularly when dealing with expensive to-evaluate objective functions (Bergstra and Bengio, 2012). In the univariate Holt Winters method, the smoothing parameters are determined using a brute-force approach, where different values are tested to minimize the error. However, when extending the method to a multivariate setting, the smoothing parameters are represented as matrices instead of scalar values. This significantly increases computational complexity, making the brute-force approach impractical due to the exponential growth in the number of possible parameter combinations. To address this challenge, we adopt a Bayesian optimization approach for selecting the optimal smoothing parameters efficiently.

Bayesian optimization is a probabilistic model-based method that intelligently determines which set of parameters should be evaluated next, rather than exhaustively searching through all possibilities (Sameen *et al.*, 2020). This approach is particularly useful in high-dimensional parameter spaces, as it reduces the number of iterations needed to find the best parameters while maintaining accuracy. The theoretical foundation of Bayesian optimization rests on two key components: a probabilistic surrogate model that captures the underlying function behavior, and an acquisition function that balances exploration of uncertain regions with exploitation of promising areas (Brochu *et al.*, 2010). The effectiveness of Bayesian optimization approach arises from its ability to build a surrogate model of the objective function using observed data points and to employ acquisition functions to guide the search toward promising regions of the parameter space. The two key components of Bayesian Optimization are therefore the surrogate model, which captures the behavior of the objective function, and the acquisition function, which balances exploration of uncertain regions with exploitation of high-performing areas.

In the present study, Gaussian Processes were employed as the surrogate model due to their mathematical tractability, ability to provide uncertainty estimates, and flexibility in modeling complex functional behaviors through appropriate kernel selection (Williams and Rasmussen, 2006). Among various kernel functions, The radial basis function kernel was selected for its smoothness and universal approximation properties (Micchelli, 2006). Among various acquisition functions, Expected Improvement (EI) was adopted to guide parameter selection. EI selects the next parameter set by estimating the potential performance gain over the current best result (Jones, 1998).

In the context of smoothing parameter selection, The Bayesian Optimization procedure was implemented iteratively as follows. First, the search space for α, β, and γ was defined as 3×3 matrices, resulting in a total of 27 parameters, each constrained within [0,1]. An initial set of parameter combinations was evaluated to fit the Gaussian Process and establish a baseline surrogate model. At each iteration, the EI was maximized to propose the next candidate parameter set, which was then evaluated by computing the training RMSE of the multivariate Holt Winters forecasts. The new observation was added to the dataset, and the GP surrogate was updated accordingly. This loop of surrogate updating and acquisition optimization continued until convergence or the maximum number of evaluations was reached. The detail flowchart is given in Figure 2.3.

Upon completion, the parameter set corresponding to the minimum training RMSE was extracted and reshaped into the 3×3 matrices. Using these optimized parameters, forecasts were generated for both training and testing datasets, and the performance was evaluated in terms of RMSE and MAE. This approach enhances computational efficiency while ensuring accurate forecasting.

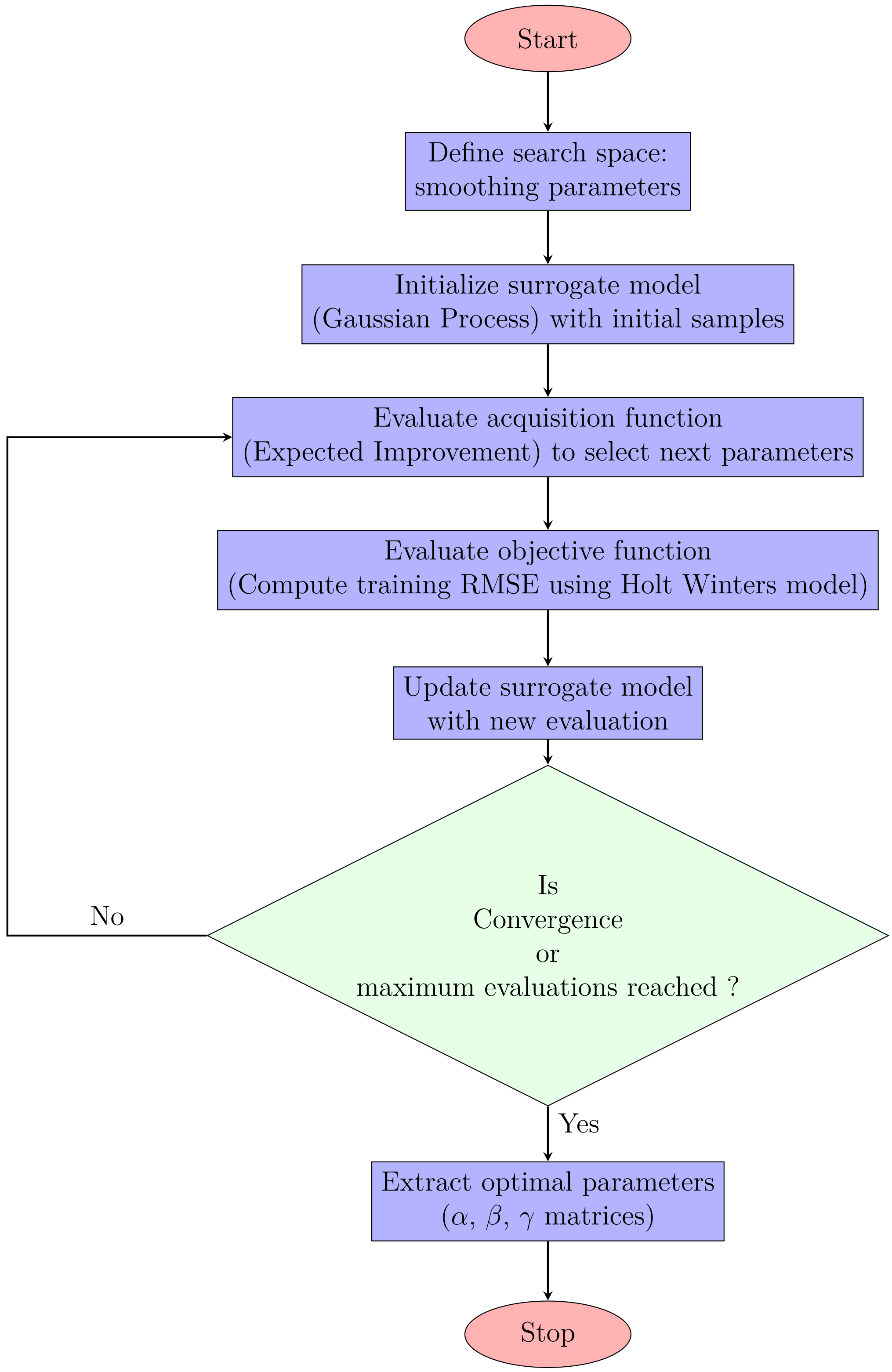

Figure 2.3: Flowchart of Bayesian Optimization for Holt Winters Parameter Tuning.

2.7.3 Modified K-fold

Traditional cross-validation techniques, such as k-fold cross-validation, are based on the assumption that data samples are independent and identically distributed. However, this assumption does not hold for time series data (Assaad and Fayek, 2021). Since time series data points are closely related in time, applying standard k-fold cross-validation can result in significant overlap between training and testing sets, leading to unreliable generalization error estimates. To address this challenge, a modified version of k-fold cross-validation has been developed specifically for time series data (Assaad and Fayek, 2021). This approach, known as time series split, evaluates models on future observations rather than random observations. In each iteration, the training and validation sets are partitioned such that the validation set always follows the training set chronologically. Figure 2 provides the time series split approach, demonstrating how the latter ensures a forward-looking evaluation for time series data.

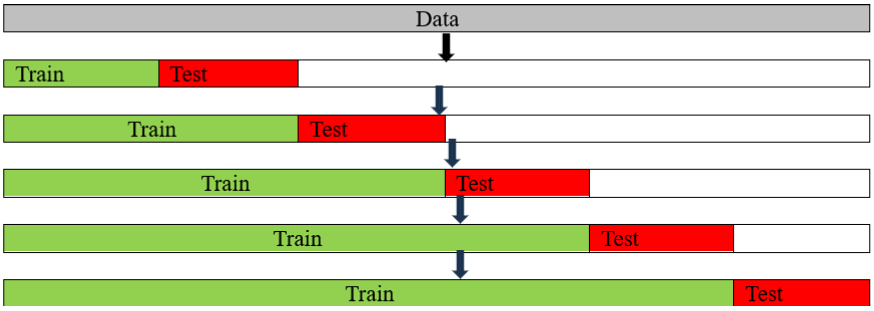

Figure 2.4: The function of modified k-fold cross-validation.

In this study, a modified k-fold cross-validation approach was employed to evaluate model performance for time series data. The dataset was split iteratively, using a growing training set and a fixed testing set to ensure that testing was always conducted on future observations. Specifically, the training and testing splits were as follows:

- Data from 1971–2017 was used for training, and the model was tested on data from 2018.

- Data from 1971–2018 was used for training, and the model was tested on data from 2019.
- Data from 1971–2019 was used for training, and the model was tested on data from 2020.
- Data from 1971–2020 was used for training, and the model was tested on data from 2021.
- Data from 1971–2021 was used for training, and the model was tested on data from 2022.

The performance of the model for each fold was evaluated using three metrics: Root Mean Square Error (RMSE), Mean Absolute Error (MAE), and Coefficient of determination (R^2). The final model performance was determined by calculating the average of these metrics across all folds, providing a comprehensive assessment of the model's accuracy and reliability. This approach was adopted to enhance the reliability of the model when incorporating new data into the existing dataset. By progressively expanding the training set with each fold, the model learns from a growing historical dataset, better capturing the underlying patterns and trends. Testing on future observations ensures that the model's performance is evaluated in a realistic forecasting scenario, providing a robust assessment of its ability to generalize to unseen data.

2.8 Correlation Analysis

Correlation analysis is a statistical method used to assess the relationship between two or more variables. Variables are said to be correlated if changes in one variable are associated with changes in another. It is applicable to both bivariate and multivariate datasets. In this study, Pearson's correlation coefficient, Spearman's rank correlation, and cross-correlation are used to evaluate the relationships between variables.

2.8.1 Pearson's Correlation Coefficient

Pearson's correlation coefficient (r) is a statistical measure used to measures the strength and direction of the linear relationship between two continuous variables (Kirch, 2008). It evaluates how one variable changes in relation to another and ranges from -1 to +1. A positive value ($r > 0$) indicates that as one variable increases, the other tends to increase as well, and vice versa. A negative value ($r < 0$) suggests that an increase in one variable is associated with a decrease in the other. When the value is close to zero $r \approx 0$, it implies a weak or no linear relationship between the variables. The Pearson's correlation coefficient is defined by (Pearson, 1896)

$$r = \frac{\sum_{i=1}^{n}(x_i - \bar{x})(y_i - \bar{y})}{\sqrt{\sum_{i=1}^{n}(x_i - \bar{x})^2 \sum_{i=1}^{n}(y_i - \bar{y})^2}}, \tag{2.54}$$

wwhere,

x_i = value of the x-variable for the i^{th} observation,

y_i = value of the y-variable for the i^{th} observation,

$\bar{x}$ = mean of the x-variable values,

$\bar{y}$ = mean of the y-variable values, and

n = number of observations.

2.8.2 Spearman's Rank Correlation Coefficient

Spearman's rank correlation coefficient (ρ) is a non-parametric measure of the monotonic relationship between two variables by comparing their ranked values rather than actual values, ranges from -1 to +1 (Wissler, 1905). It is given by (Spearman, 1987)

$$\rho = 1 - \frac{6\sum_{i=1}^{n} d_i^2}{n^3 - n}, \tag{2.55}$$

where,

d_i = difference between the ranks of x_i and y_i, and

n = number of observations.

2.8.3 Cross-Correlation

The Cross-Correlation Function (CCF) is a statistical tool used to measure the similarity between two time series as a function of their time displacement. It helps identify the extent to which one time series is related to another at different time lags, making it valuable for analyzing leading and lagging relationships between variables. The CCF is constructed using cross-correlation coefficients, which represent the correlation between the elements of two time series at varying time displacements (Bhaskaran *et al.*, 2013). Given two time series, x_t and z_t, the cross-correlation coefficient at a lag L, denoted as $R(L)$, is defined as (Carrión-García *et al.*, 2021):

$$R(L) = \frac{\sum_t (x_t - \bar{x})(z_{t-L} - \bar{z})}{\sqrt{\sum_t (x_t - \bar{x})^2}\sqrt{\sum_t (z_{t-L} - \bar{z})^2}}, \tag{2.56}$$

where,
$R(L)$ represents the cross-correlation coefficient at lag L,
x_t and z_t are the time series being analyzed, and
$\bar{x}$ and $\bar{z}$ are the mean values of x_t and z_t, respectively.

By analyzing these coefficients at different lags, we can interpret the interaction between the two series. Firstly, a significant correlation at $L = 0$ suggests an instantaneous relationship between the variables. Secondly, a significant correlation at $L > 0$ indicates that changes in x_t influence z_t with a delay of L periods. Thirdly, a significant correlation at $L < 0$ implies that changes in x_t impact z_t with a delay of L periods.

2.9 Goodness Criteria

To evaluate the performance of the methods, we utilize several standard metrics. These include the Mean Absolute Error (MAE), the Root Mean Square Error (RMSE), Nash–Sutcliffe Efficiency coefficient (NSE) and the Coefficient of Determination (R2), to assess prediction accuracy. Additionally, we apply the Akaike Information Criterion (AIC) and the Bayesian Information Criterion (BIC) for model selection, balancing goodness of fit with model complexity.

2.9.1 Mean Absolute Error (MAE)

Mean Absolute Error (MAE) is a common metric used to evaluate the accuracy of forecasting models. It measures the average magnitude of errors between predicted values and actual observed values, without considering their direction (Pertiwi, 2020). MAE is calculated as follows:

$$\text{MAE} = \frac{1}{n}\sum_{i=1}^{n}\left|Y_i - \hat{Y}_i\right|, \tag{2.57}$$

where,
Y_i is the actual value for observation i,
$\hat{Y}_i$ is the predicted value for observation i,
n is the number of observations.

MAE provides a straightforward indication of the average error magnitude in the predictions, with lower values indicating better model performance.

2.9.2 Root Mean Square Error (RMSE)

Root Mean Square Error (RMSE) is a widely used metric for assessing the accuracy of a forecasting model. It measures the average magnitude of the prediction errors, giving more weight to larger errors due to its squaring operation (Karthika and Karthikeyan, 2022). RMSE is calculated as follows:

$$\text{RMSE} = \sqrt{\frac{1}{n}\sum_{i=1}^{n}\left(Y_i - \hat{Y}_i\right)^2}, \tag{2.58}$$

where,
Y_i is the actual value for observation i,

$\hat{Y}_i$ is the predicted value for observation i,
n is the number of observations.

RMSE measures how closely the model predictions align with the actual data, where smaller values indicate better performance.

2.9.3 Coefficient of Determination

The coefficient of determination is a statistical metric that measures the proportion of the total variation in the dependent variable that is explained by the independent variable (s) and is denoted by R^2. It ranges from 0 to 1, where 0 indicates that the model does not explain any variation in the dependent variable, and 1 signifies a perfect fit. In general, a more accurate predictive model will have an R^2 value closer to 1. It can be computed by using the following formulae:

$$R^2 = 1 - \frac{\sum_{i=1}^{n} \left(Y_i - \hat{Y}_i\right)^2}{\sum_{i=1}^{n} \left(Y_i - \bar{Y}\right)^2}, \tag{2.59}$$

where,
Y_i is the actual value for observation i,
$\hat{Y}_i$ is the predicted value for observation i,
$\bar{Y}$ is the mean of actual observations,
n is the number of observations.

2.9.4 Nash–Sutcliffe Efficiency (NSE) Coefficient

The Nash–Sutcliffe Efficiency (NSE), proposed by Nash and Sutcliffe (1970), is a widely used metric to evaluate the predictive accuracy of hydrological and rainfall forecasting models. NSE measures how well the modeled or simulated values match the observed values, taking into account both the variance and bias of the predictions. A value of NSE = 1 indicates a perfect match between observed and simulated values, NSE = 0 indicates that the model predictions are no better than using the mean of observed data, and NSE < 0 indicates that the model performs worse than the mean (Melsen *et al.*, 2025). Unlike R^2, which measures only the strength of the linear relationship between observed and predicted values, NSE evaluates the actual predictive performance, making it particularly suitable for assessing rainfall or hydrological models. The equation is given by:

$$NSE = 1 - \frac{\sum_{i=1}^{n} \left(Q_{obs,i} - Q_{mod,i}\right)^2}{\sum_{i=1}^{n} \left(Q_{obs,i} - \overline{Q}_{obs}\right)^2}, \tag{2.60}$$

where:
$Q_{obs,i}$ = observed value for observation i,
$Q_{mod,i}$ = modeled/simulated value for observation i,
$\overline{Q}_{obs}$ = mean of observed values,
n = number of observations.

2.9.5 Akaike Information Criterion (AIC)

The Akaike Information Criterion (AIC) is a statistical measure used to assess the quality of a model relative to other models. It provides a way to compare models with different numbers of parameters and select the one that best balances goodness of fit with model complexity (Wang, 2005). The AIC is defined as:

$$\text{AIC} = 2k - 2\ln(P), \tag{2.61}$$

where,
k is the number of parameters in the model,
P is the maximum value of the likelihood function for the model.

The AIC penalizes models with more parameters to prevent overfitting. A lower AIC value reflects a better balance between model fit and complexity. When comparing different models, the one with the lowest AIC is typically favoured.

2.9.6 Bayesian Information Criterion (BIC)

The Bayesian Information Criterion (BIC), is a statistical criterion for model selection that penalizes model complexity more heavily than the Akaike Information Criterion (AIC). It is used to compare models with different numbers of parameters and helps in selecting the model that best balances fit and complexity (Pandit *et al.*, 2023). The BIC is defined as:

$$\mathrm{BIC} = k \ln(n) - 2 \ln(P), \tag{2.62}$$

where,
k is the number of parameters in the model,
n is the number of observations,
P is the maximum value of the likelihood function for the model.

A lower BIC value indicates a better model, with the model having the lowest BIC being preferred for its balance of fit and simplicity.

Chapter 3

Forecast based on Holt Winters Method and its Modification

3.1 Introduction

The Holt Winters method is an advanced exponential smoothing technique that integrates the Holt and Winters approaches to time series forecasting. It has been widely applied for rainfall forecasting across various regions (Rahman *et al.*, 2016; Manideep and Sekar, 2018; Aini *et al.*, 2021; Hutapea and Siahaan, 2023; Wiguna *et al.*, 2023; Hendri and Fadhlia, 2024), and has been found to be a suitable model for rainfall forecasting. Motivated by previous studies, in this chapter, we will be forecasting monthly rainfall using both Additive and Multiplicative Holt Winters method for Mizoram and South India regions. Additionally, we have introduced the Modified Holt Winters method, based on the Holt Winters approach and have used it in forecasting along with AHW and MHW. For better understanding the performance of each of the methods at each of the regions, we will be using various statistical tests along with graphical representations.

3.2 Monthly Rainfall Forecasting of Mizoram using Holt Winters Methods

In this section, we will be forecasting Mizoram rainfall using AHW and MHW, together with MOHW models. Firstly, we analysed the collected data and decomposed into its trend, seasonality, and residual components. Next, we separated our data for training (80%) and testing (20%), then forecasted the rainfall for the next years (2025-2027) using the models and evaluated the performances using error matrices like RMSE, MAE, AIC and BIC. Finally, a detailed comparison of their performances is conducted.

3.2.1 Study Area

Mizoram, one of the seven northeastern states of India, is situated between latitudes 21°58' N and 24°35' N and longitudes 92°15' E and 93°29' E (see Figure 3.1). It covers an area of 21,081 square kilometres, with 86.27 % of it being a very dense forest, while the remaining area consists of moderately dense and open forests. However, this forest cover is diminishing due to shifting cultivation and other developmental activities. Agriculture is the primary livelihood for most of Mizoram's population. The state shares international borders with Myanmar (404 kilometres) and Bangladesh (318 kilometres) and is also adjacent to three other northeastern states: Assam (123 kilometres), Tripura (66 kilometres), and Manipur (95 kilometres). Given the state's reliance on agriculture, understanding its rainfall patterns is crucial for local farmers and their crops. Climate change poses a growing concern as rising temperatures may alter precipitation patterns and impact water availability for agricultural and domestic use. Monitoring and analysing rainfall data over time can help identify shifts or trends in rainfall patterns, aiding in better water management and crop planning. Mizoram expe-

Lallawmzuali, M. and Muniyan, S. (2025). Rainfall prediction in Mizoram using the Modified Holt Winters method. *Theoreotical and Applied Climatology*, **156 (2)**, 125-137.

riences temperatures exceeding 30°C in summer, while winter temperatures range from 7°C-22°C. The state enjoys a mild climate with summer temperatures between 20°C and 29°C.

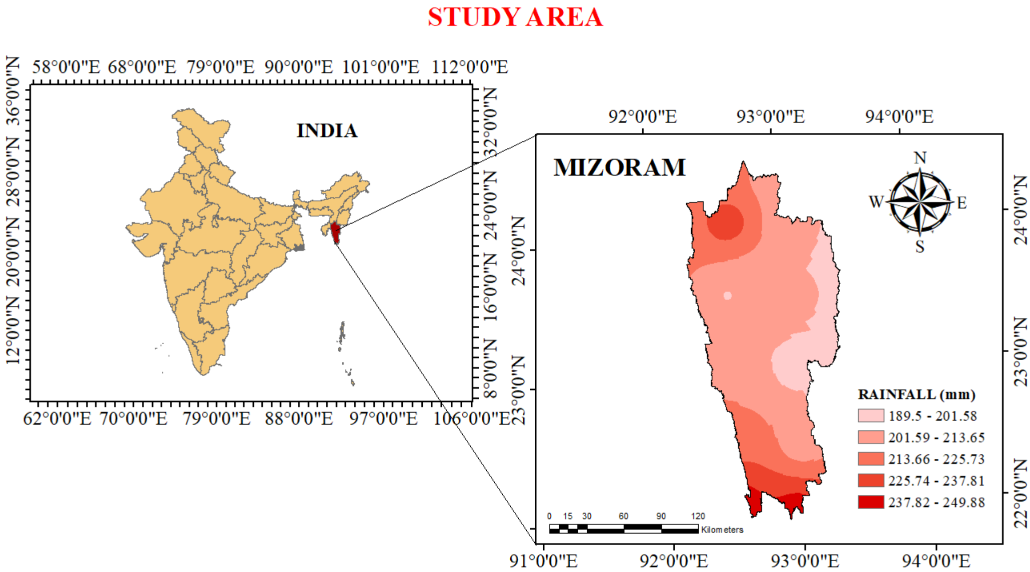

Figure 3.1: The location of the Study Area.

3.2.2 Data Collection

Historical monthly rainfall data covering a 37 year period (1986-2022) has been sourced from the State Meteorological Centre, Directorate of Science and Technology, Government of Mizoram (see Figure 3.2-3.3). The data from 1986 to 2017 was utilized for training the model, while the period from 2018 to 2022 was reserved for testing. Figure highlights substantial variability in rainfall from month to month and year to year, with some months recording close to zero rainfall and others reaching peaks as high as 700 mm. The prominent peaks suggest periodic heavy rainfall events, possibly during the monsoon season, which is typical for northeastern India. Over the decades, the graph does not show a clear increasing or decreasing trend, but rather indicates periodic high rainfall events that are followed by months of much lower precipitation. This cyclical pattern may reflect the impact of the monsoon cycle in Mizoram, where the region receives a substantial portion of its annual rainfall during the rainy season.

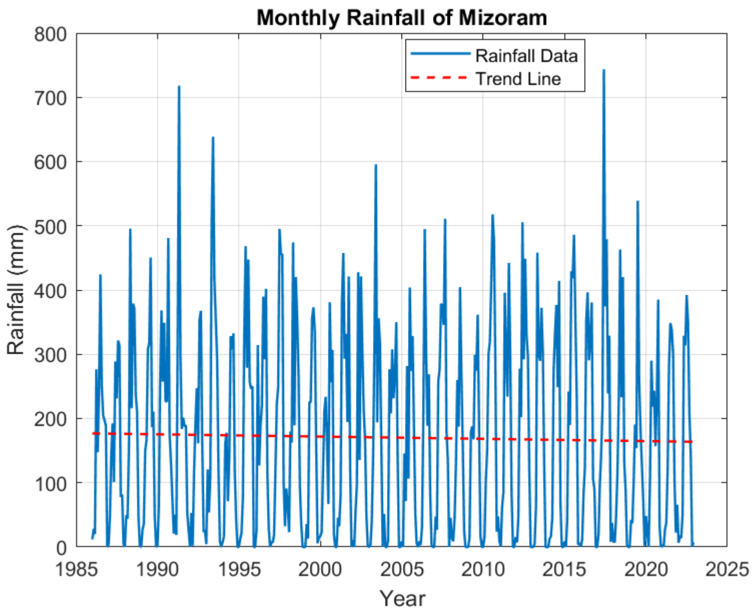

Figure 3.2: Time Series plot for Mizoram Rainfall Data (1986-2022).

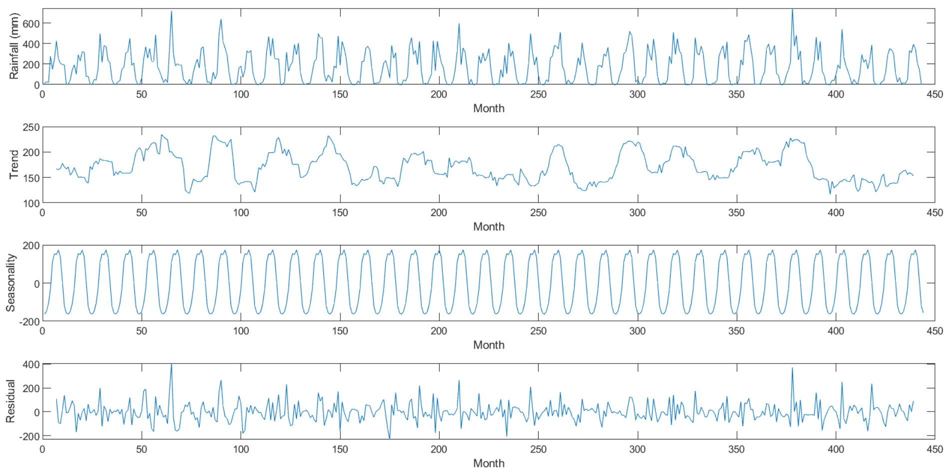

Figure 3.3: The decomposition of rainfall data for Mizoram from 1986-2022 collected by the State Meteorological Centre, DST, Government of Mizoram.

3.2.3 Data Exploration

Table 3.1 provides a descriptive statistical analysis of rainfall data in Mizoram. It indicates that July has the highest average rainfall at 539.00 mm, while January experiences the lowest average rainfall, with only 8.20 mm. June records the highest monthly rainfall at 743.50 mm, whereas January, February, March, November, and December see the lowest monthly rainfall at just 0.01 mm. May exhibits the highest rainfall variance, with a value of 17825.84 mm, indicating greater variability in rainfall, while January has the lowest variance at 228.02 mm, suggesting more consistent rainfall in that month.

Table 3.1: Mizoram rainfall data summary.

Month	Minimum (mm)	Average (mm)	Maximum (mm)	Variance (mm^2)
January	0.01	8.20	68.20	228.02
February	0.01	22.30	120.80	614.61
March	0.01	62.60	314.30	5054.86
April	13.10	144.10	368.30	7659.03
May	71.20	278.30	718.00	17 825.84
June	106.50	321.80	743.50	21 489.10
July	66.90	539.00	539.00	10 009.72
August	66.90	319.70	517.00	7697.72
September	131.00	303.80	510.80	8428.67
October	67.90	177.60	421.00	7508.35
November	0.01	48.10	250.20	3316.18
December	0.01	12.70	91.10	570.42

3.2.4 Additive Holt Winters Method (AHW)

In this study, we evaluated the performance of the AHW using rainfall data from Mizoram. The models were trained using data from 1980 to 2018, and their performance was evaluated on data from 2019 to 2022, with forecasts extended to future periods (refer to Figure 3.4). The analysis was conducted using MATLAB Version 9.13.0 (R2022b) Update 2. In applying the AHW for time series forecasting, smoothing parameters (α, β, γ) were optimized within the interval [0, 1] by minimizing the RMSE during model training. The optimal RMSE during the training phase was 99.70 with $\alpha = 0.10$, $\beta = 0.00$ and $\gamma = 0.20$. These parameters were then used to test the model on unseen data, where the RMSE improved to 89.06, indicating better performance on the test set. The MAE during testing was 58.76, and the AIC and BIC were 805.09 and 812.55, respectively, suggesting a good balance between fit and complexity. With the model performing consistently, it was then used to forecast the next periods, leveraging its ability to capture the seasonal and trend components for future predictions.

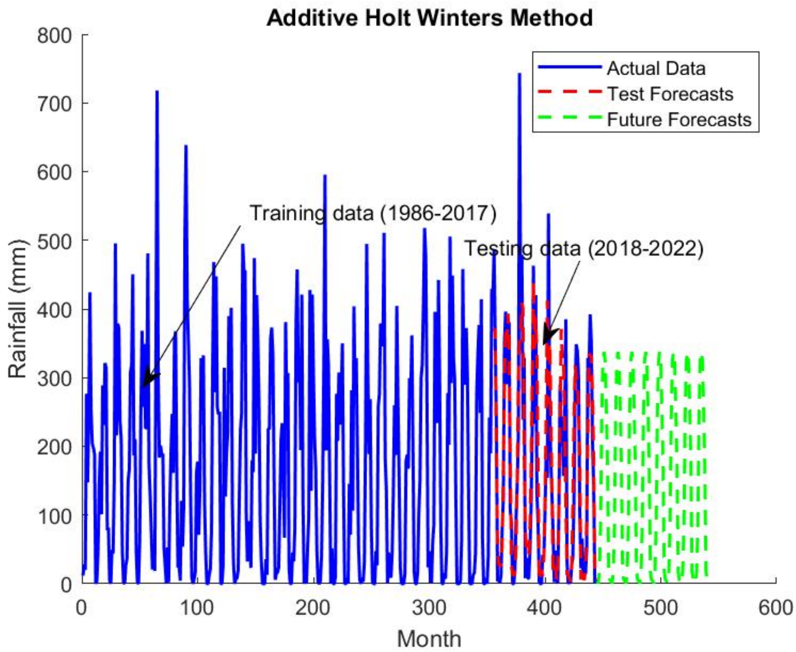

Figure 3.4: Plot illustrating the forecasts generated by the Additive Holt Winters method (AHW) for Mizoram rainfall data.

3.2.5 Multiplicative Holt Winters Method (MHW)

In this study, we used Mizoram rainfall data to assess the MHW's performance. The models were trained on data from 1980 to 2018, and their performance was evaluated on data from 2019 to 2022, with a forecast for future periods (see Figure 3.5). The analysis was conducted using MATLAB Version 9.13.0 (R2022b) Update 2. In using the MHW for forecasting, smoothing parameters were selected by evaluating different values of alpha (α), beta (β), and gamma (γ) within the interval [0, 1]. The optimal combination of parameters was determined by minimizing the RMSE during the training phase. After testing several combinations, the best-performing parameters were $\alpha = 0.70$, $\beta = 0.00$, and $\gamma = 0.70$. However, despite these efforts, the training RMSE remained high at 645.94. However, after using it for testing the data its RMSE value became lower with 396.47, with an

MAE of 280.72, suggesting significant prediction errors. The AIC was 1070.90, and the BIC was 1078.37, indicating that while the model captured some aspects of the data, it was not well-suited for forecasting in this region due to its poor overall performance. As a result, the MHW model was deemed ineffective, prompting the need for alternative models or parameter adjustments to improve forecast accuracy.

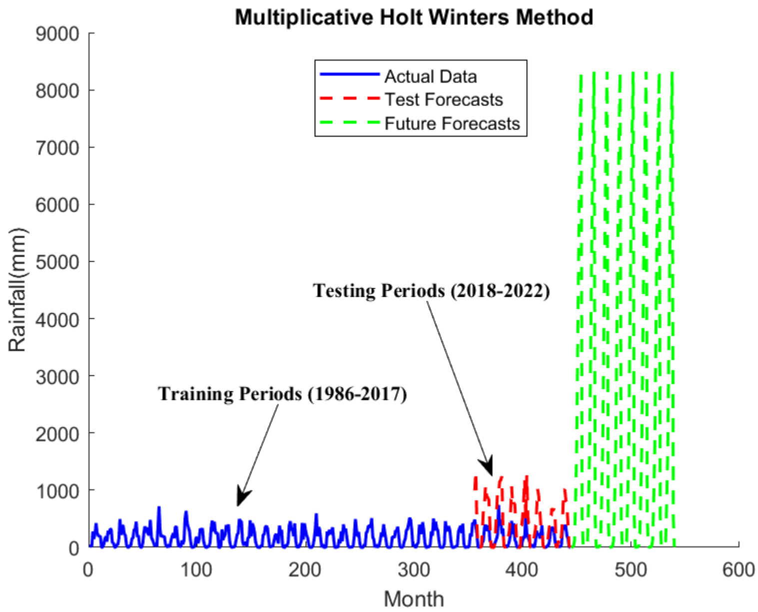

Figure 3.5: Plot depicting the forecasts produced by the Multiplicative Holt Winters method (MHW) for Mizoram rainfall data.

3.2.6 Modified Holt Winters Method (MOHW)

In using the MOHW, smoothing parameters were selected as $\alpha = 0.10$, $\beta = 1.00$, and $\gamma = 0.10$ based on minimizing the RMSE. During the training phase, the model achieved an RMSE of 98.36, and when tested during the remaining periods, the RMSE improved to 87.76, indicating good performance across both training and testing. The MAE was 58.76, showing moderate forecast deviations. Additionally, the AIC was 802.48, and the BIC was 809.95, suggesting a better fit and reduced model complexity compared to other methods, making this model suitable for forecasting in this region (see Figure 3.6). The analysis was conducted using MATLAB Version 9.13.0 (R2022b) Update 2.

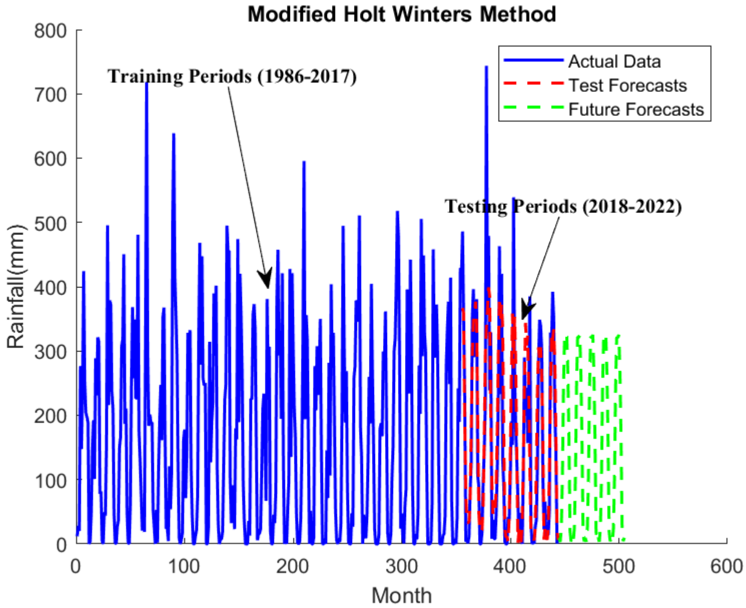

Figure 3.6: Plot showcasing the forecasts from the Modified Holt Winters method (MOHW) for Mizoram rainfall data.

3.2.7 Comparison of AHW, MHW, and MOHW

The smoothing parameters for the Holt Winters models were optimized by calculating the values that resulted in the lowest RMSE for each model during the training period. These optimized parameter values were subsequently used for testing and forecasting purposes, ensuring the highest prediction accuracy for rainfall data. The smoothing parameter values for each method are presented in Table 3.2.

Table 3.2: Summary of the optimized smoothing parameter values for each model.

Method	**Level Smoothing** (α)	**Trend Smoothing** (β)	**Seasonality Smoothing** (γ)
AHW	0.10	0.00	0.20
MHW	0.70	0.00	0.70
MOHW	0.01	1.00	0.10

The comparison of results for both the training and testing periods of the three forecasting models—MHW, AHW, and MOHW are presented in Table 3.3.

Table 3.3: Statistical evaluation of Holt Winters Method during training and testing period.

Method	**Training period**				**Testing period**			
	RMSE	**MAE**	**AIC**	**BIC**	**RMSE**	**MAE**	**AIC**	**BIC**
AHW	99.70	72.04	3153.12	3164.63	89.06	58.76	805.05	812.55
MHW	396.47	280.72	4444.91	4456.42	645.94	280.76	1070.90	1078.37
MOHW	98.26	70.71	3150.48	3161.99	87.76	58.32	802.48	809.95

The evaluation of the Holt Winters forecasting methods—AHW, MHW, and MOHW—during the training and testing periods reveals that the MOHW method demonstrates the best overall performance (see Table 3.3). In the training period, MOHW achieves the lowest RMSE (98.26) and MAE (70.71), slightly outperforming AHW (99.70 RMSE and 72.04 MAE) and significantly surpassing MHW (396.47 RMSE and 280.72 MAE). Similarly, in the testing period, MOHW continues to lead with the lowest RMSE (87.76) and MAE (58.32), compared to AHW (89.06 RMSE and 58.76 MAE) and MHW (645.94 RMSE and 280.76 MAE). Notably, the testing values for RMSE and MAE are slightly lower than the training values for all methods, indicating that the models generalize well to unseen data, with MOHW achieving the best balance. Additionally, MOHW records the lowest AIC and BIC values in both training (3150.48 and 3161.99) and testing (802.48 and 809.95) periods, reflecting its superior efficiency and accuracy. While AHW performs reasonably well, it falls short of MOHW, and MHW exhibits significantly poorer performance with high RMSE and MAE, suggesting overfitting and unsuitability for the dataset. Overall, MOHW emerges as the most effective method for accurate forecasting in this region, demonstrating consistent performance across both training and testing periods.

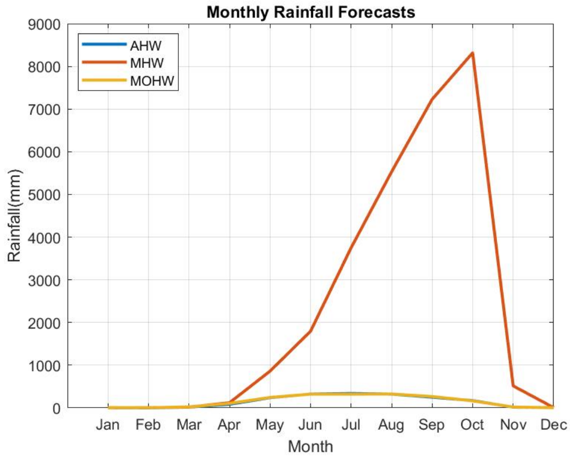

Figure 3.7: Rainfall prediction of Mizoram using AHW, MHW, MOHW for 2025.

The results presented in Figure 3.7 suggest that the MHW data is not applicable to this region and should be excluded from further analysis. Figure 3.8 shows the monthly rainfall forecasts based on two methods: AHW and MOHW.

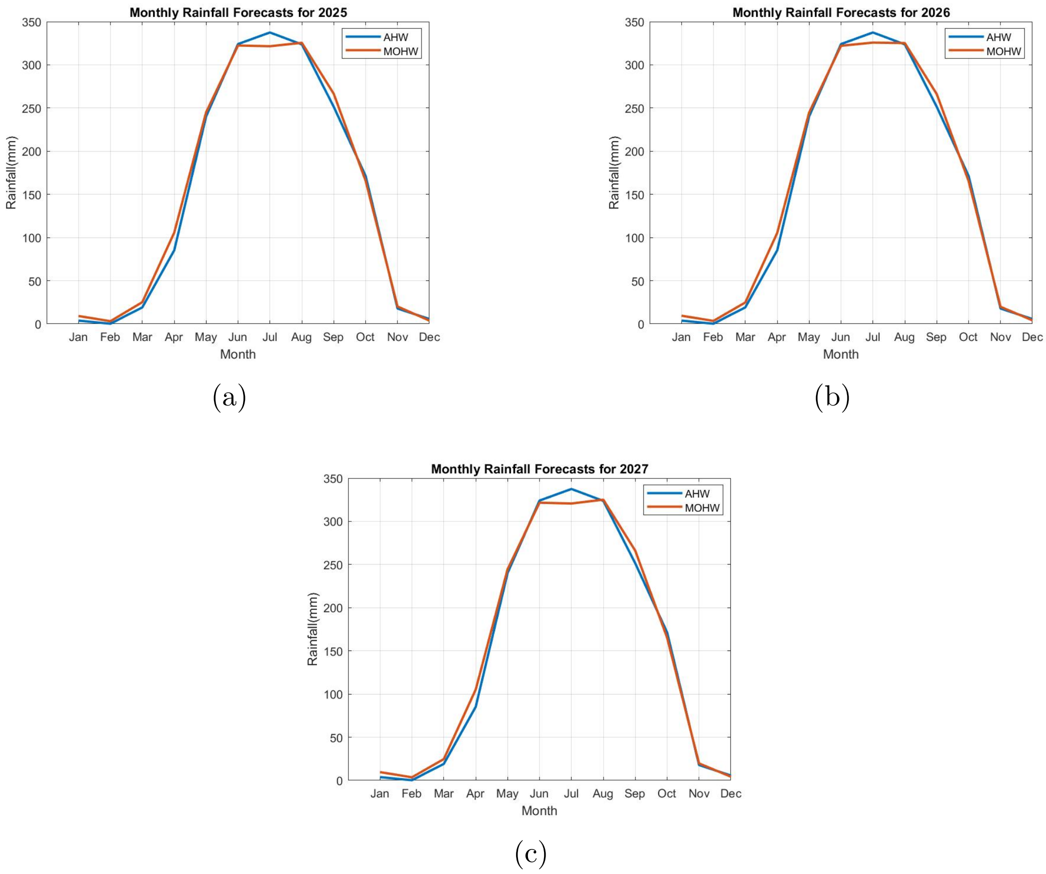

Figure 3.8: The plot illustrates the rainfall prediction by AHW and MOHW for Mizoram rainfall during 2025, 2026 and 2027.

3.2.8 Comparison with SARIMA model

The Seasonal Autoregressive Integrated Moving Average (SARIMA) method is a commonly used time series forecasting technique, particularly suited for stochastic data with seasonal patterns (William and Wei, 2006). As outlined by Box and Jenkins (1976), Palit and Popovic (2005), Shumway and Stoffer (2006), and Bouzerdoum *et al.*, 2011), SARIMA modeling follows four key steps: (1) Model Identification, which involves analyzing the stationarity of the time series and determining the optimal combination of autoregressive and moving average components; (2) Model Estimation, where the identified models are evaluated, and the most efficient one is selected; (3) Model Validation, which assesses the accuracy of the chosen model and identifies potential improvements; and (4) Model Forecasting, which predicts future values of the series, accompanied by a confidence interval to account for uncertainty.

For the Mizoram rainfall data, the SARIMA model was configured with an order of (0,1,0) and a seasonal component of 12, achieving an RMSE of 240.83 during the testing phase. In comparison, the Modified Holt Winters (MOHW) method demonstrates superior performance, with a significantly lower RMSE of 87.76. The Additive Holt Winters (AHW) method also outperforms SARIMA, achieving an RMSE of 89.06, while the Multiplicative Holt Winters (MHW) model performs poorly with an RMSE of 645.94. These results underscore the effectiveness of the MOHW and AHW methods in accurately capturing the seasonal and stochastic patterns of Mizoram rainfall data, making them more reliable forecasting approaches than SARIMA for this dataset. This finding aligns with the results reported by Bora and Hazarika (2023), who studied rainfall patterns in Assam and Meghalaya using ARIMA models and obtained average AIC values of approximately 2600 during the testing phase.

3.3 Monthly Rainfall Forecasting of South India region

In this section, we will be forecasting South India region, which are Andhra Pradesh, Tamil Nadu, Telangana, Kerala, and Karnataka rainfall using AHW and MHW, together with MOHW models. Firstly, we separated our data for training (80%) and testing (20%), then the forecasted rainfall for the year 2025 is shown using spatial mapping at each of the South Indian states based on IMD classifications, and evaluated the performances using error matrices like RMSE, MAE, AIC and BIC. Finally, a detailed comparison of their performances is conducted.

3.3.1 Study Area and Data Collection

The study was carried out in the southern part of India, focusing on the major states of Kerala, Tamil Nadu, Karnataka, Andhra Pradesh, and Telangana (formerly part of Andhra Pradesh). While the Union Territory of Puducherry was initially considered as part of the study area, it was excluded from further analysis due to its relatively small land cover. Therefore, the regions analysed in this study are limited to Telangana, Andhra Pradesh, Kerala, Karnataka, and Tamil Nadu (Table 3.4). These states, covering a significant portion of South India, are characterized by diverse geographical features and climatic conditions that play a vital role in influencing regional rainfall patterns. Figure 3.9 illustrates the location of these different states, providing a clear visual representation of the study area. Historical monthly rainfall data spanning a 51-year period (1971-2022) was obtained from the Indian Meteorological Department (IMD). For the purpose of analysis, the dataset was divided, with 80% allocated for training and the remaining 20% reserved for testing.

Muniyan, S. and Lallawmzuali, M. (2025). Assessment of Rainfall Patterns in South India: A comparative Analysis of Additive, Multiplicative, and Modified Holt Winters Methods. (Communicated)

Table 3.4: Geographical and Climatic Characteristics of South Indian States.

State	Latitude	Longitude	Average Annual Rainfall (mm)	Average Annual Temperature (°C)	Geographical Area (km^2)
Andhra Pradesh	12°37 N ≈ 19°55 N	76°45 E ≈ 84°46 E	1094	15 °C – 45 °C	162 970 km^2
Karnataka	11°30 N ≈ 18°30 N	74°16 E ≈ 78°30 E	1248	14 °C – 40 °C	191 791 km^2
Kerala	08°17 N ≈ 12°47 N	74°27 E ≈ 77°37 E	3107	22 °C – 32 °C	388 638 km^2
Telangana	15°46 N ≈ 19°47 N	77°16 E ≈ 81°43 E	961	22 °C – 32 °C	112 077 km^2
Tamil Nadu	08°05 N ≈ 13°35 N	76°15 E ≈ 80°20 E	998	20 °C – 40 °C	130 058 km^2

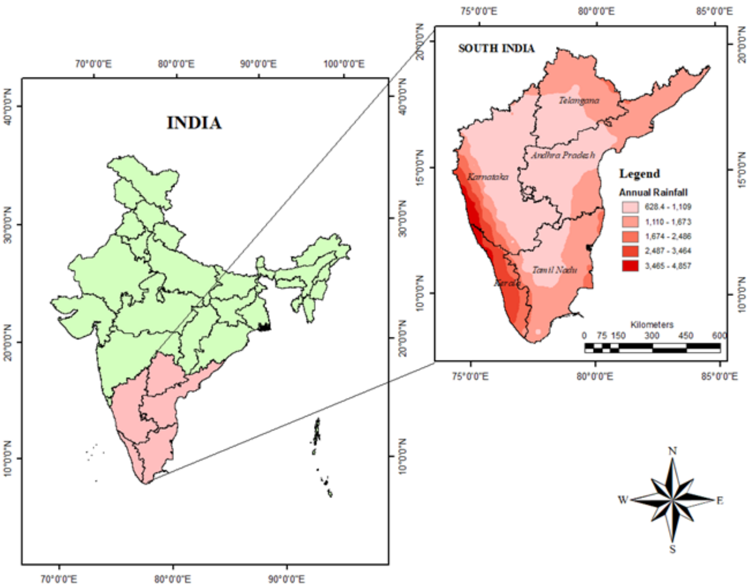

Figure 3.9: Location of the Study Area.

3.3.2 Additive Holt Winters Method (AHW)

The results of applying the Additive Holt Winters method (AHW) to South Indian states reveal varying degrees of forecasting performance based on multiple evaluation metrics. The smoothing parameters α, β, and γ demonstrate how the model adapts to the rainfall patterns of each region. In the context of optimizing the smoothing parameters for the Additive Holt Winters (AHW) model, the approach taken involved utilizing an optimization method to identify parameter values that minimize the Root Mean Square Error (RMSE). This technique is pivotal in enhancing the model's accuracy in forecasting rainfall across various regions. By systematically adjusting the smoothing parameters, the optimization process seeks to find the combination that results in the lowest RMSE value during the training phase, ensuring that the model captures the underlying patterns in the data effectively. For all states, the level parameter α was set to 0.10, indicating a moderate emphasis on recent rainfall data. The trend parameter β was consistently set to 0.00, suggesting that the model did not account for any trend in the data, which may be appropriate in regions where rainfall trends are minimal. The seasonal component γ varied slightly between states, with Andhra Pradesh having a value of 0.10 and other states like Karnataka, Kerala, Tamil Nadu, and Telangana set to 0.20, reflecting greater seasonal variations in these regions.

When evaluating the goodness of fit, Andhra Pradesh outperformed other states across multiple metrics, with a training RMSE of 48.28 and a testing RMSE of 44.04. This suggests that the AHW model effectively captured the rainfall patterns in this state. Tamil Nadu also showed relatively low error rates, with a training RMSE of 51.12 and a testing RMSE of 53.12. In contrast, Kerala demonstrated the highest testing RMSE at 136.85, indicating challenges in modeling the complex rainfall patterns in the state, possibly due to higher variability or other factors that the model did not capture well. The MAE results reinforce these findings, with Andhra Pradesh achieving the lowest error at 29.67 and Kerala showing the highest error at 92.19, further emphasizing the differences in forecast accuracy between states. The model selection criteria, including AIC and BIC, further highlight these variations. Andhra Pradesh had the lowest AIC (952.25) and BIC (960.73), indicating that the model not only fit the data well but also balanced model complexity effectively. In contrast, Kerala had the highest AIC (1235.72) and BIC (1244.20), reinforcing the view that the AHW model struggled to capture the dynamics of rainfall in this region.

The performance of the AHW model in Karnataka and Telangana also warrants attention. Karnataka exhibited a training RMSE of 65.89 and a testing RMSE of 67.33, indicating a moderate level of predictive accuracy, but not as strong as Andhra Pradesh or Tamil Nadu. The AIC and BIC values for Karnataka were 1058.40 and 1066.89, respectively, suggesting that while the model provided reasonable forecasts, it may need further refinement to improve its fit. Telangana presented a training RMSE of 61.26 and a testing RMSE of 59.78, indicating relatively good performance, though it fell short of the accuracy observed in Andhra Pradesh.

Overall, these results suggest that while the AHW model performs well in states like Andhra Pradesh and Tamil Nadu, it may require further refinement or the consideration of alternative models for regions with more complex rainfall patterns, such as Kerala. The variation in model performance across states could be attributed to factors such as geographical differences, varying rainfall distribution patterns, and potential limitations in the model's assumptions regarding trend and seasonality. Future studies may benefit from exploring hybrid models or incorporating additional data sources to enhance predictive accuracy across diverse regions. With the model performing consistently, it was then used to forecast 2025, leveraging its ability to capture the seasonal and trend components for future predictions (see Figure 3.10).

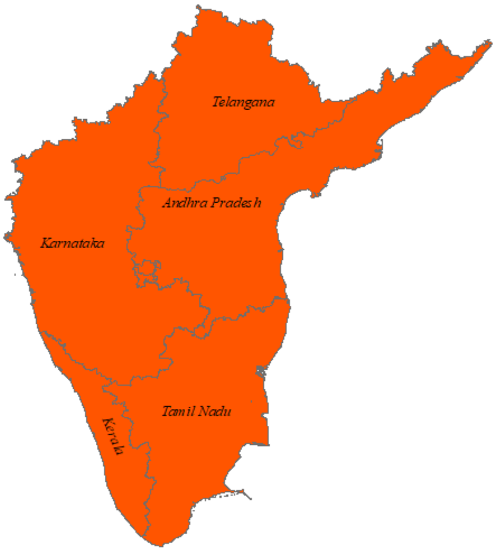

(a) Jan

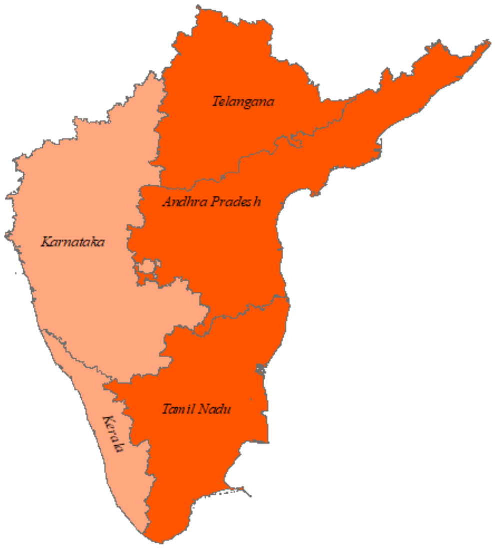

(b) Feb

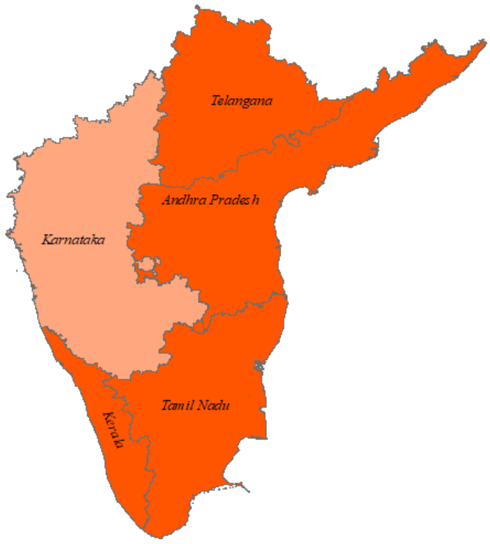

(c) Mar

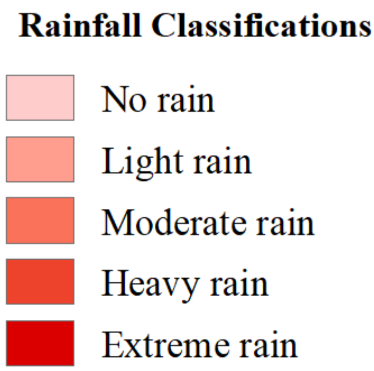

Figure 3.10: Monthly rainfall for the southern region of India in 2025, generated using the Additive Holt Winters method (AHW). The classifications, defined by the Indian Meteorological Department (IMD) (Mukheerjee *et al.*, 2016), are as follows: 0 mm indicates "No rain," 0.1 to 7.5 mm represents "Light rain," 7.6 to 64.4 mm denotes "Moderate rain," 64.5 to 244.4 mm signifies "Heavy rain," and rainfall above 244.4 mm is classified as "Extreme rain." The color-coded categories range from pale pink for "No rain" to dark red for "Extreme rain," illustrating the predicted rainfall intensities across the region for the year 2025 (Continued).

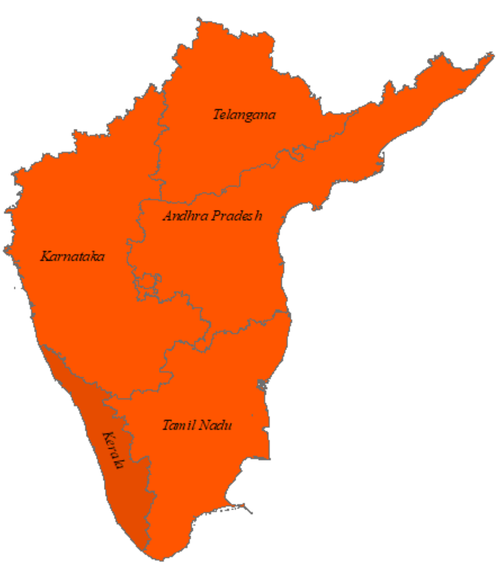

(d) Apr

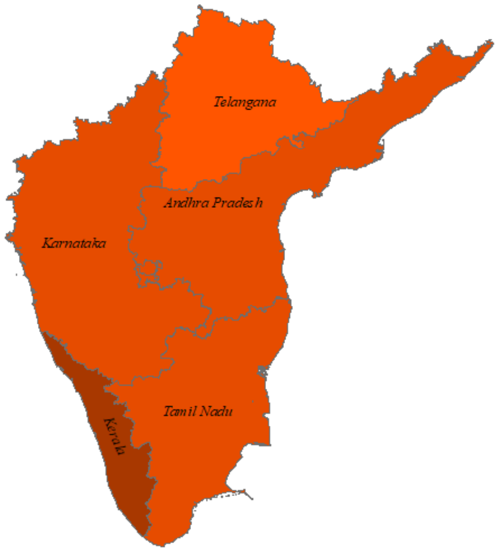

(e) May

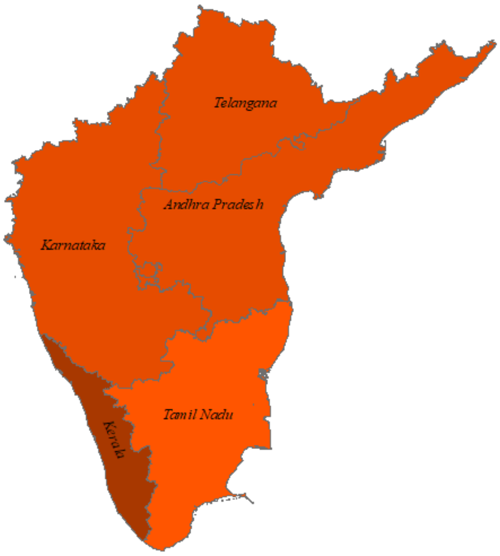

(f) Jun

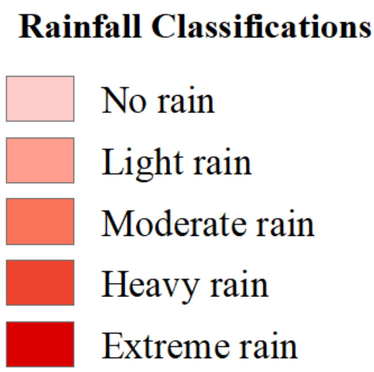

Figure 3.10: Monthly rainfall for the southern region of India in 2025, generated using the Additive Holt Winters method (AHW). The classifications, defined by the Indian Meteorological Department (IMD) (Mukheerjee *et al.*, 2016), are as follows: 0 mm indicates "No rain," 0.1 to 7.5 mm represents "Light rain," 7.6 to 64.4 mm denotes "Moderate rain," 64.5 to 244.4 mm signifies "Heavy rain," and rainfall above 244.4 mm is classified as "Extreme rain." The color-coded categories range from pale pink for "No rain" to dark red for "Extreme rain," illustrating the predicted rainfall intensities across the region for the year 2025 (Continued).

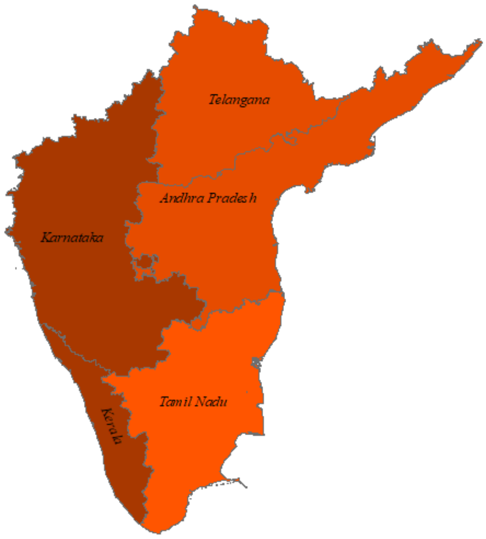

(g) Jul

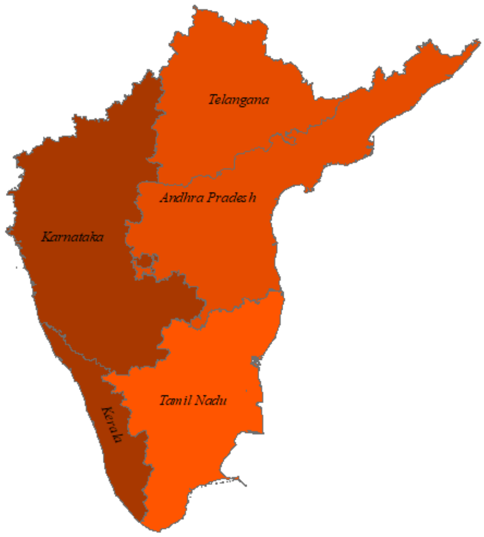

(h) Aug

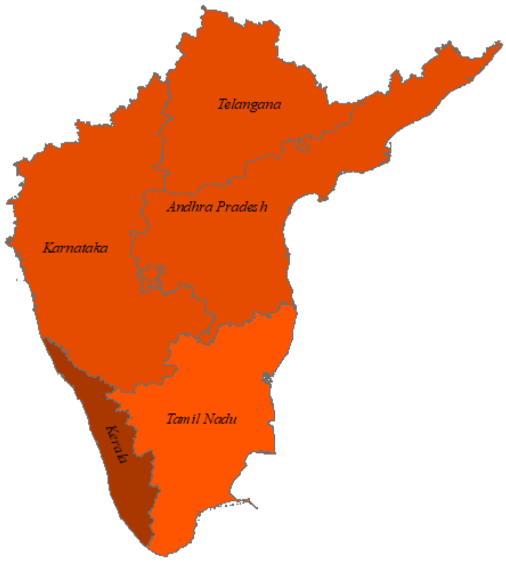

(i) Sep

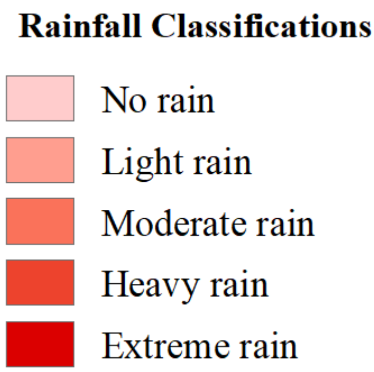

Figure 3.10: Monthly rainfall for the southern region of India in 2025, generated using the Additive Holt Winters method (AHW). The classifications, defined by the Indian Meteorological Department (IMD) (Mukheerjee *et al.*, 2016), are as follows: 0 mm indicates "No rain," 0.1 to 7.5 mm represents "Light rain," 7.6 to 64.4 mm denotes "Moderate rain," 64.5 to 244.4 mm signifies "Heavy rain," and rainfall above 244.4 mm is classified as "Extreme rain." The color-coded categories range from pale pink for "No rain" to dark red for "Extreme rain," illustrating the predicted rainfall intensities across the region for the year 2025 (Continued).

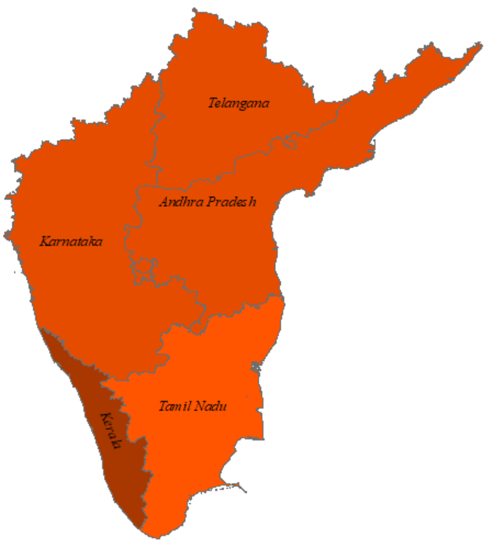

(j) Oct

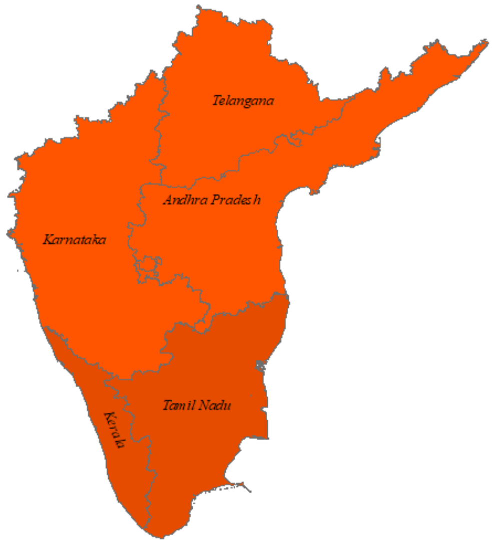

(k) Nov

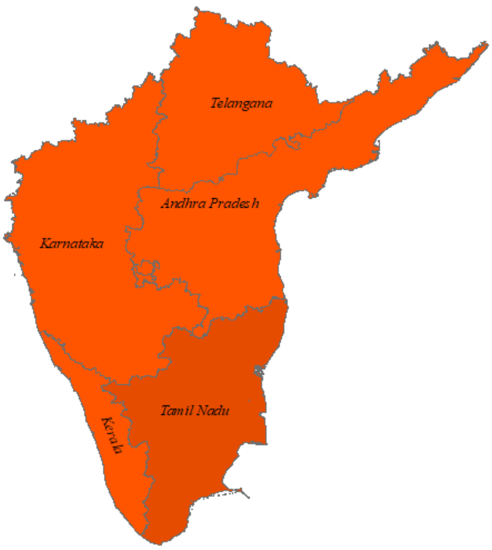

(l) Dec

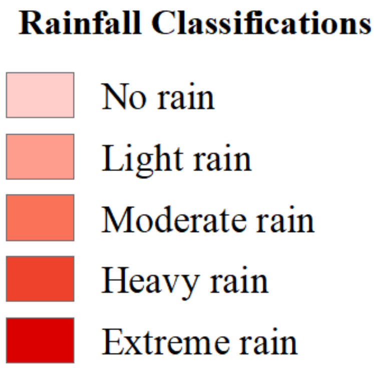

Figure 3.10: Monthly rainfall for the southern region of India in 2025, generated using the Additive Holt Winters method (AHW). The classifications, defined by the Indian Meteorological Department (IMD) (Mukheerjee *et al.*, 2016), are as follows: 0 mm indicates "No rain," 0.1 to 7.5 mm represents "Light rain," 7.6 to 64.4 mm denotes "Moderate rain," 64.5 to 244.4 mm signifies "Heavy rain," and rainfall above 244.4 mm is classified as "Extreme rain." The color-coded categories range from pale pink for "No rain" to dark red for "Extreme rain," illustrating the predicted rainfall intensities across the region for the year 2025.

3.3.3 Multiplicative Holt Winters Method (MHW)

The application of the Multiplicative Holt Winters (MHW) model across South India states yielded a range of forecasting performance as evaluated through several metrics. The smoothing parameters α, β, and γ were adjusted to suit the rainfall characteristics of each region by taking parameters that optimized lowest RMSE value. In all cases, the level parameter α was consistently set at 0.10, indicating a moderate reliance on recent observations. The trend parameter β was maintained at 0.00, suggesting that no trend adjustments were made, which may be suitable in contexts where long-term trends in rainfall are minimal. Notably, the seasonal component γ varied significantly, with values of 0.10 for Andhra Pradesh and Tamil Nadu, indicating moderate seasonal fluctuations, while Karnataka and Telangana exhibited higher values of 0.20 and 0.80, respectively, reflecting greater seasonal variability.

Andhra Pradesh demonstrated the best forecasting performance among the states, achieving a training RMSE of 55.25 and a testing RMSE of 44.02, which suggests that the MHW model effectively captured the rainfall dynamics in this region. Tamil Nadu also performed relatively well, with a training RMSE of 58.48 and a testing RMSE of 53.06, indicating robust predictive capabilities. Conversely, Karnataka's results raised concerns, with a training RMSE of 136.75 and an alarming testing RMSE of 329.52, suggesting significant challenges in modeling its rainfall patterns. The high MAE of 117.60 further underscores the model's inability to accurately predict rainfall in this state. Kerala exhibited moderate performance with a training RMSE of 141.64 and a testing RMSE of 180.51, indicating complexities in its rainfall behaviour that the MHW model struggled to accommodate effectively. Finally, Telangana's results were particularly concerning, showing an exceptionally high training RMSE of 32,591.01 and a testing RMSE of 909.75, alongside an MAE of 483.75. This suggests severe inadequacies in the model's ability to forecast rainfall in Telangana, likely due to its extreme rainfall variability or other unmodeled factors.

The model selection criteria, AIC and BIC, reflect these variations in performance. Andhra Pradesh recorded the lowest AIC (952.16) and BIC (960.65), indicating a good balance between model fit and complexity. In contrast, Karnataka and Telangana had considerably higher AIC and BIC values, signalling potential overfitting or inadequate representation of the underlying data structure. Overall, the results indicate that while the MHW model can be effective in certain states, it requires further refinement or alternative modeling approaches to better capture the intricacies of rainfall patterns, particularly in Karnataka and Telangana. With the model demonstrating consistent performance, it was subsequently employed to forecast rainfall for 2025 (see Figure 3.11).

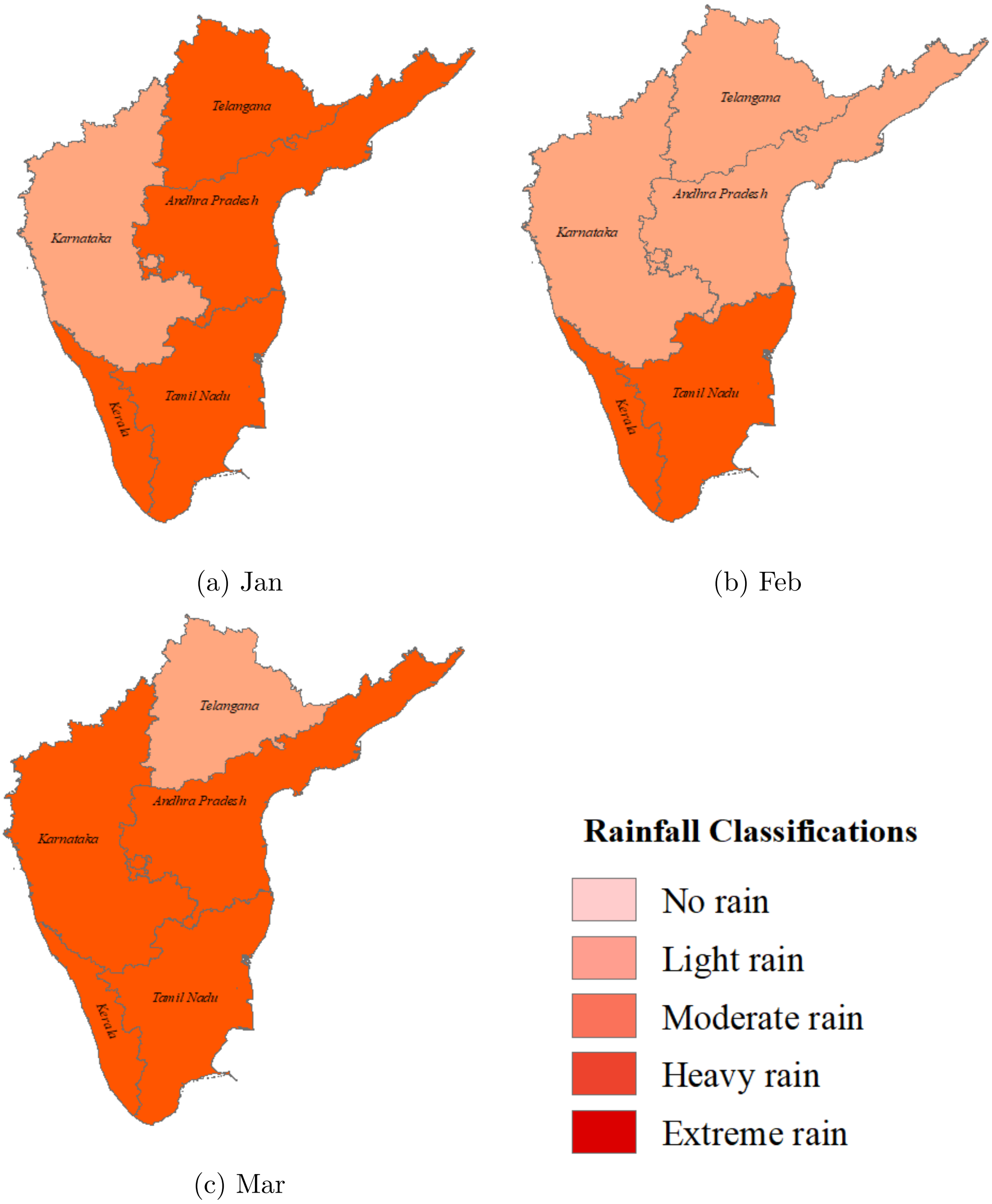

Figure 3.11: Monthly rainfall for the southern region of India in 2025, generated using the Multiplicative Holt Winters method (MHW). The classifications are same as Figure 3.10 (Continued).

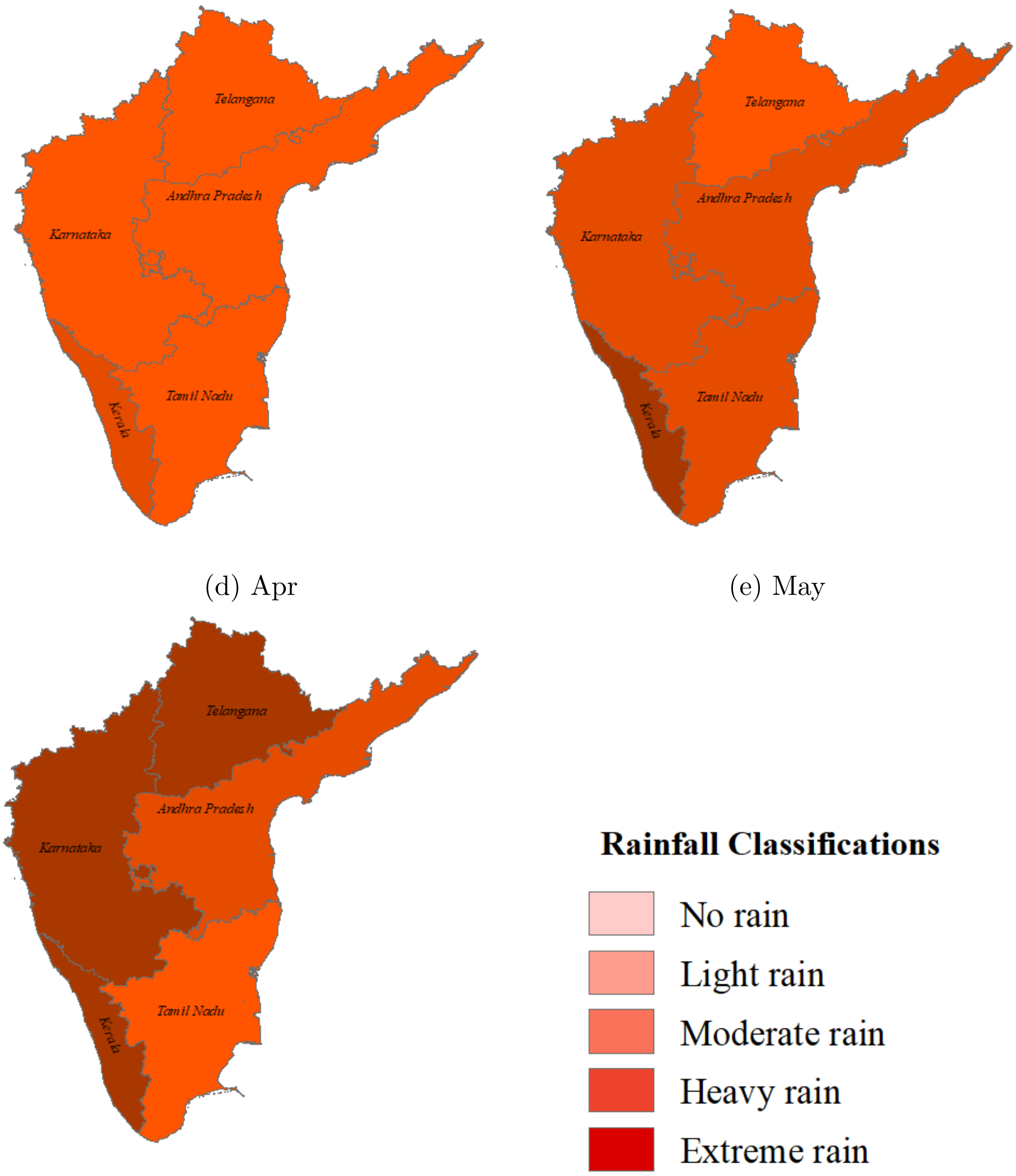

(d) Apr

(e) May

(f) Jun

Figure 3.11: Monthly rainfall for the southern region of India in 2025, generated using the Multiplicative Holt Winters method (MHW). The classifications are same as Figure 3.10 (Continued).

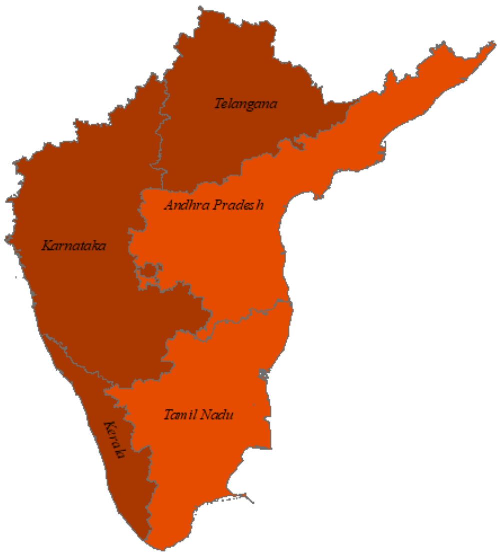

(g) Jul

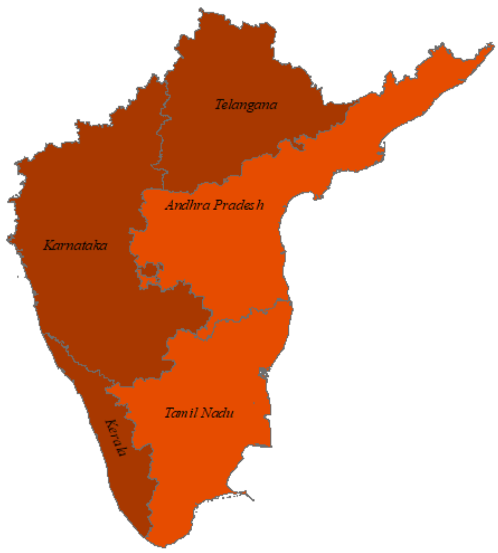

(h) Aug

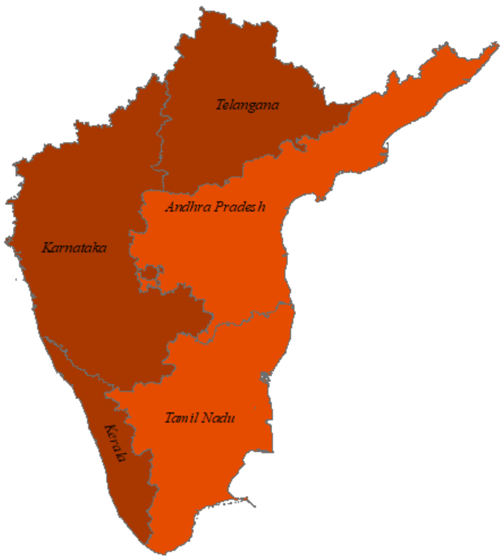

(i) Sep

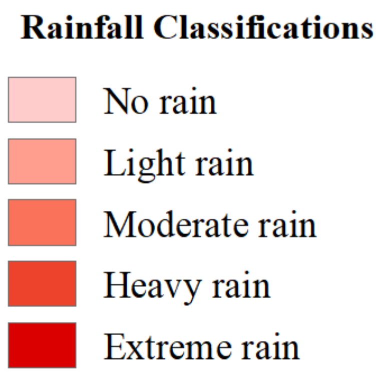

Figure 3.11: Monthly rainfall for the southern region of India in 2025, generated using the Multiplicative Holt Winters method (MHW). The classifications are same as Figure 3.10 (Continued).

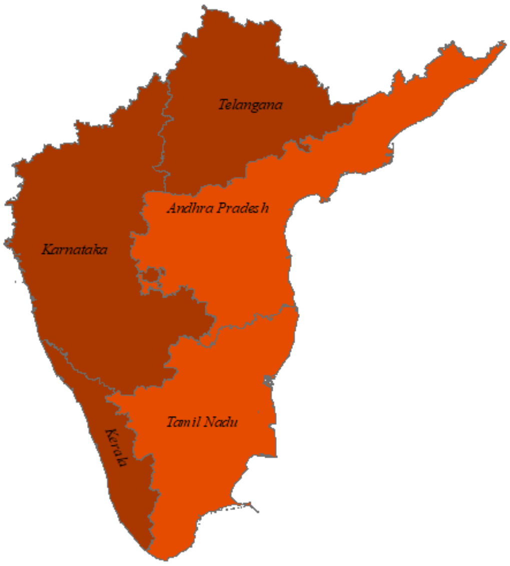

(j) Oct

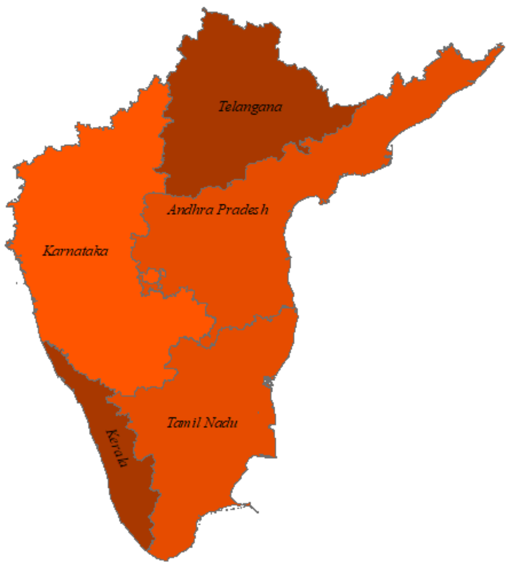

(k) Nov

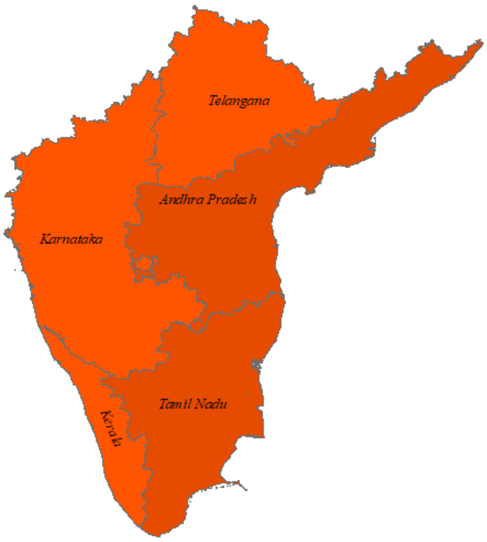

(l) Dec

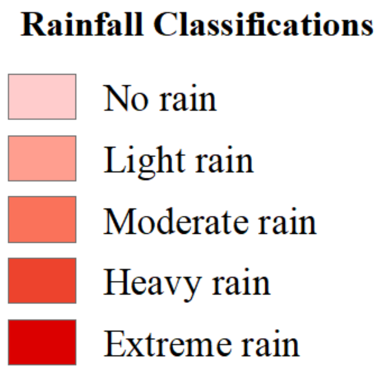

Figure 3.11: Monthly rainfall for the southern region of India in 2025, generated using the Multiplicative Holt Winters method (MHW). The classifications are same as Figure 3.10.

3.3.4 Modified Holt Winters Method (MOHW)

The results of applying the Multiplicative Additive Holt Winters method (MOHW) across South Indian states reveal varying degrees of forecasting performance, as indicated by several evaluation metrics. The smoothing parameters were consistently set with the level parameter α at 0.10 and the trend parameter β at 1.00, suggesting a strong emphasis on the trend component while maintaining a moderate influence from recent observations. The seasonal parameter γ varied, with values of 0.10 for Andhra Pradesh, Kerala, and Tamil Nadu, while Karnataka and Telangana had a γ value of 0.20, reflecting greater seasonal variations in these regions.

In terms of forecasting accuracy, Andhra Pradesh exhibited the best performance, achieving a training RMSE of 48.58 and a testing RMSE of 43.70. This indicates that the MOHW model effectively captured the rainfall dynamics in this state. Tamil Nadu also demonstrated commendable accuracy, with a training RMSE of 51.21 and a testing RMSE of 50.05. Conversely, Kerala displayed a higher testing RMSE of 134.33, suggesting difficulties in accurately modeling its rainfall patterns. Despite this, the MOHW model still performed better than AHW and MHW methods for this state, indicating an improvement in capturing complexities in rainfall data. Karnataka and Telangana showed more mixed results. Karnataka recorded a testing RMSE of 67.27, which suggests that while the model captured some aspects of rainfall patterns, it may not have fully addressed the complexities inherent to the region, leading to less accurate forecasts. Telangana exhibited a testing RMSE of 59.69, which is relatively better than Karnataka's, indicating that the model was somewhat effective in capturing the rainfall trends in this state, although there may still be significant room for improvement. The MAE results support these observations, with Andhra Pradesh attaining the lowest MAE of 29.74 and Kerala showing a significantly higher MAE of 90.10. Karnataka and Telangana had MAEs of 46.01 and 40.36, respectively, highlighting the variability in forecasting accuracy across these regions.

The model selection criteria, AIC and BIC, further emphasize the disparities in model performance. Andhra Pradesh recorded the lowest AIC (950.35) and BIC (958.84), highlighting that the model not only fit the data well but also maintained an optimal balance between model complexity and goodness of fit. In contrast, Kerala had the highest AIC (1231.08) and BIC (1239.57), emphasizing that the MOHW model, despite challenges, still managed to better capture the complexities of rainfall in comparison to the Additive and Multiplicative approaches. Given the model's consistent performance, it was then utilized to project rainfall for the year 2025 (see Figure 3.12).

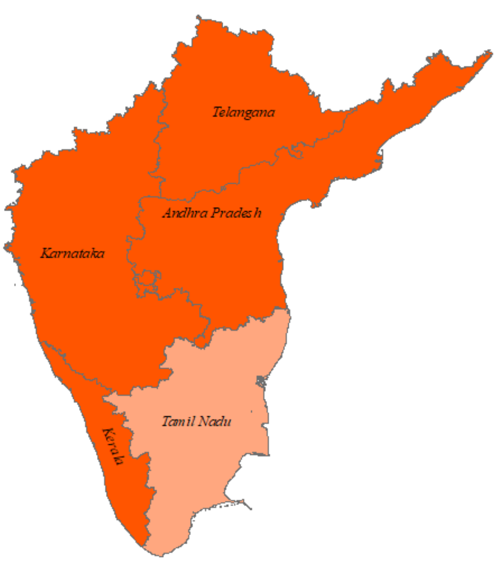

(a) Jan

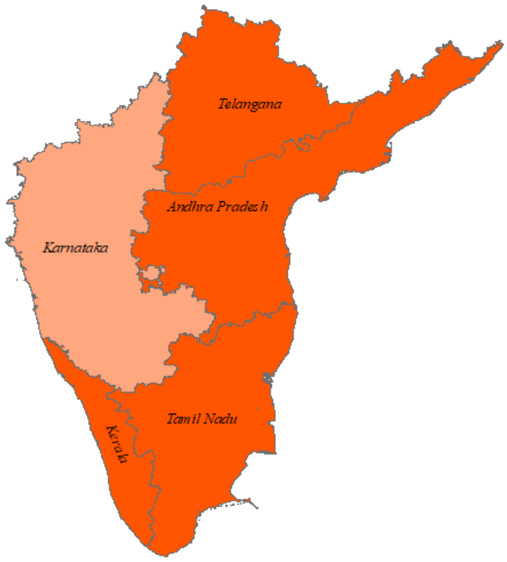

(b) Feb

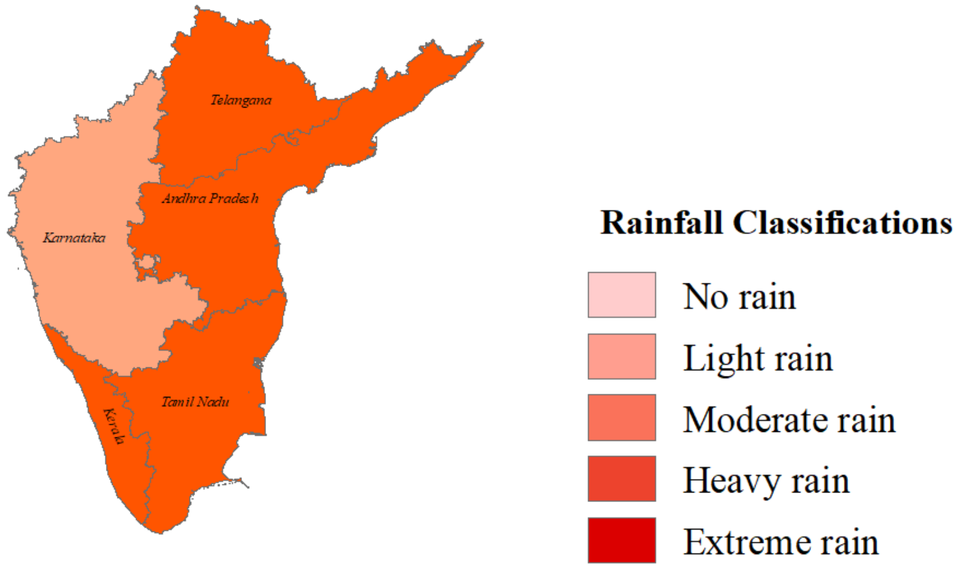

(c) Mar

Figure 3.12: Monthly rainfall for the southern region of India in 2025, generated using the Modified Holt Winters method (MOHW) model. The classifications are same as Figure 3.10 (Continued).

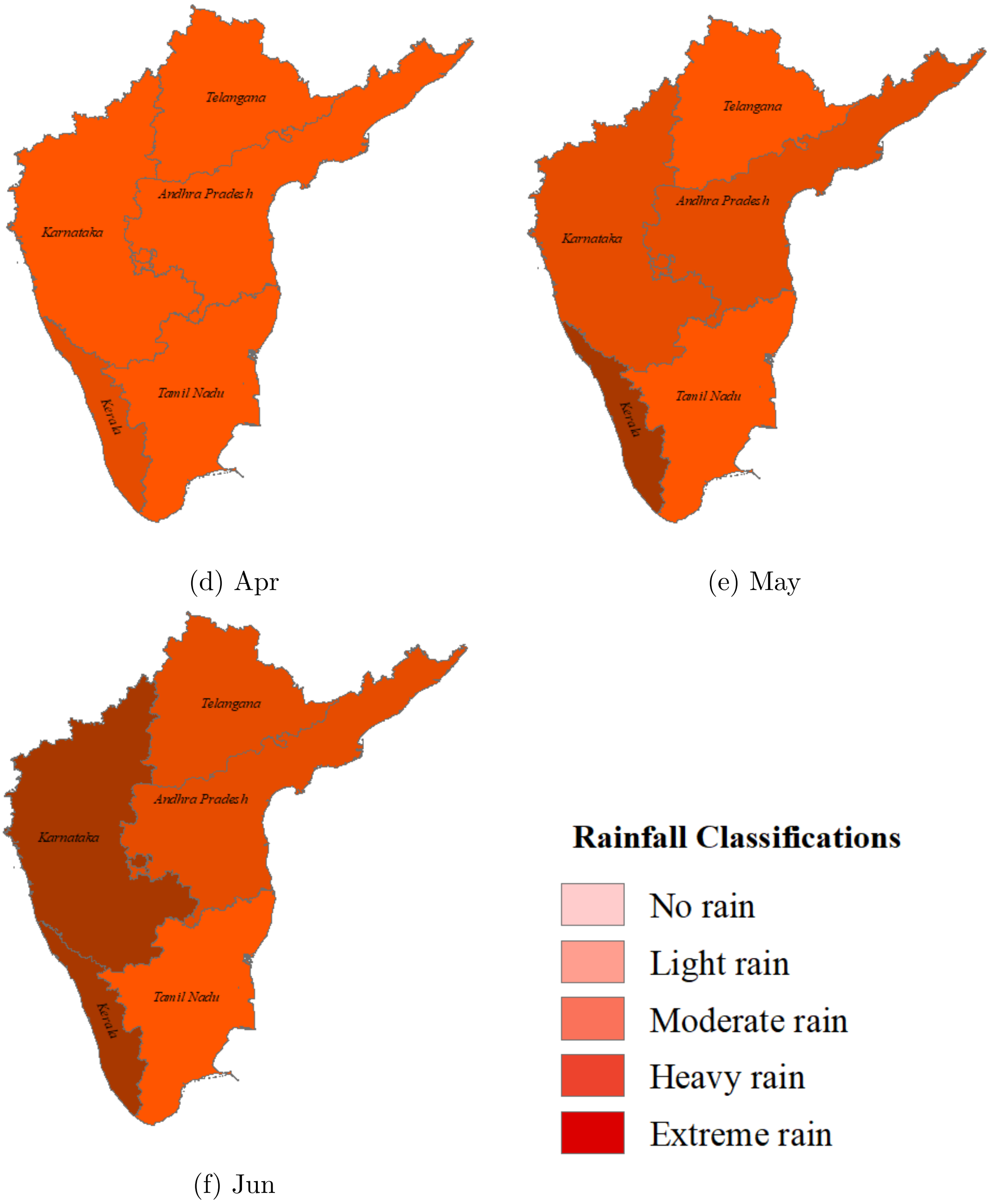

Figure 3.12: Monthly rainfall for the southern region of India in 2025, generated using the Modified Holt Winters method (MOHW) model. The classifications are same as Figure 3.10 (Continued).

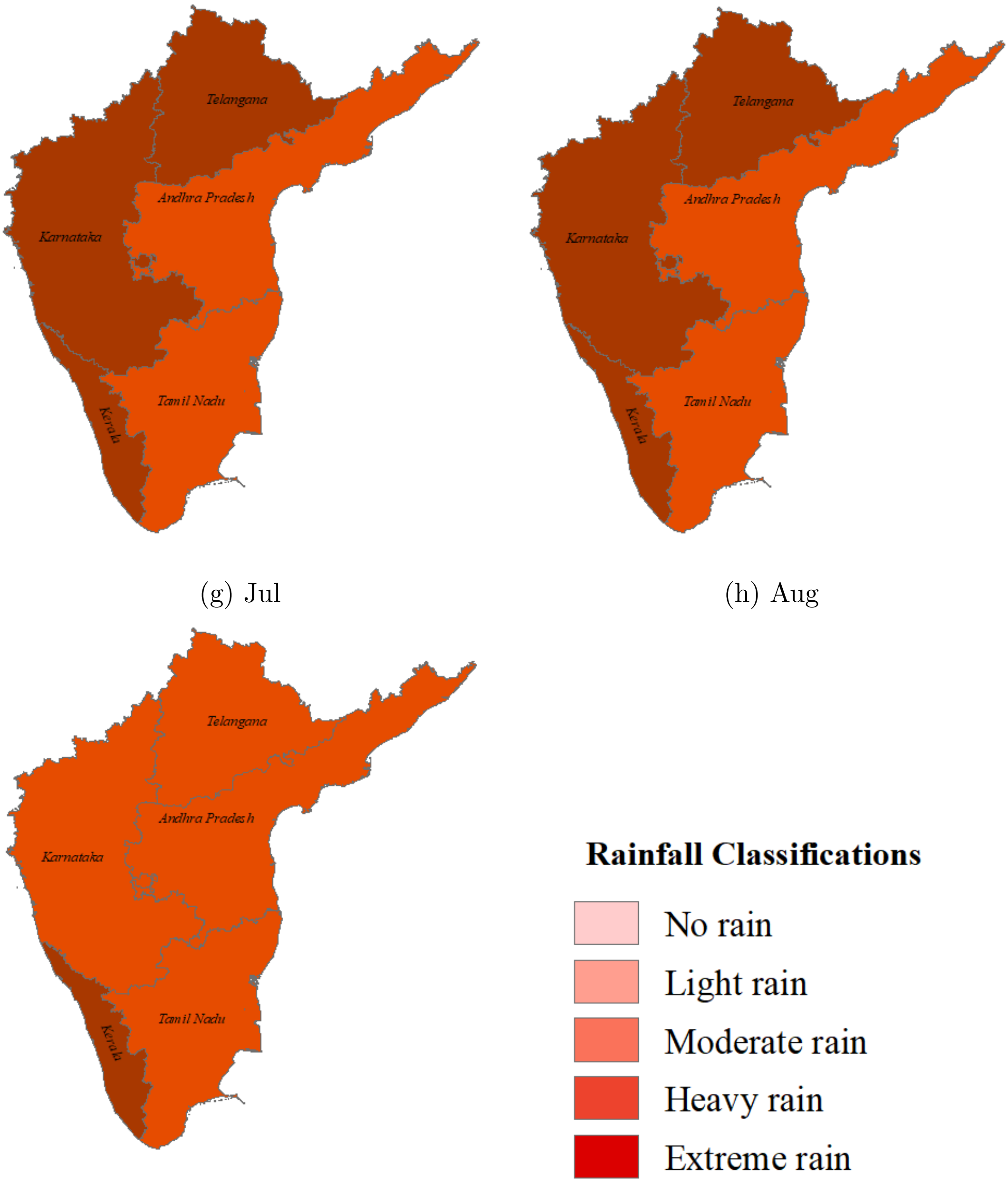

(g) Jul

(h) Aug

(i) Sep

Figure 3.12: Monthly rainfall for the southern region of India in 2025, generated using the Modified Holt Winters method (MOHW) model. The classifications are same as Figure 3.10 (Continued).

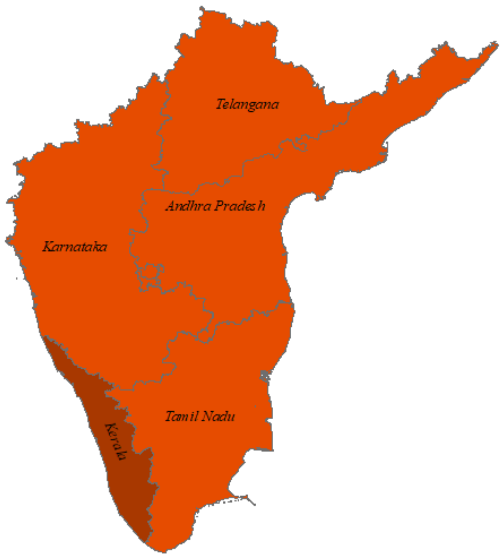

(j) Oct

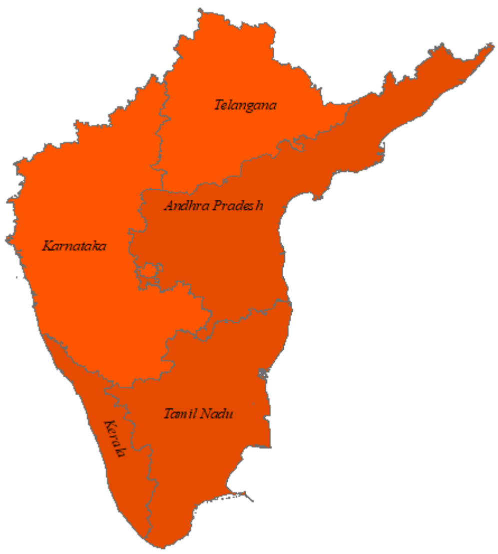

(k) Nov

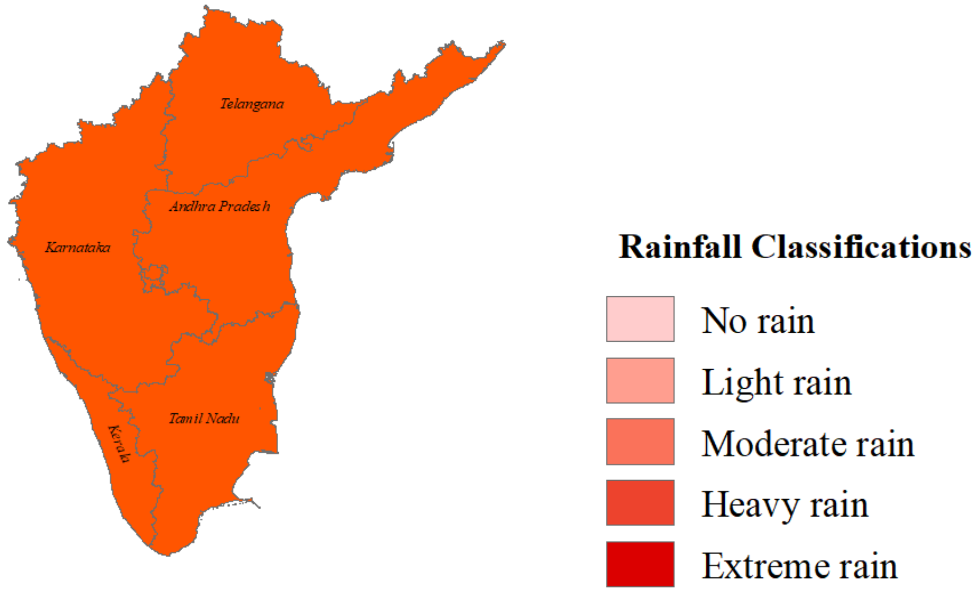

(l) Dec

Figure 3.12: Monthly rainfall for the southern region of India in 2025, generated using the Modified Holt Winters method (MOHW) model. The classifications are same as Figure 3.10.

3.3.5 Comparison of AHW, MHW, MOHW

The results from the application of the AHW, MHW, and MOHW models across South Indian states demonstrate notable variations in forecasting performance (see Table 3.5) and use for forecasting 2025 (see Figure 3.13). For Andhra

Pradesh, the MOHW model achieved the lowest testing RMSE of 43.70, closely followed by the AHW model at 44.04, while the MHW model performed slightly less effectively with an RMSE of 44.02. This suggests that the MOHW model effectively captures the rainfall patterns in the region. In Karnataka, however, the MHW model yielded an exceedingly high RMSE of 329.52, indicating significant challenges in accurately forecasting rainfall, while both the AHW and MOHW models exhibited comparable performance with RMSE values of 67.33 and 67.27, respectively. In Kerala, the MOHW model again outperformed the AHW and MHW models, recording an RMSE of 134.33 compared to 136.85 for the AHW and a much higher 180.51 for the MHW, indicating difficulties in modeling the rainfall dynamics in this state. Tamil Nadu showed similar trends, with the MOHW model yielding the best performance at an RMSE of 50.05, while the AHW and MHW models recorded RMSE values of 53.12 and 53.06, respectively. In Telangana, the MOHW model maintained a competitive edge with an RMSE of 59.69, closely followed by the AHW model at 59.78, while the MHW model presented significant forecasting challenges with a substantially higher RMSE of 909.75. Overall, the MOHW model consistently demonstrated superior forecasting capabilities across most states, outperforming both the AHW and MHW models in terms of RMSE, indicating its effectiveness in capturing the complexities of rainfall patterns in different regions. These results highlight the necessity of selecting the appropriate model based on regional characteristics to enhance rainfall forecasting accuracy.

Table 3.5: Performance evaluation of Holt Winters Methods.

State	Model	Smoothing Parameters			Goodness Criteria				
		α	β	γ	Training RMSE	RMSE	MAE	AIC	BIC
Andhra Pradesh	AHW	0.10	0.00	0.10	48.28	44.04	29.67	952.25	960.73
	MHW	0.10	0.00	0.10	55.25	44.02	29.64	952.16	960.65
	MOHW	0.10	1.00	0.10	48.58	43.70	29.74	950.35	958.84
Karnataka	AHW	0.10	0.00	0.20	65.89	67.33	46.09	1058.40	1066.89
	MHW	0.10	0.00	0.20	136.75	329.52	117.60	1455.41	1463.89
	MOHW	0.10	1.00	0.20	65.87	67.27	46.01	1058.16	1066.65
Kerala	AHW	0.10	0.00	0.20	120.93	136.85	92.19	1235.72	1244.20
	MHW	0.10	0.00	0.90	141.64	180.51	103.27	1304.94	1313.43
	MOHW	0.10	1.00	0.10	121.71	134.33	90.10	1231.08	1239.57
Tamil Nadu	AHW	0.10	0.00	0.20	51.12	53.12	33.70	999.16	1007.64
	MHW	0.10	0.00	0.10	58.48	53.06	33.80	998.85	1007.33
	MOHW	0.10	1.00	0.20	51.21	50.05	33.36	984.28	992.76
Telangana	AHW	0.10	0.00	0.20	61.26	59.78	40.35	1028.66	1037.15
	MHW	0.90	0.00	0.80	32 591.01	909.75	483.75	1709.29	1717.78
	MOHW	0.10	1.00	0.20	61.23	59.69	40.36	1028.29	1036.78

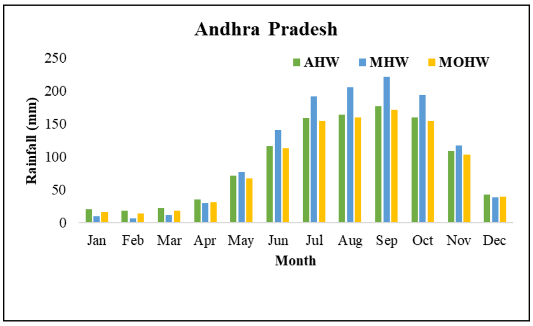

(a)

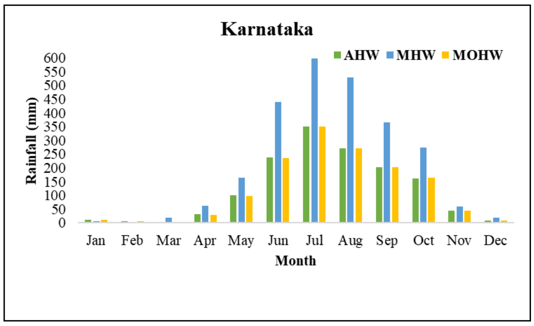

(b)

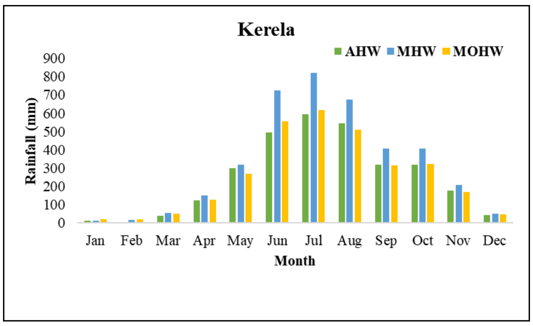

(c)

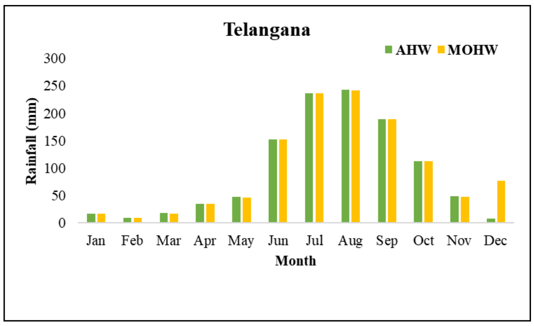

(d)

Figure 3.13: Comparison of monthly rainfall predictions for the southern region of India in 2025 using AHW, MHW, and MOHW. The Multiplicative Holt Winters method (MHW) for Telangana is excluded from the comparison due to its high RMSE value, reflecting its lower predictive accuracy compared to the other models (Continued).

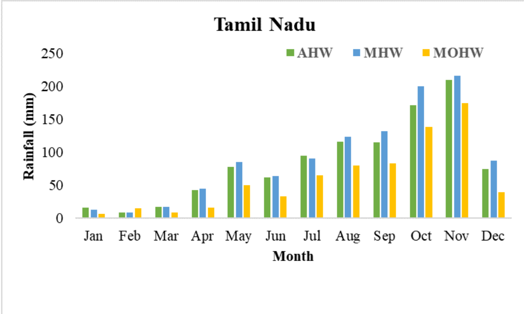

(e)

Figure 3.13: Comparison of monthly rainfall predictions for the southern region of India in 2025 using AHW, MHW, and MOHW. The Multiplicative Holt Winters method (MHW) for Telangana is excluded from the comparison due to its high RMSE value, reflecting its lower predictive accuracy compared to the other models.

3.4 Summary

The Holt Winters method, developed by Charles Holt and Peter Winters, is a widely used exponential smoothing technique for identifying patterns in changing levels, trends, and seasonal variations. In this study, we introduced the Modified Holt Winters Method (MOHW) to enhance the existing approach and compared its performance with the Additive Holt Winters (AHW) and Multiplicative Holt Winters (MHW) methods using historical rainfall data. Our analysis demonstrates that the MOHW method delivers superior forecasting performance, achieving the lowest RMSE, MAE, AIC, and BIC values during both training and testing phases. The AHW model performed well in Andhra Pradesh, Karnataka, Kerala, Tamil Nadu, and Telangana. While the MHW performed well in Andhra Pradesh but not suitable for States like Mizoram, Telangana, and Karnataka. Overall, in the study area, MOHW performed considerately well, whereas AHW is more suitable compared to MHW for forecasting rainfall but falls behind MOHW in terms of their accuracy. Our findings highlight the fact that MHW is not suitable for rainfall forecasting in our study area.

Chapter 4

An Innovative Long Range Forecast Model for Monthly Rainfall

4.1 Introduction

Regression methods have been widely used in rainfall forecasting across various regions (Ahasan *et al.*, 2010; Islam *et al.*, 2017; Sarkar *et al.*, 2023; Agrawal *et al.*, 2024). Similarly, Fourier series have proven to be highly effective in modeling and predicting the seasonal and periodic variations of rainfall patterns (Jou and Mirhashemi, 2023). However, existing methods often fail to fully capture the complex interactions between trend, cyclic, and random components, leading to limitations in forecasting accuracy. To address this gap, we propose a novel framework called the Innovative Rainfall Predictive Method (IRPM), which integrates Linear Regression, Fourier analysis, and a probabilistic approach. By incorporating trend, cyclic, and random components, IRPM provides a more comprehensive and robust methodology for rainfall forecasting, improving prediction reliability. This chapter focuses on conducting a long range trend analysis of historical rainfall data for Mizoram and meteorological sub-divisions of India using well-established techniques such as the Mann-Kendall (MK) test, Sen's slope, and

Innovative Trend Analysis (ITA). These methods will also be applied to detect future trends in monthly forecasted rainfall. Furthermore, the IRPM framework will be utilized to generate monthly rainfall forecasts, offering a data-driven approach to understanding long range rainfall patterns.

4.2 Monthly Rainfall Forecasting for Districts of Mizoram Using IRPM

In this section, we introduce a new approach called the Innovative Rainfall Predictive Method (IRPM) for rainfall forecasting. First, we analyse the collected data and identify trends using the Mann-Kendall test, Sen's slope, and Innovative Trend Analysis. Next, we apply IRPM for forecasting and validate the model using a modified K-fold cross-validation. Finally, we use the model to predict rainfall for the upcoming years and identify trends in the forecasted data.

4.2.1 Study Area and Data Collection

Mizoram is one of the seven northeastern states of India, located between latitudes 21°58'N and 24°35'N and longitudes 92°15'E and 93°29'E (see Figure 4.1). Covering a total area of 21,081 square kilometers, approximately 86.27% of the land is covered by dense forests, with the remainder consisting of moderately dense and open forests. However, this forest cover is gradually diminishing due to shifting cultivation practices and other developmental activities. Agriculture is the main livelihood for the majority of the population. Mizoram shares international borders with Myanmar (404 km) and Bangladesh (318 km), along with borders with three northeastern states: Assam (123 km), Tripura (66 km), and Manipur (95 km). Temperatures in Mizoram can exceed 30°C during the summer, while in winter they range from 7°C to 22°C, it experiences mild summers, with temperatures typically between 20°C and 29°C and its annual average rainfall is

Muniyan, S. and Lallawmzuali, M. (2026). Monthly Rainfall Forecasting in the Districts of Mizoram Using the Innovative Rainfall Predictive Method and Trend Analysis with Mann-Kendall and Innovative Trend Analysis. *Environmental Modeling & Assessment*, 1-26.

around 2,056.8 mm. For this study, we are considering eight districts of Mizoram i.e. Aizawl, Champhai, Kolasib, Lawngtlai, Lunglei, Mamit, Saiha, and Serchhip. Historical monthly rainfall data spanning 38 years (1986–2023) has been collected for each district. However, due to the unavailability of earlier records, rainfall data for Mamit is available only for a 24-year period (2000–2023). All data has been sourced from the State Meteorological Centre, Directorate of Science and Technology, Government of Mizoram.

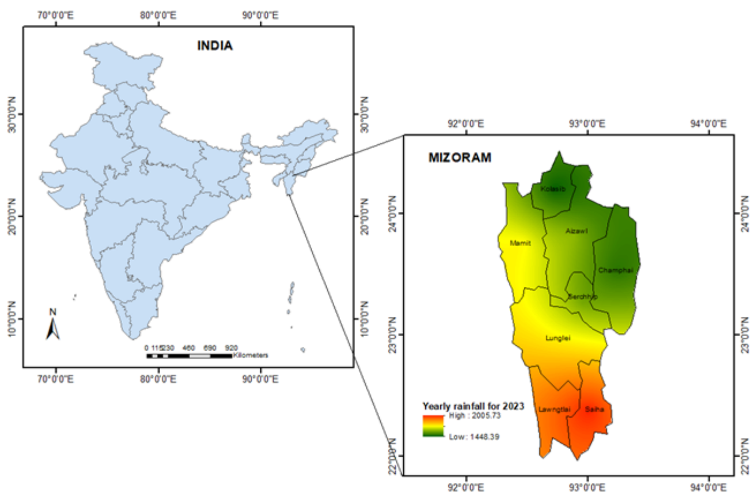

Figure 4.1: The location of the Study Area showing districts of Mizoram.

4.2.2 Analysis of Monthly Rainfall Statistics for Different Districts of Mizoram

Before conducting trend analysis, a preliminary statistical assessment is performed to estimate key statistical parameters of monthly rainfall data for the period 1986–2023 of Mizoram. This analysis provides insights into the variability and distribution of rainfall across different months and districts in Mizoram. Skewness, a measure of asymmetry in the frequency distribution of a dataset relative to its mean, is calculated for each month's rainfall series. The results reveal that all monthly rainfall series exhibit positive skewness, except for August in the districts of Mamit (-0.11), Champhai (-0.13), and Serchhip (-0.18).

The skewness values for monthly rainfall range from -0.18 to 5.41, indicating significant variation in distribution patterns. To analyze rainfall variability across different districts, the coefficient of variation (CV) technique is employed. The CV, expressed as a percentage, quantifies relative dispersion in rainfall by normalizing the standard deviation with respect to the mean. Figure 4.2 presents a spatial mapping of monthly rainfall variation over Mizoram, generated using the ordinary kriging interpolation method—a geostatistical approach that estimates rainfall values at unobserved locations based on spatial autocorrelation. The analysis highlights that the least rainfall fluctuation occurs in Aizawl during August (21.39%), followed by Aizawl in July (28.98%) and Kolasib in June (29.06%). Conversely, the highest rainfall variability is observed in Lawngtlai in February (246.04%), followed by Mamit in December (228.41%). These findings indicate spatial variability in rainfall distribution, which is crucial for understanding regional hydrological patterns and improving forecasting models.

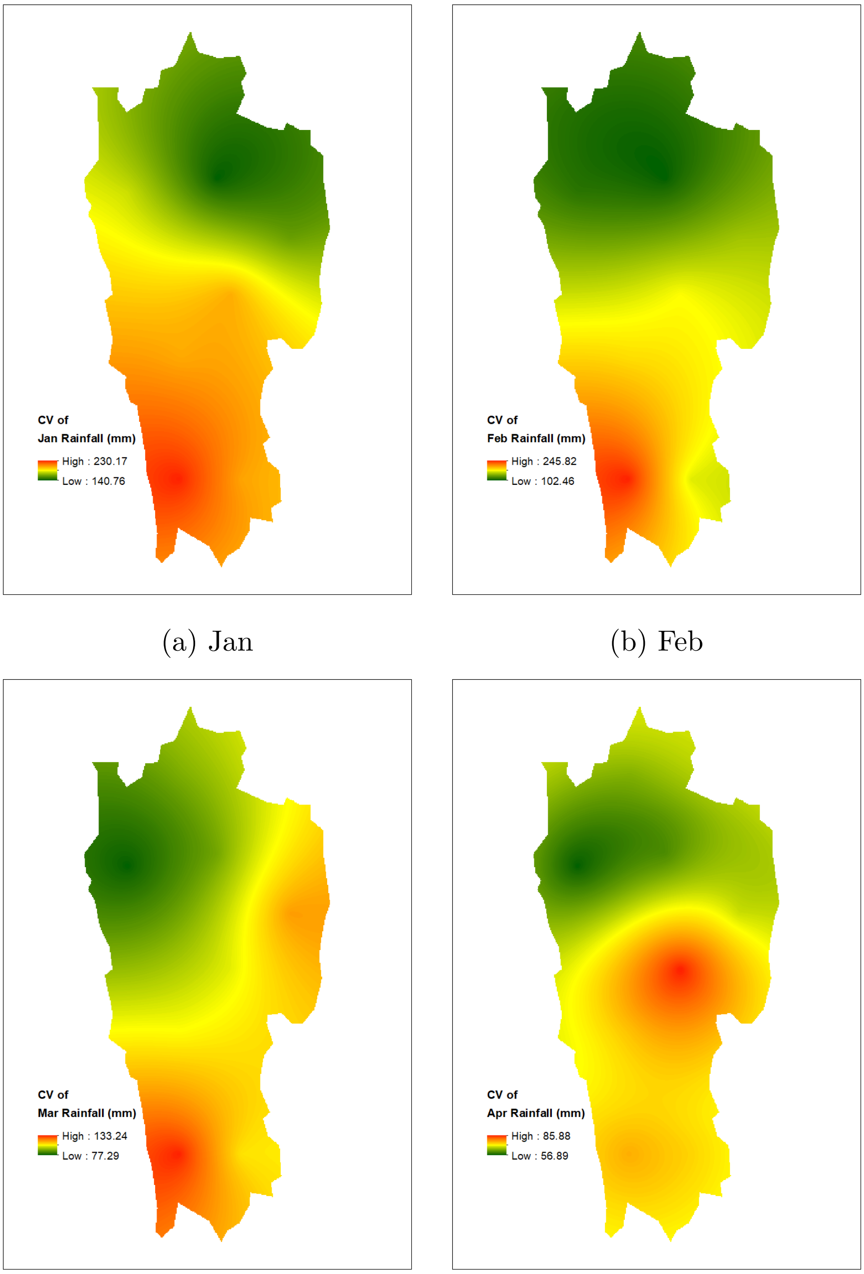

(a) Jan (b) Feb

(c) Mar (d) Apr

Figure 4.2: Spatial variation of rainfall measured using the coefficient of variation for monthly rainfall of districts of Mizoram (1986-2023) (Continued).

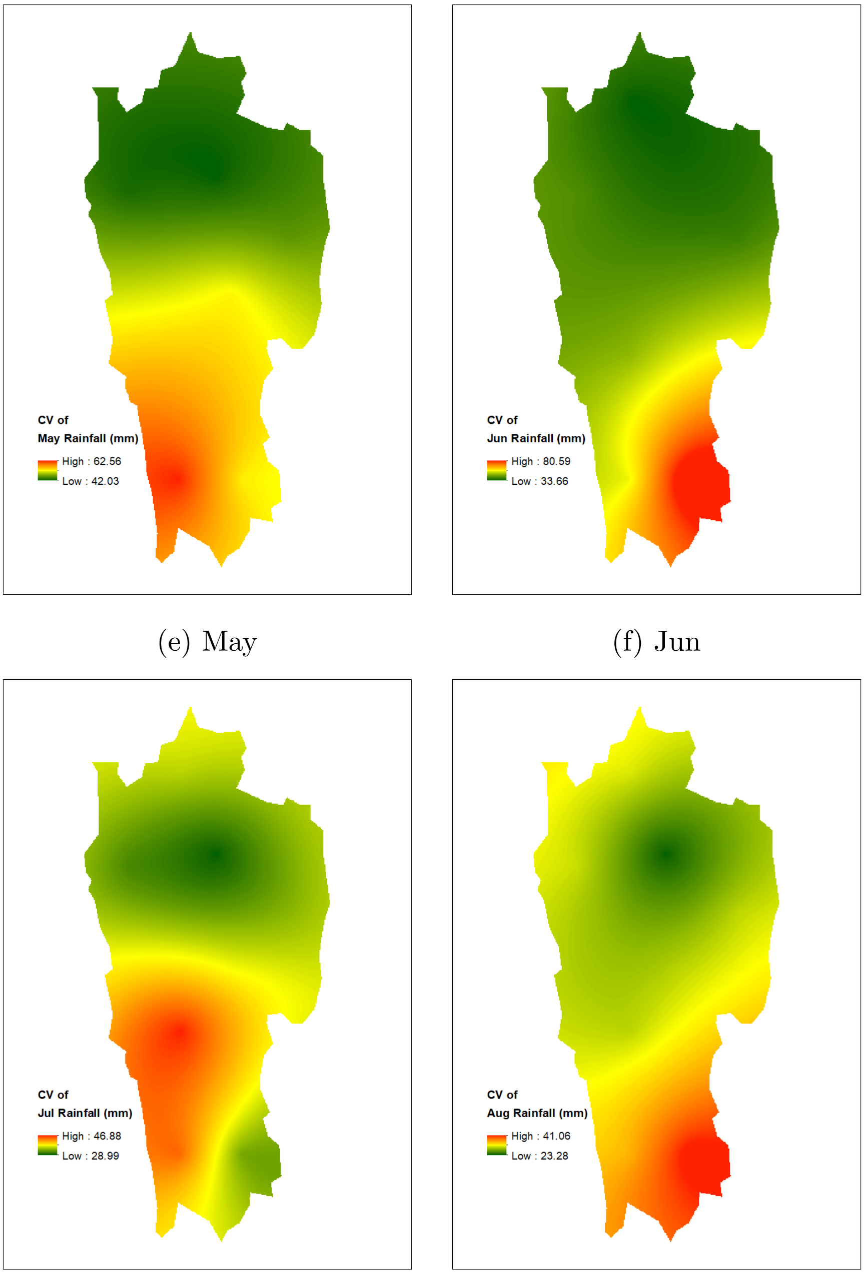

(e) May (f) Jun

(g) Jul (h) Aug

Figure 4.2: Spatial variation of rainfall measured using the coefficient of variation for monthly rainfall of districts of Mizoram (1986-2023) (Continued).

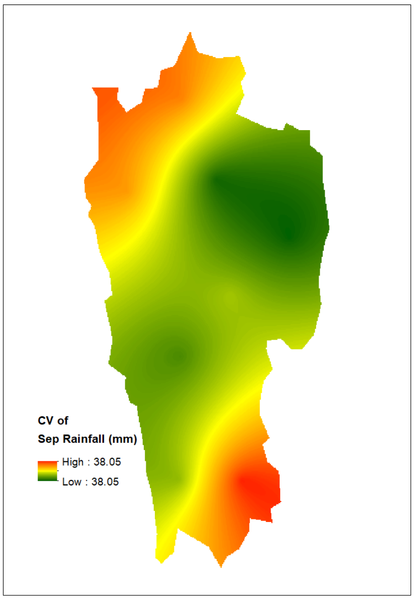

(i) Sep

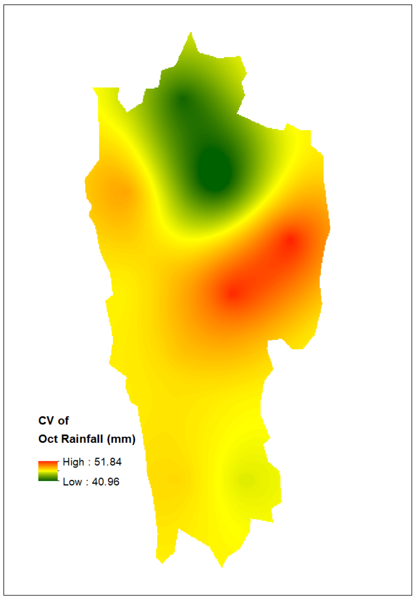

(j) Oct

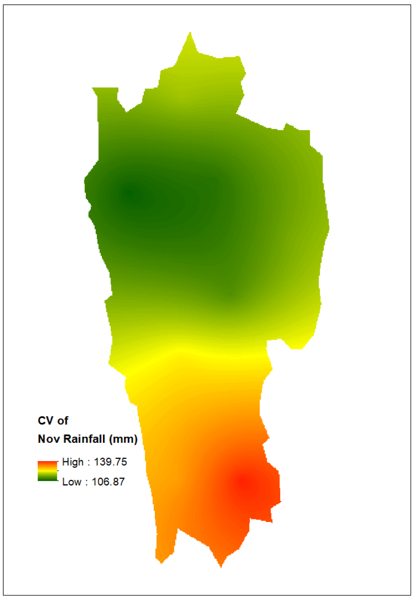

(k) Nov

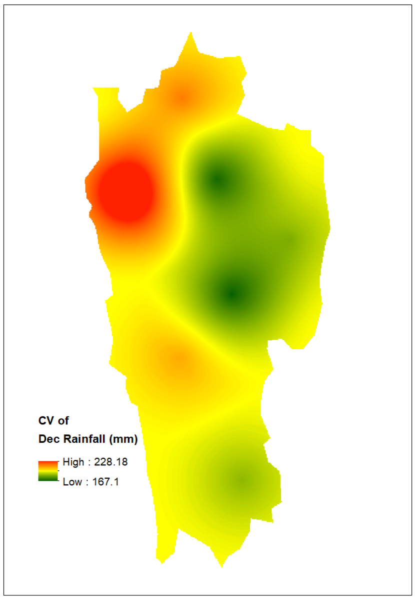

(l) Dec

Figure 4.2: Spatial variation of rainfall measured using the coefficient of variation for monthly rainfall of districts of Mizoram (1986-2023).

4.2.3 Trend Analysis of Monthly Rainfall

4.2.3.1 Using Mann-Kendal Test and Sen's Slope

The monthly rainfall trends across different districts in Mizoram were examined using the non-parametric Mann-Kendall (MK) test and Sen's slope estimator (Figure 4.4). This analysis, conducted over the period from 1986 to 2023 (at 95% confidence level) are summarized in Table 4.1 and Table 4.2. The findings highlight considerable variation in rainfall trends across different months, with some areas experiencing an increase while others show a decline. However, most of these observed trends are not statistically significant. In the MK test, a trend is considered statistically significant if the absolute Z-value ($|Z|$) exceeds 1.96. A negative Z-value represents a significant decreasing trend, whereas a positive Z-value indicates a significant increasing trend. Conversely, Z-values within the range of $|Z| \leq 1.96$ suggest that the observed trend is not statistically significant. The results of the Mann-Kendall test and Sen's slope analysis for rainfall trends in Mizoram indicate varying trends across districts and months. Aizawl's rainfall exhibits a decreasing trend throughout the year, with only February (Z = -3.19) and September (Z = -2.41) showing a statistically significant decline. The corresponding Sen's slope values further confirm this decline, with the most substantial decrease occurring in September (Q = -3.12), indicating a notable reduction in rainfall over time. Kolasib shows a decreasing trend for all months except December, with the strongest negative Z-values recorded in October (Z = -2.59) and February (Z = -2.53), indicating statistically significant declines. The Sen's slope values align with this trend, showing the steepest reductions in June (-3.68) and October (-3.54), signifying substantial declines in rainfall magnitude. Lunglei presents mixed results, with a slight increasing trend in January and December. However, March, April, and October exhibit significant decreasing trends, with October showing the most pronounced decline in rainfall (Q = -3.42). Champhai consistently shows a declining rainfall trend throughout the year, except in December, with a particularly strong decrease in February

(Z = -3.92), which is further confirmed by a substantial negative Sen's slope value. Lawngtlai exhibits a moderate decreasing trend, with statistically significant declines observed in June (Z = -2.20) and November (Z = -2.26). Serchhip experiences one of the most pronounced decreasing trends, with strong negative Z-values throughout the year, particularly in August (Z = -3.22) and February (Z = -2.93). The Sen's slope values indicate sharp declines in rainfall, most notably in July (Z = -5.76) and August (Z = -5.31), highlighting a substantial reduction in rainfall magnitude. Mamit, unlike most other districts, shows a significant increasing trend in December (Z = 2.09), suggesting a potential rise in rainfall during this period. Lastly, Saiha exhibits weak fluctuations, with slight increases in June (Q = 0.51), July (Q = 0.48), August (Q = 1.24) and December ($Q = 0$), although none of these trends are statistically significant. However, a significant decline is observed in November (Z = -2.18). Overall, the results suggest a general decline in rainfall across most districts. The months of March, April, May, and October show a consistent decreasing trend across all districts, with a gradual decline in slope magnitude. However, Mamit is the only district that exhibits a significant increase in December. Figure 4.3 shows a spatial mapping of MK values.

Table 4.1: Results of Mann–Kendall analysis of monthly rainfall of districts of Mizoram (1986–2023).

District	**Jan**	**Feb**	**Mar**	**Apr**	**May**	**Jun**	**Jul**	**Aug**	**Sep**	**Oct**	**Nov**	**Dec**
Aizawl	−0.68	−3.19*	−1.82	−1.76	−1.16	−1.06	−1.73	−0.75	−2.40*	−1.99	−1.52	−0.29
Kolasib	0.66	−2.53*	−2.31*	−0.79	−0.10	−2.00*	−1.13	−0.73	−1.08	−2.59*	−2.03*	0.70
Lunglei	0.77	−1.05	−2.17*	−2.04*	−1.51	0.05	−1.71	−0.80	−1.43	−2.61*	−1.26	1.13
Champhai	−0.14	−3.92*	−1.52	−1.72	−0.68	−2.43*	−0.84	−2.10*	−2.92*	−2.06*	−0.87	0.19
Lawngtlai	−0.29	0.48	−0.98	−1.53	−0.96	−2.2 *	−1.53	−0.65	−1.53	−1.45	−2.62*	1.96
Serchhip	0.49	−2.93*	−2.77*	−2.51*	−1.71	−2.48*	−2.68*	−3.22*	−2.77*	−2.75*	−2.44*	−0.40
Mamit	0.18	−0.98	−2.23*	−1.71	−2.31	−1.31	0.82	−1.51	−1.41	−0.57	0.68	2.09*
Saiha	−0.64	−1.44	−0.94	−0.99	−0.48	0.18	0.28	0.48	0.67	−0.06	−2.18*	0.86

***** indicates statistical significance

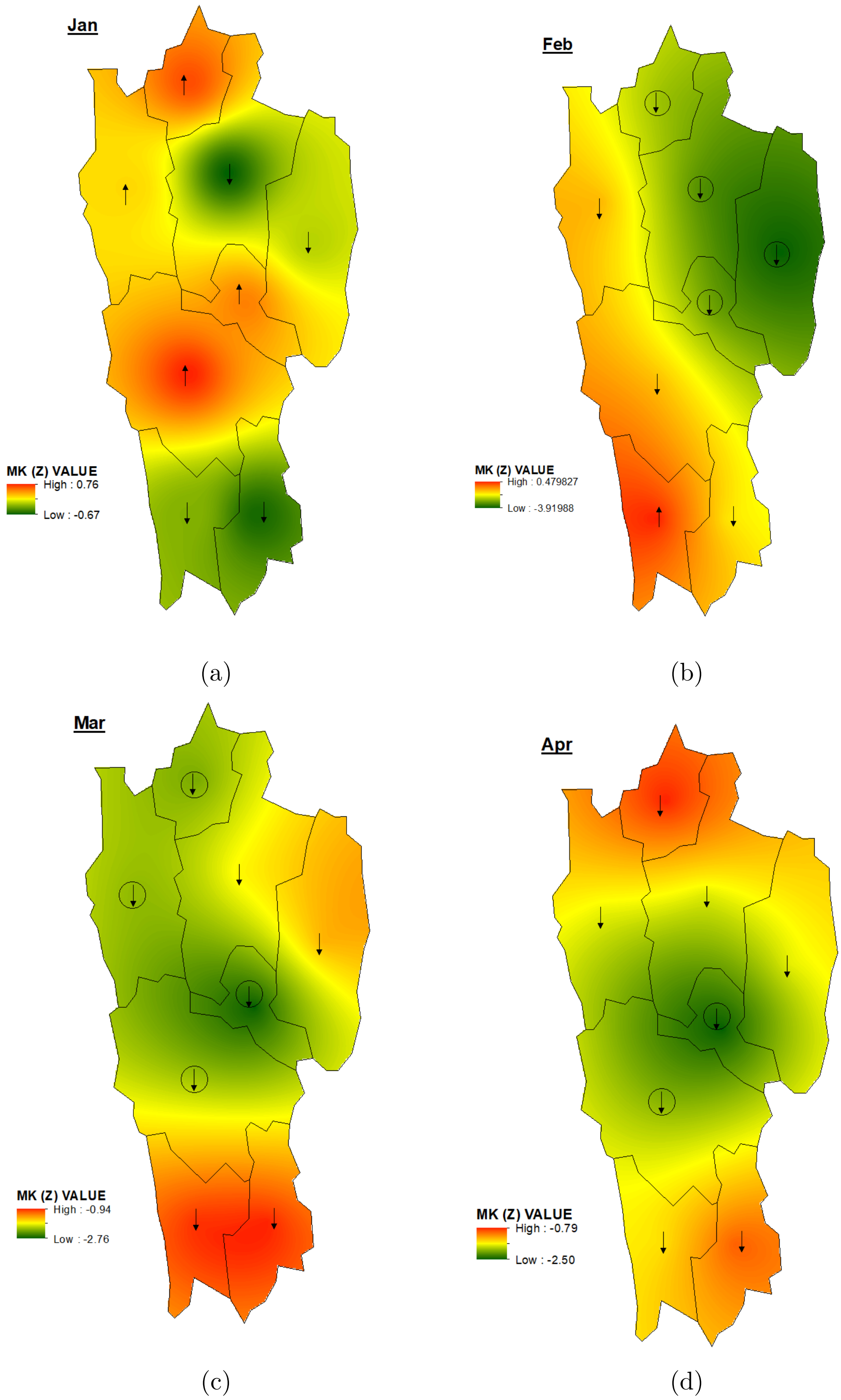

Figure 4.3: Spatial distribution of Monthly rainfall trends over Mizoram from 1986 to 2023 using the Mann-Kendall test. ↑: increasing trend; ↓: decreasing trend; ○: significant at 95% confidence (Continued).

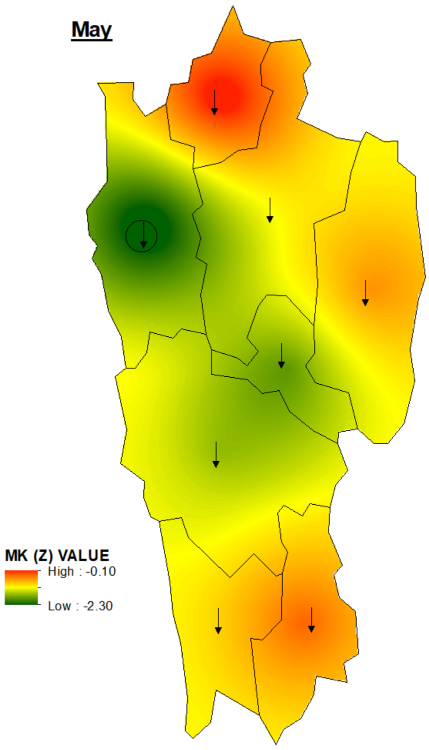

(e)

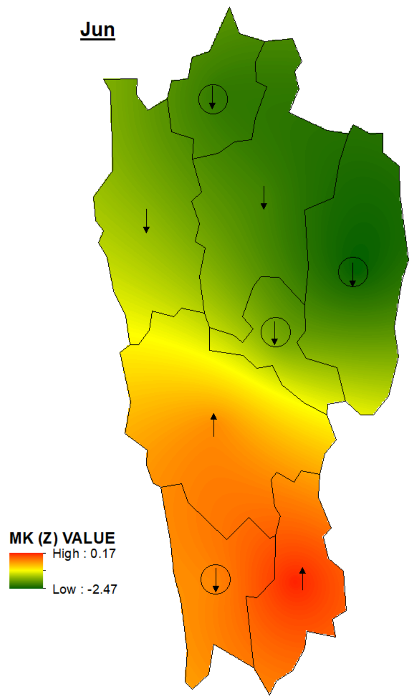

(f)

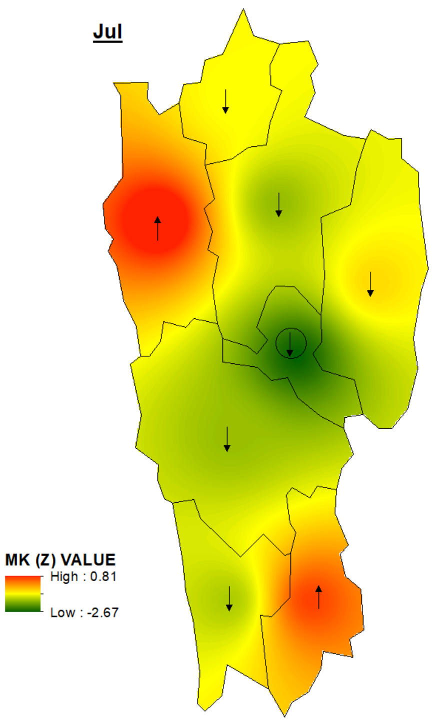

(g)

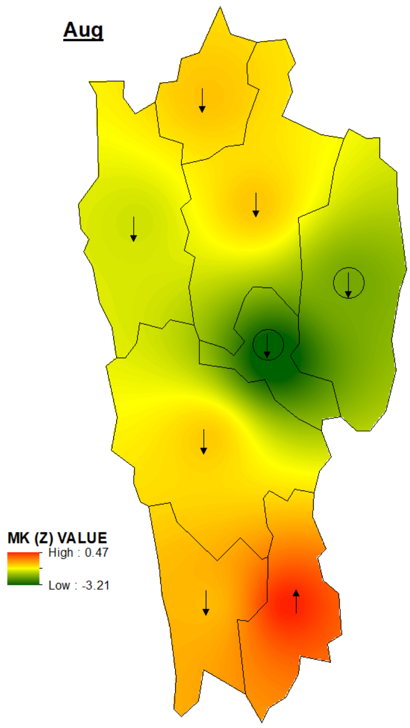

(h)

Figure 4.3: Spatial distribution of Monthly rainfall trends over Mizoram from 1986 to 2023 using the Mann-Kendall test. ↑: increasing trend; ↓: decreasing trend; ○: significant at 95% confidence (Continued).

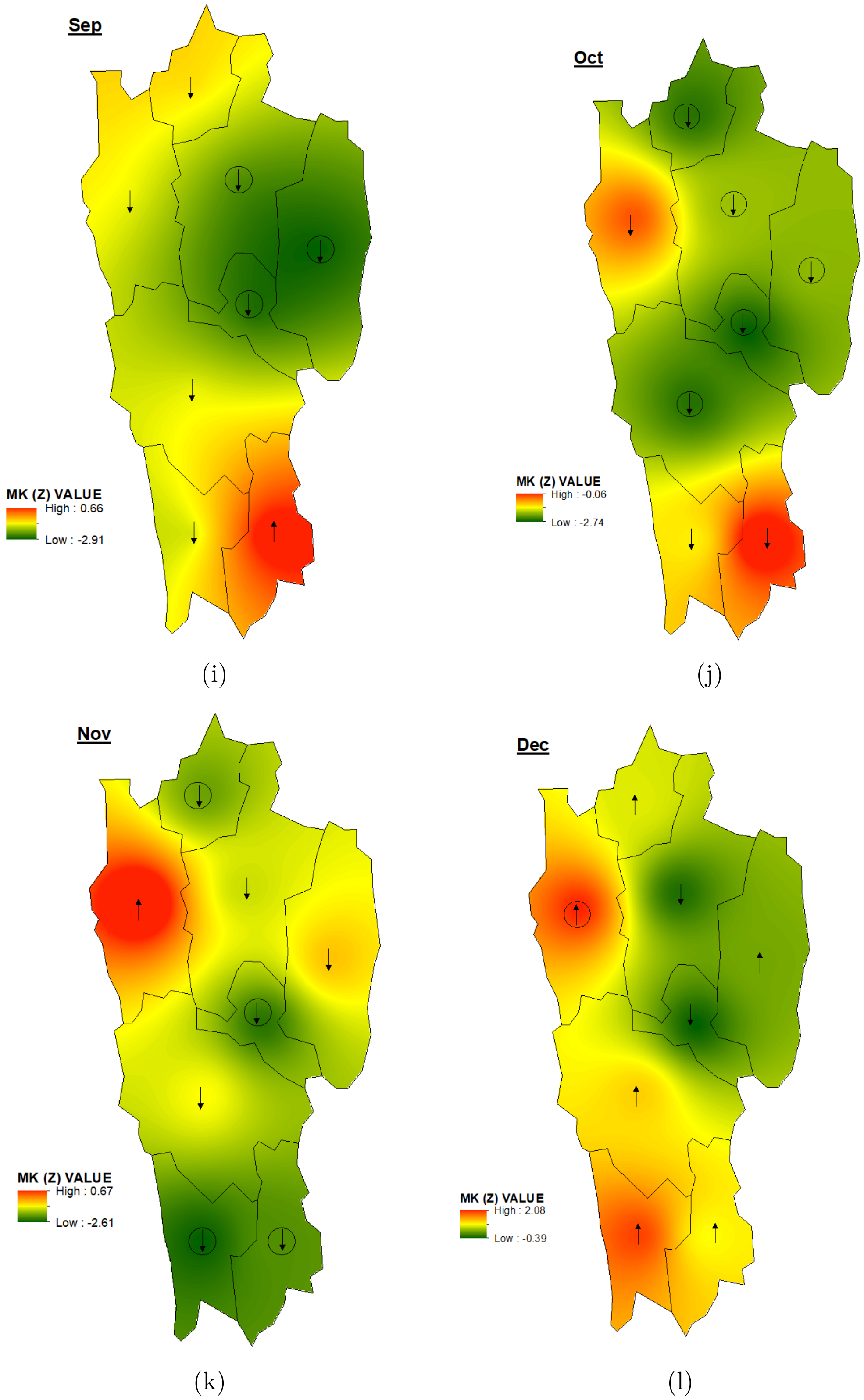

Figure 4.3: Spatial distribution of Monthly rainfall trends over Mizoram from 1986 to 2023 using the Mann-Kendall test. ↑: increasing trend; ↓: decreasing trend; ○: significant at 95% confidence.

Table 4.2: Results of Sen's Slope value of Monthly Rainfall of Districts of Mizoram (1986-2023).

District	**Jan**	**Feb**	**Mar**	**Apr**	**May**	**Jun**	**Jul**	**Aug**	**Sep**	**Oct**	**Nov**	**Dec**
Aizawl	0	0.86	−1.37	−2.07	−2.55	−2.02	−2.74	−0.99	−3.12	−2.48	−0.71	0
Kolasib	0	−1.04	−2.00	−1.41	−0.38	−3.68	−2.53	−1.53	−2.83	−3.54	−0.16	0
Lunglei	0	−0.01	−1.22	−2.27	−3.20	0.04	−3.33	−1.55	−2.57	−3.42	−0.47	0
Champhai	0	−0.30	−0.74	−1.77	−1.3	−3.42	−1.33	−3.34	−3.96	−2.73	−0.41	0
Lawngtlai	0	0	−0.45	−1.50	−2.29	−4.31	−3.43	−1.21	−2.79	−2.46	−1.60	0
Serchhip	0	−0.56	−2.40	−3.76	−4.88	−5.76	−5.31	−5.09	−2.76	−1.61	0	
Mamit	0	−0.31	−3.66	−6.32	−12.06	−6.48	2.87	−7.1	−5.07	−1.54	0.04	0
Saiha	0	0	−0.47	−0.99	−1.58	0.51	0.48	1.24	1.16	−0.22	−1.26	0

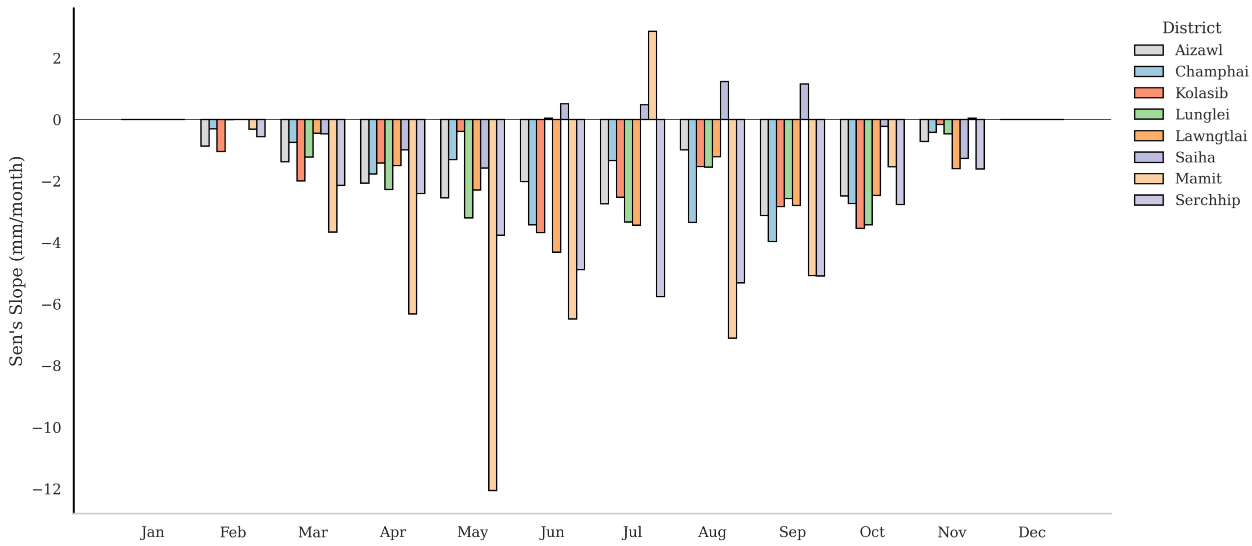

Figure 4.4: Sen's Slope results of monthly rainfall of Mizoram (1986-2023).

4.2.3.2 Using Innovative Trend Analysis

In the Innovative Trend Analysis (ITA), a slope value falling between the lower and upper limits indicates no trend. Conversely, a slope value exceeding the upper limit signifies an increasing trend, while a slope below the lower limit represents a decreasing trend at a 95% confidence level. In Aizawl, ITA slopes remain below the lower limit for all months except December, indicating a decreasing trend. December, however, exhibits no significant trend. The ITA slopes remain below the lower limit for all months, confirming a consistent decreasing trend for Champhai. In Kolasib, a decreasing trend is observed in all months except May and December, where the slope values lie between the upper and lower limits, indicating no trend. In Lunglei, no trend is detected in January, August, September, and December, while the remaining months exhibit a decreasing trend. In Lawngtlai, August displays a slope above the upper limit, signifying an increasing trend, while December shows no trend. The remaining months indicate a decreasing trend. In Saiha, no trend is observed in January, March, July, and December, as their slope values fall within the defined limits. The other months show a mix of increasing and decreasing trends, with June exhibiting the highest slope value (D = 9.03). A decreasing trend is present in all months for Serchhip except January, which shows no trend. In Mamit, a combination of increasing and decreasing trends is observed, while June, July, and October exhibit no trend. Overall, based on the ITA, 76.04% of the data exhibits a decreasing trend, 7.29% shows an increasing trend, and 16.67% indicates no trend. The graphical trend results obtained from ITA are presented in Figure 4.5 - 4.8.

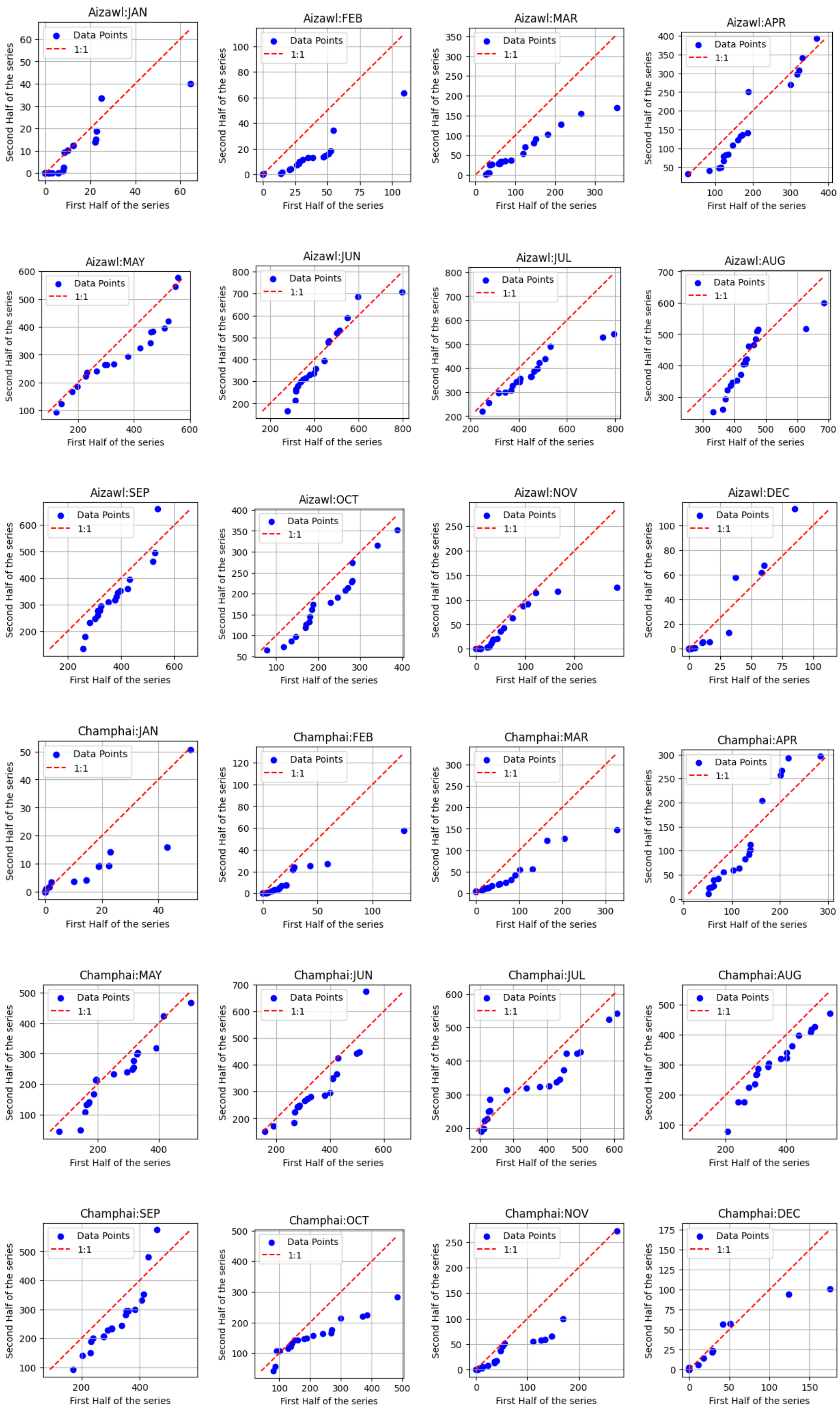

Figure 4.5: ITA results of monthly rainfall in Aizawl and Champhai from 1986-2023.

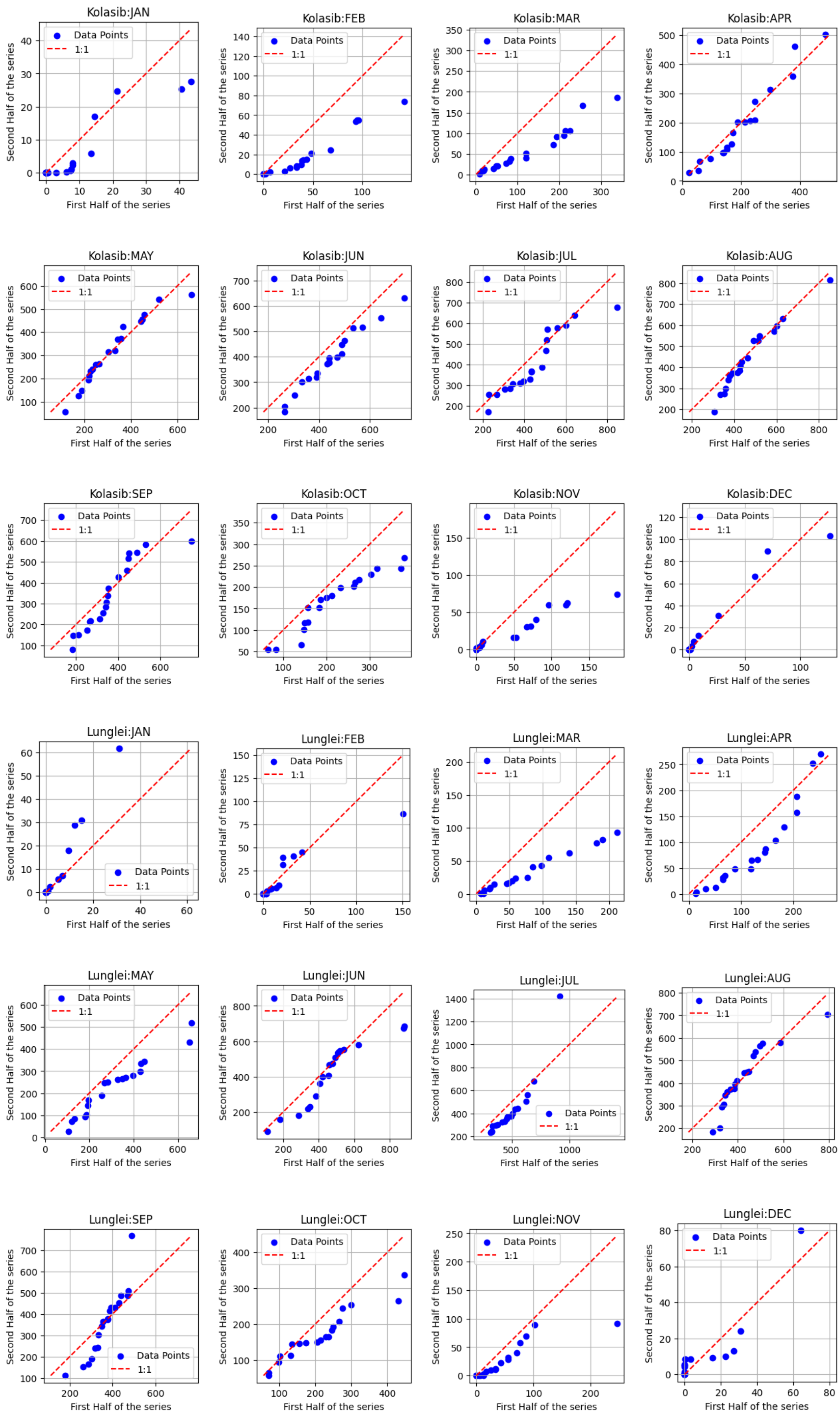

Figure 4.6: ITA results of monthly rainfall in Kolasib and Lunglei from 1986-2023.

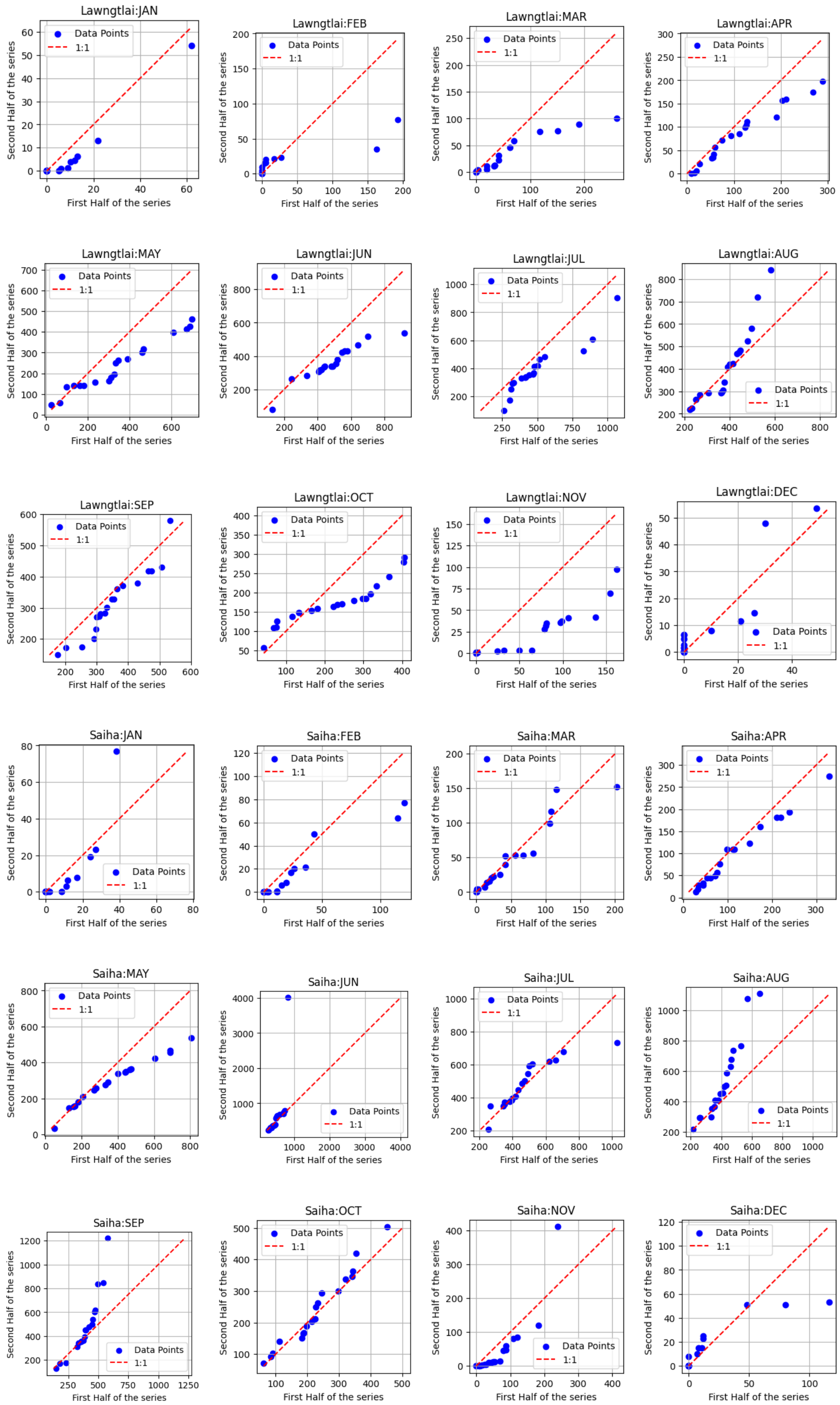

Figure 4.7: ITA results of monthly rainfall in Lawngtlai and Saiha (1986-2023).

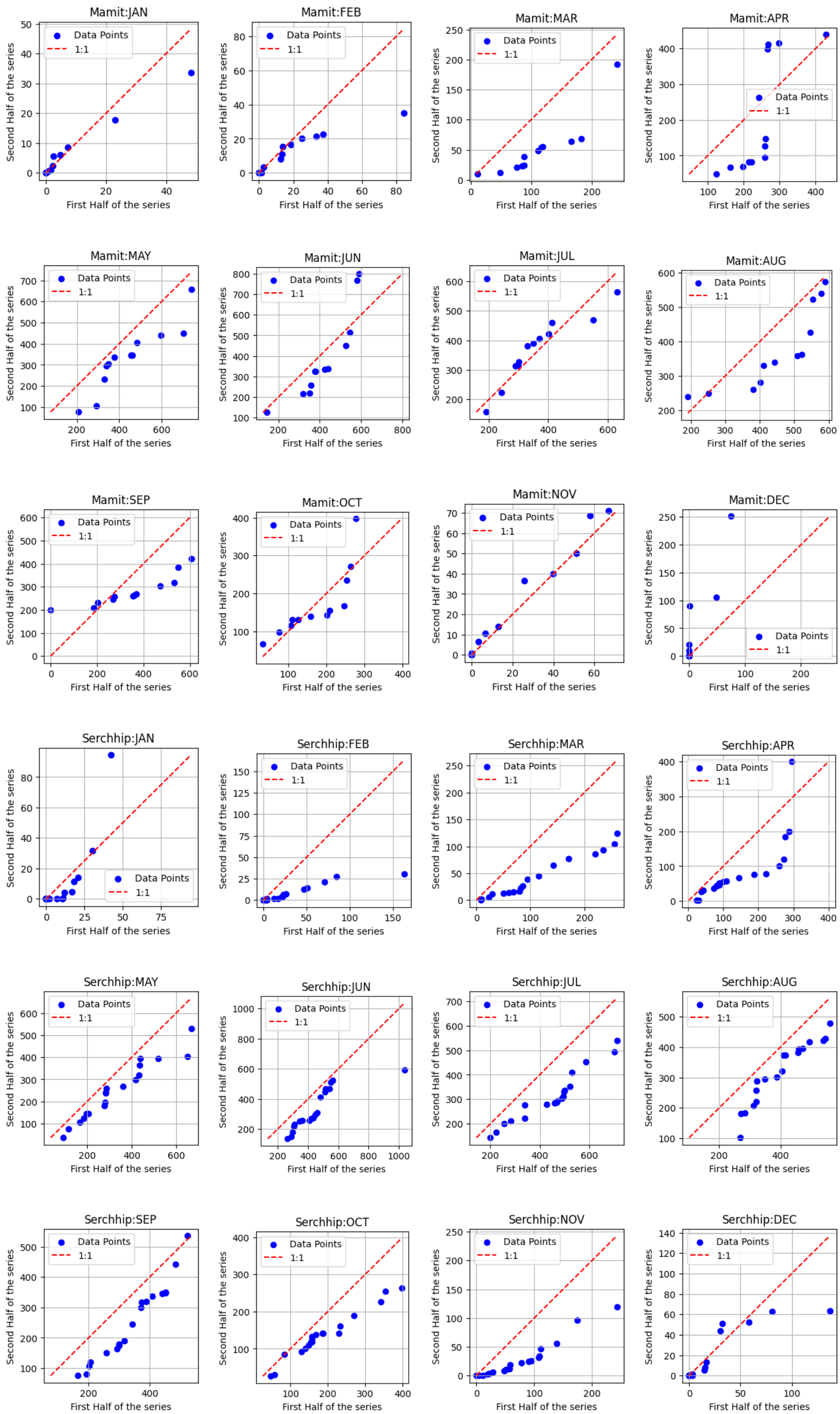

Figure 4.8: ITA results of monthly rainfall in Mamit and Serchhip (1986-2023).

4.2.3.3 Comparison of Trend Analysis

The results of the Mann-Kendall (MK) and Innovative Trend Analysis (ITA) tests for each district's rainfall are presented Figure 4.9. A comparison of these figure reveals notable differences between the two methods. According to the MK test, 79 months (82.29%) exhibit a decreasing trend, while 17 months (17.71%) show an increasing trend. In contrast, the ITA test indicates that 76.04% of the data follows a decreasing trend, 7.29% shows an increasing trend, and 16.67% exhibits no trend. Discrepancies between the two methods are evident in several cases. For example, in Aizawl, December shows a decreasing trend according to the MK test but no trend in the ITA test. Similar inconsistencies are observed in January and March in Saiha, August and September in Lunglei, and October in Mamit. Additionally, in Kolasib, January is classified as having an increasing trend based on the MK test but no trend according to ITA. The same pattern is observed in Lunglei (January), Lawngtlai (December), Serchhip (January), and Saiha (July and December). Despite these variations, both methods consistently indicate that rainfall is generally decreasing across all districts.

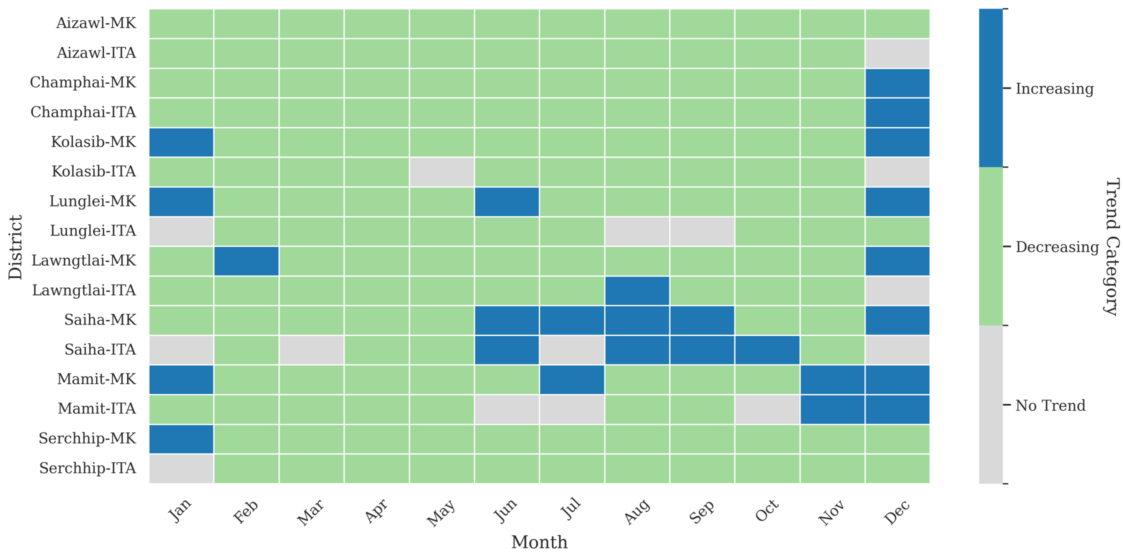

Figure 4.9: Comparison of monthly rainfall trends across the districts of Mizoram using the Mann-Kendall (MK) and Innovative Trend Analysis (ITA) methods.

4.2.4 Rainfall Prediction Using IRPM

Accurate rainfall forecasting is crucial for effective water resource management, agricultural planning, and disaster preparedness, particularly in regions with substantial seasonal variations. This study employs the Innovative Rainfall Predictive Method (IRPM) to forecast district-wise rainfall in Mizoram for the period 2024–2064. The IRPM integrates linear regression, Fourier regression, and a random probabilistic approach to enhance prediction accuracy. To further refine the forecasts, a Corrector Factor was applied, defined as the ratio of actual observed values to the sum of the three predictive components, thereby minimizing discrepancies between predicted and actual rainfall amounts. The model's predictive performance was assessed using a modified k-fold cross-validation approach, ensuring rigorous validation by partitioning the dataset into training and testing subsets. This iterative process enables continuous validation against future observations, improving reliability.

The forecasted monthly rainfall analysis for 2024 reveals distinct seasonal variations. The dry season, spanning January to February, records minimal precipitation (< 15 mm). Rainfall progressively increases in March and April, leading to the peak monsoon period from May to August, with Saiha experiencing the highest precipitation, exceeding 600 mm in June. A gradual decline follows from September to October, while November and December mark the return of dry conditions. Saiha consistently records the highest annual rainfall, whereas Champhai and Lawngtlai exhibit comparatively lower but stable precipitation trends. To evaluate the model's accuracy, Root Mean Square Error (RMSE) and Mean Absolute Error (MAE) were computed for each district. Predictive performance varied across regions, with Champhai showing the lowest RMSE (49.66) and MAE (35.87), followed closely by Aizawl (RMSE = 52.27, MAE = 36.22), indicating superior forecast reliability. In contrast, Lunglei (RMSE = 90.91, MAE = 55.49) and Saiha (RMSE = 74.59, MAE = 54.94) exhibited the highest deviations, suggesting greater challenges in accurately modeling rainfall trends in these areas. Kolasib, Lawngtlai, Mamit, and Serchhip demonstrated moderate prediction accuracy, with error values falling between these extremes.

These results highlight the spatial variability in forecasting performance. In the next section, we will analyze the forecasted monthly trends for each district using the Mann-Kendall and Sen Slope methods to assess long-term trends until 2064. The spatially forecasted rainfall projections for 10-year and 30-year periods are presented in Figure 4.10.

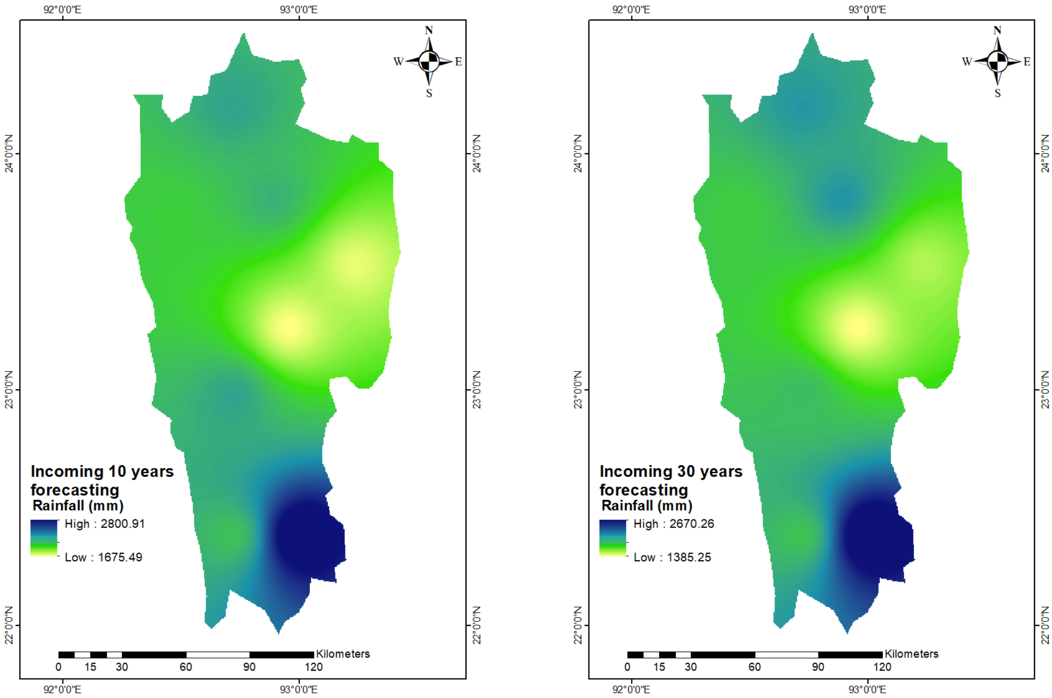

(a) Incoming 10 years

(b) Incoming 30 years

Figure 4.10: Spatial rainfall forecast for incoming 10 years and 30 years for Districts of Mizoram.

4.2.5 Comparison of IRPM with SARIMA and ARIMA

The Auto Regressive Integrated Moving Average (ARIMA) and Seasonal Auto Regressive Integrated Moving Average (SARIMA) models are widely used for rainfall forecasting (Valipour, 2015; Yavuz, 2025). In this study, the proposed Innovative Rainfall Predictive Method (IRPM) was compared with SARIMA and ARIMA using Mean Absolute Error (MAE) as the evaluation metric. MAE provides valuable insights into the accuracy and reliability of each model's predictions. The results reveal that the IRPM consistently exhibits significantly lower MAE values across all districts of Mizoram when compared to SARIMA and ARIMA, indicating superior predictive performance. The comparative results are presented in Figure 4.11. Among all districts, Champhai recorded the lowest MAE for IRPM, while Saiha exhibited the highest MAE under ARIMA. ARIMA generally produced the highest MAE values across districts, except for Mamit, where its MAE was slightly lower than that of SARIMA, underscoring its relatively poor fit for this regional dataset. SARIMA showed intermediate performance, with MAE values consistently lower than ARIMA but higher than IRPM. Based on these findings, the IRPM outperforms both ARIMA and SARIMA in forecasting rainfall across the districts of Mizoram, demonstrating its potential as a more reliable and accurate predictive model for the region.

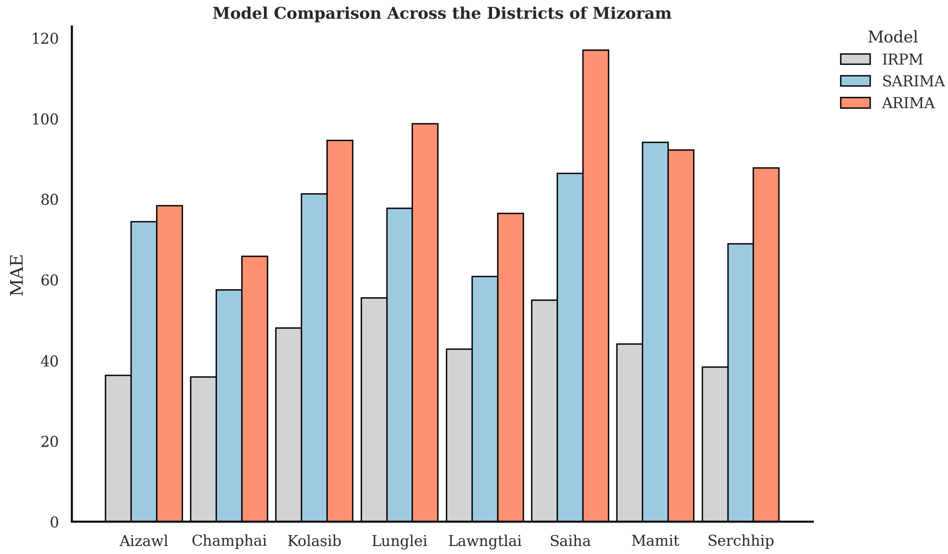

Figure 4.11: Comparative MAE performance of IRPM, SARIMA, and ARIMA models across districts of Mizoram.

4.2.6 Long Range Trend Analysis using Mann-Kendall and Sen's Slope Method

The forecasted monthly rainfall trends for 2024–2064, derived using the IRPM method and analyzed through the Mann-Kendall (MK) and Sen's Slope tests, exhibit notable spatial and temporal variability across each district of Mizoram. To better understand these patterns, the Z-values for each month were spatially mapped using the kriging interpolation technique, providing a detailed visualization of regional rainfall trends (Figure 4.14), also the Z-values and Q-values for each month are presented in Table 4.3 and Table 4.4.

The Mann-Kendall test was applied to assess the statistical significance of rainfall trends across different districts in Mizoram. Z-values were computed for each month, and significance was determined based on the threshold [-1.96,1.96], where values beyond this range indicate significant trends. The results reveal substantial spatial variability in rainfall trends. Champhai, Lawngtlai, Serchhip, and Mamit exhibit the highest number of significant months (10 out of 12), with predominant decreasing trends. Notably, Champhai and Serchhip show exclusively decreasing trends across all significant months, indicating a sustained reduction in rainfall. Lawngtlai and Mamit also exhibit strong decreasing trends, with Mamit showing two months of increasing trends. Aizawl and Saiha present moderate significance, with 9 significant months. Aizawl follows a predominantly decreasing trend, while Saiha exhibits a mixed pattern, with four months showing an increase and five months indicating a decline. Kolasib and Lunglei demonstrate the least number of significant months (7 and 8, respectively), both characterized by a consistent decreasing trend.

The Sen's Slope test further quantifies the magnitude and direction of these trends. A negative Q-value indicates a decreasing trend, while a positive value signifies an increasing trend. The analysis reveals distinct regional variations in rainfall patterns. Champhai and Serchhip exhibit the most pronounced declining trends, with all 12 months showing negative slopes. Serchhip, in particular, has the steepest average decline (-0.981), followed by Champhai (-0.569), suggesting a substantial reduction in long-term rainfall. Aizawl, Lunglei, Lawngtlai, and Kolasib also show predominantly decreasing trends, with over 10 months exhibiting negative slopes, reinforcing the Mann-Kendall findings of persistent declines in precipitation.

In contrast, Saiha stands out as the only district with a notable increasing trend (see Figure 4.15), with 8 out of 12 months showing positive slopes, its average slope (0.315) suggests a moderate rise in rainfall, particularly during the monsoon season. Mamit shows a mixed trend, with 3 months experiencing an increase and 9 months showing a decline, resulting in an overall negative trend (−0.912). These findings highlight regional disparities in rainfall trends, with most districts experiencing declining precipitation levels. The observed downward trends emphasize the need for proactive water management strategies, particularly in districts like Champhai and Serchhip, where rainfall reduction is most pronounced. Further refinements in forecasting models incorporating additional climatic parameters such as temperature and humidity could enhance predictive accuracy and inform sustainable resource management.

Table 4.3: Results of Mann–Kendall analysis of monthly rainfall of districts of Mizoram (2024–2064).

District	**Jan**	**Feb**	**Mar**	**Apr**	**May**	**Jun**	**Jul**	**Aug**	**Sep**	**Oct**	**Nov**	**Dec**
Aizawl	−0.45	−6.16*	−5.58*	−2.92*	−3.52*	−1.66	−3.17*	−4.35*	−6.14*	−5.31*	−3.19*	1.76
Kolasib	−1.38	−5.68*	−7.07*	−1.86	−1.94	−4.15*	−2.36*	−1.63	−2.56*	−5.00*	−3.60*	0.83
Lunglei	0.7	−2.82*	−7.69*	−4.30*	−2.84*	−0.93	−1.23	−2.97*	−4.80*	−4.78*	−3.42*	−0.33
Champhai	−0.10	−4.55*	−5.48*	−2.24*	−3.17	−3.82*	−3.44	−4.95*	−5.61*	−4.80*	−2.97	−1.03
Lawngtlai	−2.82*	−3.27*	−4.25*	−4.83*	−4.12*	−4.65*	−1.84	1.94	−4.10*	−7.07*	−6.19*	3.60*
Serchhip	−0.73	−5.20*	−7.64*	−3.90*	−4.35*	−4.30	−5.38*	−4.93*	−5.98*	−6.01*	−5.81	−0.06
Mamit	−2.94*	−5.43*	−5.85*	−4.70*	−5.92*	−2.79*	1.74	−5.72*	−6.08	−1.69	3.44*	5.82*
Saiha	3.32*	−3.6 *	−2.01*	−3.19*	−2.46*	1.71	3.39*	2.99*	2.09*	1.21	−3.90*	1.16

* indicates statistical significance

Table 4.4: Results of Sen's Slope value of monthly rainfall of districts of Mizoram (2024–2064).

District	**Jan**	**Feb**	**Mar**	**Apr**	**May**	**Jun**	**Jul**	**Aug**	**Sep**	**Oct**	**Nov**	**Dec**
Aizawl	−0.01	−0.3	−0.61	−0.5	−0.79	−0.32	−0.8	−0.45	−0.93	−0.79	−0.27	0.06
Kolasib	−0.01	−0.35	−0.78	−0.25	−0.22	−1.22	−0.52	−0.45	0.74	−1.12	−0.26	0.02
Lunglei	0.01	−0.09	−0.49	−0.58	−1.01	−0.14	−1.01	−0.14	−0.31	−0.53	−0.77	−1.16
Champhai	−0.01	−0.17	−0.44	−0.30	−0.67	−1.14	−0.47	−1.01	−1.05	−1.22	−0.29	−0.06
Lawngtlai	−0.03	−0.12	−0.31	−0.63	−0.92	−1.35	−0.98	0.35	−0.82	−0.69	−0.54	0.05
Serchhip	−0.01	−0.29	−0.77	−0.85	−1.19	−1.78	−1.79	−1.56	−1.71	−1.18	−0.58	−0.06
Mamit	−0.05	−0.26	1.10	−1.76	−4.24	−0.89	0.37	−1.79	−1.65	−0.15	0.12	0.46
Saiha	0.03	−0.08	−0.18	0.31	−0.68	2.21	0.51	1.1	0.83	0.17	−0.45	0.01

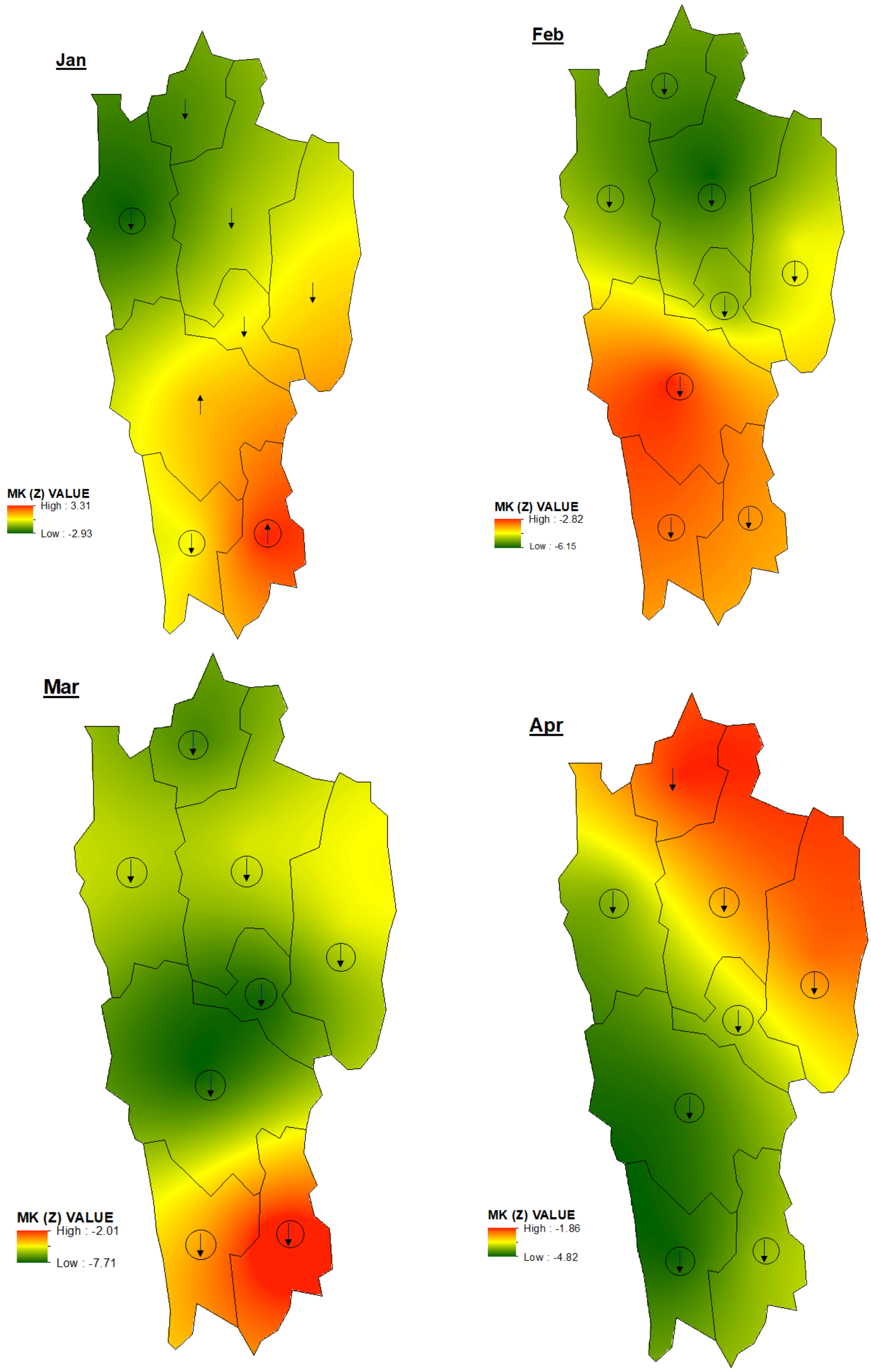

Figure 4.12: Spatial variations in trends of monthly rainfall using Mann-Kendall during 2024–2064 across Mizoram (Continued).

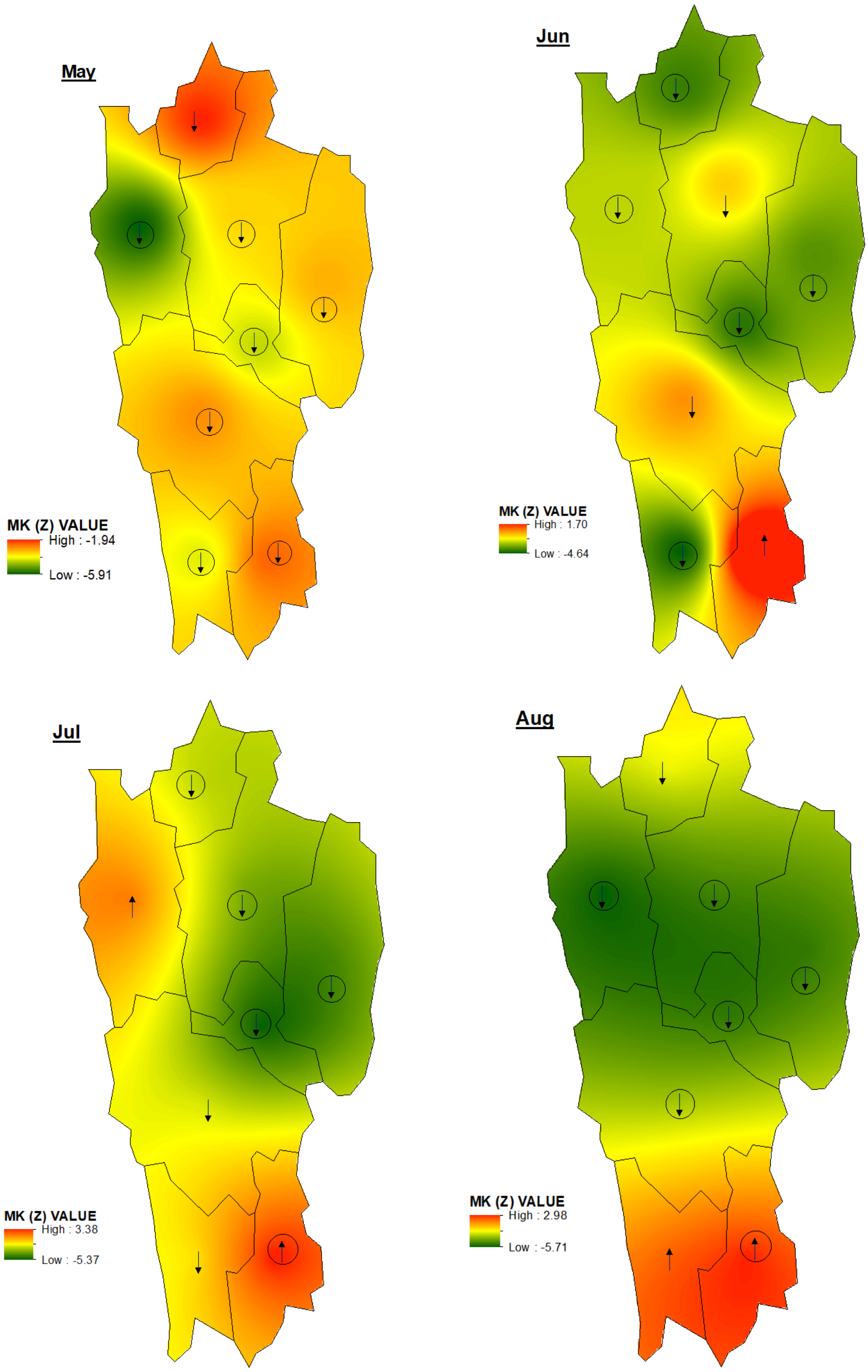

Figure 4.13: Spatial variations in trends of monthly rainfall using Mann-Kendall during 2024–2064 across Mizoram (Continued).

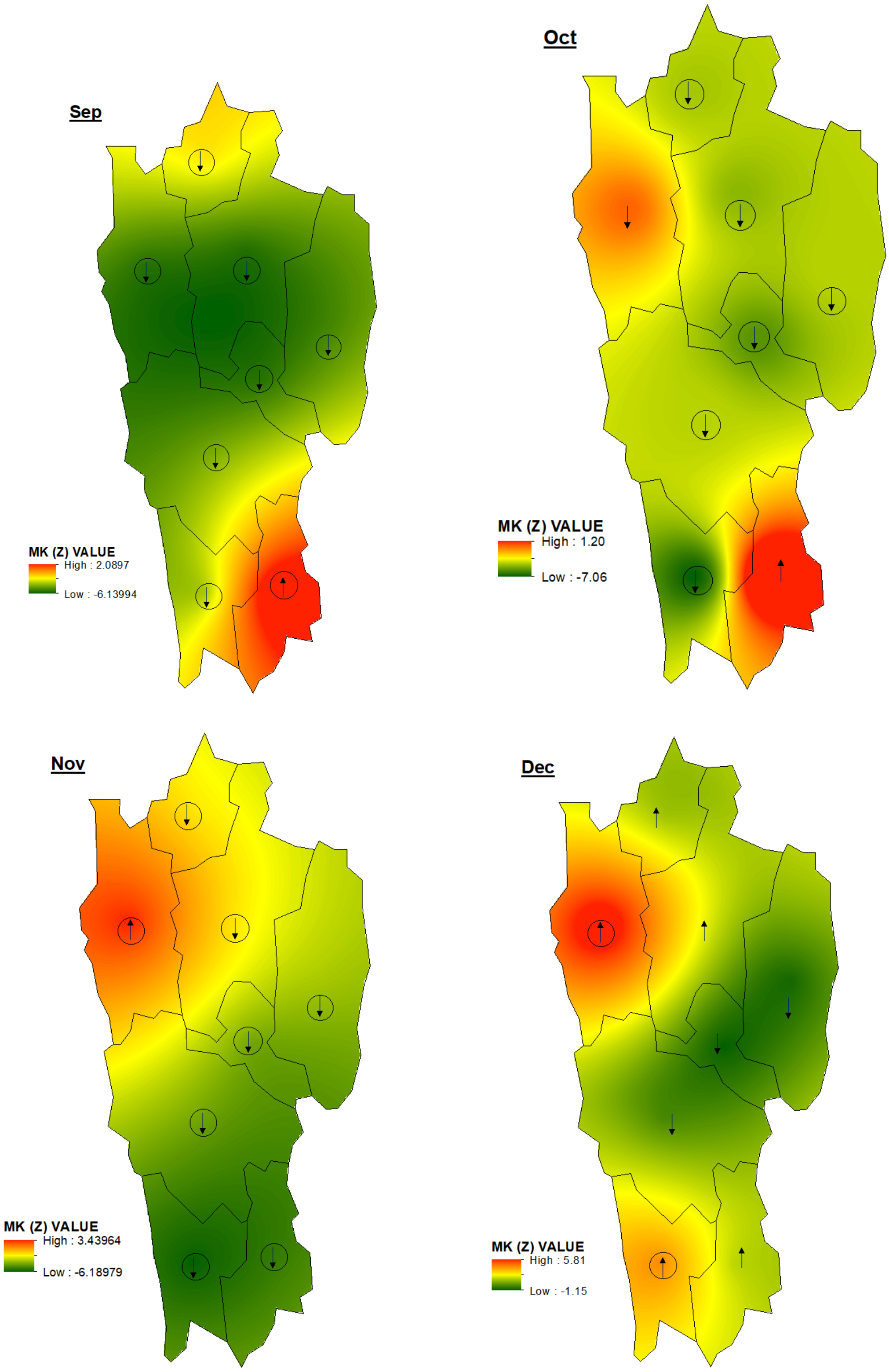

Figure 4.14: Spatial variations in trends of monthly rainfall using Mann-Kendall during 2024–2064 across Mizoram.

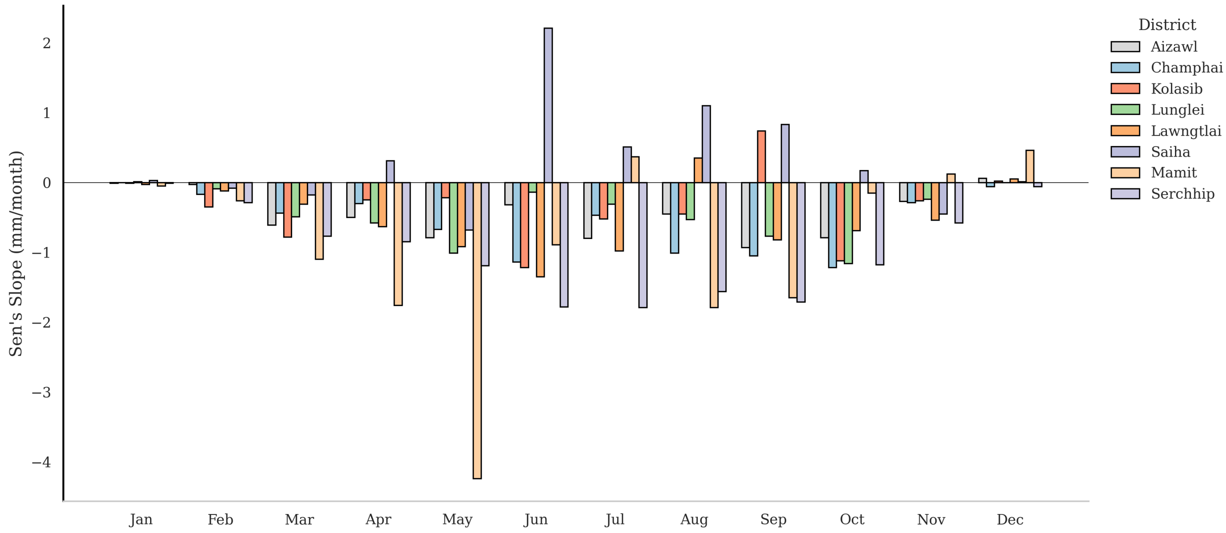

Figure 4.15: Sen's Slope results of monthly rainfall across Mizoram (2024-2064).

4.3 Long Range Monthly Rainfall Forecasting for Meteorological Subdivisions of India

In this section, we employed similar approach as Mizoram (Section 4.2) for Meteorological Sub-divisions of India. The trend analysis has been conducted for past and present data as well as future forecasted data for 34 Sub-divisions. The findings have been presented spatially using ArcGis for better clarity. Moreover, the model accuracy has been tested using various statistical methods.

4.3.1 Study Area and Data Source

India is geographically situated between latitudes 8.4°N and 37.6°N and longitudes 68.7°E and 97.25°E. The country is broadly classified into four distinct climatic zones: North-West India, North-East India, Central India, and Peninsular India, based on the distribution patterns of rainfall and temperature. India experiences a wide range of climatic conditions due to its diverse physiography and geographical extent. On average, India receives approximately 117 mm of rain-

Muniyan, S. and Lallawmzuali, M. (2025). Long Range Forecast Modeling and Trend Analysis of Monthly Rainfall across Metrological Sub-divisions of India using An Innovative Rainfall Predictive Method. (Communicated) fall annually, with 80% of it occurring during the monsoon months (Praveen *et al.*, 2020). The Indian Meteorological Department (IMD) has divided the country into 34 meteorological subdivisions (see Figure 4.16) excluding Andaman & Nicobar Island and Lakshadweep. For this study, rainfall data spanning 51 years (1971–2022) was obtained from IMD.

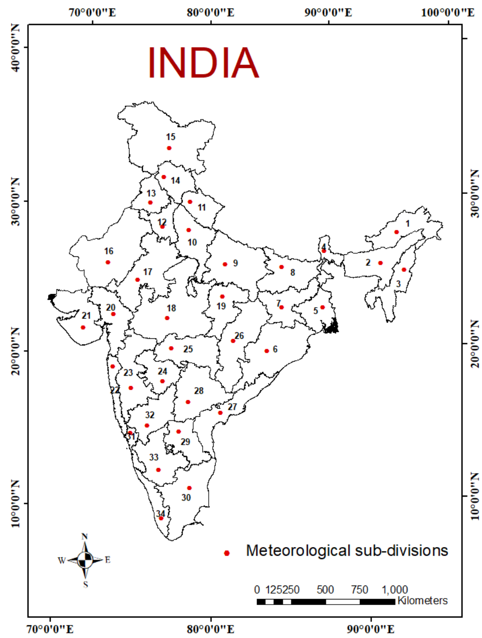

Figure 4.16: Location of Study Area.

Region Labels:

1 Arunachal Pradesh

2 Assam and Meghalaya

3 Nagaland, Manipur, Mizoram and Tripura

4 Sub-Himalayan West Bengal and Sikkim

5 Gangetic West Bengal

6 Orissa

7 Jharkhand

8 Bihar

9 East Uttar Pradesh

10 West Uttar Pradesh

11 Uttarakhand

12 Haryana, Chandigarh, and Delhi

13 Punjab

14 Himachal Pradesh

15 Jammu and Kashmir

16 West Rajasthan

17 East Rajasthan

18 West Madhya Pradesh

19 East Madhya Pradesh

20 Gujarat Region

21 Saurashtra and Kutch

22 Konkan and Goa

23 Madhya Maharashtra

24 Marathwada

25 Vidarbha

26 Chhattisgarh

27 Coastal Andhra Pradesh and Yanam

28 Telangana

29 Rayalaseema

30 Tamil Nadu, Puducherry and Karaikal

31 Coastal Karnataka

32 North Interior Karnataka

33 South Interior Karnataka

34 Kerala

4.3.2 Statistical Summary of Rainfall

During the study period, India experienced an average annual rainfall of 1160.12 mm. Based on rainfall data from 1971 to 2022, the majority of the rainfall occurred between June and September, with July receiving the highest amount at 280.95 mm. In contrast, the driest months were from November to February, with December recording the least rainfall at 14.93 mm (see Figure 4.17). The contributions of June, July, August, and September to the total annual rainfall were 14.37%, 24.22%, 22.05%, and 14.52%, respectively. Meanwhile, November, December, January, and February accounted for 2.48%, 1.29%, 1.52%, and 1.93% of the annual rainfall. Additionally, March, April, May, and October contributed 2.43%, 3.29%, 5.41%, and 6.49%, respectively.

An analysis of annual rainfall data from 1971 to 2022 was conducted for 34 meteorological sub-divisions across India. The results reveal that the regions with the highest average rainfall were Coastal Karnataka (3517.16 mm), Kerala (3086.69 mm), and Konkan & Goa (2811.23 mm). Conversely, the lowest average rainfall was observed in West Rajasthan (329.82 mm), Haryana, Delhi, and Chandigarh (522.27 mm), and Saurashtra & Kutch (550.52 mm). The standard deviation of rainfall varied between 530.53 mm and 142.64 mm across the sub-divisions. Arunachal Pradesh showed the highest variation at 530.53 mm, followed by Konkan & Goa (519.45 mm) and Coastal Karnataka (478.63 mm). On the other hand, the lowest variations were noted in Haryana, Delhi, and Chandigarh (142.64 mm), Western Rajasthan (144.58 mm), and North Interior Karnataka (149.94 mm). Rainfall skewness values ranged from −0.78 to 2.28 across the sub-divisions. Negative skewness was identified in Tamil Nadu (−0.78), Odisha (−0.19), Kerala (−0.15), and Bihar (−0.08), while the remaining sub-divisions displayed positive skewness.

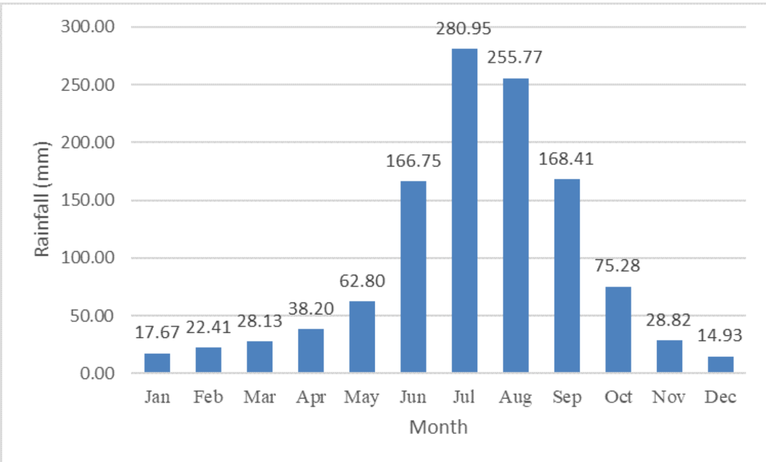

Figure 4.17: Meteorological Sub-divisions monthly rainfall trends from 1971-2022.

4.3.3 Monthly Trend Analysis Using MK and Sen's Slope Test

The monthly rainfall trends for thirty-four meteorological sub-divisions of India were analyzed using the non-parametric Mann-Kendall (MK) test and Sen's slope estimator. The results, covering the period from 1971 to 2022 and evaluated at a 95% confidence level. These analyses reveal substantial variability in rainfall trends across months and regions, with some showing increasing patterns and others exhibiting declines. However, the majority of these trends are not statistically significant (Table 4.5). In the MK test, Z-values with $|Z| > 1.96$ indicate statistically significant trends, where a negative Z-value corresponds to a significant decreasing trend and a positive Z-value indicates a significant increase.

Z-values within $|Z| \leq 1.96$ suggest no statistically significant trend. Among the months, January exhibits the highest positive Z-value, highlighting a significant increase in rainfall, likely attributed to western disturbances or pre-monsoon activities. Conversely, February records the highest negative Z-value, indicating a notable decline in rainfall, potentially reflecting broader climatic changes or shifts in monsoon dynamics. Sen's slope (Q) complements the MK test by quantifying the magnitude of increasing or decreasing trends. For instance, February, which shows the most significant negative Z-value (-3.34) in Arunachal Pradesh, also has a corresponding Q value of -0.58, indicating a substantial reduction in rainfall over time. Similarly, in the northeastern states of Nagaland, Manipur, Mizoram, and Tripura, February and July show sharp negative trends with Z-values of -2.84 (Q = -0.58) and -2.06, respectively. On the other hand, regions like Coastal Karnataka and Kerala, which exhibit significant positive Z-values, have corresponding positive Q values, such as 3.06 (March) and 2.70 (March), respectively, indicating an increase in rainfall magnitude.

Spatial mapping of MK Z-values, visualized using the ordinary kriging interpolation method, provides a geo-statistical overview of rainfall variations across India (Figure 4.20). The meteorological sub-divisions of Arunachal Pradesh show consistent declines in rainfall across most months, with Z-values ranging from -3.34 in February to -0.13 in May, signifying substantial reductions, particularly in February (Table 4.6). Assam and Meghalaya exhibit declining trends, especially in November (Z = -2.18, Q = -0.48), indicating reduced post-monsoon rainfall. However, minor increases in May (Z = 0.81, Q = 0.11) remain statistically insignificant. In the northeastern states, sharp negative trends in February (Z = -2.84, Q = -0.58) and July (Z = -2.06, Q = -0.40) suggest broader climatic shifts affecting monsoon patterns. Sub-Himalayan West Bengal and Sikkim show mixed trends, with a slight increase in March (Z = 1.22, Q = 0.22) but declines in July (Z = -1.97, Q = -0.37). Gangetic West Bengal exhibits negative trends in most months, such as February (Z = -1.44, Q = -0.23), with minor increases in May (Z = 1.11, Q = 0.18). Western regions like Konkan and Goa show consistent positive trends, with significant Z-values of 2.58 in March and 2.50 in July, indicating substantial rainfall increases. Corresponding Q-values for these months, such as 0.42 and 0.36, respectively, emphasize the magnitude of these trends. Coastal Karnataka also displays increasing rainfall trends, particularly in March (Z = 3.06, Q = 0.48) and April (Z = 2.99, Q = 0.44), suggesting enhanced precipitation during these months. Kerala similarly records positive trends, with Z-values of 2.70 in March (Q = 0.39) and 1.78 in September (Q = 0.28), highlighting growing rainfall patterns. In contrast, northern and central regions, such as East Uttar Pradesh, exhibit declining rainfall during monsoon months, with significant Z-values of -2.69 in August and -2.23 in September, accompanied by Q-values of -0.52 and -0.48, respectively, reflecting reductions in monsoon precipitation. Gujarat and surrounding regions also show declining trends, particularly in May (Z = -1.92, Q = -0.34) and June (Z = -1.35, Q = -0.28).

Table 4.5: Mann–Kendall Z values for Monthly Rainfall (1971–2022) Across Meteorological Sub-divisions of India.

Regions	**Jan**	**Feb**	**Mar**	**Apr**	**May**	**Jun**	**Jul**	**Aug**	**Sep**	**Oct**	**Nov**	**Dec**
Arunachal Pradesh	−2.21*	−3.34*	−1.65	−0.99	−0.13	−1.03	−0.88	−0.42	−0.28	−1.73	−1.97	−1.78
Assam and Meghalaya	−1.20	−1.13	−0.25	0.02	0.81	−0.34	−1.89	−1.27	−0.62	−0.13	−2.18*	−1.78
Nagaland, Manipur, Mizoram and Tripura	−0.04	−2.84*	−1.24	−2.62*	−1.37	−2.79*	−2.06*	−1.35	−1.00	−0.03	−2.85*	0.46
Sub-Himalayan West Bengal and Sikkim	−1.06	−1.07	1.22	0.83	−0.71	−0.54	−1.97	−0.28	−1.13	−0.99	−1.60	−1.30
Gangetic West Bengal	−0.58	−1.44	−0.92	−0.51	1.11	−0.45	−1.29	−1.09	−0.02	−0.02	−1.27	0.68
Orissa	0.58	−1.73	−1.14	−0.09	1.88	−0.09	0.61	−0.13	1.63	0.68	−0.47	−0.08
Jharkhand	−1.70	−2.23*	−0.74	−1.04	0.88	−0.88	−1.35	−1.24	−0.98	−0.02	−1.95	−0.70
Bihar	−1.59	−1.05	−0.51	0.40	1.35	0.28	−0.89	−0.64	−1.03	−0.80	−2.68*	−1.05
East Uttar Pradesh	−1.03	−0.91	−0.36	−0.57	0.50	−0.84	−2.17*	−2.69*	−2.23*	−1.10	−1.40	−1.68
West Uttar Pradesh	0.45	−0.46	−0.61	0.32	1.04	−1.81	−1.91	−2.61*	−0.77	−0.81	−0.21	−1.10
Uttarakhand	−0.25	−0.62	−1.07	0.55	1.24	0.61	0.94	0.69	0.42	−0.89	−0.55	−1.25
Haryana, Chandigarh and Delhi	0.02	−0.39	−0.17	0.81	1.10	−0.39	−1.43	−2.70*	1.31	−0.92	0.48	−0.61
Punjab	0.62	−1.04	−0.86	0.78	0.61	−0.43	−2.11*	−2.25*	1.51	−0.10	0.83	−0.31
Himachal Pradesh	−0.48	−0.54	−0.89	−0.04	−0.40	0.06	−0.62	1.38	1.31	−0.99	−0.17	−0.73
Jammu and Kashmir	0.62	−0.36	−1.68	−0.95	−1.52	1.42	0.33	0.06	0.69	0.07	0.16	−1.01
West Rajasthan	0.25	0.09	1.97	1.59	0.50	1.42	0.37	0.92	1.36	0.33	0.40	−0.35
East Rajasthan	0.23	−1.34	1.62	1.11	−0.03	0.18	−0.42	0.42	1.37	−0.48	−0.33	−0.10
West Madhya Pradesh	0.42	−0.59	1.23	0.44	−0.52	0.00	2.00*	−1.27	1.08	0.08	−0.68	−0.29
East Madhya Pradesh	−0.36	−0.59	0.51	0.72	0.95	0.02	−0.13	−1.96	0.54	−0.04	−0.32	−0.32
Gujarat Region	−0.58	−0.96	0.62	−0.01	−1.92	−1.35	0.88	−0.48	1.62	0.95	−1.06	0.65
Saurashtra, Kutch and Diu	−0.49	−1.19	1.36	1.48	−0.62	−0.91	1.48	0.83	2.34	1.33	0.14	0.87
Konkan and Goa	2.25*	0.29	2.58*	1.32	0.70	0.84	2.50*	0.29	2.16*	2.27*	1.33	1.95
Madhya Maharashtra	0.09	−0.52	0.89	−0.10	−1.07	0.53	2.23	0.59	1.68	1.32	−0.92	0.47
Marathwada	−0.41	0.54	1.20	0.68	−1.02	0.45	0.80	−0.32	1.50	0.39	−1.18	−0.76
Vidarbha	−0.46	−1.39	0.69	−0.58	−0.92	−0.39	1.55	−1.40	2.19*	−0.56	−1.10	−1.53
Chhattisgarh	0.46	−0.71	0.77	1.00	1.97	0.29	−0.21	−1.25	1.30	0.12	−1.72	0.98
Coastal Andhra Pradesh	1.43	−1.06	0.48	0.37	0.54	0.13	1.39	−0.02	0.53	−1.10	0.20	1.07
Telangana	0.43	0.16	0.96	1.22	0.40	0.10	−0.04	−0.10	2.03*	−0.42	−0.52	0.20
Rayalaseema	1.25	0.25	1.52	1.28	0.79	1.74	−0.01	0.95	0.24	−0.80	−1.17	0.59
Tamil Nadu and Pondicherry	1.96	0.15	−0.43	0.24	0.03	0.09	−1.13	1.37	−2.45*	−0.16	0.81	−0.01
Coastal Karnataka	1.94	2.28*	3.06*	2.99*	1.16	−1.53	−0.04	−0.02	2.49*	2.26*	−0.36	1.95
North Interior Karnataka	1.13	1.18	2.08	1.88	0.89	−0.19	0.58	0.27	0.28	0.15	−0.73	1.52
South Interior Karnataka	3.75*	2.96*	1.73	2.01	1.15	−1.84	−0.22	0.92	−0.76	1.35	−0.07	1.72
Kerala	1.31	0.67	2.70*	0.99	1.03	−1.87	−0.64	0.69	1.78	1.65	0.04	0.49

* indicates statistical significance

Table 4.6: Sen's Slope (Q) Values for Monthly Rainfall (1971–2022) Across Meteorological Sub-divisions of India.

Regions	**Jan**	**Feb**	**Mar**	**Apr**	**May**	**Jun**	**Jul**	**Aug**	**Sep**	**Oct**	**Nov**	**Dec**
Arunachal Pradesh	−0.63	−1.19	−0.87	−0.79	−0.08	−1.33	−1.21	−0.45	−0.44	−1.10	−0.36	−0.31
Assam and Meghalaya	−0.10	−0.20	−0.07	0.03	0.61	−0.34	−2.58	−1.51	−0.54	−0.10	−0.27	−0.12
Nagaland, Manipur, Mizoram and Tripura	0.00	−0.58	−0.06	−1.73	−1.53	−2.63	−1.97	−1.04	−0.78	−0.03	−0.67	0.00
Sub-Himalayan West Bengal and Sikkim	−0.11	−0.19	0.32	0.34	−0.42	−0.53	−2.90	−0.34	−1.10	−0.71	−0.17	−0.07
Gangetic West Bengal	−0.03	−0.20	−0.14	−0.14	0.58	−0.46	−1.04	−0.93	−0.01	−0.06	−0.11	0.00
Orissa	0.01	−0.13	−0.11	−0.03	0.54	−0.08	0.41	−0.16	1.04	0.40	−0.04	0.00
Jharkhand	−0.12	−0.27	−0.04	−0.14	0.28	−0.49	−1.20	−0.99	−0.65	−0.01	−0.07	0.00
Bihar	−0.09	−0.06	−0.02	0.05	0.33	0.26	−0.97	−0.41	−0.82	−0.28	−0.04	−0.01
East Uttar Pradesh	−0.09	−0.06	−0.01	−0.02	0.06	−0.44	−1.03	−1.62	−1.60	−0.24	−0.02	−0.03
West Uttar Pradesh	0.05	−0.05	−0.02	0.01	−0.11	−0.65	−1.47	−2.31	−0.50	−0.07	0.00	−0.02
Uttarakhand	−0.08	−0.19	−0.41	0.12	0.43	0.38	1.04	0.53	0.36	−0.14	−0.02	−0.73
Haryana, Chandigarh and Delhi	0.00	−0.03	−0.01	0.02	0.16	−0.12	−0.96	−1.68	0.52	−0.01	0.00	−0.01
Punjab	0.09	−0.22	−0.12	0.06	0.76	−0.11	−1.26	−1.66	0.71	0.00	0.00	−0.01
Himachal Pradesh	−0.26	−0.35	−0.55	−0.03	−0.12	0.03	−0.46	0.95	0.75	−0.15	−0.02	−0.12
Jammu and Kashmir	0.35	−0.23	−1.54	−0.40	−0.42	0.48	0.23	0.04	0.22	0.02	0.02	−0.33
West Rajasthan	0.00	0.00	0.03	0.04	0.04	0.28	0.14	0.59	0.28	0.01	0.00	0.00
East Rajasthan	0.04	−0.02	0.02	0.01	0.00	0.07	−0.26	0.32	0.65	−0.01	0.00	0.00
West Madhya Pradesh	0.01	−0.01	0.02	0.00	−0.03	−0.01	1.72	−1.45	0.95	0.01	−0.01	0.00
East Madhya Pradesh	−0.01	−0.05	0.01	0.02	0.05	0.01	0.14	−2.29	0.40	−0.01	0.00	0.00
Gujarat Region	0.00	0.00	0.00	0.00	−0.01	−0.95	1.03	−0.65	1.54	0.08	0.00	0.00
Saurashtra, Kutch and Diu	0.00	0.00	0.00	0.00	0.00	−0.54	1.62	0.62	1.39	0.06	0.00	0.00
Konkan and Goa	0.00	0.00	0.00	0.01	0.06	1.22	6.77	0.93	4.37	1.51	−0.08	0.00
Madhya Maharashtra	0.00	0.00	0.01	−0.01	−0.11	0.36	1.52	0.42	1.17	0.51	−0.08	0.00
Marathwada	0.00	0.00	0.02	0.02	−0.08	0.23	0.66	−0.40	1.19	0.21	−0.04	0.00
Vidarbha	−0.01	−0.06	0.03	−0.01	−0.04	−0.24	1.35	−1.01	1.65	−0.25	−0.02	−0.01
Chhattisgarh	0.02	−0.05	0.03	0.08	0.13	0.17	−0.18	−0.86	0.86	0.06	−0.05	0.00
Coastal Andhra Pradesh	0.04	−0.04	0.02	0.07	0.15	0.06	0.57	−0.02	0.29	−0.84	0.11	0.10
Telangana	0.00	0.00	0.04	0.11	0.05	0.04	−0.04	−0.08	1.61	−0.31	−0.05	0.00
Rayalaseema	0.02	0.00	0.04	0.12	0.18	0.50	−0.01	0.47	0.17	−0.57	−0.65	0.12
Tamil Nadu and Pondicherry	0.10	0.00	−0.05	0.04	0.01	0.02	−0.33	0.45	−0.98	−0.10	0.83	−0.02
Coastal Karnataka	0.00	0.00	0.08	0.52	0.90	−2.82	−0.86	−0.03	3.77	1.82	−0.19	0.10
North Interior Karnataka	0.00	0.00	0.07	0.23	0.21	−0.03	0.32	0.09	0.12	0.17	−0.10	0.01
South Interior Karnataka	0.01	0.01	0.10	0.39	0.52	−0.88	−0.15	0.48	−0.41	0.68	−0.03	0.11
Kerala	0.05	0.05	0.49	0.47	1.21	3.30	−1.19	1.09	2.64	1.69	0.06	0.13

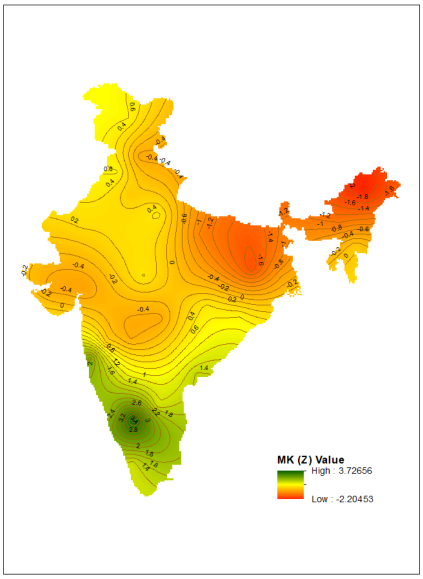

(a) Jan

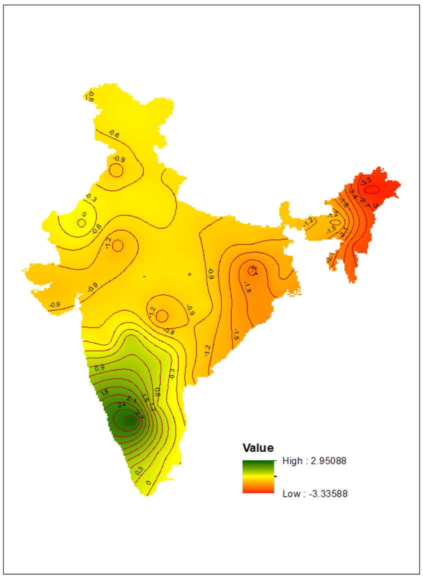

(b) Feb

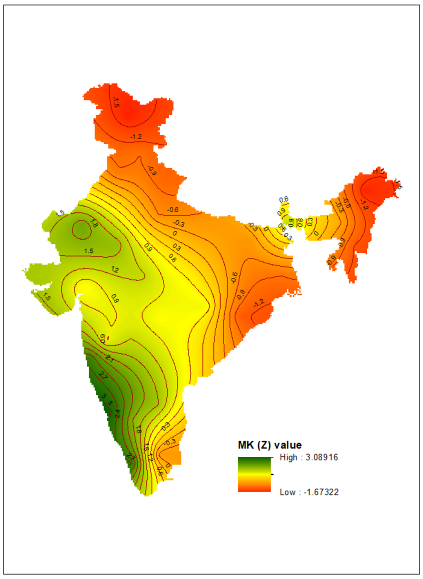

(c) Mar

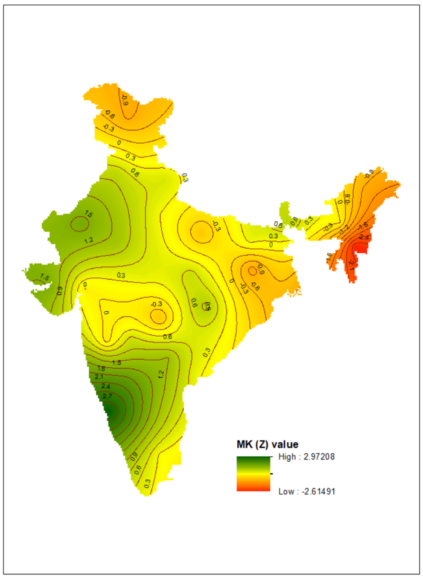

(d) Apr

Figure 4.18: Spatial distributions of monthly rainfall (1971-2022) across Meteorological sub-divisions of India using the Mann-Kendall test (Continued).

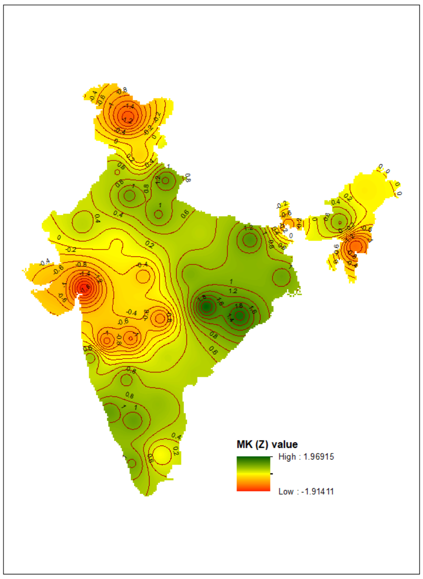

(e) May

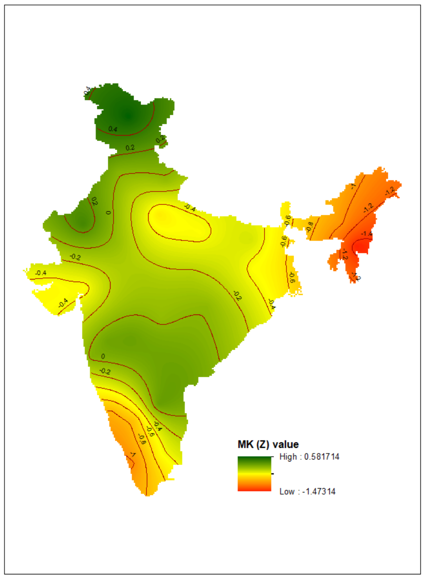

(f) Jun

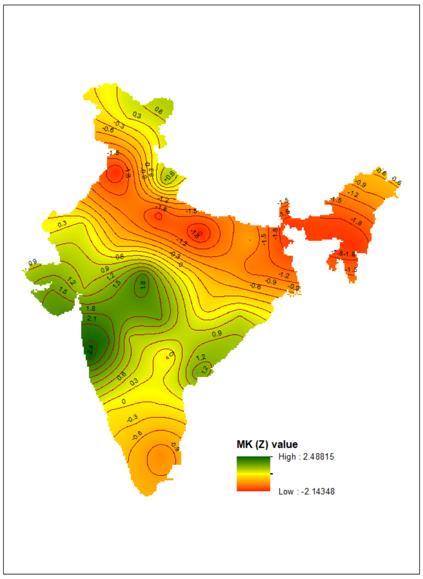

(g) Jul

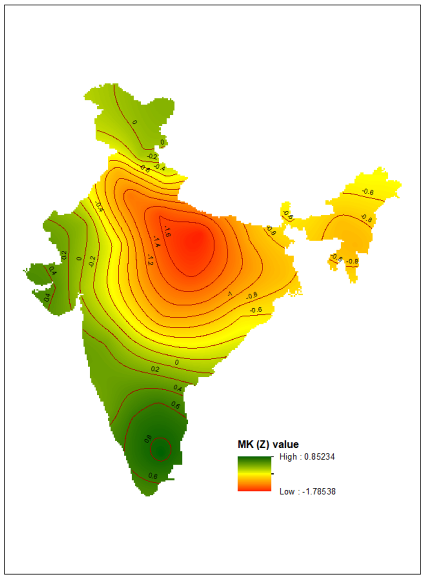

(h) Aug

Figure 4.18: Spatial distributions of monthly rainfall (1971-2022) across Meteorological sub-divisions of India using the Mann-Kendall test (Continued).

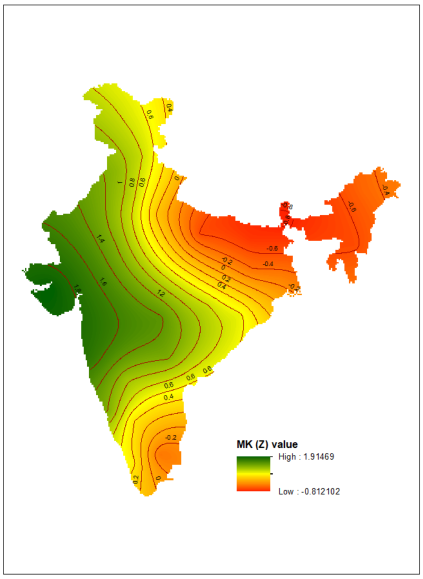

(i) Sep

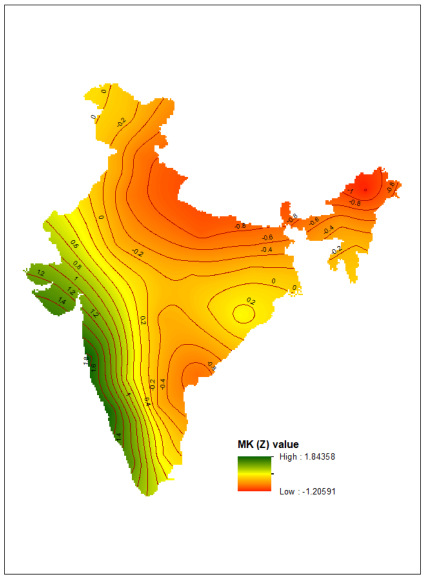

(j) Oct

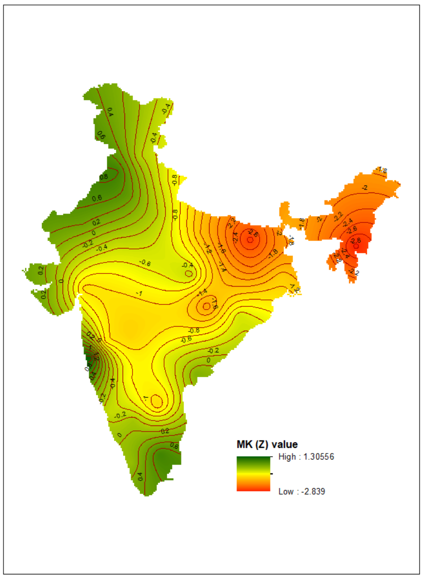

(k) Nov

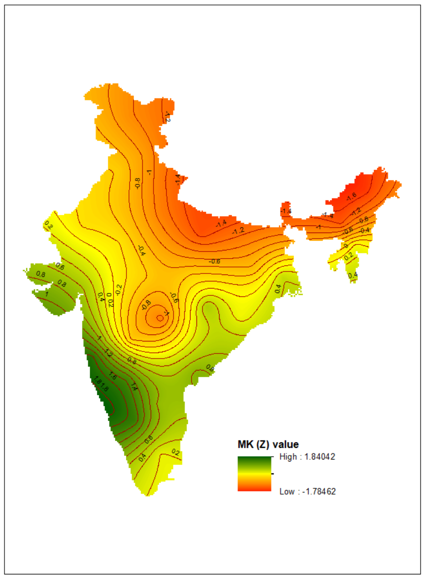

(l) Dec

Figure 4.18: Spatial distributions of monthly rainfall (1971-2022) across Meteorological sub-divisions of India using the Mann-Kendall test.

4.3.4 Rainfall Forecasting and Long Range Monthly Trend Analysis

4.3.4.1 Rainfall Forecast

Accurate rainfall forecasting is critical for effective water resource management and planning, particularly in regions experiencing significant variations in rainfall patterns. In this study, the Innovative Rainfall Predictive Method (IRPM) was utilized, integrating linear regression, Fourier regression, and a random probabilistic approach to improve prediction accuracy. To further refine the predictions, a Corrector Factor was applied. This factor, calculated as the ratio of actual observed values to the sum of the three predictive components, adjusted for discrepancies between predicted and actual rainfall amounts. The mean of the monthly corrector factors was computed to standardize adjustments across months, ensuring consistent and reliable model outputs. The model's performance was evaluated using a modified k-fold cross-validation approach (Table 4.7). This iterative process involved dividing the dataset into training and testing subsets, ensuring that predictions were always validated on future observations. Specifically, the dataset was divided as follows:

- Data from 1971–2017 was used for training, and the model was tested on 2018 data.
- Data from 1971–2018 was used for training, and the model was tested on 2019 data.
- Data from 1971–2019 was used for training, and the model was tested on 2020 data.
- Data from 1971–2020 was used for training, and the model was tested on 2021 data.
- Data from 1971–2021 was used for training, and the model was tested on 2022 data.

The forecasted monthly rainfall analysis reveals significant spatial and temporal variability across India's meteorological sub-divisions, with notable extremes (Figure 4.21). Konkan & Goa experience the highest rainfall, peaking at 1075.93 mm in July, followed by Coastal Karnataka with 1053.75 mm in the same month, underscoring the dominance of the southwest monsoon. Sub-Himalayan West Bengal and Sikkim also receive substantial rainfall, with a maximum of 601.53 mm in July. In contrast, Tamil Nadu and Rayalaseema exhibit post-monsoon rainfall reliance, with Tamil Nadu peaking at 176.01 mm in November. The model's performance, evaluated using Root Mean Square Error (RMSE), Mean Absolute Error (MAE), and the coefficient of determination (R^2), highlighted variability in predictive accuracy across regions. Sub-Himalayan West Bengal and Sikkim achieved high accuracy with an R^2 of 0.93 and an RMSE of 61.29, while Vidarbha and Chhattisgarh demonstrated strong performance with R^2 values of 0.94 and 0.95 and RMSE values of 31.84 and 32.62, respectively. However, regions such as Jammu and Kashmir and West Rajasthan exhibited lower predictive accuracy, with R^2 values of 0.67 and RMSE of 33.67 and 26.92, respectively. Coastal regions like Konkan and Goa faced challenges, with high RMSE values, such as 119.22, reflecting the complexity of capturing rainfall variability in these areas. Overall, the IRPM model demonstrated robust performance, particularly in regions with consistent rainfall patterns, while highlighting the need for further refinements to address complex rainfall dynamics in certain areas. The rainfall prediction and forecasting were performed in Python software (version 3.11) and the map pings were done in Arc GIS (version 10.8) software.

Table 4.7: Model Validation Results of the Modified K-Fold Cross-Validation Method for the Innovative Rainfall Predictive Method (IRPM).

Meteorological Sub-divisions	RMSE	MAE	R^2
Arunachal Pradesh	61.21	43.82	0.85
Assam and Meghalaya	59.54	41.46	0.91
Nagaland, Manipur, Mizoram, Tripura	38.66	29.36	0.88
Sub-Himalayan West Bengal	61.29	38.42	0.93
Sikkim	40.86	30.98	0.89
Orissa	37.41	27.96	0.92
Jharkhand	31.15	22.38	0.91
Bihar	44.15	28.38	0.84
East Uttar Pradesh	31.63	20.56	0.88
West Uttar Pradesh	23.84	15.84	0.88
Uttarakhand	33.95	24.82	0.91
Haryana, Chandigarh and Delhi	21.39	15.29	0.84
Punjab	23.70	15.70	0.84
Himachal Pradesh	26.81	24.03	0.86
Jammu and Kashmir	33.67	25.93	0.67
West Rajasthan	26.92	18.37	0.67
East Rajasthan	28.58	16.06	0.91
West Madhya Pradesh	38.90	22.10	0.92
East Madhya Pradesh	36.23	21.63	0.92
Gujarat Region	57.86	28.33	0.82
Saurashtra and Kutch	44.15	28.12	0.73
Konkan and Goa	119.22	67.18	0.93
Madhya Maharashtra	35.84	22.69	0.91
Marathwada	38.34	27.21	0.84
Vidarbha	31.84	18.24	0.94
Chhattisgarh	32.62	21.99	0.95
Coaltal Andhra Pradesh and Yanam	31.43	20.32	0.84
Telangana	39.72	23.98	0.89
Rayalaseema	32.76	21.70	0.68
Tamil Nadu, Puducherry and Karaikal	29.23	19.73	0.84
Coastal Karnataka	102.26	62.32	0.93
North Interior Karnatak	26.00	17.51	0.85
South Interior Karnataka	36.17	18.61	0.87
Kerala	97.18	62.75	0.84

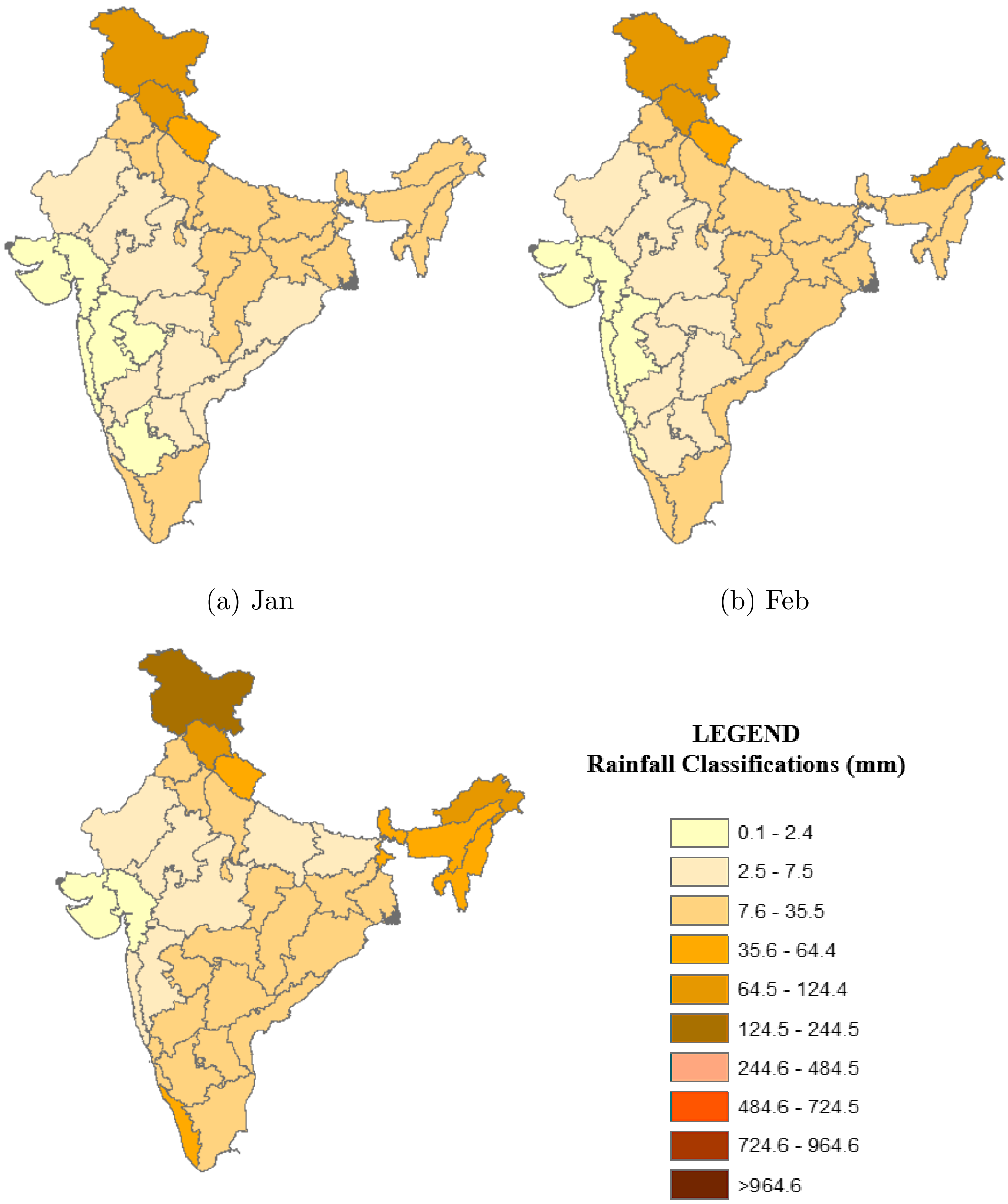

(a) Jan

(b) Feb

(c) Mar

Figure 4.19: Rainfall Prediction for 2026 Using IRPM (Continued).

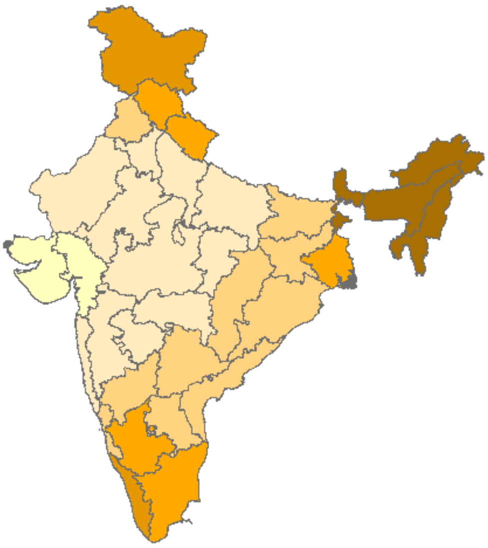

(d) Apr

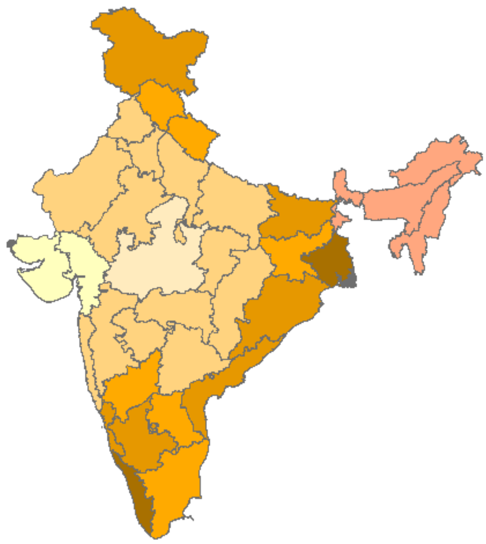

(e) May

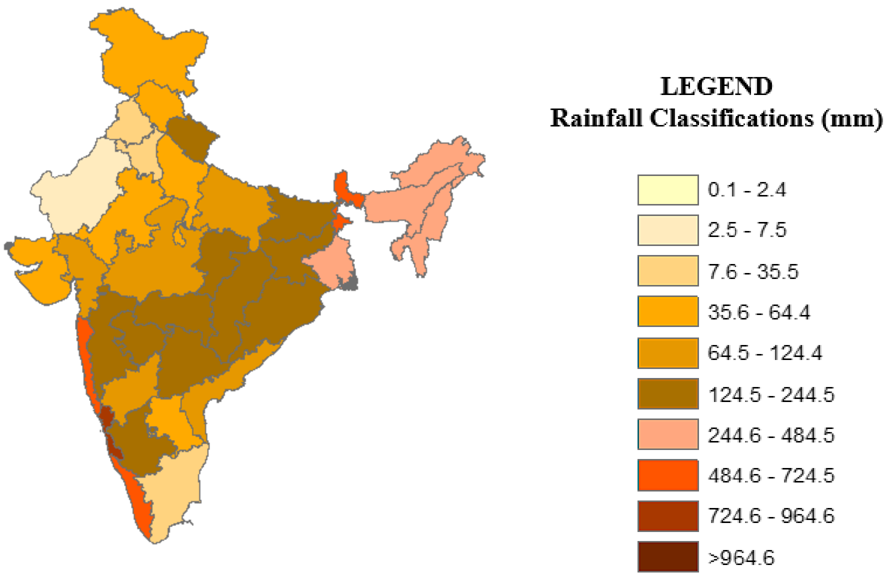

(f) Jun

Figure 4.19: Rainfall Prediction for 2026 Using IRPM (Continued).

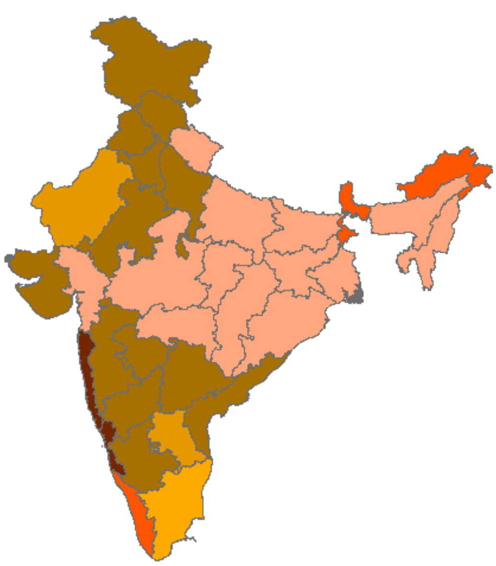

(g) Jul

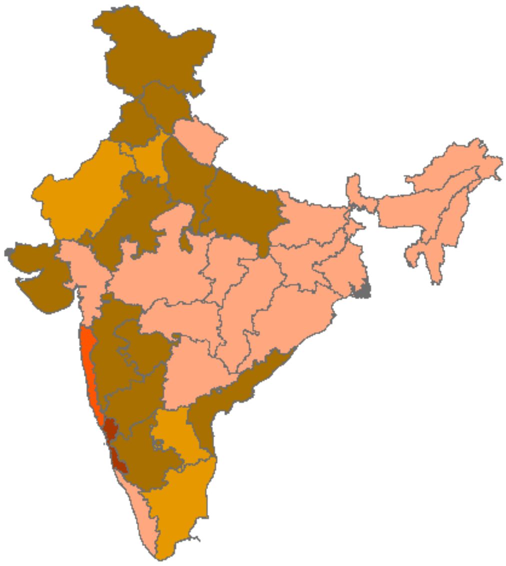

(h) Aug

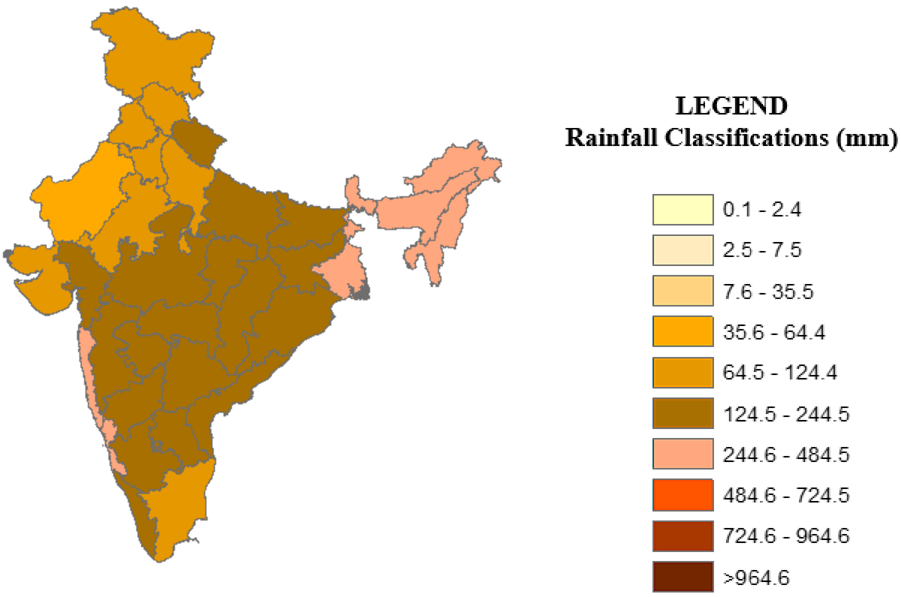

(i) Sep

Figure 4.19: Rainfall Prediction for 2026 Using IRPM (Continued).

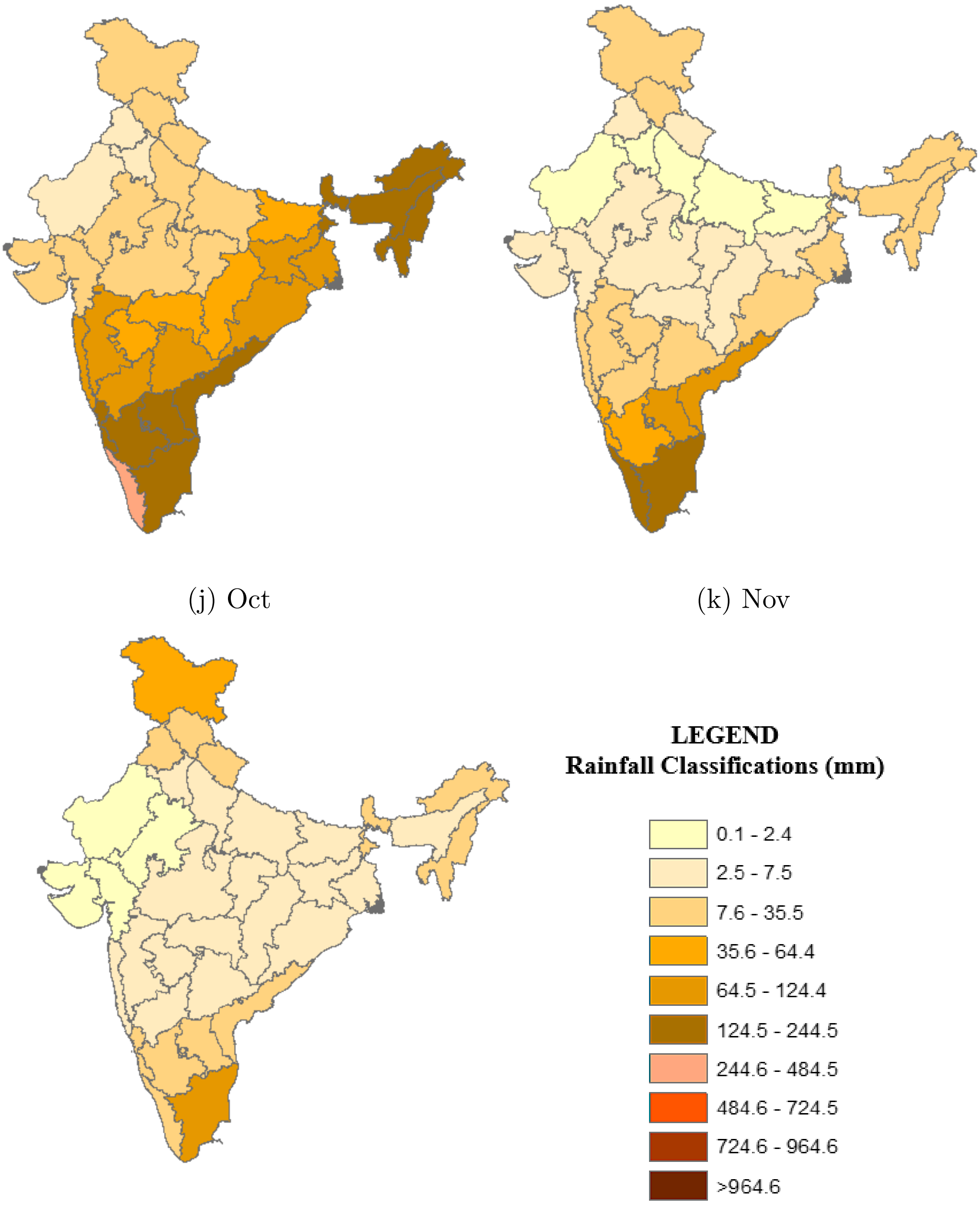

(j) Oct

(k) Nov

(l) Dec

Figure 4.19: Rainfall Prediction for 2026 Using IRPM.

4.3.4.2 Mann-Kendall Test

The forecasted monthly rainfall trends for 2023–2075, derived using the IRPM method and analysed through the Mann-Kendall (MK) test, exhibit notable spatial and temporal variability across India's meteorological sub-divisions (Table 4.8). To better understand these patterns, the Z-values for each month were spatially mapped using the kriging interpolation technique, providing a detailed visualization of regional rainfall trends (Figure 4.20). The findings reveal consistent declines in regions such as Arunachal Pradesh, Nagaland, Manipur, Mizoram, and Tripura, with sharp reductions observed during February (Z = -6.13 to -5.55) and July (Z = -6.92 to -5.66). Similarly, significant monsoon rainfall reductions are evident in Sub-Himalayan West Bengal and Sikkim, as well as in northern and central regions like East Uttar Pradesh and Jharkhand, particularly during July and August (Z = -7.98 to -7.03). Conversely, strong positive trends are detected in southern and western regions, including Konkan & Goa, Coastal Karnataka, and Kerala, during pre-monsoon and post-monsoon months. Coastal Karnataka records the most pronounced increase in April (Z = 9.00), while Kerala shows substantial gains in October (Z = 8.10). Mixed trends are observed in regions like Assam and Meghalaya, where declining rainfall in July (Z = -6.46) contrasts with increases in May (Z = 5.69). Seasonal analyses indicate declining monsoon rainfall in northern and central India, likely attributed to weakened monsoon circulation. In contrast, intensified western disturbances and enhanced local convective systems contribute to increased rainfall in southern coastal regions during pre- and post-monsoon periods. These findings, supported by spatial mapping, emphasize the urgent need for region-specific adaptation strategies. Addressing significant rainfall declines is critical to ensuring sustainable water management, agricultural productivity, and resilience to climate change across diverse meteorological sub-divisions in India.

Table 4.8: Mann-Kendall test values for monthly rainfall (2023-2075) across meteorological sub-divisions of India forcasted using IRPM.

Regions	**Jan**	**Feb**	**Mar**	**Apr**	**May**	**Jun**	**Jul**	**Aug**	**Sep**	**Oct**	**Nov**	**Dec**
Arunachal Pradesh	−7.17*	−6.13*	−4.06*	−3.07*	−1.37	−3.75*	−6.92*	−2.71*	−2.81*	−4.84*	−4.46*	−7.63*
Assam and Meghalaya	−3.72*	−4.73*	−2.01*	1.38	5.69*	2.45*	−6.46*	−3.76*	−1.25	−1.29	−5.89*	−4.30*
Nagaland, Manipur, Mizoram and Tripura	3.81*	−5.55*	−5.93*	−6.10*	−6.35*	−6.62*	−5.66*	−4.13*	−4.22*	0.83	−6.54*	1.27
Sub-Himalayan West Bengal and Sikkim	−3.43*	−1.40	3.42*	1.62	−1.74	−1.51	−7.03*	−2.30*	−5.61*	−3.64*	−3.56*	−2.49*
Gangetic West Bengal	3.04*	−1.73	−4.63*	−3.48*	5.12*	−1.92	−2.79*	−4.08*	−0.29	3.09*	−2.63*	0.89
Orissa	4.08*	−4.10*	−4.47*	1.46	4.55*	−0.92	4.27*	0.97	5.22*	4.44*	−2.15*	3.89*
Jharkhand	−3.45*	−4.19*	−3.39*	−2.25*	7.09*	−2.11*	−5.23*	−4.70*	−3.61*	−0.48	−2.69*	−3.81*
Bihar	−2.39*	0.42	4.21*	−0.62	6.95*	2.14*	−7.98*	−3.24*	−1.96	−1.76	−6.01*	−4.00*
East Uttar Pradesh	−1.21	−0.61	−1.30	−3.12	4.92	−1.40	−7.98*	−7.66*	−7.38*	−1.78	−7.22*	−6.48*
West Uttar Pradesh	4.66*	−0.67	1.05	−2.68*	4.43*	−3.40*	−7.17*	−7.17*	−4.24*	1.02	−4.05*	−3.75*
Uttarakhand	1.84	−0.86	−3.69*	1.33	0.62	1.67	3.43*	1.18	1.37	1.60	−4.55*	−5.15*
Haryana, Chandigarh and Delhi	1.54	−1.48	2.08*	0.37	3.18*	1.92	−7.66*	−5.07*	5.17*	1.76	−5.01*	−3.84*
Punjab	3.04*	−4.17*	−2.20*	−0.95	−4.57*	2.01*	−7.36*	−3.70*	2.22*	1.74	−3.70*	−4.35*
Himachal Pradesh	−2.75*	2.19*	−3.62*	−1.49*	−2.85*	0.67	−3.45*	4.51*	5.72*	−1.43	−0.34	−3.56*
Jammu and Kashmir	1.73	0.18	−4.25*	−3.35*	−4.93*	5.33*	0.59	−0.56	2.14*	−0.50	2.25*	−4.36*
West Rajasthan	2.39*	3.45*	4.40*	3.59*	1.96	4.47*	1.14	5.28*	4.36*	1.35	3.01*	3.29*
East Rajasthan	4.27*	−2.45*	4.35*	1.59	1.82	−1.51	−2.03*	2.66*	3.34*	−0.70*	−7.36*	−3.13*
West Madhya Pradesh	0.26	−1.16	3.87*	1.74	−1.46	0.86	6.46*	−3.27*	3.57*	1.54	−6.04*	−1.59
East Madhya Pradesh	−2.83*	−2.38*	4.08*	2.38*	6.02*	−1.74	0.23	−8.26*	2.50*	−2.11*	−2.80*	−1.21
Gujarat Region	0.70	−2.72*	5.00*	1.49	−4.49*	−5.29*	1.57	−1.08	6.51*	2.14*	−7.00*	3.61*
Saurashtra, Kutch and Diu	0.92	−4.14*	4.88*	3.31*	0.97	−4.32*	4.96*	4.38*	6.81*	0.10	−5.37*	2.20*
Konkan and Goa	7.28*	5.86*	4.73*	4.21*	3.39*	3.75*	5.69*	2.99*	5.39*	4.57*	−2.03*	4.08*
Madhya Maharashtra	2.08*	−1.24	3.04*	−4.88*	−5.71*	0.34	5.04*	2.72*	3.57*	3.01*	−3.40*	1.41
Marathwada	−4.10*	−0.91	2.60*	2.15*	−3.78*	0.75	3.50*	−2.90*	3.78*	2.42*	−5.25*	−4.28*
Vidarbha	−1.08	−6.64*	4.38*	−0.42	−2.08*	−1.40	4.60*	−4.93*	4.16*	−2.99*	−3.21*	−4.90*
Chhattisgarh	2.99*	−0.20	4.92*	3.37*	2.93*	−1.74	−1.40	−3.67*	4.21*	−1.67	−1.78	2.82*
Coastal Andhra Pradesh	4.24*	−1.87	1.24	−1.22	−1.10	2.23	4.68*	0.97	2.58*	−3.70*	−0.75	5.28*
Telangana	2.66*	−4.17*	3.75*	5.56*	0.20	0.28	1.11	−0.50	4.33*	−2.30*	−4.14*	−1.51
Rayalaseema	−0.28	−1.85	3.54*	4.28*	4.43*	4.52*	2.36*	2.25*	1.95	−3.86*	−1.22	2.22*
Tamil Nadu and Pondicherry	3.59*	2.44*	0.20	3.18*	1.41	−1.05	−1.13	3.20*	−6.07*	−1.74	−2.19*	−1.35
Coastal Karnataka	5.39*	4.87*	5.22*	9.00*	7.55*	−5.66*	−2.33*	−1.21	5.69*	6.53*	1.37	4.95*
North Interior Karnataka	3.04*	1.52	4.46*	5.94*	3.76*	−1.73	2.60*	2.30*	−0.97	−0.24	−4.62*	1.57
South Interior Karnataka	3.86*	2.82*	4.74*	4.63*	4.73*	−3.42*	0.92	4.52*	−2.23*	6.19*	1.85	3.97*
Kerala	4.57*	2.25*	6.35*	4.32*	5.17*	−3.81*	−1.43	4.33*	4.10*	8.10*	−1.19	1.87

***** indicates statistical significance

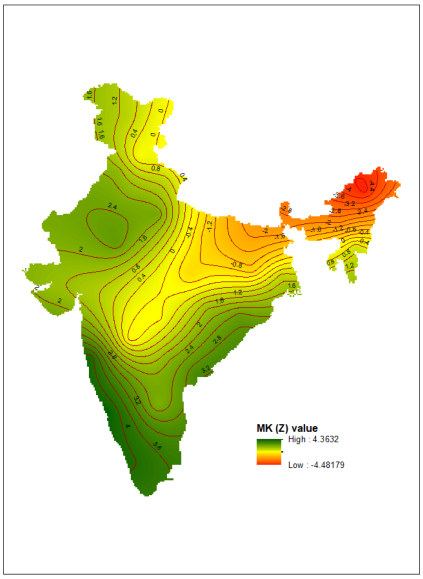

(a) Jan

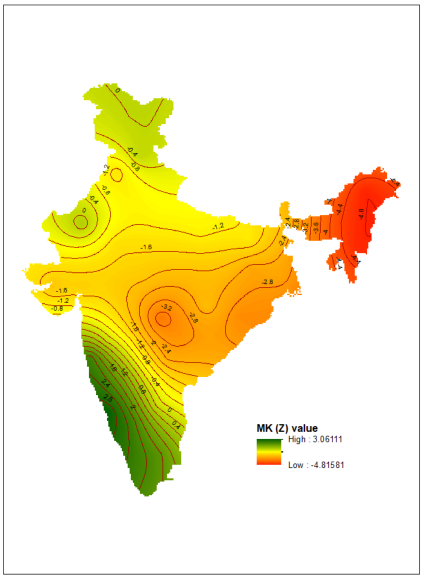

(b) Feb

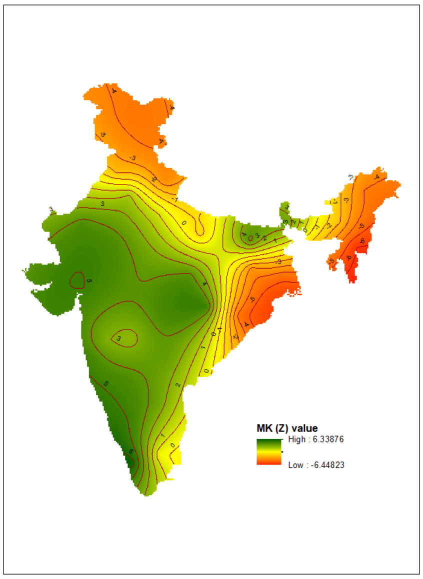

(c) Mar

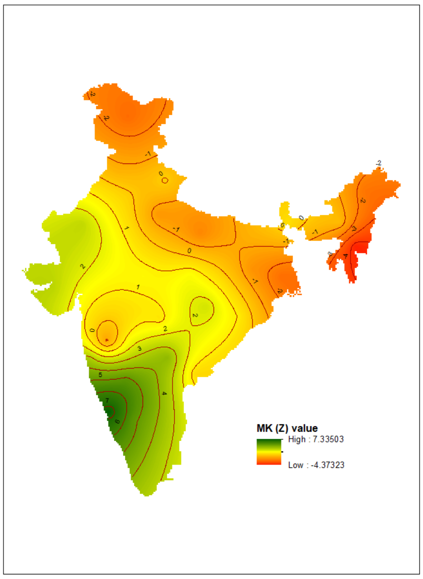

(d) Apr

Figure 4.20: Spatial distributions of monthly rainfall (2023-2074) across Meteorological sub-divisions of India using the Man-Kendall test (Continued).

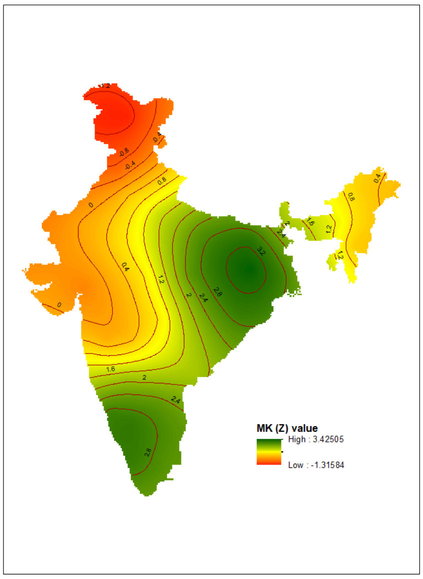

(e) May

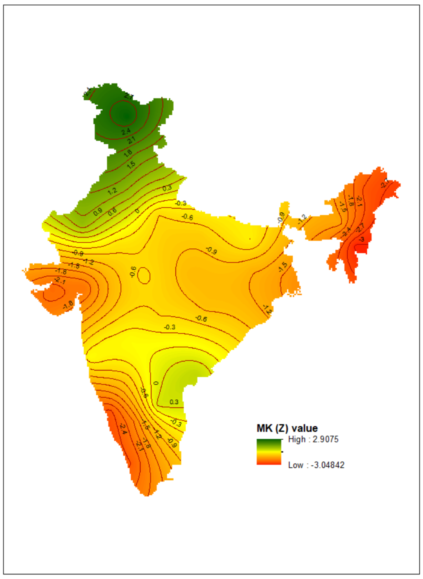

(f) Jun

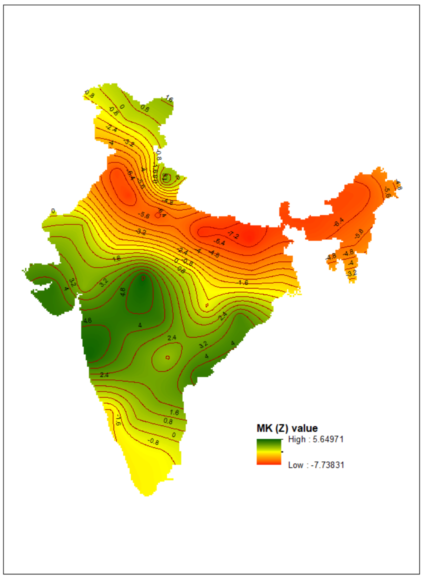

(g) Jul

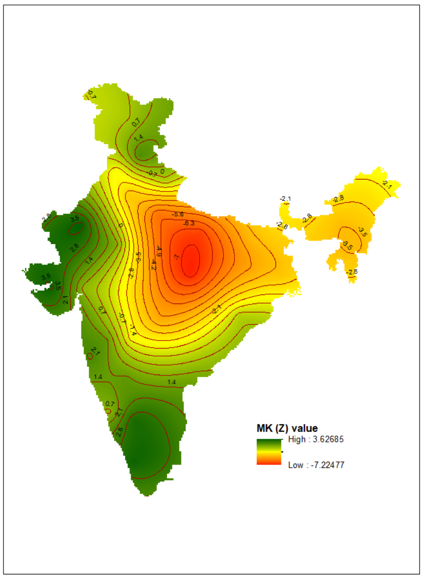

(h) Aug

Figure 4.20: Spatial distributions of monthly rainfall (2023-2074) across Meteorological sub-divisions of India using the Man-Kendall test (Continued).

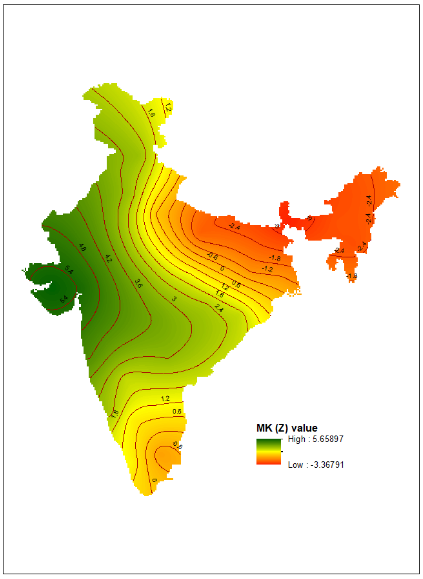

(i) Sep

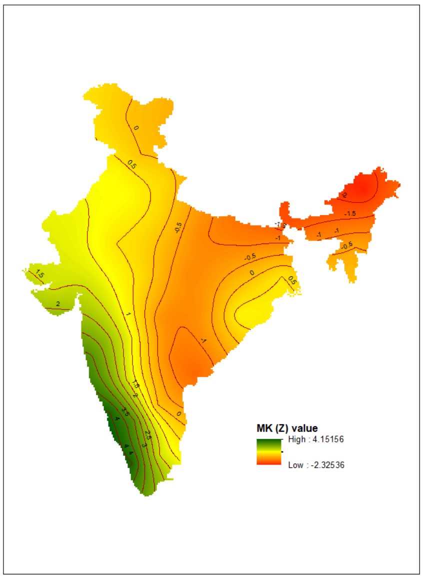

(j) Oct

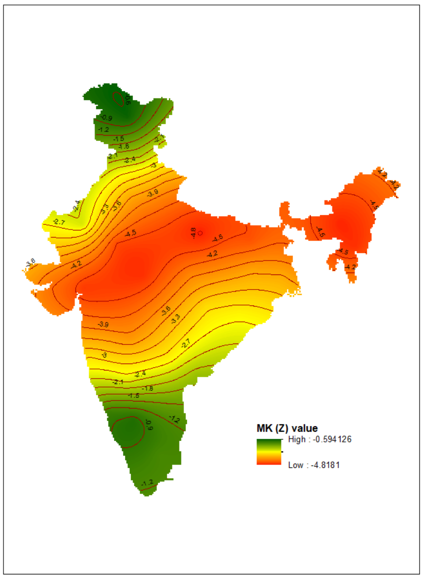

(k) Nov

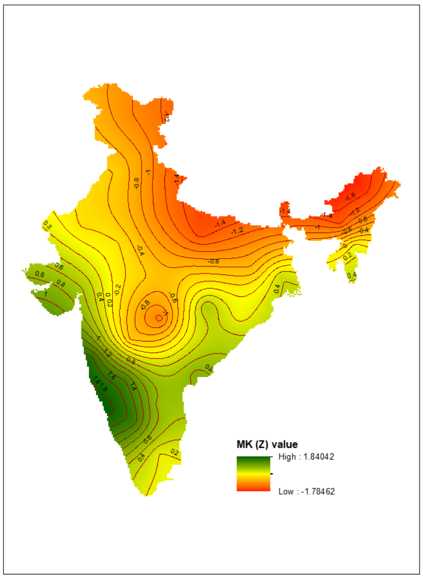

(l) Dec

Figure 4.20: Spatial distributions of monthly rainfall (2023-2074) across Meteorological sub-divisions of India using the Man-Kendall test.

4.3.4.3 Sen's Slope Test

The Sen slope analysis of forecasted monthly rainfall trends for 2023–2075 highlights significant spatial and temporal variability across India's meteorological subdivisions, emphasizing both declining and increasing rainfall trends (Table 4.9). Declining trends are most pronounced in northeastern regions such as Arunachal Pradesh, which exhibits the steepest reduction in October (-0.441 mm/year), and Nagaland, Manipur, Mizoram, and Tripura, where June shows a sharp decline of -0.923 mm/year. Similarly, Sub-Himalayan West Bengal and Sikkim demonstrate significant monsoon reductions, particularly in July (-0.864 mm/year), indicating potential challenges for regions dependent on consistent monsoon rainfall for agriculture and water resources. Other regions, including Jharkhand, Bihar, and East Uttar Pradesh, also show declining rainfall trends during critical monsoon months, which could exacerbate water scarcity and impact crop yields. Conversely, regions like Konkan and Goa display the highest positive trend in July (+1.93 mm/year), reflecting intensified monsoon activity. Coastal Karnataka and Kerala also show substantial increases, with August and September reporting positive trends of +1.254 mm/year and +0.771 mm/year, respectively, suggesting potential risks of flooding and infrastructure challenges in these areas. Mixed patterns are observed in Gangetic West Bengal and Telangana, where pre-monsoon months like May exhibit increasing rainfall trends, while monsoon months display declining trends, highlighting the shifting dynamics of rainfall distribution across seasons. In central and western India, regions like Saurashtra, Kutch, and Diu show positive rainfall trends during the late monsoon months, with September witnessing an increase of +0.707 mm/year. Similarly, Vidarbha and Madhya Maharashtra exhibit moderate increases in July (+0.506 mm/year and +0.485 mm/year, respectively), which may benefit agricultural activities in these regions. However, East Rajasthan and Chhattisgarh show mixed trends, with slight increases in some months but significant declines in others, indicating variability in rainfall reliability. Overall, the analysis underscores the uneven distribution of rainfall trends across India, with some regions experiencing enhanced monsoon precipitation while others face significant reductions. These patterns reflect the complex interplay of climatic factors influencing rainfall variability and point to the need for region-specific water resource management and climate adaptation strategies.

Table 4.9: Sen's Slope Analysis of Forecasted Monthly Rainfall (2023-2075) Across Meteorological Sub-divisions of India Using IRPM.

Region	**Jan**	**Feb**	**Mar**	**Apr**	**May**	**Jun**	**Jul**	**Aug**	**Sep**	**Oct**	**Nov**	**Dec**
Arunachal Pradesh	−0.22	−0.38	−0.26	−0.24	−0.07	−0.29	−0.44	−0.22	−0.18	−0.44	−0.19	−0.16
Assam and Meghalaya	−0.04	−0.08	−0.07	0.06	0.27	0.15	−0.80	−0.33	−0.11	−0.04	−0.13	−0.05
Nagaland, Manipur, Mizoram and Tripura	0.02	−0.16	−0.20	−0.54	−0.55	−0.92	−0.62	−0.37	−0.20	0.06	−0.27	0.01
Sub-Himalayan West Bengal and Sikkim	−0.04	−0.02	0.09	0.03	−0.10	−0.14	−0.86	−0.27	−0.33	−0.25	−0.08	−0.03
Gangetic West Bengal	0.02	−0.02	−0.08	−0.12	0.27	−0.17	−0.18	−0.43	−0.02	0.13	−0.05	0.00
Orissa	0.03	−0.06	−0.05	0.02	0.17	−0.02	0.25	0.02	0.39	0.14	−0.06	0.03
Jharkhand	−0.03	−0.08	−0.02	−0.04	0.16	−0.19	−0.39	−0.35	−0.28	−0.01	−0.02	−0.01
Bihar	−0.02	0.00	0.02	0.00	0.21	0.09	−0.37	−0.20	−0.17	−1.10	−0.04	−0.02
East Uttar Pradesh	−0.01	−0.01	0.00	−0.02	0.06	−0.09	−0.68	−0.58	−0.49	−0.05	−0.02	−0.03
West Uttar Pradesh	0.04	−0.01	0.01	−0.02	0.03	−0.18	0.50	−0.73	−0.18	0.01	−0.01	−0.03
Uttarakhand	0.02	−0.03	−0.14	0.02	0.01	0.07	0.30	0.15	0.07	0.05	−0.03	−0.09
Haryana, Chandigarh and Delhi	0.01	−0.02	0.02	0.00	0.03	0.03	−0.31	−0.53	0.22	0.01	−0.02	−0.03
Punjab	0.06	−0.07	−0.03	−0.01	−0.04	0.02	−0.47	−0.51	0.13	0.01	−0.02	−0.04
Himachal Pradesh	−0.08	−0.04	−0.21	−0.03	−0.07	0.00	−0.28	0.26	0.21	−0.04	0.00	−0.09
Jammu and Kashmir	0.16	0.01	−0.35	−0.12	−0.17	0.13	0.01	−0.03	0.16	0.00	0.03	−0.15
West Rajasthan	0.01	0.02	0.04	0.04	0.02	0.08	0.06	0.15	0.14	0.01	0.01	0.01
East Rajasthan	0.01	−0.13	0.03	0.00	0.01	−0.03	−0.06	0.12	0.17	−0.01	−0.03	−0.01
West Madhya Pradesh	0.00	−0.01	0.03	0.00	0.00	0.04	0.42	−0.27	0.32	0.02	−0.05	−0.01
East Madhya Pradesh	−0.03	−0.05	0.05	0.01	0.06	−0.06	0.00	−0.71	0.16	−0.06	−0.03	−0.01
Gujarat Region	0.00	0.00	0.00	0.00	−0.02	−0.36	0.37	−0.03	0.41	0.03	−0.05	0.01
Saurashtra, Kutch and Diu	0.00	0.00	0.00	0.00	0.00	−0.25	0.57	0.37	0.71	0.00	−0.05	0.00
Konkan and Goa	0.01	0.00	0.02	0.01	0.07	0.27	1.93	0.36	1.51	0.46	−0.04	0.02
Madhya Maharashtra	0.00	0.00	0.02	−0.02	−0.06	0.02	0.49	0.21	0.26	0.15	−0.06	0.01
Marathwada	−0.01	0.00	0.03	0.01	−0.05	0.03	0.31	−0.15	0.28	0.08	−0.09	−0.02
Vidarbha	0.00	−0.05	0.06	0.00	−0.01	−0.03	0.51	−0.43	0.49	−0.13	−0.05	−0.03
Chhattisgarh	0.03	0.00	0.05	0.04	0.02	−0.10	−0.88	−0.26	0.32	−0.04	−0.02	0.01
Coastal Andhra Pradesh	0.04	−0.03	0.01	−0.02	0.00	0.09	0.19	0.01	0.13	−0.23	−0.01	0.11
Telangana	0.02	−0.02	0.06	0.04	0.00	0.01	0.05	−0.04	0.39	−0.16	−0.06	0.00
Rayalaseema	0.00	−0.01	0.04	0.06	0.07	0.20	0.06	0.12	0.07	−0.18	−0.06	0.01
Tamil Nadu and Pondicherry	0.06	−0.03	0.00	0.06	0.02	−0.02	−0.06	0.15	−0.28	−0.06	0.24	−0.07
Coastal Karnataka	0.03	0.01	0.09	0.19	0.38	−0.92	−0.32	−0.06	1.25	0.66	0.03	0.06
North Interior Karnataka	0.01	0.00	0.05	0.06	0.07	−0.04	0.08	0.08	−0.02	−0.02	−0.08	0.00
South Interior Karnataka	0.01	0.01	0.06	0.14	0.19	−0.22	0.01	0.22	−0.10	0.24	0.06	0.03
Kerala	0.04	0.02	0.19	0.20	0.44	−0.61	−0.31	0.65	0.77	0.58	−0.02	0.01

4.3.5 Comparison with other forecasting models

We evaluated the forecasting performance of SARIMA and IRPM, by calculating two widely used error measures: RMSE and MAE (Figure 4.21). These metrics offer clear insights into both the accuracy and consistency of the model predictions. Our analysis revealed that across all studied regions, the IRPM model consistently outperformed SARIMA, achieving lower RMSE and MAE values. This indicates that IRPM produces more precise and reliable forecasts than the SARIMA approach in every geographical area studied.

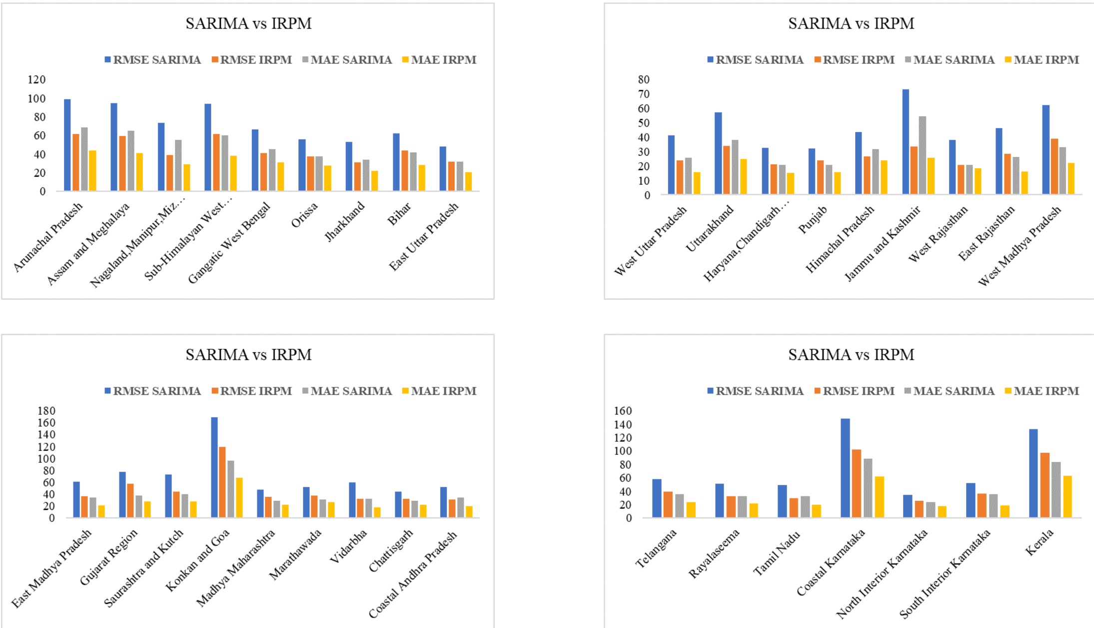

Figure 4.21: Comparison of SARIMA and IRPM using RMSE for Meteorological Sub-divisions of India.

4.3.6 Discussion

Analysing historical rainfall trends is crucial for effective water resource management, agriculture, ecosystem sustainability, and public health. Marumbwa *et al.* (2019) emphasized the significance of such analyses in understanding climatic variability. In this study, rainfall data from 1972–2022 across 34 meteorological sub-divisions in India was examined to identify trends and forecast rainfall for the next 50 years. The Mann-Kendall and Sen's slope tests revealed notable spatial and temporal variability, with increasing trends observed in regions like Coastal Karnataka and Kerala during March, and declining trends in Arunachal Pradesh and other Northeastern States during February and July. January exhibited the highest positive trend, while February showed the most negative trend. Regionally, western areas such as Konkan and Goa experienced rising rainfall patterns, whereas northern and central regions, including East Uttar Pradesh and Gujarat, showed reductions in monsoon rainfall. These findings are consistent with previous studies—-Mirza *et al.* (1998) reported stable rainfall patterns in Sub-Himalayan and Gangetic Bengal, Murali *et al.* (2022) observed positive trends in Telangana, and Praveen *et al.* (2020) identified significant monsoon rainfall declines in 11 out of 17 divisions from 1901–2015. The consistency of these results with the current study strengthens the reliability of the observed monthly rainfall trends.

Accurate rainfall forecasting is essential for proactive water resource management. This study utilized the Innovative Rainfall Predictive Method (IRPM), which integrates linear regression, Fourier regression, and a random probabilistic approach, further refined by a corrector factor to adjust discrepancies between observed and predicted rainfall. The model's performance was validated using a modified K-fold cross-validation method with data from 1971 to 2022. Previous research has explored various forecasting techniques to improve predictive accuracy. For example, Shrestha *et al.* (2017) applied artificial neural networks for rainfall prediction, demonstrating their effectiveness in capturing non-linear climatic patterns. Similarly, Boukabara *et al.* (2019) highlighted the advantages of data assimilation techniques in enhancing weather and precipitation forecasts. Building on these approaches, the IRPM model combines statistical and probabilistic methods to improve forecast reliability. The IRPM model's results revealed significant spatial and temporal rainfall variability across India. High predictive accuracy was observed in regions like Vidarbha ($R^2 = 0.94$) and Sub-Himalayan West Bengal ($R^2 = 0.93$), while lower performance was noted in topographically complex regions such as Jammu & Kashmir ($R^2 = 0.67$). These findings are consistent with Kumar *et al.* (2020), who reported challenges in rainfall prediction for mountainous and heterogeneous terrains. Overall, the IRPM model demonstrated robust performance, particularly in regions with consistent rainfall patterns, while highlighting the need for further refinements to capture complex rainfall dynamics in coastal and mountainous areas.

Global warming and climate change, driven by rising global temperatures and glacier melting, are significantly altering precipitation patterns worldwide (IPCC, 2021). Studies such as Hansen *et al.* (2017) and Jones and Ricketts (2019) highlight how changing atmospheric dynamics and oceanic circulations contribute to regional rainfall variability. Understanding long term rainfall trends is critical for mitigating climate-induced risks, particularly in monsoon-dependent regions like India. Using the IRPM, this study forecasts rainfall trends for 2025–2075, analysed through the MK test and Sen's slope method, revealing substantial spatial and temporal variability. The projected rainfall trends for 2025–2075 reveal significant spatial and temporal variability across India, with northeastern and central regions experiencing sharp declines, while coastal and western areas exhibit rising trends. These increasing trends align with Praveen *et al.* (2020), who attributed rising rainfall in Kerala and Coastal Karnataka to intensified convective systems and western disturbances. Similarly, Boukabara *et al.* (2019) highlighted the role of shifting oceanic temperatures and intensified el niño-southern oscillation patterns in amplifying rainfall variability in coastal and western India. The IPCC Sixth Assessment Report (2021) also predicts an increase in extreme rainfall events in South Asia, driven by rising sea surface temperatures and enhanced moisture convergence. Overall, the rainfall projections for 2025–2075 highlight an uneven distribution of precipitation across India, with some regions facing increasing monsoon rainfall, while others experience significant declines. These trends align with global climate studies (Hansen *et al.*, 2017; IPCC, 2021) that link climate change to altered monsoon dynamics. While regions with declining rainfall must prepare for water shortages, areas with increasing rainfall may face flooding risks. The study emphasizes the urgent need for region-specific adaptation strategies, including sustainable water resource management, resilient agricultural planning, and flood mitigation measures, to counteract the adverse effects of climate change on rainfall patterns.

4.4 Summary

Understanding long range rainfall trends is crucial for mitigating climate-induced risks, particularly in monsoon-dependent regions where rainfall variability significantly impacts agriculture, water resources, and disaster management. This chapter is dedicated to analyzing past and future rainfall trends to develop effective climate adaptation strategies. To achieve this, we conducted a study covering India. A district-wise trend analysis of Mizoram's historical rainfall data using the MK test, Sen's slope, and ITA methods revealed that most districts exhibit decreasing rainfall trends, though many are not statistically significant at the 95% confidence level. However, Aizawl, Kolasib, Champhai, and Serchhip show significant declines, particularly in February, September, and October, with the steepest reductions confirmed by Sen's slope values. In contrast, Mamit is the only district displaying a statistically significant increase in December. Across all districts, March, April, May, and October consistently exhibit declining rainfall trends, indicating a long-term reduction in precipitation that may impact regional hydrological stability and water management. Long-term forecasts using the IRPM from 2024 to 2064 indicate a prevailing decline in rainfall across most districts. Champhai and Serchhip experience the steepest reductions, with slopes of -0.981 and -0.569, respectively. Significant decreasing trends are also observed in Aizawl, Lunglei, Lawngtlai, and Kolasib, reinforcing concerns about declining rainfall. Conversely, Saiha emerges as the only district with a notable increasing trend (average slope = 0.315), while Mamit exhibits mixed results. Expanding our analysis beyond Mizoram, we conducted a trend assessment across 34 meteorological sub-divisions in India. Significant increasing rainfall trends were observed in March and September across five sub-divisions, signalling shifts in pre- and post-monsoon patterns. July exhibited intensified monsoon activity in some regions but declines in others. No notable changes occurred in May and December. The IRPM demonstrated strong predictive reliability (RMSE: 21.39–102.26, R^2: 0.67–0.95). Future projections from 2023 to 2075 reveal sharp declines in rainfall across northeastern states and eastern India, raising concerns about water security. In contrast, Coastal Karnataka, Kerala, and Konkan & Goa exhibit increasing trends, indicating heightened flood risks during peak monsoon periods. Central and western India displays mixed rainfall patterns, reflecting the complex variability of the monsoon system. Additionally, the IRPM outperforms both ARIMA and SARIMA in forecasting rainfall across the study area, demonstrating its potential as a more reliable and accurate predictive model for the region.

This study underscores the importance of detailed rainfall trend analysis for effective climate adaptation strategies. The findings provide valuable insights for the efficient planning and management of water resources, ensuring reliable water allocation across different sectors. The presence of significant trends in specific months necessitates careful planning for water availability and food security.

Chapter 5

Multivariate Holt Winters Method for Forecasting Rainfall

5.1 Introduction

Time series forecasting has emerged as a vital analytical tool for modeling historical rainfall data and predicting future rainfall patterns (Malik *et al.*, 2023). Among the various forecasting methods, exponential smoothing techniques have gained prominence due to their simplicity, adaptability, and ability to capture both trend and seasonality components in time series data. Holt Winters method is one type of exponential smoothing method, making it suitable for data with linear and seasonality patterns. These models have been widely employed in rainfall forecasting studies, with performance commonly evaluated using error metrics such as Mean Absolute Error (MAE), Root Mean Square Error (RMSE), and Mean Absolute Percentage Error (MAPE) (Rafian, 2022; Hutapea and Siahaan, 2023; Aini *et al.*, 2021; Wiguna *et al.*, 2023; Karthika and Karthikeyan, 2022; Pandit *et al.*, 2023; Irwan *et al.*, 2023). Despite their effectiveness, traditional univariate Holt Winters methods have a significant limitation: they do not account for external meteorological factors such as temperature, humidity, which

Muniyan, S. and Lallawmzuali, M. (2025). Multivariate Holt Winters Method for Forecasting Rainfall. (Communicated) are known to influence rainfall patterns (Guhathakurta *et al.*, 2011).

Univariate forecasting refers to prediction based solely on past values of a single variable, offering simplicity and interpretability. However, it often fails to capture the interdependencies between multiple factors influencing the target variable. In contrast, multivariate forecasting considers multiple correlated variables simultaneously, enabling the modeling of their dynamic relationships and improving predictive accuracy (Shah and Dimitrov, 2022). Several multivariate techniques have been successfully applied in rainfall forecasting. For example, Vector Autoregression (VAR) and Multiple Linear Regression (MLR) models have shown promising results. Nauval *et al.* (2022) applied the VAR model to forecast monthly rainfall in Cilacap, Indonesia, achieving high predictive accuracy as measured by RMSE and MAPE. Shahin *et al.* (2014) used VAR to study rainfall trends in the Jessore region of Bangladesh, revealing a downward trend. Nugroho *et al.* (2014) found VAR to outperform ARIMA in forecasting rainfall in Semarang, Central Java, evidenced by lower MAE and MAPE values. Ahmed and Mohamed (2021) employed MLR to predict precipitation rates in Khartoum, Sudan, with considerable success.

Given the strengths of multivariate models, researchers have proposed multivariate extensions of exponential smoothing techniques. Pfeffermann and Allon (1989) were among the first to develop a multivariate exponential smoothing framework, demonstrating its superiority over univariate and autoregressive models in forecasting correlated time series, such as tourism and economic data (Athanasopoulos *et al.*, 2011). However, the application of multivariate Holt Winters methods to rainfall forecasting remains underexplored. Motivated by this hole, in this chapter, we seek to bridge this gap by developing two advanced forecasting models: a Multivariate Additive Holt Winters (MAHW) model and a Multivariate Modified Holt Winters (MMOHW) model, both of which integrate auxiliary meteorological variables to enhance prediction accuracy. By incorporating cross-variable dependencies, these models aim to provide a more robust and comprehensive framework for rainfall forecasting, ultimately supporting better climate adaptation and decision-making.

5.2 Study Area and Data Collection

The Historical monthly rainfall, temperature, and humidity of 1986-2023 are obtained from the State Meteorological Centre, Directorate of Science and Technology, Government of Mizoram.

5.3 Data Exploration

The statistical analysis of monthly rainfall, temperature, and humidity from 1986-2023, as presented in Table 5.1, provides valuable insights into the region's climate patterns.

The monthly rainfall in Mizoram from 1986 to 2023 exhibits significant variability, ranging from 0 mm to a maximum of 743.5 mm. The Standard Deviation (SD), which measures the extent of fluctuations in monthly rainfall, varies between 14.95 mm and 144.86 mm, indicating considerable differences in rainfall distribution across months. The skewness, ranging from -0.16 to 2.8, suggests that while some months have a nearly symmetrical distribution of rainfall, others exhibit a strong right-skewed pattern, with occasional extreme rainfall events. Additionally, the kurtosis values, which range from -0.42 to 8.06, reflecting variations in the peakedness of the distribution, with some months experiencing more uniform rainfall while others show highly irregular and extreme variations.

The monthly temperature in Mizoram from 1986 to 2023 exhibits a relatively stable pattern, with mean temperatures ranging from 15.06°C to 24.08°C. The standard deviation, which measures the extent of variability, remains low, ranging from 0.54°C to 1.26°C, indicating minimal fluctuations across months over the years. The recorded temperatures range from a minimum of 12.6°C to a maximum of 25.7°C, reflecting a moderate overall variation. The skewness of the temperature distribution ranges from -0.42 to 0.72, suggesting a nearly symmetrical distribution with only slight deviations. Additionally, the kurtosis values range from -1.03 to 0.78, indicating a relatively flat distribution without extreme peaks or heavy tails, reinforcing the overall stability of temperature patterns in Mizoram over the observed period.

The monthly humidity in Mizoram from 1986 to 2023 varies significantly, ranging from 30.28% to 90.92%. The standard deviation, which measures the fluctuations in humidity levels, ranges from 3.84% to 10.88%, indicating moderate to high variability across different months. The skewness values range from -0.27 to 0.64, suggesting that the humidity distribution is nearly symmetrical, with slight deviations in certain months. The kurtosis values range from -1.39 to 0.33, indicating a generally flat distribution, meaning the humidity levels do not exhibit extreme peaks or heavy tails. Notably, the only positive kurtosis value (0.3) was observed in April, while all other months show negative kurtosis, implying that the humidity distribution in most months is more uniform and lacks significant extremes.

Table 5.1: Descriptive Statistics of Rainfall, Temperature, and Humidity (1986–2023).

Variable	Min (mm)	Mean (mm)	Max (mm)	SD (mm)	Skewness	Kurtosis
Rainfall (Jan)	0.00	7.99	68.20	14.95	2.80	8.06
Rainfall (Feb)	0.00	21.67	120.80	24.72	1.99	5.71
Rainfall (Mar)	0.00	62.37	314.30	70.15	2.02	4.26
Rainfall (Apr)	13.10	141.58	368.28	87.68	0.87	0.24
Rainfall (May)	71.20	273.32	718.00	135.16	1.15	1.84
Rainfall (Jun)	106.50	320.42	743.50	144.86	0.97	0.97
Rainfall (Jul)	66.90	317.79	539.00	99.44	−0.16	−0.04
Rainfall (Aug)	156.90	344.24	517.90	86.55	−0.06	−0.42
Rainfall (Sep)	131.00	301.80	510.80	91.38	0.47	−0.23
Rainfall (Oct)	67.90	174.87	421.00	87.13	1.14	0.94
Rainfall (Nov)	0.00	48.30	250.20	56.83	1.84	3.68
Rainfall (Dec)	0.00	141.13	91.10	25.26	1.83	2.24
Temperature (Jan)	12.64	15.06	16.77	0.93	−0.41	−0.09
Temperature (Feb)	14.24	17.33	20.42	1.26	−0.12	0.74
Temperature (Mar)	19.00	20.86	23.09	0.87	−0.10	−0.01
Temperature (Apr)	21.29	23.35	25.30	1.01	0.15	0.78
Temperature (May)	22.38	24.08	25.70	0.72	−0.42	−0.06
Temperature (Jun)	22.71	23.96	24.99	0.70	0.13	−0.35
Temperature (Jul)	23.02	23.98	24.99	0.54	−1.03	−1.03
Temperature (Aug)	22.84	23.96	25.54	0.66	−0.42	−0.42
Temperature (Sep)	22.32	23.43	24.61	0.54	−0.24	−0.24
Temperature (Oct)	20.02	22.03	23.47	0.70	0.61	0.61
Temperature (Nov)	17.20	19.22	21.23	0.79	0.72	0.72
Temperature (Dec)	14.25	16.13	17.94	0.83	−0.32	−0.32
Humidity (Jan)	31.53	51.73	74.42	10.88	0.14	−0.69
Humidity (Feb)	30.28	48.33	68.65	9.27	0.16	−0.50
Humidity (Mar)	35.66	50.06	68.58	7.58	0.11	−0.02
Humidity (Apr)	48.48	61.29	83.62	8.30	0.64	0.33
Humidity (May)	61.49	72.58	85.73	6.27	0.54	−0.52
Humidity (Jun)	70.26	81.49	90.84	4.99	−0.27	−0.49
Humidity (Jul)	77.68	84.62	90.92	3.84	−0.12	−0.98
Humidity (Aug)	76.87	85.12	91.51	4.29	−0.17	−1.40
Humidity (Sep)	77.76	84.87	92.20	4.55	−0.14	−1.39
Humidity (Oct)	68.16	81.77	90.93	5.86	−0.21	−0.83
Humidity (Nov)	54.23	71.82	86.29	8.58	−0.16	−0.87
Humidity (Dec)	39.86	61.45	82.64	10.54	−0.16	−0.55

5.4 Correlation of the Meteorological Variables

The correlation analysis demonstrates a strong positive relationship between meteorological variables and rainfall. The Pearson correlation coefficient indicates that temperature and rainfall are positively correlated (0.7074), while humidity and rainfall also exhibit a strong correlation (0.6734), suggesting that increases in temperature and humidity are generally associated with higher rainfall. Similarly, the Spearman's rank correlation values further confirm this association, with temperature showing a correlation of 0.7523 with rainfall and humidity showing 0.7136. These results suggest that both temperature and humidity significantly influence rainfall patterns, with a slightly stronger monotonic relationship observed in the Spearman correlation.

The cross-correlation analysis further highlights the temporal dependencies between these variables (Figure 5.1). The highest correlation between rainfall and temperature (0.8015) occurs at lag 0, indicating that changes in temperature and rainfall occur simultaneously. In contrast, rainfall and humidity show a maximum correlation of 0.8261 at lag -1, meaning that variations in humidity precede changes in rainfall by one time step, making humidity a potential predictor for rainfall fluctuations. Overall, the analysis demonstrates that temperature and humidity significantly influence rainfall patterns, with humidity playing a leading role in rainfall variations. These findings are crucial for improving forecasting models, particularly in the context of multivariate approaches like the Multivariate Holt Winters method, which can effectively account for these interdependencies in long range rainfall prediction.

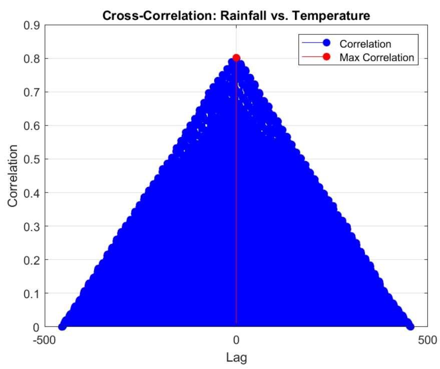

(a) The highest correlation between Rainfall and Temperature occurs at lag 0.

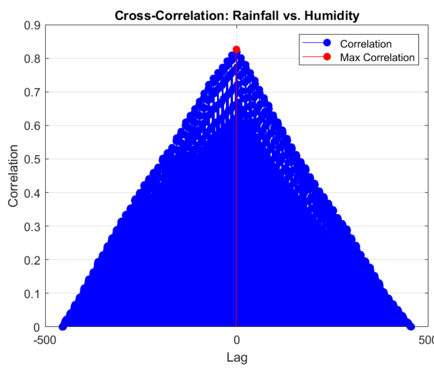

(b) The highest correlation between Rainfall and Humidity occurs at lag -1.

Figure 5.1: Cross Correlation of Rainfall vs Temperature, and Rainfall vs Humidity for Mizoram data of 1986-2023.

5.4.1 Decomposition of Meteorological Variables

The decomposition of rainfall, temperature, and humidity of Mizoram from 1986-2023 are presented in Figure 5.2. The decomposition process separates each variable into trend, seasonal, and residual components, allowing us to understand their underlying structures. The trend component reveals long-term variations, indicating whether the variable exhibits an upward or downward pattern over time. The seasonal component highlights periodic fluctuations that repeat at regular intervals, confirming the presence of seasonality in the data. The residual component captures random variations that cannot be explained by trend or seasonality. By decomposing these variables, we can visually examine the presence of seasonal patterns, which is essential for selecting an appropriate forecasting method. Since the Holt Winters method relies on level, trend, and seasonal components, confirming the existence of seasonality is a critical step before applying the model.

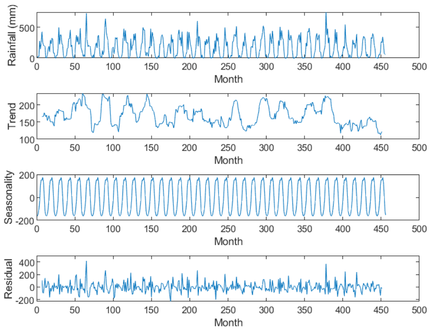

(a) Rainfall

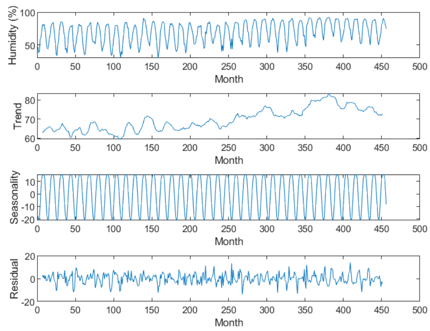

(b) Humidity

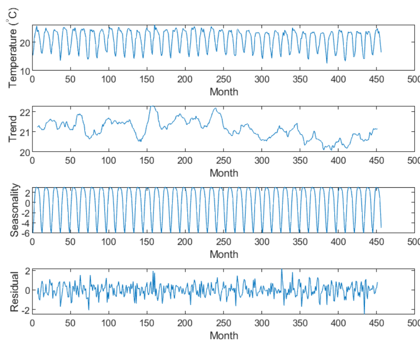

(c) Temperature

Figure 5.2: The decomposition plot of Rainfall, Humidity, and Temperature for Mizoram from 1986-2023.

5.5 Monthly Rainfall Forecasting of Mizoram using Multivariate Holt Winters Methods

In this section, we will be forecasting Mizoram rainfall using MAHW and MMOHW. Firstly, we separated our data for training (80%) and testing (20%). Next, to optimize model performance, the smoothing parameters were fine-tuned within the interval [0,1] using the Bayesian optimization approach, and evaluated the performances using error matrices. Finally, we used the model to forecast monthly rainfall for the next years.

5.5.1 Multivariate Additive Holt Winters Method (MAHW)

As rainfall is influenced by multiple meteorological factors, we employed a Multivariate Additive Holt Winters method (MAHW), incorporating rainfall, temperature, and humidity as key predictors. The dataset, spanning from 1986 to 2023, was used for model development. For training and evaluation, the data was split into 80% for training and 20% for testing (Figure 5.3). The analysis was conducted using MATLAB Version 9.13.0 (R2022b) Update 2. To optimize model performance, the smoothing parameters were fine-tuned within the interval [0,1] using the Bayesian optimization approach, with the final parameter values presented in Table 5.2. Bayesian optimization is known to efficiently find the best hyperparameter settings compared to traditional grid and random searches, as it builds a probabilistic model to guide the search process (Shakya *et al.*, 2022). This approach accelerates convergence and improves accuracy by strategically selecting the most promising hyperparameter values. The model's performance was evaluated using Root Mean Square Error (RMSE) and Mean Absolute Error (MAE). The results indicate that the model effectively captures rainfall variations, demonstrating strong predictive performance with minimal error. For the training period (80% of data), the model achieved an RMSE of 58.96 and an MAE of 28.89, while for the testing period (20% of data), it attained an RMSE of 52.97 and an MAE of 26.15. The relatively low RMSE and MAE values suggest that incorporating temperature and humidity significantly enhances forecasting accuracy. Utilizing this method, rainfall forecasts were generated for future time periods (Figure 5.4). The relatively low RMSE and MAE values suggest that incorporating temperature and humidity significantly enhances a reliable forecasting with NSE 0.64.

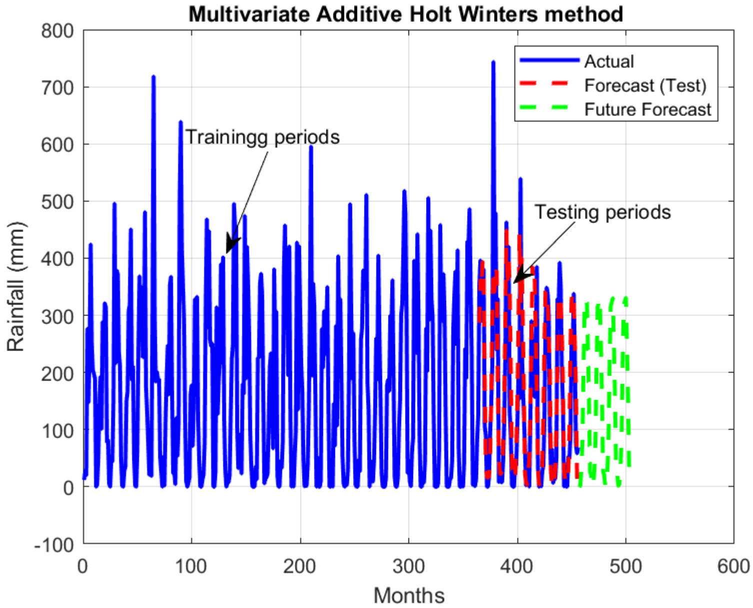

Figure 5.3: Plot illustrating Rainfall forecasts for Mizoram generated by the MAHW.

Table 5.2: Smoothing parameters for MAHW identified using the Brute-Force approach.

Component	**Smoothing parameters**		
Level	$\alpha_{11} = 0.1503$	$\alpha_{12} = 0.8184$	$\alpha_{13} = 0.4962$
	$\alpha_{21} = 0.0995$	$\alpha_{22} = 0.5471$	$\alpha_{23} = 0.5591$
	$\alpha_{31} = 0.6201$	$\alpha_{32} = 0.0811$	$\alpha_{33} = 0.5849$
Trend	$\beta_{11} = 0.0930$	$\beta_{12} = 0.2631$	$\beta_{13} = 0.1357$
	$\beta_{21} = 0.2664$	$\beta_{22} = 0.5716$	$\beta_{23} = 0.2618$
	$\beta_{31} = 0.8245$	$\beta_{32} = 0.1544$	$\beta_{33} = 0.2645$
Seasonality	$\gamma_{11} = 0.1407$	$\gamma_{12} = 0.0006$	$\gamma_{13} = 0.3897$
	$\gamma_{21} = 0.2471$	$\gamma_{22} = 0.1327$	$\gamma_{23} = 0.9720$
	$\gamma_{31} = 0.9064$	$\gamma_{32} = 0.1359$	$\gamma_{33} = 0.9065$

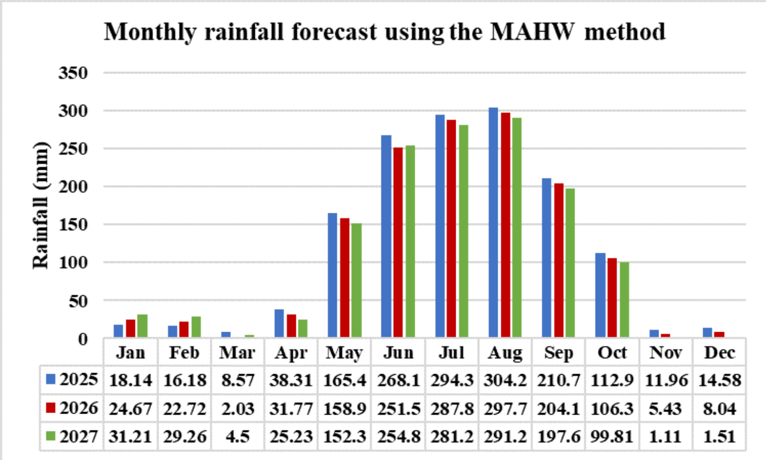

Figure 5.4: Monthly rainfall forecasting of Mizoram using the MAHW method from 2025-2027.

5.5.2 Multivariate Modified Holt Winters Method (MMOHW)

In this study, we evaluated the performance of the MMOHW for rainfall prediction in Mizoram using meteorological variables—temperature, humidity, and rainfall. The models were trained on 80% of the dataset and tested on the remaining 20%, with forecasts extended to future periods (see Figure 5.5). All analyses were conducted using MATLAB Version 9.13.0 (R2022b) Update 2. For time series forecasting with the MMOHW method, the smoothing parameters (α, β, γ) were optimized within the interval [0, 1] using a Bayesian optimization approach, minimizing the RMSE during training. The optimal RMSE achieved in the training phase was 54.45, with the corresponding parameters presented in Table 5.3. When applied to unseen test data, the model demonstrated improved performance, yielding a lower RMSE of 51.80. Similarly, the MAE decreased from 25.60 (training) to 21.33 (testing), indicating a well-balanced model with strong generalization capability. The consistent performance of the MMOHW method suggests its effectiveness in capturing both seasonal and trend components of the time series data. Consequently, the model was employed to generate future rainfall forecasts (see Figure 5.6, demonstrating its potential for reliable meteorological predictions with NSE value of 0.67.

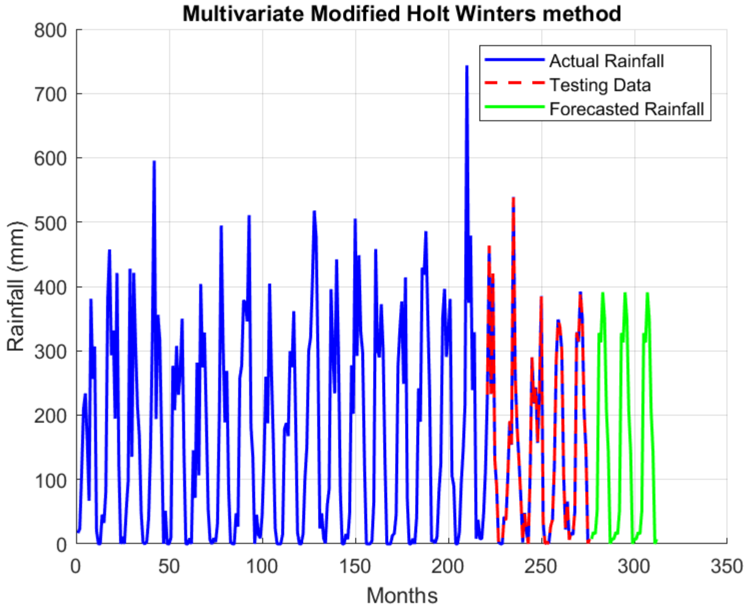

Figure 5.5: Plot illustrating Rainfall forecasts for Mizoram generated by the MMOHW.

Table 5.3: Smoothing parameters for the Multivariate Modified Holt Winters method (MMOHW) identified using the Brute-Force approach.

Component	**Smoothing parameters**		
Level	$\alpha_{11} = 0.2889$	$\alpha_{12} = 0.0799$	$\alpha_{13} = 0.8821$
	$\alpha_{21} = 0.1237$	$\alpha_{22} = 0.0002$	$\alpha_{23} = 0.7440$
	$\alpha_{31} = 0.5455$	$\alpha_{32} = 0.6927$	$\alpha_{33} = 0.1720$
Trend	$\beta_{11} = 0.9670$	$\beta_{12} = 0.0020$	$\beta_{13} = 0.0274$
	$\beta_{21} = 0.7688$	$\beta_{22} = 0.7790$	$\beta_{23} = 0.6929$
	$\beta_{31} = 0.3923$	$\beta_{32} = 0.7928$	$\beta_{33} = 0.8042$
Seasonality	$\gamma_{11} = 0.4211$	$\gamma_{12} = 0.76808$	$\gamma_{13} = 0.4146$
	$\gamma_{21} = 0.2584$	$\gamma_{22} = 0.8103$	$\gamma_{23} = 0.9023$
	$\gamma_{31} = 0.0435$	$\gamma_{32} = 0.2104$	$\gamma_{33} = 0.5011$

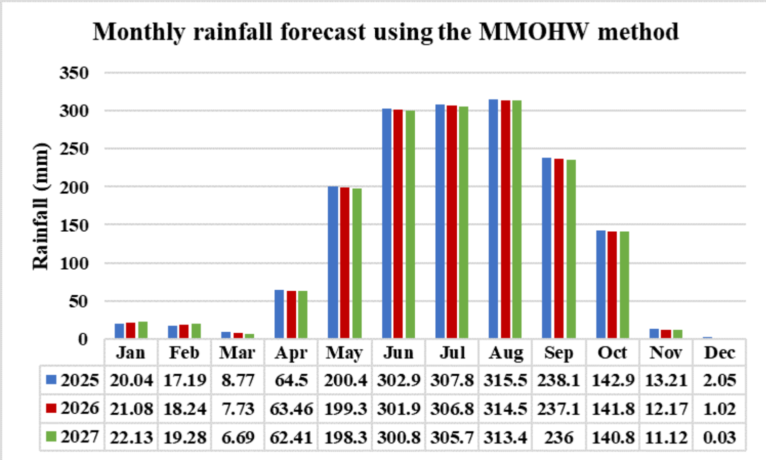

Figure 5.6: Monthly rainfall forecast for Mizoram (2025–2027) using the MMOHW.

5.6 Influence of Variables

In the previous analysis, three variables i.e. rainfall, temperature, and humidity, were used together. In this section, we investigate the impact on model performance when one of these variables is removed.

5.6.1 Rainfall with Temperature

Since temperature exhibits a significant correlation with rainfall, it was considered as a predictor in both the MAHW and MMOHW methods. The dataset comprised average monthly rainfall and temperature data for Mizoram from 1986 to 2023. 80% of the data was used for training, and the remaining 20% was reserved for testing. Smoothing parameters were optimized using a brute-force approach within the interval [0,1]. For the MAHW (Rainfall + Temperature) model, the smoothing parameters yielding the lowest RMSE during the training phase were:

$$\alpha_{11} = 0.0764,\ \alpha_{12} = 0.6260,\ \alpha_{21} = 0.4280,\ \alpha_{22} = 0.6920;$$
$$\beta_{11} = 0.0065,\ \beta_{12} = 0.4821,\ \beta_{21} = 0.4886,\ \beta_{22} = 0.9873;$$
$$\gamma_{11} = 0.2290,\ \gamma_{12} = 0.5293,\ \gamma_{21} = 0.9786,\ \gamma_{22} = 0.2844$$

Using these parameters, the RMSE values for the training and testing periods were 69.15 and 63.31, respectively, while the MAE values were 36.23 and 30.43. Although these results indicate good prediction, the performance was not good enough compare to the MAHW (Rainfall + Temperature + Humidity) model, which achieved lower RMSE and MAE values in both training and testing phases. For the MMOHW (Rainfall +Temperature) model, the optimal smoothing parameters were:

$$\alpha_{11} = 0.1131,\ \alpha_{12} = 0.3406,\ \alpha_{21} = 0.2384,\ \alpha_{22} = 0.3406;$$
$$\beta_{11} = 0.9846,\ \beta_{12} = 0.8239,\ \beta_{21} = 0.9978,\ \beta_{22} = 0.9201;$$
$$\gamma_{11} = 0.4001,\ \gamma_{12} = 0.9846,\ \gamma_{21} = 0.5110,\ \gamma_{22} = 0.5262$$

With these parameters, the RMSE values during training and testing were 72.19 and 65.82, respectively, while the corresponding MAE values were 39.30 and 33.38. These error metrics are again higher than those from the MMOHW (Rainfall + Temperature + Humidity) model. Thus, excluding humidity makes the model comparatively less suitable for rainfall forecasting in this region.

5.6.2 Rainfall with Humidity

Based on correlation analysis, humidity shows a significant relationship with rainfall. To assess the predictive potential of humidity alone (in the absence of temperature), we applied both the Multivariate Additive Holt Winters (MAHW) and Multivariate Modified Holt Winters (MMOHW) methods using monthly rainfall and humidity data from Mizoram for the period 1986–2023. The dataset was split into 80% for training and 20% for testing. Smoothing parameters were optimized using a brute-force search within the interval [0,1]. For the MAHW (Rainfall + Humidity) model, the smoothing parameters that yielded the lowest RMSE during training were:

$$\alpha_{11} = 0.1824,\ \alpha_{12} \ = 0.5877,\ \alpha_{21} = 0.3457,\ \alpha_{22} \ = 0.0020;$$
$$\beta_{11} = 0.0037,\ \beta_{12} \ = 0.6930,\ \beta_{21} = 0.9610,\ \beta_{22} \ = 0.3838;$$
$$\gamma_{11} = 0.4185,\ \gamma_{12} \ = 0.2780,\ \gamma_{21} = 0.8992,\ \gamma_{22} \ = 0.9390$$

With these parameters, the RMSE values for training and testing were 73.10 and 66.86, respectively. The corresponding MAE values were 41.35 (training) and 33.13 (testing). Compared to the MAHW (Rainfall + Temperature + Humidity) model, which yielded lower error values, this configuration is relatively less effective for rainfall forecasting. For the MMOHW (Rainfall + Humidity) model, the smoothing parameters were optimized in the same manner, which were:

$$\alpha_{11} = 0.4279,\ \alpha_{12} \ = 0.4174,\ \alpha_{21} = 0.6783,\ \alpha_{22} \ = 0.3675;$$
$$\beta_{11} = 0.0037,\ \beta_{12} \ = 0.0764,\ \beta_{21} = 0.4435,\ \beta_{22} \ = 0.9999;$$
$$\gamma_{11} = 0.4185,\ \gamma_{12} \ = 0.3993,\ \gamma_{21} = 0.6370,\ \gamma_{22} \ = 0.3177$$

The RMSE values obtained were 83.65 for the training set and 77.31 for the testing set, while the MAE values were 46.16 and 40.51, respectively. These results further confirm that excluding temperature leads to a decline in model performance, and that humidity alone is not sufficient for achieving optimal prediction accuracy. 0verall, the models that incorporate all three variables consistently outperform those with only two, highlighting the importance of multi-variable integration in rainfall forecasting.

5.7 Comparison of Univariate and Multivariate Holt Winters Methods

This section presents a comparative analysis of univariate and multivariate Holt Winters methods, including the Additive Holt Winters (AHW), Modified Holt

Winters (MOHW), Multivariate Additive Holt Winters (MAHW), and Multivariate Modified Holt Winters (MMOHW) models. The performance of these models was evaluated using Root Mean Square Error (RMSE) and Mean Absolute Error (MAE) on both training and testing datasets (Figure 5.7). The AHW model yielded RMSE values of 99.70 for training and 89.06 for testing, with corresponding MAE values of 72.04 and 58.76. The MOHW model showed slightly improved performance, with training RMSE and MAE of 98.26 and 70.71, and testing RMSE and MAE of 87.76 and 58.32, respectively. In contrast, the multivariate models demonstrated significantly better accuracy. The MAHW model achieved RMSE values of 58.96 (training) and 52.97 (testing), and MAE values of 28.89 and 26.15. Similarly, the MMOHW model recorded RMSE values of 56.45 and 51.80, and MAE values of 25.60 and 21.33 for training and testing, respectively. These results clearly indicate that the inclusion of multiple variables—such as temperature and humidity—substantially enhances forecasting performance. Among all models, the MMOHW method produced the lowest error metrics, suggesting it is the most effective for rainfall prediction in this region.

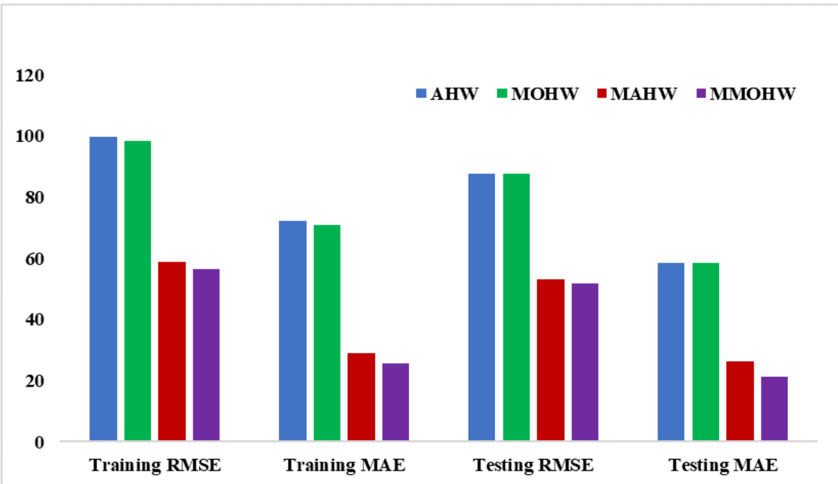

Figure 5.7: Comparison of Holt Winters method during training and testing of RMSE and MAE.

5.8 Comparison of Multivariate Methods

The comparison of multivariate models is presented in Table 5.4, highlighting the performance of each method based on key evaluation metrics such as RMSE and MAE for both training and testing datasets. The models compared include the Multivariate Linear Regression (MLR) model, the Vector Autoregressive (VAR) model, and the multivariate Holt Winters method. This comparison helps to identify the most accurate and reliable model for forecasting rainfall patterns.

Multilinear Regression (MLR) is a statistical method used to model the relationship between one dependent variable and multiple independent variables (Ge and Wu, 2020). MLR has been widely applied by researchers for rainfall forecasting (Ahmed and Mohamed, 2021; Sulca *et al.*, 2024). In this study, we utilized monthly rainfall data from 1986 to 2022 for Mizoram, where rainfall serves as the dependent variable, while temperature and humidity are considered independent variables. The dataset was split into 80% for training and 20% for testing to evaluate the model's performance. The RMSE for the training period was 98.38, while for the testing period, it was 90.15. Additionally, the MAE was 75.96 for the training data and 69.59 for the testing data. The Vector Autoregressive (VAR) model is a robust multivariate time series approach that captures the linear interdependencies among multiple variables. Unlike univariate autoregressive models, VAR models allow for dynamic interactions and feedback effects between the variables in the system (Rosita and Estuningsih, 2018). In this study, the VAR model was employed to analyze and forecast rainfall patterns based on its own past values as well as those of temperature and humidity. Before applying the VAR model, the stationarity of the individual time series was assessed using the Augmented Dickey-Fuller (ADF) test. Only stationary series were used, while non-stationary series were differenced accordingly. The dataset, covering the period from 1986 to 2023, was split into 80% for training and 20% for testing. The model was trained on the training set, and its performance was evaluated using Root Mean Squared Error (RMSE) and Mean Absolute Error (MAE). The training RMSE and MAE were found to be 84.91 and 62.18, respectively, while the testing RMSE and MAE were 90.90 and 66.98, respectively.

Table 5.4: Performance Comparison of Multivariate Models.

Method	**Training period**		**Testing period**	
	RMSE	**MAE**	**RMSE**	**MAE**
MLRM	98.38	90.15	75.96	69.59
VAR	84.91	62.18	90.90	66.98
MAHW	58.96	28.89	52.97	26.15
MMOHW	56.45	25.60	51.80	21.33

5.9 Summary

The Holt Winters method, originally developed by Holt (1957) and Winters (1960), has been widely used for time series forecasting due to its ability to capture level, trend, and seasonal components. Traditionally, it functions as a univariate model, relying solely on the historical behaviour of a single variable. However, rainfall is a complex phenomenon influenced by multiple climatic factors such as temperature and humidity. Therefore, relying on univariate models alone may not be sufficient for accurate long range forecasting. Recognizing this limitation, and in the absence of any prior established multivariate extension of the Holt Winters framework, this study introduces two novel approaches: the Multivariate Additive Holt Winters (MAHW) and the Multivariate Modified Holt Winters (MMOHW) methods. These models are designed to incorporate additional variables, making them more suitable for forecasting complex environmental time series like rainfall.

The performance evaluation conducted using historical rainfall, temperature, and humidity data from Mizoram (1986–2023) demonstrates that the proposed multivariate Holt Winters models significantly outperform traditional univariate approaches. Among all the models assessed, the Multivariate Modified Holt Winters (MMOHW) model exhibited the lowest RMSE and MAE values, highlighting its superior ability to capture both seasonal and interannual rainfall variability.

Further analysis showed that excluding one variable (either temperature or humidity) from the multivariate models resulted in higher error values, reinforcing the importance of multi-variable integration. The proposed multivariate methods also outperformed traditional statistical approaches such as Multiple Linear Regression (MLR) and Vector Auto Regression (VAR) in terms of forecasting accuracy, further validating their effectiveness. The forecasts generated using the MMOHW model aligned well with historical trends and provided consistent and reliable predictions for future periods and use it for prediction for upcoming periods. Overall, the multivariate extensions proposed in this study mark a significant advancement in Holt Winters method's forecasting, providing a more robust and context-sensitive solution for rainfall prediction for Mizoram.

Chapter 6

Conclusion

Water is essential for daily life, supporting vital needs such as drinking, domestic tasks, and various industries, including agriculture and manufacturing. However, managing water resources effectively remains a global challenge. Water exists primarily in three forms: surface water, groundwater, and precipitation (Abdullah *et al.*, 2021). Rainfall plays a critical role in sustaining both surface and groundwater supplies, making its analysis and prediction essential for water management strategies. Over the past four decades, researchers have extensively studied rainfall forecasting and extreme hydrological events. Mathematical models have proven crucial for predicting rainfall and extreme events by analyzing historical data. Time series analysis, a key tool in this effort, examines data patterns over time to forecast future values. Accurate forecasting relies on identifying data patterns (Hanke and Wychern, 2005). With the growing challenges of climate change and increasing extreme weather events, accurate rainfall forecasting has become more important.

This chapter summarizes the previous chapters and presents concluding remarks based on the key research findings. The primary aim of this study was to develop a Long Range Forecasting (LRF) model for predicting monthly rainfall in various regions of India. Monthly rainfall data were analyzed using statistical techniques, and trends were investigated using the Mann-Kendall (MK) test, Sen's slope estimator, and the Innovative Trend Analysis (ITA) test. The study employed Additive Holt Winters (AHW) and Multiplicative Holt Winters (MHW) models for forecasting, along with a newly proposed variant—the Modified Holt Winters (MOHW) method. Additionally, a novel hybrid approach called the Innovative Rainfall Predictive Method (IRPM) was developed, which integrates three essential components: linear, cyclic, and random. Recognizing that rainfall is influenced by other meteorological variables, a multivariate forecasting framework was also introduced using the Multivariate Holt Winters approach. Model performance was assessed using standard evaluation metrics such as RMSE, MAE, NSE, modified K-fold cross-validation, and the coefficient of determination (R^2). Additionally, for models comparison AIC and BIC were used.

Chapter 1 describes the study's background and motivation, highlighting the challenges posed by climatic variability in India and the gap in conventional forecasting techniques. It lays out the research problem, reviews existing literature exploring global and regional studies, clearly defines the research objectives, and their significance.

Chapter 2 details the methodology adopted in this study, including the implementation of both traditional and advanced forecasting models. The MOHW model is proposed as an enhancement to the classical Holt Winters framework, and the IRPM model is introduced as a hybrid structure integrating linear regression, Fourier series, and a probabilistic random component. Additionally, two multivariate models—Multivariate Additive Holt Winters (MAHW) and Multivariate Modified Holt Winters (MMOHW)—are developed to include temperature and humidity variables, with model parameters optimized using brute-force approach and Bayesian optimization. The correlations among the variables are determined using Pearson's Correlation Coefficient, Spearman's Rank Correlation Coefficient, and Cross-correlation. These models are rigorously validated using standard error metrics using RMSE, MAE, NSE, R^2, and a modified K-fold cross-validation approach to ensure model reliability. Additionally, models are compared using AIC and BIC.

Chapter 3 focuses on rainfall forecasting in two distinct regions—Mizoram in

Northeast India and five South Indian states: Andhra Pradesh, Telangana, Tamil Nadu, Kerala, and Karnataka. The data were divided into 80% (1986-2016) for training and 20% (2018-2022) for testing. The Holt Winters method is an advanced exponential smoothing technique that integrates the Holt and Winters method for time series forecasting (Kalekar, 2004). The Holt Winters method features two variations based on the type of seasonal component: AHW and MHW. The AHW method is appropriate when seasonal variations are consistent over time. On the other hand, the MHW is appropriate when seasonal variations are proportional to the level of the series. These two methods have been successfully applied for forecasting rainfall around the globe (Irwan *et al.*, 2023; Rafian, 2022; Sinay *et al.* 2017). Due to this success, the AHW and MHW methods were applied to these regions. The smoothing parameters were determined using a Brute-force approach, where the values corresponding to the minimum RMSE during the training period were selected and subsequently applied for testing as well as for forecasting the future periods. Some of the key findings are summarized below:

- The AHW model performed well in Karnataka, Mizoram and Tamil Nadu, yielding relatively lower values of RMSE and MAE during training and testing periods, but struggled in Kerala due to high rainfall variability.
- The MHW model showed strong forecasting performance in Andhra Pradesh and Tamil Nadu but exhibited high RMSE and MAE in Karnataka and Kerala, indicating poor model adaptability in those states. It performed particularly poorly in Mizoram and Telangana, likely due to overfitting.

Although the AHW and MHW methods perform well in certain regions, it cannot be concluded that one consistently outperforms the other across all regions, as their effectiveness largely depends on regional rainfall patterns. A major limitation of the MHW model is its inability to handle zero values in the dataset. To address this issue and to develop a more robust model applicable across diverse regions, the MOHW model is proposed. The MOHW consistently outperforms both AHW and MHW by achieving lower RMSE and MAE during both training and testing periods across all study regions. Moreover, when compared with the SARIMA model, the MOHW demonstrates superior performance, establishing it as a more reliable choice for long range rainfall forecasting in these areas and is used for forecasting the upcoming periods.

Chapter 4 introduces the IRPM for rainfall forecasting. This model integrates three components: linear, cyclic and random, which are combined into a single predictive component and further adjusted using a corrector factor. The model was first applied to the districts of Mizoram and then extended to a national scale through the application of the IRPM model to all 34 meteorological subdivisions of India. Rainfall trends were assessed using the MK test, Sen's slope, and ITA, followed by forecasting with IRPM. The model was evaluated using RMSE, MAE, modified K-fold cross validation, coefficient of determination and its performance was compared with ARIMA and SARIMA models.

In the first part of the chapter, monthly rainfall data from 1986 to 2023 for Mizoram's districts were analyzed. The results indicated mostly decreasing trends, with Aizawl, Kolasib, Champhai, and Serchhip showing significant declines—particularly in February, September, and October. Mamit was the only district to show a statistically significant increase in December. March, April, May, and October consistently exhibited declining trends across all districts, which may have significant implications for water resource management and agricultural planning. ITA results confirmed these observations, showing that 76.04% of the data followed a decreasing trend, 7.29% exhibited an increasing trend, and 16.67% remained stable. MK results showed a higher trend detection sensitivity, with 82.29% of the data classified as decreasing. Spatial mapping of Z-values reinforced the widespread nature of these declining trends. IRPM was then used to forecast rainfall from 2024 to 2064 across Mizoram. The model, enhanced with a corrector factor and validated through modified K-fold cross-validation, delivered reliable forecasts by minimizing the error metrics. Peak monsoon rainfall was projected between May and August, with Saiha expected to receive over 600 mm in

June. Champhai showed the lowest RMSE and MAE, indicating high predictive accuracy, while Lunglei and Saiha showed higher deviations. Long term trend analysis using MK and Sen's slope confirmed persistent rainfall declines in most districts, particularly Champhai and Serchhip. Only Saiha showed a statistically significant increasing trend.

In the second part, following the same methodology, monthly rainfall trends were examined across India's 34 meteorological subdivisions from 1972 to 2022. MK and Sen's slope tests revealed significant spatial and temporal variability. Increasing trends were found in March and September in areas like West Rajasthan, Konkan & Goa, and Coastal/North Interior Karnataka. July also showed increasing trends in some areas, while declining trends were observed in others, including Northeast and Eastern India. No significant changes were found in May and December. The IRPM model was applied to project rainfall up to 2075, achieving RMSE values between 21.39 and 102.26 and R^2 values between 0.67 and 0.95. As mentioned in the first part, this indicates sharp rainfall declines in Northeast India during February and July and in regions like Jharkhand, Bihar, and Uttar Pradesh during peak monsoon months. In contrast, increasing trends were noted in parts of Karnataka, Kerala, and Konkan & Goa. These mixed patterns underscore the complexity of monsoon dynamics and the need for regional forecasting models. The results provide essential insights for planning water allocation, ensuring food security, and managing agriculture under a changing climate.

Lastly, the IRPM model outperformed both the ARIMA and SARIMA models in every region evaluated.

Chapter 5 introduces multivariate modeling by extending the Holt Winters framework to incorporate temperature and humidity, acknowledging the limitations of traditional univariate approaches. This study proposes two novel multivariate models: MAHW and MMOHW. The models were evaluated using historical data from Mizoram (1986–2023), and the data were divided into 80% (training) and 20% (testing). The smoothing parameters were obtained using Bayesian optimization techniques. Based on our findings, the multivariate outperformed univariate Holt Winters method by having lower RMSE and MAE during training and testing periods. Additionally, the MMOHW performed better than MAHW. Furthermore, the exclusion of either temperature or humidity resulted in significantly higher errors, demonstrating the importance of including multiple variables. The multivariate models also outperformed classical statistical approaches like Multiple Linear Regression (MLR) and Vector Auto Regression (VAR). The forecasts generated by MMOHW closely aligned with historical patterns and provided reliable projections for future periods with NSE value of 0.67. These findings establish the multivariate models as a significant advancement in rainfall forecasting, offering more context-sensitive and accurate tools for climate adaptation in Mizoram.

Chapter 6 is a conclusion.

This thesis concludes with the development of reliable and adaptable Long Range rainfall forecasting systems through innovative time series models. Key contributions include:

- A new Modified Holt Winters (MOHW) model suitable for chaotic rainfall patterns.
- The IRPM model, integrating linear, cyclic, and random components with improved forecast accuracy through a corrector factor;
- Multivariate extensions (MAHW and MMOHW), incorporating temperature and humidity to improve rainfall prediction.
- Based on our study conducted in different regions, our model shows reliable rainfall forecasting performance.
- Application of these models across districts, regions, and national zones with robust validation techniques.
- Long term trend analysis in this study shows that most regions exhibit a decreasing trend.

- Long term projections extending up to 2075, offering valuable tools for strategic planning and policy formulation.

In summary, this study has successfully addressed the research objectives and filled a critical gap in Long Range rainfall forecasting in India. The models developed are interpretable, scalable, and empirically validated, making them suitable for real-world deployment. They hold great promise for climate-sensitive sectors such as agriculture, disaster management, and water governance. As climate variability continues to reshape monsoonal behavior, the forecasting frameworks presented here provide a solid foundation for future innovations in rainfall prediction and environmental resilience planning.

The limitations of the study are as follows:

- The study focuses solely on monthly rainfall data and does not generate daily-level forecasts, which means short-term events such as daily storms or dry spells cannot be captured.
- Several important meteorological variables that could influence rainfall prediction accuracy — such as wind patterns, sunshine duration, and surface air pressure — were not included in the analysis.
- Rainfall data were not examined at the level of individual rain gauge stations but were instead aggregated at subdivision and regional levels. As a result, local variations and micro climatic effects may have been overlooked.

Future work could address these limitations by incorporating daily data, including additional meteorological variables, and analyzing data at finer spatial scales.

Bibliography

Abeysingha, N.S., Jayasekara, J.M.N.S. and Meegastenna, T.J. (2017). Streamflow trends in up and midstream of Kirindi Oya river basin in Srilanka and its linkages to rainfall. *Mausam*, **68(1)**, 99–110.

Afshar, N.R. and Fahmi, H. (2012). Rainfall forecasting using Fourier series. *Journal of Civil Engineering and Architecture*, **6(9)**, 1258-1262.

Agrawal, A., Adke, A., Hood, V., Bambale, R. and Shelke, P. (2024). Forecasting Rainfall Utilizing Simple Linear Regression. In *2024 ASU International Conference in Emerging Technologies for Sustainability and Intelligent Systems (ICETSIS)*, IEEE, 1348–1352.

Ahasan, M., Chowdhary, M.A. and Quadir, D. (2010). Variability and trends of summer monsoon rainfall over Bangladesh *Journal of Hydrology and Meteorology*, **7(1)**, 1–17.

Ahmed, H.A.Y. and Mohamed, S.W. (2021). Rainfall prediction using multiple linear regressions model. In *2020 International Conference on Computer, Control, Electrical, and Electronics Engineering (ICCCEEE)*, IEEE, 1–5.

Ahmed, S.A. (2023). Detection of spatiotemporal patterns of rainfall trends, using non-parametric statistical techniques in Karnataka state, India *Environ. Monit. Assess.*, **195(7)**, 1-20.

Aini, A.N., Intan, P.K. and Ulinnuha, N. (2021). Prediction of average of monthly rain in Pasuruan using the Holt-Winters exponential smoothing method. *Jurnal Riset Sains dan Teknologi*, **5(2)**, 117–122.

Alam, N.M., Jana, C., Barman, D., Sharma, B., Singh, D., Mishra, P.K. and Sharma, N.K. (2018). Twentieth Century Rainfall Trends of Uttarakhand, India: A Spatio-Temporal Analysis. *Climate Change and Environmental Sustainability*, **6(2)**, 104–113.

Alivia, C.A. and Biswas, A. (2016). Development of a monthly rainfall prediction model using ARIMA techniques in Krishnanagar sub-division, Nadia District, West Bengal. *International Journal of Engineering Studies and Technical Approach*, **2(2)**, 18–26.

Anand, B., Karunanidhi, D., Subramani, T., Srinivasamoorthy, K. and Suresh, M. (2020). Long-term trend detection and spatiotemporal analysis of groundwater levels using GIS techniques in lower Bhavani river basin, Tamil Nadu, India. *J. Environ. Dev. Sustain.*, **22(4)**, 2779–2800.

Asmat, A., Wahid, S.N.S. and Deni, S.M. (2021). Identifying rainfall patterns using Fourier series: A case of daily rainfall data in Sarawak, Malaysia. *Journal of Physics: Conference Series*, **1988(1)**, 012086.

Assaad, R.H. and Fayek, S. (2021). Predicting the price of crude oil and its fluctuations using computational econometrics: deep learning, LSTM, and convolutional neural networks. *Econometric Research in Finance*, **6(2)**, 119–137.

Athanasopoulos, G., Hyndman, R.J., Song, H. and Wu, D.C. (2011). The tourism forecasting competition. *International Journal of Forecasting*, **27(3)**, 822–844.

Attri, S.D. and Tyagi, A. (2010) Climate profile of India. *Environment Monitoring and Research Center*, India Meteorology Department: New Delhi, India.

Banerjee, A.K., Sen, P.N. and Raman, C.R.V. (1978). On foreshadowing south-west monsoon rainfall over India with mid tropospheric circulation anomaly of April. *Indian Journal of Meteorology and Geophysics*, **29**, 425–431.

Bari, S.H., Rahman, M.T., Hussain, M.M. and Ray, S. (2015). Forecasting monthly precipitation in Sylhet city using ARIMA model. *Journal of Civil and Environmental Research*, **7(1)**, 69–78.

Bergmeir, C. and Benítez, J.M. (2012). On the use of cross validation for time series predictor evaluation. *Information Sciences*, **191**, 192-213.

Bergstra, J. and Bengio, Y. (2012). Random search for hyper parameter optimization. *Journal of Machine Learning Research*, **13(1)**, 281-305.

Bhakar, S.R., Bansal, A.K., Chhajed, N. and Purohit, R.C. (2006). Frequency analysis of consecutive days maximum rainfall at Banswara, Rajasthan, India. *ARPN Journal of Engineering and Applied Sciences*, **1(3)**, 64–67.

Bhaskaran, K., Gasparrini, A., Hajat, S., Smeeth, L. and Armstrong, B. (2013). Time series regression studies in environmental epidemiology. *International Journal of Epidemiology*, **42(4)**, 1187–1195.

Blanford, H.F. (1884). On the connection of the Himalaya snowfall with dry winds and seasons of drought in India. *Proceedings of the Royal Society of London*, **37**, 3–22.

Boukabara, S.A., Garrett, K., Chen, W., Iturbide-Sanchez, F., Grassotti, C., Kongoli, C. and Ferraro, R. (2019). MiRS: A new approach to satellite-based microwave rainfall retrievals. *IEEE Journal of Selected Topics in Applied Earth Observations and Remote Sensing*, **12(4)**, 1225–1244.

Bouzerdoum, M., Mellit, A. and Pavan, A.M. (2011). A hybrid model (SARIMA-SVM) for short-term power forecasting of a small-scale grid-connected photovoltaic plant. *Solar Energy*, **98**, 226–235.

Box, G.E.P. and Jenkins, G.M. (1976). *Time Series Analysis: Forecasting and Control*. Holden-Day Inc., California.

Box, G.E.P., Jenkins, G.M., Reinsel, G. C. and Ljung, G. M. (2015). *Time series analysis: forecasting and control*. John Wiley and Sons.

Brito, A.G.R., Rivero Villaverde, A., Lau Quan, A. and Ruíz Pérez, M.E. (2021). Comparison between SARIMA and Holt–Winters models for forecasting monthly streamflow in the western region of Cuba. *SN Applied Sciences*, **3(6)**, 671.

Brochu, E., Cora, V.M. and De Freitas, N. (2010). A tutorial on Bayesian optimization of expensive cost functions, with application to active user modeling and hierarchical reinforcement learning. *arXiv preprint arXiv:1012.2599*.

Brown, R.G. (1956). Exponential smoothing for predicting demand. *Little*.

Brown, R.G. and Meyer, R.F. (1961). The fundamental theorem of exponential smoothing. *Operations Research*, **9(5)**, 673-685.

Callot, L.A., Kock, A.B. and Medeiros, M.C. (2017). Modeling and forecasting large realized covariance matrices and portfolio choice. *Journal of Applied Econometrics*, **32(1)**, 140-158.

Caloiero, T., Coscarelli, R. and Ferrari, E. (2018). Application of the innovative trend analysis method for the trend analysis of rainfall anomalies in Southern Italy. *Water Resources Management*, **32(15)**, 4971–4983.

Caloiero, T., Coscarelli, R., Ferrari, E. and Mancini, M. (2011). Trend detection of annual and seasonal rainfall in Calabria (Southern Italy). *International Journal of Climatology*, **31(1)**, 44–56.

Carrión-García, A., Jabaloyes, J. and Grisales, A. (2021). The growth of COVID-19 in Spain: A view based on time-series forecasting methods. In *Data Science for COVID-19*, Academic Press, 643–660.

Chandler, R.E. and Wheater, H.S. (2002). Analysis of rainfall variability using generalized linear models: A case study from the west of Ireland. *Water Resources Research*, **38(10)**, 1–10.

Charaniya, N.A. and Dudul, S.V. (2011). Committee of artificial neural networks for monthly rainfall prediction using wavelet transform. In *2011 International Conference on Business, Engineering and Industrial Applications*, IEEE, 125–129.

Chowdhury, R.K. and Beecham, S. (2010). Australian rainfall trends and their relation to the southern oscillation index. *Hydrological Processes: An International Journal*, **24(4)**, 504–514.

Cyril, A., Mulangi, R.H. and George, V. (2019). Bus passenger demand modelling using time-series techniques and big data analytics. *The Open Transportation Journal*, **13(1)**, 41-47.

Danbatta, S.J., Muhammad, A., Varol, A. and Abdurrahaman, D.T. (2025). Forecasting monthly rainfall using hybrid time-series models and Monte Carlo simulation amidst security challenges: A case study of five districts from northern Nigeria. *Environment, Development and Sustainability*, **27**, 13815–13837.

Das, P.K. (1987). Short- and long-range monsoon prediction in India. In *Monsoons*, 549–578.

Dash, S.K., Jenamani, R.K., Kalsi, S.R. and Panda, S.K. (2007). Some evidence of climate change in twentieth-century India. *Climatic Change*, **85**, 299–321.

Deb, C., Zhang, F., Yang, J., Lee, S.E. and Shah, K.W. (2017). A review on time series forecasting techniques for building energy consumption. *Renewable and Sustainable Energy Reviews*, **74**, 902-924.

DelSole, T. and Shukla, J. (2002). Linear prediction of Indian monsoon rainfall. *Journal of Climate*, **15(24)**, 3645–3658.

Djakaria, I. and Saleh, S.E. (2021). Covid-19 forecast using Holt-Winters exponential smoothing. In *Journal of Physics: Conference Series*, **1882(1)**, 012033.

Duhan, D. and Pandey, A. (2013). Statistical analysis of long term spatial and temporal trends of precipitation during 1901–2002 at Madhya Pradesh, India. *Atmospheric Research*, **122**, 136–149.

Encik, R. and Sugiarto, S. (2016). Holt-Winter forecasting method to predict the number of visitors to the library of Riau University. *FMIPA Repository*, **7(1)**, 1-8.

Ewa, W. and Chmielowski, K. (2016). The use of Holt Winters method for forecasting the amount of sewage inflowing into the wastewater treatment plant in NowySącz. *Environmental Protection and Natural Resources*, **27(2)**, 7-12.

Fahrudin, T.M., Ambariawan, R.P. and Kamisutara, M. (2021). Demand forecasting of the automobile sales using least square, single exponential smoothing and double exponential smoothing. *Petra International Journal of Business Studies (IJBS)*, **4(2)**, 122-130.

Feng, G., Cobb, S., Abdo, Z., Fisher, D.K., Ouyang, Y., Adeli, A. and Jenkins, J.N. (2016). Trend analysis and forecast of precipitation, reference evapotranspiration, and rainfall deficit in the Blackland Prairie of Eastern Mississippi. *Journal of Applied Meteorology and Climatology*, **55(7)**, 1425–1439.

Gadgil, S., Rajeevan, M. and Nanjundiah, R. (2005). Monsoon prediction–Why yet another failure?. *Current Science*, **88(9)**, 1389–1400.

Gajbhiye, S., Meshram, C., Singh, S.K., Srivastava, P.K. and Islam, T. (2015). Precipitation trend analysis of Sindh River basin, India, from 102-year record (1901–2002). *Atmospheric Science Letters*, **17(1)**, 71–77.

Ge, Y. and Wu, H. (2020). Prediction of corn price fluctuation based on multiple linear regression analysis model under big data. *Neural Computing and Applications*, **32**, 16843-16855.

Gosain, A.K., Rao, S. and Basuray, D. (2006). Climate change impact assessment on hydrology of Indian River basins. *Current Science*, **90**, 346–353.

Goswami, B., Venugopal, V., Sengupta, D., Madhusoodanan, M. and Xavier, P. (2006). Increasing trend of extreme rain events over India in a warming environment. *Science*, **314**, 1442–1445.

Goswami, G. and Prasad, R.K. (2023). Trend analysis of rainfall pattern in Arunachal Pradesh (India). *Environmental Modeling & Assessment*, **28(6)**, 1093–1125.

Gouda, K.C., Nikhilasuma, P., Benke, M. and Agnihotri, G. (2024). Assessment of rainfall variability over Karnataka state in India. *Natural Hazards Research*, **4(2)**, 246–254.

Gowariker, V.A.S.A.N.T., Thapliyal, V., Kulshrestha, S.M., Mandal, G.S., Roy, N.S. and Sikka, D.R. (1991). A power regression model for long range forecast of southwest monsoon rainfall over India. *Mausam*, **42(2)**, 125–130.

Gowariker, V.A.S.A.N.T., Thapliyal, V., Sarker, R.P., Mandal, G.S. and Sikka, D.R. (1989). Parametric and power regression models: new approach to long range forecasting of monsoon rainfall in India. *Mausam*, **40(2)**, 115–122.

Gowri, L., Manjula, K.R., Sasireka, K. and Deepa, D. (2022). Assessment of statistical models for rainfall forecasting using machine learning technique. *Journal of Soft Computing in Civil Engineering*, **6(2)**, 51–67.

Guhathakurta, P., Sreejith, O.P. and Menon, P.A. (2011). Impact of climate change on extreme rainfall events and flood risk in India. *Journal of Earth System Science*, **120**, 359–373.

Guhathakurta, P. and Rajeevan, M. (2008). Trends in the rainfall pattern over India. *International Journal of Climatology: A Journal of the Royal Meteorological Society*, **28**, 1453–1469.

Gupta, M., Srivastava, P.K., Islam, T. and Ishak, A.M.B. (2014). Evaluation of TRMM rainfall for soil moisture prediction in a subtropical climate. *Environmental Earth Sciences*, **71**, 4421–4431.

Haghighatjou, P., Akhoond-Ali, A.M. and Nazemosadat, M.J. (2013). Non-parametric kernel estimation of annual precipitation over Iran. *Theoretical and Applied Climatology*, **112**, 193–200.

Haghighatjou, P., Akhoond-Ali, A.M., Behnia, A.K. and Chinipardaz, R. (2009). A comparison of parametric and nonparametric density functions for estimating annual precipitation in Iran. *Research Journal of Environmental Sciences*, **3(1)**, 62–70.

Hamid, A.T., Sharif, M. and Archer, D. (2014). Analysis of temperature trends in Sutlej River Basin, India. *Journal of Earth Science and Climatic Change*, **5**, 222–225.

Hanke, J.E. and Wichern, D.W. (2005). Business Forecasting. Pearson, Prentice Hall, New Jersey, ISBN: 0-13-122856-0. Reviewed in *International Journal of Forecasting*, **22(4)**, 823–824.

Hansen, J., Sato, M. and Ruedy, R. (2017). Global Temperature Trends and Their Implications. *Proceedings of the National Academy of Sciences*, **114(9)**, 2283–2290.

Hastenrath, S. (1995). Recent advances in tropical climate prediction. *Journal of Climate*, **8(6)**, 1519–1532.

Hastenrath, S. (1988). Prediction of Indian monsoon rainfall: further exploration. *Journal of Climate*, **1(3)**, 298–304.

He, J., Feng, P., Wang, B., Zhuang, W., Zhang, Y., Liu, D.L., Cleverly, J., Huete, A. and Yu, Q. (2022). Centennial annual rainfall pattern changes show an increasing trend with higher variation over northern Australia. *Journal of Hydrometeorology*, **23(8)**, 1333–1349.

Hendri, E.P. and Fadhlia, S. (2024). Time series data analysis: The Holt-Winters model for rainfall prediction in West Java. *International Journal of Applied Mathematics, Sciences, and Technology for National Defense*, **2(1)**, 1–8.

Hippenstiel, R.D. (2017). Detection theory: applications and digital signal processing. *CRC Press*.

Holt, C.C. (1957). Forecasting seasonals and trends by exponentially weighted averages (O.N.R. Memorandum No. 52), Carnegie Institute of Technology, Pittsburgh USA.

Holt, C.C. (2004). Forecasting seasonals and trends by exponentially weighted moving averages. *International Journal of Forecasting*, **20(1)**, 5–10.

Hutapea, T.A. and Siahaan, A.Y. (2023). Rainfall forecasting using the Holt-Winters exponential smoothing method in North Padang Lawas. *Journal of Student Research*, **1(2)**, 378–393.

Hyndman, R.J. and Athanasopoulos, G. (2018). Forecasting: Principles and Practice, *OTexts*.

Ingsrisawang, L., Ingsriswang, S., Somchit, S., Aungsuratana, P. and Khantiyanan, W. (2008). Machine learning techniques for short-term rain forecasting system in the Northeastern part of Thailand. *World Academy of Science, Engineering and Technology*, **31 (7)**, 248–253.

IPCC. (2021). *Climate Change 2021: The Physical Science Basis*. Intergovernmental Panel on Climate Change, Sixth Assessment Report.

Irwan, A.M., Karwangsic, E. and Ahmar, A.S. (2023). Rainfall forecasting in Makassar city using triple exponential smoothing method. *ARRUS Journal of Social Sciences and Humanities*, **3(1)**, 52–58.

Isabella, M.M., Ambujam, N.K. and Krishnan, S. (2020). Trend analysis of streamflow and its relation to rainfall in the lower Tamiraparani sub-basin of Tamil Nadu, India. *Applied Ecology & Environmental Research*, **18(1)**, 863–878.

Islam, T., Rico-Ramirez, M.A., Han, D. and Srivastava, P.K. (2012). A Joss–Waldvogel disdrometer derived rainfall estimation study by collocated tipping bucket and rapid response rain gauges. *Atmospheric Science Letters*, **13(2)**, 139–150.

Islam, M.S., Siddika, S.E. and Masum, S.I.H. (2017). Rainfall prediction in south-eastern part of Bangladesh by linear regression method. *International Journal of Emerging Research in Management and Technology*, **6(4)**.

Jain, S.K., Kumar, V. and Saharia, M. (2013). Analysis of rainfall and temperature trends in northeast India. *International Journal of Climatology*, **33**, 968–978.

Jain, S.K. and Kumar, V. (2012). Trend analysis of rainfall and temperature data for India. *Current Science*, **102(1)**, 37–42.

Jaswal, A.K., Karandikar, A.S., Gujar, M.K. and Bhan, S.C. (2015). Seasonal and annual rainfall trends in Himachal Pradesh during 1951–2005. *Mausam*, **66(2)**, 247–264.

Jayawardene, H.K.W.I., Jayewardene, D.R. and Sonnadara, D.U.J. (2015). Interannual variability of precipitation in Sri Lanka, *Journal of the National Science Foundation of Sri Lanka*, **43(1)**, 75–82.

Jones, D.R., Schonlau, M. and Welch, W.J. (1998). Efficient global optimization of expensive black-box functions. *Journal of Global Optimization*, **13(4)**, 455-492.

Jones, P.D. and Ricketts, D. (2019). The impact of climate variability on global precipitation patterns, *Climate Dynamics*, **52(3–4)**, 1595–1612.

Jou, P.H. and Mirhashemi, S.H. (2023). Frequency analysis of extreme daily rainfall over an arid zone of Iran using Fourier series method, *Applied Water Science*, **13(1)**, 16.

Junaid, M.N. and Santhanakrishnan, P.T. (2021). Rainfall trend analysis by Mann-Kendall test and Sen's slope estimator: A case study of Gummidipoondi Sub-basin, Tamil Nadu, India, *International Journal of Scientific & Engineering Research*, **12(6)**, 575.

Jyostna, B., Meena, A., Rathod, S., Tuti, M.D., Choudhary, K., Lama, A., Kumar, A.T., Reddy, B.N.K., Bhanusree, D., Rakesh, J. and Swarnaraj, A.K. (2025). Multiscale rainfall forecasting using a hybrid ensemble empirical mode decomposition and LSTM model, *Modeling Earth Systems and Environment*, **11(2)**, 1–15.

Kahya, E. and Kalayci, S. (2004). Trend analysis of streamflow in Turkey, *Journal of Hydrology*, **289(1)**, 128–144.

Kalayci, S. and Kahya, E. (2006). Assessment of streamflow variability modes in Turkey: 1964–1994, *Journal of Hydrology*, **324(1–4)**, 163–177.

Kalekar, P.S. (2004). Time series forecasting using Holt-Winters exponential smoothing, *Kanwal Rekhi School of Information Technology*, **4329008(13)**, 1–13.

Kanchan, P. and Shardoor, N.K.B. (2021). Rainfall analysis and forecasting using deep learning technique, *Journal of Informatics Electrical and Electronics Engineering (JIEEE)*, **2(2)**, 1–11.

Karmakar, S. and Simonovic, S.P. (2008). Bivariate flood frequency analysis using copula with parametric and nonparametric marginals, in *Proceedings of the 4th International Symposium on Flood Defence*, Toronto, Ontario.

Karpouzos, D.K., Kavalieratou, S. and Babajimopoulos, C. (2010). Trend analysis of precipitation data in Pieria region (Greece), *European Water*, **30**, 31–40.

Karthika, D. and Karthikeyan, K. (2021). Estimation of electrical energy consumption in Tamil Nadu using univariate time-series analysis, *Annals of Optimization Theory and Practice*, **4(2)**, 31–37.

Karthika, D. and Karthikeyan, K. (2022). Analysis of mathematical models for rainfall prediction using seasonal rainfall data: A case study for Tamil Nadu, India, in *2022 First International Conference on Electrical, Electronics, Information and Communication Technologies (ICEEICT), IEEE*, 1–4.

Kendall, M. G. (1975). *Rank Correlation Methods*. Charles Griffin, London, 4.

Khaniya, B., Jayanayaka, I., Jayasanka, P. and Rathnayake, U. (2019). Rainfall trend analysis in Uma Oya basin, Sri Lanka, and future water scarcity problems in perspective of climate variability. *Advances in Meteorology*, **2019**, 3636158.

Kirch, W. (2008). Pearson's correlation coefficient. *Encyclopedia of Public Health*, **1**, 1090–1091.

Krishnakumar, K.N., Rao, G.P. and Gopakumar, C.S. (2009). Rainfall trends in twentieth century over Kerala, India. *Atmospheric Environment*, **43(11)**, 1940–1944.

Kronmal, R. and Tarter, M. (1968). The estimation of probability densities and cumulative by Fourier series method. *American Statistical Association Journal*, **63**, 925–952.

Kumar, K.K., Soman, M.K. and Kumar, K.R. (1995). Seasonal forecasting of Indian summer monsoon rainfall: a review. *Weather*, **50(12)**, 449–467.

Kumar, K., Verma, S., Sahu, R. and Verma, M. (2023). Analysis of rainfall trends in India, incorporating non-parametric tests and wavelet synopsis over the last 117 years. *Journal of Environmental Informatics Letters*, **10**, 74–88.

Kumar, P., Singh, R.K. and Bandyopadhyay, A. (2020). Improving rainfall prediction using machine learning techniques: A case study of Indian monsoon regions. *Theoretical and Applied Climatology*, **141(3–4)**, 1243–1254.

Kumar, V. and Jain, S.K. (2010). Trends in seasonal and annual rainfall and rainy days in Kashmir Valley in the last century. *Quaternary International*, **212(1)**, 64–69.

Kumar, V., Jain, S.K. and Singh, Y. (2010). Analysis of long-term rainfall trends in India. *Hydrological Sciences Journal – Journal des Sciences Hydrologiques*, **55(4)**, 484–496.

Lallianthanga, R.K., Lalmalsawma S. Hrahsel L. and Lalthanpuia. (2018). Climate Profile of Mizoram: A tabular and graphical representation of meteorological data of eight district of Mizoram. *Mizoram State Climate Change Cell, Mizoram Science, Technology and Innovation*

Council (MISTIC), Directorate of Science and Technology, Government of Mizoram.

Li, X., Shang, W. and Wang, S. (2019). Text-based crude oil price forecasting: A deep learning approach. *International Journal of Forecasting*, **35(4)**, 1548-1560.

Li, P.W. and Lai, E.S. (2004). Short-range quantitative precipitation forecasting in Hong Kong. *Journal of Hydrology*, **288(1–2)**, 189–209.

Longobardi, A. and Villani, P. (2010). Trend analysis of annual and seasonal rainfall time series in the Mediterranean area. *International Journal of Climatology*, **30(10)**, 1538–1546.

Lv, Y., Duan, Y., Kang, W., Li, Z. and Wang, F.Y. (2014). Traffic flow prediction with big data: A deep learning approach. *IEEE transactions on intelligent transportation systems*, **16(2)**, 865-873.

Madhusoodhanan, C.G., Sreeja, K.G. and Eldho, T.I. (2016). Climate change impact assessments on the water resources of India under extensive human interventions. *Ambio*, **45(6)**, 725–741.

Madolli, M.J., Himanshu, S.K., Patro, E.R. and De Michele, C. (2022). Past, present and future perspectives of seasonal prediction of Indian summer monsoon rainfall: A review. *Asia-Pacific Journal of Atmospheric Sciences*, **58(4)**, 591–615.

Mahmoud, M. and Smadi, A. (2006). Sudden change in rainfall characteristics in Amman, Jordan during the mid 1950s. *American Journal of Environmental Sciences*, **2(3)**, 84–91.

Malik, P., Dangi, A.S., Thakur, A.S., Parihar, A.P.S., Sharma, U. and Mishra, L. (2023). An analysis of time series analysis and forecasting techniques. *International Journal of Advance Research and Innovative Ideas in Education*, **9(5)**, 1364-1374.

Manideep, K. and Sekar, K.R. (2018). Rainfall prediction using different methods of Holt winters algorithm: A big data approach. *International Journal of Pure and Applied Mathematics*, **119(15)**, 379-386.

Mann, H.B. (1945). Nonparametric tests against trend. *Econometrica: Journal of the Econometric Society*, **13(3)**, 245-259.

Marumbwa, F.M., Cho, M.A. and Chirwa, P.W. (2019). Analysis of spatio-temporal rainfall trends across southern African biomes between 1981 and 2016. *Physics and Chemistry of the Earth*, **114**, 102808.

Matham, P.K., Pattanayak, S., Kolagani, N. and Shankari, U. (2024). Rain-fed Agriculture and Use of Groundwater: Winners and Losers-A Review of Literature of Experiences in India. *Current Agriculture Research Journal*, **12(2)**, 515-529.

Melsen, L.A., Puy, A., Torfs, P.J. and Saltelli, A. (2025). The rise of the Nash-Sutcliffe efficiency in hydrology. *Hydrological Sciences Journal*, **70(1)**, 1-12.

Micchelli, C.A., Xu, Y. and Zhang, H. (2006). Universal kernels. *Journal of Machine Learning Research*, **7**, 2651-2667.

Mirza, M.Q., Warrick, R.A., Ericksen, N.J. and Kenny, G.J. (1998). Trends and persistence in precipitation in the Ganges, Brahmaputra and Meghna river basins. *Hydrological Sciences Journal*, **43**, 845-858.

Mohammad, A., Saleh, O. and Abdeen, R.A. (2006). Occurrences algorithm for string searching based on brute-force algorithm. *Journal of Computer Science*, **2(1)**, 82-85.

Mohanty, U.C., Sinha, P., Mohanty, M.R., Maurya, R.K.S. and Rao, M.N. (2019). A review on the monthly and seasonal forecast of the Indian summer monsoon. *Mausam*, **70(3)**, 425-442.

Mondal, A., Lakshmi, V. and Hashemi, H. (2018). Intercomparison of trend analysis of multisatellite monthly precipitation products and gauge measurements for river basins of India. *Journal of Hydrology*, **565**, 779-790.

Monir, M.M., Rokonuzzaman, M., Sarker, S.C., Alam, E., Islam, M.K. and Islam, A.R.M.T. (2023). Spatiotemporal analysis and predicting rainfall trends in a tropical monsoon-dominated country using MAKESENS and machine learning techniques. *Scientific Reports*, **13(1)**, 13933-13959.

Mooley, D.A. and Parthasarathy, B. (1984). Fluctuations in All-India summer monsoon rainfall during 1871–1978. *Climatic Change*, **6**, 287-301.

Mudelsee, M. (2019). Trend analysis of climate time series: A review of methods. *Earth-science reviews*, **190**, 310-322.

Mukherjee, S., Ballav, S., Soni, S., Kumar, K. and Kumar, D. U. (2016). Investigation of dominant modes of monsoon ISO in the northwest and eastern Himalayan region. *Theoretical and Applied Climatology*, **125**, 489-498.

Murali, A., Rangarajan, S., Thattai, D., Kamaraj, M., Varadharajan, D., Bhutia, S.Y. and Islam, M.N. (2022). Trend Analysis of Precipitation (1901–2015) over Telangana State, India. In *India II: Climate Change Impacts, Mitigation and Adaptation in Developing Countries*, 351-382.

Nainggolan, G.F.H., Andryana, S. and Gunaryati, A. (2021). Pencarian Berita Pada Web Portal Menggunakan Algoritma Brute Force String Matching. *JIPI (Jurnal Ilmiah Penelitian dan Pembelajaran Informatika)*, **6(1)**, 1-10.

Nash, J.E. and Sutcliffe, J.V. (1970). River flow forecasting through conceptual models part I—A discussion of principles. *Journal of hydrology*, **10(3)**, 282-290.

Nauval, F., Yollanda, M., Devianto, D., Harjupa, W., Andarini, D.F., Saufina, E., Purwaningsih, A., Rahmatia, F., Pratama, R., Trismidianto and Harjana, T. (2022). Monthly Rainfall prediction using vector autoregressive models based on ENSO and IOD phenomena in Cilacap. In *International Conference on Radioscience, Equatorial Atmospheric Science and Environment*, Singapore: Springer Nature, 395-406.

Ndaumanu, R.I. (2020). Studi Komparatif Algoritma Fisher Yates dengan Brute Force pada Permainan Kartu 24. *JEPIN (Jurnal Edukasi dan Penelitian Informatika)*, **6(1)**, 95-100.

Norzaida, A., Zalina, M.D. and Fadhilah, Y. (2016). Application of Fourier series in managing the seasonality of convective and monsoon rainfall. *Hydrological Sciences Journal*, **61(10)**, 1967–1980.

Nugroho, A., Hartati, S. and Mustofa, K. (2014). Vector autoregression (VAR) model for rainfall forecast and isohyet mapping in Semarang–Central Java–Indonesia. *International Journal of Advanced Computer Science and Applications*, **5(11)**, 123-130.

Nusyirwan, H and Ahmad, F. (2020). Forecasting seasonal time series data using the Holt-Winters exponential smoothing methods of additive models. *Journal Matematika Integratif*, **16(2)**, 151–157.

Onoz, B. and Bayazit, M. (2003). The power of statistical tests for trend detection. *Turkish Journal of Engineering and Environmental Sciences*, **27**, 247–251.

Palit, A. K. and Popovic, D. (2005). *Computational Intelligence in Time Series Forecasting*. Springer-Verlag, London.

Pandey, V., Pandey, P.K., Chakma, B., Ranjan, P. (2024). Influence of short- and long-term persistence on identification of rainfall temporal trends using different versions of the Mann-Kendall test in Mizoram, Northeast India. *Environmental Science and Pollution Research*, **31(7)**, 10359-10378.

Pandit, C.K., Lal, A.K. and Singh, U.S. (2023). Rainfall forecasts by mathematical model using monthly rainfall data for Ranchi District of Jharkhand in India. *International Journal of Mathematics Trends and Technology-IJMTT*, **69(8)**, 62-67.

Partal, T. and Kahya, E. (2006). Trend analysis in Turkish precipitation data. *Hydrological Processes*, **20(9)**, 2011–2026.

Patra, J.P., Mishra, A., Singh, R. and Raghuwanshi, N.S. (2012). Detecting rainfall trends in twentieth century (1871–2006) over Orissa State, India. *Climatic Change*, **111**, 801–817.

Paulo, A.A., Rosa, R.D. and Pereira, L.S. (2012). Climate trends and behaviour of drought indices based on precipitation and evapotranspiration in Portugal. *Natural Hazards and Earth System Sciences*, **12(5)**, 1481–1491.

Pearson, K. (1896). VII. Mathematical contributions to the theory of evolution.—III. Regression, heredity, and panmixia. Philosophical Transactions of the Royal Society of London. *Series A, containing papers of a mathematical or physical character*, **187**, 253-318.

Pertiwi, D.D. (2020). Applied exponential smoothing Holt-Winters method for rainfall forecast in Mataram city. *Journal of Intelligent Computing and Health Informatics*, **1(2)**, 46–49.

Pfeffermann, D. and Allon, J. (1989). Multivariate exponential smoothing: Method and practice. *International Journal of Forecasting*, **5(1)**, 83–98.

Piccialli, F., Giampaolo, F., Prezioso, E., Camacho, D. and Acampora, G. (2021). Artificial intelligence and healthcare: Forecasting of medical bookings through multi-source time-series fusion. *Information Fusion*, **74**, 1-16.

Poornima, S. and Pushpalatha, M. (2019). Prediction of rainfall using intensified LSTM based recurrent neural network with weighted linear units. *Atmosphere*, **10(11)**, 668.

Praveen, B., Talukdar, S., Shahfahad, Mahato, S., Mondal, J., Sharma, P., Islam, A.R.M.T. and Rahman, A. (2020). Analyzing trend and forecasting of rainfall changes in India using non-parametrical and machine learning approaches. *Scientific Reports*, **10(1)**, 10342.

Rafian, M.D. (2022). Rainfall data analysis using the Spearman methods, Mann-Kendall methods, and Holt-Winters exponential smoothing. *Bogor: Institut Pertanian Bogor*.

Rahman, M.H., Salma, U., Hossain, M.M. and Khan, M.T.F. (2016). Revenue forecasting using Holt–Winters exponential smoothing. *Research & Reviews: Journal of Statistics*, **5(3)**, 19–25.

Rajeevan, M., Guhathakurta, P. and Thapliyal, V. (2000). New models for long range forecasts of summer monsoon rainfall over North West and Peninsular India. *Meteorology and Atmospheric Physics*, **73(3)**, 211–225.

Rajeevan, M., Pai, D.S., Anil Kumar, R. and Lal, B. (2007). New statistical models for long-range forecasting of southwest monsoon rainfall over India. *Climate Dynamics*, **28**, 813–828.

Rajeevan, M. (2001). Prediction of Indian summer monsoon: Status, problems and prospects. *Current Science*, **11**, 1451–1457.

Ramesh, K. and Iyengar, R.N. (2017). Forecasting Indian monsoon rainfall including within year seasonal variability. *International Journal of Civil Engineering and Technology*, **8(2)**, 390-399.

Reddy, J.R., Ganesh, T., Venkateswaran, M. and Reddy, P. (2017). Forecasting of monthly mean rainfall in Coastal Andhra. *International Journal of Statistics and Applications*, **7(4)**, 197–204.

Ribeiro, R.C.M., Marques, G.T. and Junior, P.C. (2019). Holt-Winters forecasting for Brazilian natural gas production. *International Educative Research Foundation and Publisher*, **7(6)**, 119–129.

Rosita, T. and Estuningsih, R.D. (2018). Vector Autoregressive (VAR) for Rainfall Prediction. *International Journal of Engineering and Management Research (IJEMR)*, **8(2)**, 96-102.

Sahai, A.K., Grimm, A.M., Satyan, V. and Pant, G.B. (2003). Long-lead prediction of Indian summer monsoon rainfall from global SST evolution. *Climate Dynamics*, **20(7)**, 855–863.

Salas, J.D. (1993). Analysis and modelling of hydrological time series. *Handbook of hydrology*, **19**, 1-19.

Sameen, M.I., Pradhan, B. and Lee, S. (2020). Application of convolutional neural networks featuring Bayesian optimization for landslide susceptibility assessment. *Catena*, **186**, 104249.

Santoso, B.W., Sundawa, F. and Azhari, M. (2016). Implementasi Algoritma Brute Force Sebagai Mesin Pencari (Search Engine) Berbasis Web Pada Database. *Jurnal Sisfotek Global*, **6(1)**, 1-12.

Sarkar, S., Srivastava, A. and Kaur, E.A. (2023). Prediction rainfall with regression analysis. *International Journal for Research in Applied Science and Engineering Technology*, **11(3)**, 1934–1943.

Sarker, R.P. and Thapliyal, V. (1988). Climate change and variability. *Mausam*, **39**, 127–138.

Sati, V. P. and Rinawma, P. (2014). Practices of shifting cultivation and its implications in Mizoram, North-East India: a review of existing research. *Nature and Environment*, **19(2)**, 179-187.

Saxena, H., Aponte, O., McConky, K.T. (2019). A hybrid machine learning model for forecasting a billing period's peak electric load days. *International Journal of Forecasting*, **35(4)**, 1288-1303.

Şen, Z. (2012). Innovative trend analysis methodology. *Journal of Hydrologic Engineering*, **17(9)**, 1042–1046.

Sen, P.K. (1968). Estimates of the regression coefficient based on Kendall's tau. *Journal of the American Statistical Association*, **63**, 1379–1389.

Shadmani, M., Marofi, S. and Roknian, M. (2012). Trend analysis in reference evapotranspiration using Mann-Kendall and Spearman's Rho tests in arid regions of Iran. *Water Resources Management*, **26(1)**, 211–224.

Shah, V. and Dimitrov, S. (2022). A comparative study of univariate time-series methods for sales forecasting. *International Journal of Business and Data Analytics*, **2(2)**, 187–216.

Shahin, M. A., Ali, M. A. and Ali, A. S. (2014). Vector autoregression (VAR) modeling and forecasting of temperature, humidity, and cloud coverage. *Computational Intelligence Techniques in Earth and Environmental Sciences*, 29–51.

Shakya, A., Biswas, M. and Pal, M. (2022). Classification of radar data using Bayesian optimized two-dimensional convolutional neural network. In *Radar Remote Sensing* (pp. 175–186). Elsevier.

Sharma, C.S., Panda, S.N., Pradhan, R.P., Singh, A. and Kawamura, A. (2016). Precipitation and temperature changes in Eastern India by multiple trend detection methods. *Atmospheric Research*, **180**, 211–225.

Shejule, P.A. and Pekkat, S. (2024). Hybrid model for multistep-ahead rainfall forecast in Northeast India: A comparative study. *Journal of Hydrometeorology*, **25(8)**, 1221–1236.

Shrestha, D.L., Robertson, D.E., Wang, Q.J., Pagano, T.C., Hapuarachchi, H.P. and Tuteja, N.K. (2017). A Bayesian framework for probabilistic seasonal streamflow forecasting using hydrological modeling and climate predictors. *Water Resources Research*, **51(1)**, 428–446.

Shumway, R.H. and Stoffer, D.S. (2006). Time series analysis and its applications. With R examples. *Springer Texts in Statistics*, 47–82.

Sinay, L.J., Pentury, T. and Anakotta, D. (2017). Rainfall forecasting in Ambon city using the Holt-Winters exponential smoothing method. *Barekeng: Jurnal Ilmu Matematika dan Terapan*, **11(2)**, 101–108.

Singh, T., Sharma, N., Satakshi, and Kumar, M. (2023). Analysis and forecasting of air quality index based on satellite data. *Inhalation Toxicology*, **35(1-2)**, 24-39.

Singh, P. and Borah, B. (2013). Indian summer monsoon rainfall prediction using artificial neural network. *Stochastic Environmental Research and Risk Assessment*, **27**, 1585–1599.

Soltani, M., Rousta, I. and Modir T.S. (2013). Using Mann-Kendall and time series techniques for statistical analysis of long-term precipitation in Gorgan weather station. *World Applied Sciences Journal*, **28(7)**, 902–908.

Soltani, S., Saboohi, R. and Yaghmaei, L. (2012). Rainfall and rainy days trend in Iran. *Climatic Change*, **110(1)**, 187–213.

Spearman, C. (1987). The proof and measurement of association between two things. *The American journal of psychology*, **100(3/4)**, 441-471.

Srivastava, P.K., Han, D., Rico-Ramirez, M.A. and Islam, T. (2014). Sensitivity and uncertainty analysis of mesoscale model downscaled hydrometeorological variables for discharge prediction. *Hydrological Processes*, **28**, 4419–4432.

Subaeki, B. (2017). Ptimalisasi perbandingan algoritma brute force dan knuth-morris—pratt untuk meningkatkan kecepatan pencarian data pada aplikasi mobile tentang hewan vertebrata. *Jurnal Techno-Socio Ekonomika Universitas Sangga Buana YPKP*, **10(3)**, 278-291.

Subash, N. and Sikka, A.K. (2014). Trend analysis of rainfall and temperature and their relationship over India. *Theoretical and Applied Climatology*, **117(3–4)**, 449–462.

Sulaiman, N.H., Kamarudin, M., Khairul, A., Dasuki, A., Amran, M., Azaman, F., Abidin, I.Z. and Hairoma, N. (2015). Trend analysis of Pahang River using non-parametric analysis: Mann-Kendall's trend test. *Malaysian Journal of Analytical Sciences*, **19(6)**, 1327–1334.

Sulca, J., Takahashi, K., Espinoza, J.C., Tacza, J., Zubieta, R., Mosquera, K. and Apaestegui, J. (2024). A multiple linear regression model for the prediction of summer rainfall in the northwestern Peruvian Amazon using large-scale indices. *Climate Dynamics*, **62(5)**, 4431-4451.

Tabari, H., Marofi, S., Aeini, A., Talaee, P. H. and Mohammadi, K. (2011). Trend analysis of reference evapotranspiration in the western half of Iran. *Agricultural and Forest Meteorology*, **151**, 128–136.

Talbot, P.W., Rabiti, C., Alfonsi, A., Krome, C., Kunz, M.R., Epiney, A., Wang, C. and Mandelli, D. (2020). Correlated synthetic time series generation for energy system simulations using Fourier and ARMA signal processing. *International Journal of Energy Research*, **44(10)**, 8144–8155.

Tedjopurnomo, D.A., Bao, Z., Zheng, B., Choudhury, F.M. and Qin, A.K. (2020). A survey on modern deep neural network for traffic prediction:

Trends, methods and challenges. IEEE Transactions on Knowledge and Data Engineering, **34(4)**, 1544-1561.

Thapliyal, V. and Rajeevan, M. (2003). Updated operational models for long range forecasts of Indian summer monsoon rainfall. *Mausam*, **54**, 495–504.

Thapliyal, V. and Kulshreshtha, S.M. (1991). Climate changes and trends over India. *Mausam*, **42**, 333–338.

Tian, F., Yang, Y., Han, S., Moiwo, J. and Qiu, G. (2010). Determination of the period of major runoff decline and related driving factors in Ye River Basin, North China. *Journal of Water and Climate Change*, **1(2)**, 154–163.

Treppiedi, D., Cipolla, G., Francipane, A., Cannarozzo, M. and Noto, L.V. (2023). Investigating the reliability of stationary design rainfall in a Mediterranean region under a changing climate. *Water*, **15(12)**, 2245-2259.

Uba, E.S. and Bakari, H.R. (2015). An application of time series analysis in modeling monthly rainfall data for Maiduguri, North Eastern Nigeria. *Mathematical Theory and Modeling*, **5(11)**, 24–33.

Valipour, M. (2015). Long-term runoff study using SARIMA and ARIMA models in the United States. *Meteorological Applications*, **22(3)**, 592–598.

Walker, G.T. (1923). Correlation in seasonal variation of weather. VIII: A preliminary study of world weather. *Memoirs of India Meteorological Department*, **24**, 75–131.

Walker, G.T. (1925). Correlation in seasonal variations of weather—A further study of world weather. *Monthly Weather Review*, **53(6)**, 252–254.

Wang, X., Xie, N. and Yang, L. (2022). A flexible grey Fourier model based on integral matching for forecasting seasonal PM2.5 time series. *Chaos, Solitons and Fractals*, **162**, 112417.

William, W. and Wei, S. (2006). Time series analysis: univariate and multivariate methods. *USA, Pearson Addison Wesley, Segunda edicion*, **10**, 212-235.

Wiguna, I.K., Utami, N.L., Parwita, W.G., Udayana, I.P. and Sudipa, I.G. (2023). Rainfall forecasting using the Holt-Winters exponential smoothing method. *Jurnal Info Sains: Informatika dan Sains*, **13(01)**, 15–23.

Wilks, D.S. (2011). Statistical methods in the atmospheric sciences. *Academic press*, **100**.

Williams, C.K., and Rasmussen, C.E. (2006). Gaussian processes for machine learning. *Cambridge, MA: MIT press*, **2(3)**, 4.

Wilson, B.T., Knight, J.F. and McRoberts, R.E. (2018). Harmonic regression of Landsat time series for modeling attributes from national forest inventory data. *ISPRS Journal of Photogrammetry and Remote Sensing*, **137**, 29–46.

Winters, P.R. (1960). Forecasting sales by exponentially weighted moving averages. *Management Science*, **6(3)**, 324–342.

Wissler, C. (1905). The Spearman correlation formula. *Science*, **22(558)**, 309–311.

Wu, L., Zhao, C., Li, J., Yan, Y., Han, Q., Li, C. and Zhu, J. (2023). Impact of extreme climates on land surface phenology in Central Asia. *Ecological Indicators*, **146**, 109832.

Yang, Y., Yu, H. and Sun, Z. (2017). Aircraft failure rate forecasting method based on Holt-Winters seasonal model. *IEEE 2nd International Conference on Cloud Computing and Big Data Analysis*, 520–524.

Yang, Y., Lin, H., Guo, Z. and Jiang, J. (2007). A data mining approach for heavy rainfall forecasting based on satellite image sequence analysis. *Computers & Geosciences*, **33(1)**, 20–30.

Yavuz, V.S. (2025). Forecasting monthly rainfall and temperature patterns in Van Province, Türkiye, using ARIMA and SARIMA models: A long-term climate analysis. *Journal of Water and Climate Change*, **16(2)**, 800–818.

Yeditha, P.K., Anusha, G.S., Nandikanti, S.S.S. and Rathinasamy, M. (2023). Development of monthly scale precipitation-forecasting model for Indian subcontinent using wavelet-based deep learning approach. *Water*, **15(18)**, 3244-3250.

Yorucu, V. (2003). The analysis of forecasting performance by using time series data for two Mediterranean islands. *Review of Social, Economic and Business Studies*, **2**, 175-196.

Yue, S., Pilon, P. and Cavadias, G. (2002). Power of the Mann–Kendall and Spearman's rho tests for detecting monotonic trends in hydrological series. *Journal of Hydrology*, **259**, 254–271.

Zhang, Q., Xu, C.Y., Zhang, Z.X., Chen, Y.Q. and Liu, C.L. (2008). Spatial and temporal variability of extreme precipitation during 1960–2005 in the Yangtze River Basin and possible association with large-scale circulation. *Journal of Hydrology*, **353**, 215–227.

Zhang, S., Jing, X., Yue, T. and Wang, J. (2020). Performance assessment of rainwater harvesting systems: Influence of operating algorithm, length and temporal scale of rainfall time series. *Journal of Cleaner Production*, **253**, 120044.

BIO-DATA OF THE CANDIDATE

Personal Information:

Name	: MARINA LALLAWMZUALI
Father's name	: K. LALRAMNGHAKA
Mother's name	: B. LALCHHUANKIMI
Date of Birth	: 12.08.1999
Nationality	: Indian
Gender	: Female
Marital Status	: Single
Present Address	: Kulikawn, Aizawl, Mizoram.
Permanent Address	: Farkawn
Email	: lallawmzuali1999@gmail.com

Academic Records:

Xth	: M.B.S.E. (2014)
XIIth	: M.B.S.E. (2016)
B.Sc.(Hons - Mathematics)	: M.Z.U. (2019)
MSc (Mathematics)	: D.U. (2021)

(MARINA LALLAWMZUALI)

LIST OF RESEARCH PUBLICATIONS/ ACCEPTED/ COMMUNICATIONS

(1) **Lallawmzuali, M.** and Muniyan, S. (2023). Analysis of Rainfall Trend and Its Pattern in Uttarakhand Using Appropriate Probability Distributive Functions. In *International Conference on Mathematical Analysis and Application in Modeling, Singapore: Springer Nature Singapore*, 343-351.

(2) **Lallawmzuali, M.** and Muniyan, S. (2024). Probability analysis of annual and monthly rainfall in Mizoram, India: evaluating goodness of fit and identifying best probability distributions. *Mausam*, **75(3)**, 815-822.

(3) **Lallawmzuali, M.** and Muniyan, S. (2025). Rainfall prediction in Mizoram using the modified Holt Winters method. *Theoretical and Applied Climatology*, **156(2)**, 125-137.

(4) Muniyan, S. and **Lallawmzuali, M.** (2026).Monthly Rainfall Forecasting in the Districts of Mizoram Using the Innovative Rainfall Predictive Method and Trend Analysis with Mann-Kendall and Innovative Trend Analysis. *Environmental Modeling & Assessment*, 1-26.

(5) Muniyan, S. Lallawmzuali, M. and Roy, A. (2026). A Novel Statistical Approach to Water Balance Modeling for the State of MIZORAM, INDIA. *Advances in Applied Mathematics: Modeling, Simulation, and Real-World Applications, IIPSeries*, **6**. (Accepted)

(6) Muniyan, S. and **Lallawmzuali, M.** (2025). Assessment of Rainfall Patterns in South India: A comparative Analysis of Additive, Multiplicative, and Modified Holt Winters Methods. (Under Review)

(7) Muniyan, S. and **Lallawmzuali, M.** (2025). Long Range Forecast Modeling and Trend Analysis of Monthly Rainfall across Metrological Subdivisions of India using An Innovative Rainfall Predictive Method. (Under Review)

(8) Muniyan, S. and **Lallawmzuali, M.** (2025). Multivariate Holt Winters Method for Forecasting Rainfall. (Under Review)

CONFERENCES/ SEMINARS/ WORKSHOPS

(1) Attended “Short Term Course on Research and Publication Ethics” during 01^{st}–07^{th} October 2021, organized by UGC-Human Resource Development Centre, Mizoram University, India.

(2) Participated as a trainee in the “One Week Training Program on Mathematical Modelling and Computing” organised by Department of Mathematics and Computer Science, Mizoram University, Aizawl-796004, Mizoram (India) held during 26^{th} April, 2022 to 2^{nd} May, 2022.

(3) Participated as a trainee in the “Teacher’s Enrichment Workshop GROUPS, RINGS, AND NUMBER THEORY” organised by Department of Mathematics and Computer Science, Mizoram University, Aizawl-796004, Mizoram (India) held during $12^{th} - 17^{th}$ December, 2022.

(4) Attended and presented a paper entitled “A review on Long Range Forecasting Models” in the ”National Conference on Recent Developments in Mathematics and Computer Science (NCRDMCS23)” during $13^{th} - 14^{th}$ March, 2023 organized by the Mizoram Mathematical Research Association (MMRA) and Department of Mathematics, Govt. Champhai College (GCC), India.

(5) Attended “National Workshop on Role of Mathematics Modelling in Environment (NWRMME-2023)” during $18^{th} - 19^{th}$ May, 2023, organized by the Department of Mathematics and Computer Science, Mizoram University, India.

(6) Attended “National Seminar on Role of Number Theory and Graph Theory in Mathematical Science” during $12^{th} - 13^{th}$ June, 2023.

(7) Attended and presented a paper entitled “Analysis of Rainfall Trend and its Pattern in Uttarakhand using Appropriate Probability Distributive Functions” in the ”International Conference on Mathematical Analysis in Modelling (ICMAAM 2023)” during $09^{th} - 11^{th}$ October, 2023 organized by the Department of Mathematics and CMBE, Jadavpur University, India.

(8) Attended and presented a paper entitled “Probability Analysis of Monthly Rainfall Pattern in Kerela” in the ”International Conference on Recent Advances in Mathematical, Physical, and Chemical Sciences (ICRAMPC-2024)” during $21^{st} - 23^{rd}$ February, 2024 organized by School of Physical Sciences, Mizoram University, India.

(9) Attended and presented a paper entitled “Identifying the best fit probability distribution functions for monthly rainfall in Bihar” in the ”International Conference on Climate Change and Natural Resources Management for Sustainable Development (ICNS-2024)” during $13^{rd} - 15^{th}$ March, 2024 organized by the School of Earth Sciences and Natural Resources Management, Mizoram University, India.

(10) Attended and presented a paper entitled “Study on climate change through prediction of rainfall in Uttarakhand region” in the ”International Conference on Mathematics and Applications in Science, Technology and Society-2024” during $09^{th} - 10^{th}$ May, 2024 organized by the Department of Mathematics, Assam Don Bosco University, India.

(11) Attended and presented a paper entitled “Rainfall Prediction in Mizoram using the Modified Holt Winters Method” in the ”Two Days International Conference on Recent Advances in the Development of Environment and Natural Resource Management” during $04^{th} - 05^{th}$ February, 2025 organized by School of Earth Sciences and Natural Resource Management, Pachhunga University College in Collaboration with MISTIC, Directorate of Science and Technology, Govt. of Mizoram, India.

(12) Attended and presented a paper entitled “Assessment of Rainfall Patterns in South India: A comparative Analysis of Additive, Multiplicative, and Modified Holt Winters Methods” in the ”International Conference on Mathematical Science and Engineering” during $09^{th} - 11^{th}$ June, 2025 organized by the Department of Mathematics and Computer Science, Mizoram University, India.

(13) Attended "Two Days International Workshop on Artificial Intelligence Applications And Ethics" during $28^{th} - 29^{th}$ April, 2026 organized by Department of Mathematics and Computer Science, Mizoram University, India.

PARTICULARS OF THE CANDIDATE

NAME OF CANDIDATE	: MARINA LALLAWMZUALI
DEGREE	: DOCTOR OF PHILOSOPHY
DEPARTMENT	: MATHEMATICS AND COMPUTER SCIENCE
TITLE OF THESIS	: LONG RANGE FORECAST MODELING ON CHAOTIC ENVIRONMENTAL TIMES SERIES AND STUDY ON RAINFALL PATTERNS IN DIFFERENT REGIONS OF INDIA
DATE OF ADMISSION	: 17.09.2021

APPROVAL OF RESEARCH PROPOSAL:

1. DRC	: 13.04.2022
2. BOS	: 24.05.2022
3. SCHOOL BOARD	: 07.06.2022
MZU REGISTRATION NO.	: 2108961
Ph.D. REGISTRATION NO.	: MZU/Ph.D./1778 of 17.09.2021
EXTENSION	: NA

(Prof. S. SARAT SINGH)
Head of Department
Dept. of Maths. and Comp. Sc.,
Mizoram University, Mizoram.

ABSTRACT

LONG RANGE FORECAST MODELING ON CHAOTIC ENVIRONMENTAL TIMES SERIES AND STUDY ON RAINFALL PATTERNS IN DIFFERENT REGIONS OF INDIA

AN ABSTRACT SUBMITTED IN PARTIAL FULFILLMENT OF THE REQUIREMENTS FOR THE DEGREE OF DOCTOR OF PHILOSOPHY

MARINA LALLAWMZUALI
MZU REGISTRATION NUMBER: 2108961
Ph.D. REGISTRATION NO: MZU/Ph.D./1778 of 17.09.2021

DEPARTMENT OF MATHEMATICS AND COMPUTER SCIENCE

SCHOOL OF PHYSICAL SCIENCES

NOVEMBER, 2025

LONG RANGE FORECAST MODELING ON CHAOTIC ENVIRONMENTAL TIMES SERIES AND STUDY ON RAINFALL PATTERNS IN DIFFERENT REGIONS OF INDIA

BY

MARINA LALLAWMZUALI

Department of Mathematics and Computer Science

Supervisor : Prof. M. Sundararajan

Submitted

In partial fulfillment of the requirement of the Degree of Doctor of Philosophy in Mathematics of Mizoram University, Aizawl

ABSTRACT

Rainfall is a critical component of the hydrological cycle, serving as the primary source of surface and groundwater recharge and sustaining agricultural and ecological systems. However, rainfall exhibits an inherently chaotic nature, making accurate long-range forecasting a significant scientific and practical challenge. In India, where water resources and agriculture are heavily dependent on rainfall, developing robust forecasting frameworks is vital for climate adaptation, disaster preparedness, and sustainable water governance. Over the past four decades, researchers have extensively studied rainfall forecasting and extreme hydrological events. Mathematical models have proven crucial for predicting rainfall and extreme events by analyzing historical data. Time series analysis, a key tool in this effort, examines data patterns over time to forecast future values. With the growing challenges of climate change and the increasing frequency of extreme weather events, accurate rainfall forecasting has become more important than ever.

The primary aim of this study is to develop a Long Range Forecasting (LRF) model for predicting monthly rainfall in various regions of India. Monthly rainfall data were analyzed using statistical techniques, and trends were investigated with the Mann-Kendall (MK) test, Sen's slope estimator, and the Innovative Trend Analysis (ITA) test. The study employed Additive Holt Winters (AHW) and Multiplicative Holt Winters (MHW) models for forecasting, along with a newly proposed model—the Modified Holt Winters (MOHW) method. Additionally, a novel hybrid approach called the Innovative Rainfall Predictive Method (IRPM) was developed, which integrates three essential components: linear, cyclic, and random. Recognizing that rainfall is influenced by other meteorological variables, a multivariate forecasting framework was also introduced using the Multivariate Holt Winters approach. Model performance was assessed using standard evaluation metrics such as RMSE, MAE, NSE, modified K-fold cross-validation, and the coefficient of determination (R^2). For model comparison, AIC and BIC criteria were also applied.

The objectives of this research are as follows:

- To carry out an extensive statistical analysis of the rainfall data that will be collected from different rainfall regions of India.
- To develop an appropriate mathematical model on chaotic time series for Long Range Forecasting taking into consideration the three components of linear trend, cyclic trend and random events.
- To develop a LRF System of time series inbuilt with the proposed model.
- To study on the rainfall patterns in different regions of India.

Chapter 1 introduces the research background, highlighting the chaotic nature of rainfall processes and the challenges of existing forecasting techniques. It also reviews relevant literature and defines the objectives and significance of the study.

Chapter 2 presents the methodology adopted in this study, including the implementation of both traditional and advanced forecasting models. The MOHW model was proposed as an enhancement to the classical Holt Winters framework, and the IRPM model was introduced as a hybrid structure integrating linear regression, Fourier series, and a probabilistic random component. Additionally, two multivariate models—Multivariate Additive Holt Winters (MAHW) and Multivariate Modified Holt Winters (MMOHW)—were developed to include temperature and humidity variables, with model parameters optimized using brute-force search and Bayesian optimization. Correlations among the variables were determined using Pearson's Correlation Coefficient, Spearman's Rank Correlation Coefficient, and cross-correlation. These models were rigorously validated using RMSE, MAE, NSE, R^2, and a modified K-fold cross-validation approach to ensure reliability. Additionally, models were compared using AIC and BIC.

Chapter 3 focuses on rainfall forecasting in two distinct regions—Mizoram in Northeast India and five South Indian states: Andhra Pradesh, Telangana, Tamil Nadu, Kerala, and Karnataka using the AHW and MHW methods as baseline models, followed by the MOHW method. Model parameters were optimized using brute-force search and Bayesian optimization. Compared with the SARIMA model, MOHW demonstrates superior performance, establishing it as a reliable choice for long-range rainfall forecasting and was applied to forecast future periods.

Chapter 4 introduces the IRPM for rainfall forecasting. This model integrates linear, cyclic, and random components into a single predictive framework, adjusted using a corrector factor. The model was first applied to the districts of Mizoram and then extended nationally to all 34 meteorological subdivisions of India. Rainfall trends were assessed using the MK test, Sen's slope, and ITA, followed by forecasting with IRPM. The model was evaluated using RMSE, MAE, modified K-fold cross-validation, and the coefficient of determination. IRPM demonstrates superior predictive performance compared to ARIMA and SARIMA, with forecasts extending up to 2075, revealing both declining and region-specific increasing trends.

Chapter 5 extends the univariate Holt Winters method by including temperature and humidity in MAHW and MMOHW models. Applied to Mizoram, results show that MMOHW achieves the best predictive accuracy, outperforming classical methods such as Multiple Linear Regression (MLR) and Vector Auto Regression (VAR). This highlights the importance of incorporating multiple climatic variables in forecasting frameworks.

Chapter 6 is devoted for summary and conclusion.

Finally, a list of references is given at the end.